Motor and Sensor Network Topologies as Translators between Motor Control and Human Locomotion

Schumacher, Christian

(2020)

Motor and Sensor Network Topologies as Translators between Motor Control and Human Locomotion

Zur Erlangung des Grades eines Doktors der Naturwissenschaften (Dr. rer. nat.) vorgelegte Dissertation im Fachbereich Humanwissenschaften von Christian Schumacher aus Bonn
Tag der Einreichung: 10.12.2019, Tag der Prüfung: 28.05.2020

1. Gutachten: Prof. André Seyfarth
2. Gutachten: Prof. Auke Jan Ijspeert
Darmstadt – D 17

TECHNISCHE
UNIVERSITÄT
DARMSTADT

Human Sciences
Department
Institut of Sport Science
Lauflabor Locomotion
Laboratory

Motor and Sensor Network Topologies as Translators between Motor Control
and Human Locomotion

Doctoral thesis in Human Sciences by Christian Schumacher

1. Review: Prof. André Seyfarth
2. Review: Prof. Auke Jan Ijspeert

Date of submission: 10.12.2019
Date of thesis defense: 28.05.2020

Darmstadt – D 17
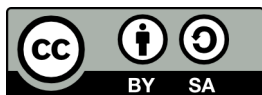
For my wife Katharina and my family

Erklärungen laut Promotionsordnung

§8 Abs. 1 lit. c PromO

Ich versichere hiermit, dass die elektronische Version meiner Dissertation mit der schriftlichen Version übereinstimmt.

§8 Abs. 1 lit. d PromO

Ich versichere hiermit, dass zu einem vorherigen Zeitpunkt noch keine Promotion versucht wurde. In diesem Fall sind nähere Angaben über Zeitpunkt, Hochschule, Dissertationsthema und Ergebnis dieses Versuchs mitzuteilen.

§9 Abs. 1 PromO

Ich versichere hiermit, dass die vorliegende Dissertation selbstständig und nur unter Verwendung der angegebenen Quellen verfasst wurde.

§9 Abs. 2 PromO

Die Arbeit hat bisher noch nicht zu Prüfungszwecken gedient.

Darmstadt, den 10.12.2019

C. Schumacher

Abstract

Human locomotion requires a complex interplay of the mechanical, sensor, neural and motor systems of motor control. Still, cyclic locomotion tasks such as walking and running can be described by simple mechanical concepts, as identified by biomechanical *Template models*. This dissertation asks how the complex motor control system produces simple patterns of human locomotion and aims to identify mechanisms of motor control to bridge the gap between the sophisticated body morphology and the low-dimensional structure of locomotion. Inspired by previous research, this work hypothesises that networks of the motor and sensor systems can provide structural solutions to simplify motor control. Three studies investigate the role of these networks for generating elementary behaviours of locomotion. Two works evaluate the motor network during steady-state locomotion and the response to unforeseen balance perturbations, while one study addresses sensor networks in dynamic hopping motions.

The first study, a meta-analysis, reviews the specific role of biarticular muscles for multi-joint coordination. The framework of *locomotor subfunctions* helps to categorise the diverse literature from biomechanics, biology and robotics. Conceptual models indicate that biarticular muscles can sense and act in global leg coordinates (leg length and orientation) instead of joint coordinates if the leg design approximates the human anatomy. Evidence from human experiments shows benefits for coordinating the segmented leg, improving motion economy and controlling angular momentum. While many of these principles provide the potential to enhance robotic system designs, these concepts await further exploitation in robotic hardware.

While the main body of experimental studies focused on steady-state motions, only a limited amount of research comprised unforeseen perturbation scenarios to study biarticular muscles. To fill this gap of knowledge, the second work investigates the role of biarticular muscles to realign the upper-body after postural balance perturbations. A new device is used to produce specific, impulse-like pitch perturbations with only minimal effects on the centre of mass dynamics. Subjects respond with intense reflex activity in biarticular thigh muscles, while monoarticular muscles respond only moderately. This study provides strong evidence that biarticular muscles are preferably used to realign the upper-body.

The final study investigates the function of blended reflex pathways to generate steady-state hopping patterns. A neuromechanical simulation model predicts pathway-specific activation patterns resulting in different motion characteristics: performance, efficiency and safety. These results indicate that elementary compositions in the sensor network can produce task-relevant behaviours. Novel *sensor-motor maps* visualise the solution space of the predicted hopping patterns to evaluate the specific feedback contributions for generating a repulsive leg function. These maps are compact, united and consistent over changes in body morphology and environment, which suggests a simple learning problem.

In summary, this thesis investigates peripheral networks of motor control, namely networks of muscle and sensory mechanoreceptors, and their function for simplifying the control task of the neural system. The main contribution of this work is the identification of the supporting role of these networks that allows the

neural system to exploit the fundamental dynamics of locomotion. These results stimulate future research on human experiments and robotic demonstrators to validate the conceptual theory presented here.

Abstract

Die menschliche Fortbewegung erfordert ein komplexes Zusammenspiel von mechanischen, sensorischen, neuronalen und motorischen Systemen der motorischen Kontrolle. Trotz dieser Komplexität, lassen sich zyklische Bewegungen wie Gehen und Laufen durch einfache mechanische Konzepte abbilden, die in biomechanischen *Templatemodellen* beschreiben werden. Diese Dissertation untersucht, wie die komplizierten Prozesse der motorischen Kontrolle simple Bewegungsmuster zur menschlichen Fortbewegung erzeugen. Dafür werden Mechanismen der motorischen Kontrolle untersucht, um die Lücke zwischen der komplexen Körpermorphologie und der niedrigdimensionalen Struktur der Fortbewegung zu schließen. Basierend auf vorheriger Forschung wird in dieser Arbeit die Hypothese aufgestellt, dass Netzwerke der motorischen und sensorischen Systeme strukturelle Lösungen liefern, die dazu beitragen können das motorische Kontrollproblem zu vereinfachen.

Drei Studien untersuchen die Rolle dieser Netzwerke in der Erzeugung elementarer Bewegungsmuster. Zwei Arbeiten evaluieren das motorische Netzwerk bei stationären Bewegungen und unvorhergesehenen Gleichgewichtsstörungen. Die dritte Studie untersucht Sensornetzwerke in dynamischen Sprungbewegungen.

Die erste Studie, eine Metaanalyse, führt die Forschung zur spezifischen Rolle von zweigelenkigen Muskeln in der Koordination mehrerer Segmente zusammen. Das Konzept der *locomotor subfunctions* hilft die Literatur aus Biomechanik, Biologie und Robotik zu kategorisieren. Templatemodelle deuten darauf hin, dass zweigelenkige Muskeln bei einer menschen-ähnlichen Beingeometrie in globalen Beinkoordinaten (Beinlänge und -ausrichtung) agieren, anstatt auf einzelne Gelenke zu wirken. Zweigelenkige Muskeln vereinfachen die Koordination des segmentierten Beins, erzeugen effizientere Bewegungen und regulieren den Drehimpuls der Segemente, wie Experimente zeigen. Viele dieser Prinzipien offenbaren Verbesserungspotentiale für die Anwendung in robotischen Systemen, jedoch werden diese Konzepte bis dato nur selten genutzt.

Während der Großteil der experimentellen Studien stationäre Bewegungen untersucht, befassen sich nur wenige Studien mit unvorhergesehenen Störungen, um zweigelenkige Muskeln zu erforschen. Um diese Lücke zu schließen, untersucht die zweite Studie dieser Arbeit die Reaktion zweigelenkiger Muskeln auf Störungen der Oberkörperbalance. Mit Hilfe eines neuen Systems werden starke und impulsartige Störungen der Oberkörperhaltung mit minimalen Auswirkungen auf die Schwerpunktdynamik erzeugt. Alle Probanden reagieren mit intensiven Reflexen in den zweigelenkigen Oberschenkelmuskeln, während eingelenkige Muskeln nur mäßige Reaktionen zeigen. Diese Studie liefert starke Belege für die wichtige Rolle von zweigelenkigen Oberschenkelmuskeln zur Kontrolle der Oberkörperhaltung.

Die letzte Studie untersucht die Funktion gemischter Reflexsignale zur Erzeugung von stationären Hüpfbewegungen. Ein neuromechanisches Simulationsmodell erzeugt signalspezifische Aktivierungsmuster, die zu unterschiedlich ausgeprägten Bewegungsformen in Bezug auf Leistung, Effizienz und Sicherheit führen. Diese Ergebnisse deuten darauf hin, dass elementare Verschaltungen von Rezeptoren aufgabenrelevantes

Verhalten hervorrufen können. Neuartige *sensor-motor maps* visualisieren den Lösungsraum der generierten Sprungmuster, um die Beiträge der verschiedenen Reflexsignale zur Erzeugung einer abdrückenden Beinfunktion zu bewerten. Diese Karten sind kompakt, einheitlich und konsistent in Bezug auf Änderungen der Körpermorphologie und -umgebung, was das Erlernen einer solchen Topologie stark vereinfacht.

Zusammenfassend untersucht diese Dissertation periphere Netzwerke der motorischen Kontrolle, nämlich Netzwerke von Muskeln und Mechanorezeptoren, und deren Funktion zur Vereinfachung der Kontrollaufgabe des neuronalen Systems. Der Hauptbeitrag dieser Arbeit ist die Identifizierung der unterstützenden Rolle solcher Netzwerke, die es dem neuronalen System ermöglichen, die grundlegende Templatedynamik der Fortbewegung auszunutzen. Diese Ergebnisse regt zukünftige Forschung durch menschlichen Experimente und robotische Demonstratoren an, um das hier vorgestellte konzeptionelle Verständnis zu validieren.

Contents

List of Figures

List of Tables

Acronyms

AMP Angular Momentum Perturbator.

BF biceps femoris.
BFlh biceps femoris long head.
BFsh biceps femoris short head.

CE contractile element.
CoM center of mass.
CoP center of pressure.
CPG central pattern generator.

DoF degrees of freedom.

ECC excitation-contraction-coupling.
EMG electromyographic data.

FFB muscle force feedback.
FMCH force-modulated compliant hip.

GAS gastrocnemius.
GASL gastrocnemius lateral head.
GASM gastrocnemius medial head.
GLU gluteus maximus.
GRA gracilis.
GRF ground reaction force.

HAM hamstrings.

IL iliacus.
IMU inertial measurement unit.
IP inverted pendulum.

LFB muscle fibre length feedback.

MTC muscle-tendon-complex.

nmPG neuromechanical pattern generator.

PAM pneumatic artificial muscle.
PS psoas major.

RF rectus femoris.
RI1 first response window.
RI2 second response window.
RI3 third response window.

SAR sartorius.
SD standard deviation.
SE serial elastic element.
SEA serial elastic actuator.
SLIP spring-loaded inverted pendulum.
SM semimembranosus.
SOL soleus.
SSC stretch-shortening cycle.
ST semitendinosus.

TA tibialis anterior.
TFL tensor fasciae latae.

VAS vastus.
VASI vastus intermedius.
VASL vastus lateralis.
VASM vastus medialis.
VFB muscle fibre velocity feedback.
VL vastus lateralis.
VPP virtual pivot point.

WEMG EMG of normal walking.

1 Introduction

Motivation

Humans can to perform a variety of movements to interact with the environment. In sports, for instance, these may range from an artistic performance of rhythmic gymnastics over a precise throw of darts to highly dynamic long jump with an impulse-like force generation. These are just some examples in which a wide set of skills are required to execute the desired motion task successfully. To enable such remarkable performance, the human body, as well as its *motor control*[1] system, must be flexible and adaptable to meet the changing requirements of the task or the environment. This requires coordinating more than a hundred joints or degrees of freedom (DoF) in the human body. More than 250 muscles are controlled by millions of neurons in the spinal cord and the brain, which in turn, receive afferent signals from thousands and more receptors (Prochazka and Ellaway, 2012). While these numbers testify the vast complexity of the human body, they also motivate to ask how such complex systems collaborate successfully to execute the desired movement.

In light of this complex interplay and the multitude of involved components, it seems even more fascinating that highly simplified biomechanical template models can describe fundamental behaviour during locomotion (Full and Koditschek, 1999). For instance, the behaviour of the leg during walking and running can be represented by the spring-loaded inverted pendulum (SLIP) model, which consists of a point mass that is supported by a force-generating leg spring (Blickhan, 1989; Geyer et al., 2006). While some of these simplifications may only apply for confined or cyclic movements, they indicate that, during cyclic locomotion, the complex body is coordinated in line with simple motion patterns or concepts.

This thesis asks about the processes that produce these simple behaviours in a highly complex system and aims to identify mechanisms in the regulation of cyclic human locomotion. This knowledge will help to progress in multiple research disciplines or technological developments and can have a considerable impact on our society. For example, a detailed understanding of the human motor control system and its organisation can be used as biologically-inspired templates for improving hardware designs or control approaches in robotic systems or assistive devices, e.g. leg prosthetics or exoskeletons. Moreover, in-depth knowledge about the processes and mechanisms involved could lead to improve diagnostics and more efficient therapies in the medical sciences.

The motor control loop

In order to build a common understanding and terminology, this section will present a brief overview of the involved systems and their function in the movement regulation.

---

[1]All processes that are involved in regulating the movement are called motor control.

An appropriate motion execution is the result of a complex interplay of different systems in the motor control loop (Figure 1.1), which continuously interact with each other (Pearson et al., 2006; Nishikawa et al., 2007; Montúfar et al., 2015).
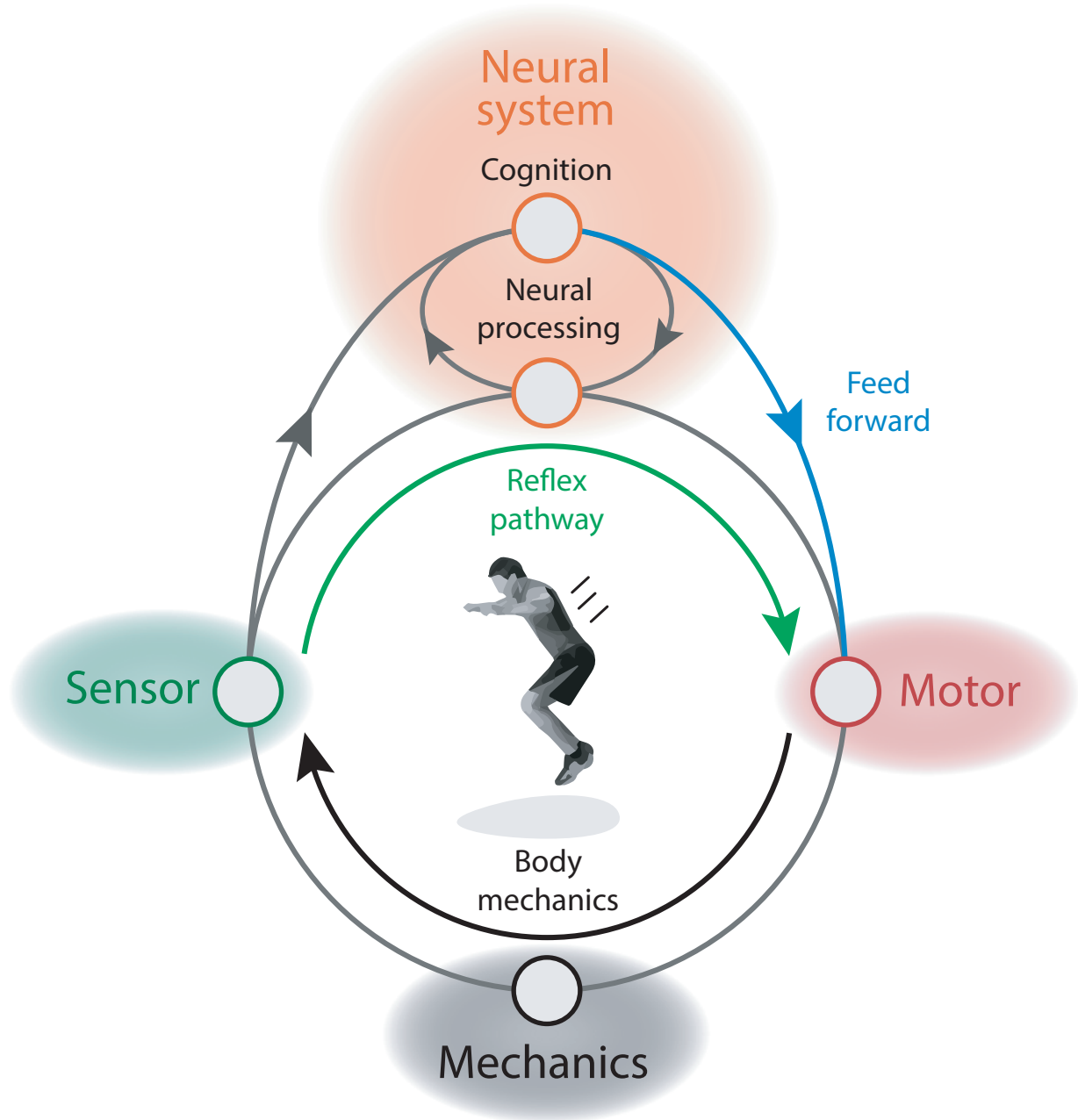
Figure 1.1: Simplified visualization of the motor control loop: Body mechanics interact with the environment **(Mechanics)**. Receptors in the body sense different stimuli and generate a neural signal **(Sensor)**, which is then processed in the spinal cord or higher centers **(neural system)**. Reflexes or feed forward signals can contribute to generate motor commands which produce muscular contractions **(Motor)** exerting forces on the body mechancis.

The body mechanics interact with the environment by exerting forces on the ground, objects or fluids

(Winter, 2009). Receptors sense states about the environment or the generated behaviour and the body, and communicate these states in the form of electrical signals to the central nervous system (Prochazka and Yakovenko, 2001). Here, many regions in the brain and spinal cord contribute to the processing in order to compute motor commands. This computation can include feedback signals, central pattern generator (CPG) (Grillner, 1975; Ijspeert, 2008; Kiehn, 2016) or feed forward commands, e.g. by internal or forward models (Francis and Wonham, 1976; Wolpert et al., 1995). Finally, muscle fibres contract in response to these motor commands and generate forces that act on bones to drive joints.

Problem statement

Based on this foundation, this section presents current challenges in the research of motor control.

Motor control is more than neural control

Because the mechanical, sensor, neural and motor systems are inevitably coupled, human motor control can not just be understood as a control problem that needs to be solved by the neural system alone (Nishikawa et al., 2007). Given sufficient resources, artificial neural networks alone can theoretically approximate any function (Hornik, 1991; Leshno et al., 1993). Therefore, it seems likely that the neural system (in the brain and spinal cord) is theoretically able to learn arbitrary movements, concerning the constraints of the body and the environment. It should be noted, however, that this strategy would require enormous resources of computation or attention, due to the high redundancy of the system (Henneman et al., 1965; Bernstein, 1967), uncertainty of the environment or sensor noise. In biology, this would reduce the 'fitness' of survival of the living organism[2]. Consequently, a major question of motor control is not, if the neural control system is capable of generating appropriate motor commands – it certainly is[3]. Rather, the question should be, to what extent can control be simplified and out-sourced to other structures, which do not require effortful computations or attention of the neural control system (Montúfar et al., 2015). This perspective helps to identify contributions of embodied systems. For example, one could ask for the simplest possible neural control topology to achieve the desired movement in a simulation model (Full and Koditschek, 1999; Brown and Loeb, 2000; Pearson et al., 2006). A comparison of e.g. muscle models with different levels of complexity, like in Haeufle et al. (2010) and Haeufle et al. (2012), could help to identify the contributions of muscular properties for the execution of movements and reductions of neural *control effort* (Haeufle et al., 2014).

Isolated approaches may not permit to identify rules of integration

In order to better understand the complex interplay in the motor control loop, we need to understand how different systems generate behaviour and what rules are used to integrate these in the collective behaviour. All parts take advantage of each other and contribute to the emergent behaviour. Therefore, the systems of the motor control loop should be studied in isolation *and* combination to identify mechanisms

---

[2]The existence of dense, local clusters in the network topology of the brain suggests that an economical brain function was indeed the result of an evolutionary optimisation (Bassett and Bullmore, 2006; Achard and Bullmore, 2007).

[3]The case of Mr. Ian Waterman or 'IW', who suffered from a total deafferentation, showed that even in the absence of proprioception, basic locomotion is possible (Cole and Cole, 1995).

of individual components while also reflecting these in the aggregate function[4] (Chiel and Beer, 1997; Dickinson et al., 2000; Ting et al., 2015). Approaches which decompose muscular activity, e.g. into *muscle synergies* (d'Avella et al., 2003; Tresch and Jarc, 2009), will most likely not be able to identify synthesising rules of individual functions because these approaches are limited to study the outcome of the neural system. Without specific intervention or active manipulation, they do not permit to discriminate between contributions of e.g. sensor or neural systems. Purely computational approaches of machine learning (black box models) will also not result in a deeper understanding of the specific interplay of mechanical, sensor, neural and motor systems in humans. While these approaches are useful to replicate neural functions, they lack the ability to identify contributions of control embodiment (if not combined with robotic systems or white-box models).

Research has identified a detailed understanding of specific mechanisms, but rules of integration remain open (Dickinson et al., 2000; Sartori et al., 2017; Frigon, 2017). Such synthesis should be evaluated in a wide range of behaviours and motion tasks (Frigon, 2017) and might also redefine individual functions (Dickinson et al., 2000). In this context, combined methodologies from different fields are required to meet the specific constraints and limitations of the individual systems at different levels: computational methods, experimental studies and robotic demonstrators (Kalveram and Seyfarth, 2009; Frigon, 2017). White-box models in simulation or hardware can replicate different functionalities of individual systems, including control embodiment (Pfeifer and Bongard, 2007). They can be build based upon experimental observations or theoretical considerations and test specific hypotheses regarding different levels of abstraction (see template – anchor concept, Full and Koditschek, 1999; Pearson et al., 2006).

Sensor and motor network topologies are poorly understood

In the motor control loop (Figure 1.1), sensor and motor systems embody the interface of the body mechanics and the neural system. By this, receptors and muscles (or motor units) establish a translation of states of the mechanical system (expressed as e.g. forces, kinematics, body properties like stiffness or inertia) and the neural system (expressed as electrochemical signals). In both systems, a high level of redundancy is found. For example, up to 500 muscle spindles can contribute to sense the state of one mammalian muscle (Prochazka and Ellaway, 2012) and multiple muscles can act on a single joint. Thereby, receptors and muscles form structural network topologies. Research has identified a detailed understanding of the individual units and their properties, like muscle spindle transfer functions or force-length and force-velocity relationships of the muscle (Prochazka and Gorassini, 1998; Hosoda et al., 2017; Siebert and Rode, 2014). However, little is known about the composition of multiple units and their contribution to the collective function of the network. Depending on the specific properties of the receptors and muscles, translations between the mechanical and neural systems are subject to limitations in e.g. dynamic response behaviour or bandwidth. Such constraints can challenge or support the control system (Chiel and Beer, 1997; Nishikawa et al., 2007). It remains open how specific topologies of these interfacing networks (and their constraints) affect the control of movements.

---

[4]This approach has been called *neuromechanics* to express the close relation of the mechanical and neural control system (Nishikawa et al., 2007; Ting et al., 2015).

Research approach

This section presents the global research approach that is used throughout this thesis to address the mentioned challenges and gaps of knowledge.

This thesis covers individual systems and their interplay that compose the aggregate function to meet the complex structure of the motor control loop. The motor control problem is thus interpreted as a composition of multiple puzzle pieces that need to be composed to create a bigger picture. For this, interdisciplinary methods from different research field are required (Nishikawa et al., 2007; Frigon, 2017), e.g. from motion science, neuroscience, psychology, and robotics.

Within this global framework, contributions of the two interfacing systems in the human motor control loop, namely motor and sensor systems, are highlighted to fill the mentioned research gap. This thesis aims at investigating the structural topology of motor and sensor networks and their contribution to simplifying neural control in cyclic locomotion. The fundamental research question is, if these network topologies enable the translation of low-dimensional (biomechanical) locomotion templates into a neural representation, such that the neural system can control the motion task more efficiently. For this, two relevant examples are chosen to study the capabilities of these networks to generate task-specific and cyclic locomotion: (1) muscle group arrangements in the human leg and (2) compositions of sensor pathways. In order to satisfy the specific requirements of these network topologies, the following perspectives are taken.

Macro-perspective: Composition of muscular functions in the human leg architecture

This macro-perspective aims at investigating how different muscle groups in the leg can contribute to generating a global leg behaviour. This is non-trivial because of the redundant and asymmetric human leg architecture. Despite – or because of – this complex network of muscles, the integrative leg function generates simple behaviours during cyclic locomotion (Geyer et al., 2006; Ivanenko et al., 2007). Is this observation a result of the neural system or, at least partially, from an advantageous arrangement of the motor system? This perspective evaluates the global leg architecture concerning its capability to provide a well-suited structural solution that allows the neural system to make use of the fundamental structure of locomotion, as identified by biomechanical template models.

Micro-perspective: Composition of sensory functions in a neuro-mechanical template model

This micro-perspective targets to identify how sensor networks of different receptors generate task-specific motion characteristics at a small scale – if a single muscle drives a single joint. For this, a *neuro-mechanical template model* for hopping is used. In order to study if the sensor network in a parsimony reflex model is sufficient to access the simple template structure of the hopping motion (Blickhan, 1989; McMahon and Cheng, 1990), different sensory signals are blended. The aim here is to work out the fundamental mechanisms of sensory blending and the dynamic interactions of the neural and mechanical systems (Full and Koditschek, 1999; Pearson et al., 2006; Nishikawa et al., 2007).

Thesis Overview

The previously mentioned research approach is represented by three articles that spread over three chapters, one per article. At the date of the thesis submission, two of the three articles are published in peer-reviewed journals while one article is submitted and currently under review.

The individual articles cover different systems in the motor control loop (Figure 1.2): (1) motor networks, (2) reactive control and (3) sensor networks. For these, research methodologies of meta-analysis, human experiment and computer simulations are used. In the following, each article will briefly be introduced.
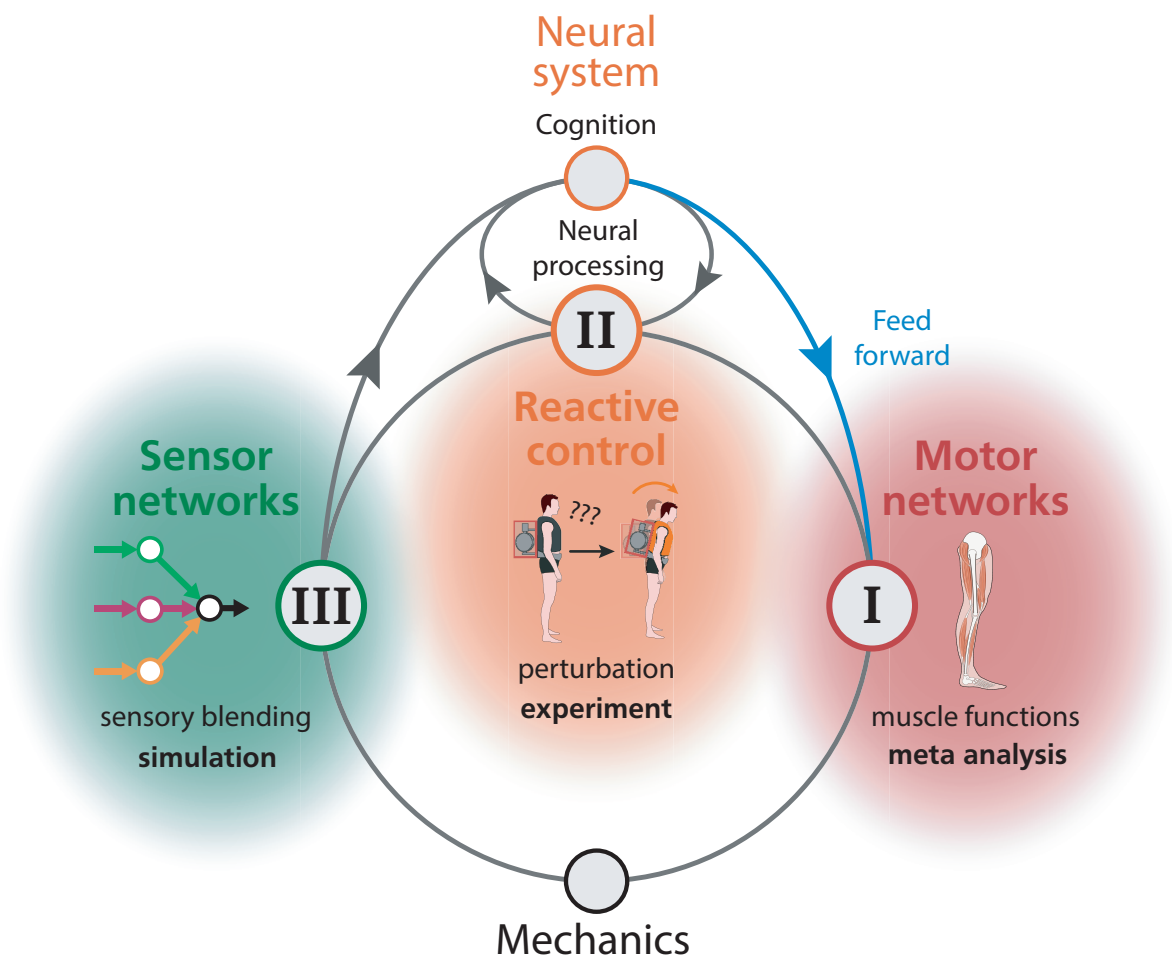
Figure 1.2: Thesis contributions (Articles I to III) in the motor control loop: muscle networks in the human leg during cyclic locomotion (**I**), reflex responses after unforeseen perturbations (**II**) and blending of different sensory pathways in sensor network (**III**).

Article I: Biarticular muscles in Light of Template Models, Experiments and Robotics: A review

The first article of this thesis presents a broad perspective on the functions of motor networks in the human leg architecture. While many studies exist that focus on a particular muscle function, it remains open how individual muscle contributions are integrated into the global leg behaviour. Reviewing research from the

fields of biomechanics, biology and robotics provides an interdisciplinary overview of state of the art and lay the foundation for the following chapters.

Within the complex network of muscles, joint impedance and torques are a superposition of multiple (antagonistic) muscles. Also, *biarticular muscles* act on more than one joint. Previous research indicates that biarticular muscles and their arrangement might play a key role in multi-joint coordination and subsequently the global leg behaviour (Hof, 2001; Dean and Kuo, 2008; Lakatos et al., 2014; Sharbafi et al., 2016; Sharbafi et al., 2017; Sarmadi et al., 2019). Therefore, this article hypothesises that biarticular structures contribute to simplify neural control.

In order to integrate research from different fields, gaits and methods, the framework of *locomotor subfunctions* is used (Seyfarth, Grimmer, et al., 2013; Sharbafi and Seyfarth, 2017). This approach allows categorising the contribution of different muscles on the global limb function of (1) the stance leg, (2) the swing leg and (3) the balanced upper body for generating appropriate behaviour in cyclic locomotion. In this framework, an overview of template models is given to understand the fundamental requirements of bipedal locomotion better. Based on this, evidence from human experiments is reviewed to identify specific contributions of biarticular muscle function. Conceptual and experimental insights are then reflected and validated in light of robotic applications and demonstrators.

This meta-analysis provides a macro perspective on the function of motor networks in the leg architecture and integrates contributions and constraints from the mechanical, sensor and neural systems. This chapter identifies topics of high research activity and aims at combining these results in a bigger picture.

Article II: Biarticular muscles are Most Responsive to Upper-body Pitch Perturbations in Human Standing

Article I identified gaps of knowledge and provided new hypotheses on the function of biarticular muscles (Chapter 2). Conceptual models suggest that biarticular muscles are preferably used to control angular momentum, e.g. for balancing the upper body (Hof, 2001; Lakatos et al., 2014; Sarmadi et al., 2019). However, experimental evidence for such kind of function is still missing, especially in the context of sudden and unforeseen perturbations.

Article II (Chapter 3) addresses this gap of knowledge by investigating the role of biarticular muscles for regulating upper-body balance after perturbations of angular momentum in human. Applying a new type of perturbation (for the first time) allows for exerting specific and impulse-like torque perturbations to the subject's upper body. First, the efficacy of the perturbation device is validated. Then, contributions of major mono- and biarticular leg muscles are identified by evaluating reactions of muscular activity in response to the perturbation. Finally, these results are reflected in the light of neural control strategies of reactive and anticipatory muscle recruitment.

Article III: Sensor-motor Maps for Describing Linear Reflex Composition in Hopping

The final article investigates the capabilities of sensor network topologies to generate specific motion tasks through changes in sensor pathway composition. A novel approach, called *sensor-motor maps*, is developed to relate elementary units of proprioception in the human body (Golgi tendon organs, muscle spindles) to specific characteristics of the generated motion.

In order to identify individual and combined (blended) contributions, the model of Geyer et al. (2003) is extended by a simple model of sensory integration. The neuromechanical template model generates a simple repetitive hopping motion to focus on the reflex contribution stemming from monosynaptic transmissions. Different characteristics of hopping are evaluated to assess the functional contribution of the sensor network: (1) ability to generate cyclic and steady-state hopping patterns (stability), (2) ability to produce dynamic and highly energetic hopping motions (performance) and (3) ability to create motions with low costs of transport (efficiency). Further, variations of the body morphology and the environment are considered to investigate the robustness of the system.

This article uses a holistic approach that integrates the mechanical, sensor, neural and motor systems in the motor control system (as motivated in this thesis). This approach allows to decompose fundamental logics of sensory blending in the sensor network and evaluates these results for generating goal-directed behaviours in the stance leg.

References

S. Achard and E. Bullmore (2007). "Efficiency and cost of economical brain functional networks". In: *PLoS computational biology* 3.2, e17.

D. S. Bassett and E. Bullmore (2006). "Small-world brain networks". In: *The neuroscientist* 12.6, pp. 512–523.

N. A. Bernstein (1967). "The co-ordination and regulation of movements". In:

R. Blickhan (1989). "The spring-mass model for running and hopping". In: *Journal of biomechanics* 22.11-12, pp. 1217–1227.

I. E. Brown and G. E. Loeb (2000). "A Reductionist Approach to Creating and Using Neuromusculoskeletal Models". In: *Biomechanics and Neural Control of Posture and Movement*. Ed. by J. M. Winters and P. E. Crago. New York, NY: Springer New York, pp. 148–163.

H. J. Chiel and R. D. Beer (1997). "The brain has a body: adaptive behavior emerges from interactions of nervous system, body and environment". In: *Trends in neurosciences* 20.12, pp. 553–557.

J. Cole and J. O. Cole (1995). *Pride and a daily marathon*. MIT Press.

A. d'Avella, P. Saltiel, and E. Bizzi (2003). "Combinations of muscle synergies in the construction of a natural motor behavior". In: *Nature neuroscience* 6.3, p. 300.

J. C. Dean and A. D. Kuo (2008). "Elastic coupling of limb joints enables faster bipedal walking". In: *Journal of the Royal Society Interface* 6.35, pp. 561–573.

M. H. Dickinson et al. (2000). "How animals move: an integrative view". In: *science* 288.5463, pp. 100–106.

B. A. Francis and W. M. Wonham (1976). "The internal model principle of control theory". In: *Automatica* 12.5, pp. 457–465.

A. Frigon (2017). "The neural control of interlimb coordination during mammalian locomotion". In: *Journal of neurophysiology* 117.6, pp. 2224–2241.

R. J. Full and D. E. Koditschek (1999). "Templates and anchors: neuromechanical hypotheses of legged locomotion on land". In: *Journal of Experimental Biology* 202.23, pp. 3325–3332.

H. Geyer, A. Seyfarth, and R. Blickhan (2006). "Compliant leg behaviour explains basic dynamics of walking and running". In: *Proceedings of the Royal Society of London B: Biological Sciences* 273, pp. 2861–2867.

H. Geyer, A. Seyfarth, and R. Blickhan (2003). "Positive force feedback in bouncing gaits?" In: *Proceedings of the Royal Society of London. Series B: Biological Sciences* 270.1529, pp. 2173–2183.

S. Grillner (1975). "Locomotion in vertebrates: central mechanisms and reflex interaction". In: *Physiological reviews* 55.2, pp. 247–304.

D. F. B. Haeufle et al. (2012). "Integration of intrinsic muscle properties, feed-forward and feedback signals for generating and stabilizing hopping". In: *Journal of The Royal Society Interface* 9.72, pp. 1458–1469.

D. Haeufle, S. Grimmer, and A. Seyfarth (2010). "The role of intrinsic muscle properties for stable hopping—stability is achieved by the force–velocity relation". In: *Bioinspiration & biomimetics* 5.1, p. 016004.

D. Haeufle et al. (2014). "Quantifying control effort of biological and technical movements: an information-entropy-based approach". In: *Physical Review E* 89.1, p. 012716.

E. Henneman, G. Somjen, and D. O. Carpenter (1965). "Functional Significance of Cell Size in Spinal Motoneurons." In: *Journal of neurophysiology* 28.3, pp. 560–580.

A. Hof (2001). "The force resulting from the action of mono-and biarticular muscles in a limb". In: *Journal of biomechanics* 34.8, pp. 1085–1089.

K. Hornik (1991). "Approximation capabilities of multilayer feedforward networks". In: *Neural networks* 4.2, pp. 251–257.

K. Hosoda et al. (2017). "Actuation in Legged Locomotion". In: *Bioinspired Legged Locomotion*. Elsevier, pp. 563–622.

A. J. Ijspeert (2008). "Central pattern generators for locomotion control in animals and robots: a review". In: *Neural networks* 21.4, pp. 642–653.

Y. P. Ivanenko et al. (2007). "Modular control of limb movements during human locomotion". In: *Journal of Neuroscience* 27.41, pp. 11149–11161.

K. T. Kalveram and A. Seyfarth (2009). "Inverse biomimetics: How robots can help to verify concepts concerning sensorimotor control of human arm and leg movements". In: *Journal of Physiology-Paris* 103.3-5, pp. 232–243.

O. Kiehn (2016). "Decoding the organization of spinal circuits that control locomotion". In: *Nature Reviews Neuroscience* 17.4, p. 224.

D. Lakatos et al. (2014). "Design and control of compliantly actuated bipedal running robots: Concepts to exploit natural system dynamics". In: *Humanoid Robots (Humanoids), 2014 14th IEEE-RAS International Conference on*. IEEE, pp. 930–937.

M. Leshno et al. (1993). "Multilayer feedforward networks with a nonpolynomial activation function can approximate any function". In: *Neural networks* 6.6, pp. 861–867.

T. McMahon and G. Cheng (1990). "The mechanism of running: how does stiffness couple with speed?" In: *Journal of Biomechanics* 23, pp. 65–78.

G. Montúfar, K. Ghazi-Zahedi, and N. Ay (2015). "A theory of cheap control in embodied systems". In: *PLoS computational biology* 11.9, e1004427.

K. Nishikawa et al. (2007). "Neuromechanics: An integrative approach for understanding motor control". In: *Integrative and Comparative Biology* 47.1, pp. 16–54.

K. Pearson, Ö. Ekeberg, and A. Büschges (2006). "Assessing sensory function in locomotor systems using neuro-mechanical simulations". In: *Trends in neurosciences* 29.11, pp. 625–631.

R. Pfeifer and J. Bongard (2007). *How the body shapes the way we think: a new view of intelligence*. MIT press.

A. Prochazka and P. Ellaway (2012). "Sensory systems in the control of movement." In: *Comprehensive Physiology* 2.4, pp. 2615–2627.

A. Prochazka and M. Gorassini (1998). "Models of ensemble firing of muscle spindle afferents recorded during normal locomotion in cats". In: *Journal of Physiology* 507.1, pp. 277–291.

A. Prochazka and S. Yakovenko (2001). "Locomotor Control: From Spring-like Reactions of Muscles to Neural Prediction". In: *The Somatosensory System: Deciphering the Brain's Own Body Image* November 2016, pp. 141–181.

A. Sarmadi et al. (2019). "Concerted control of stance and balance locomotor subfunctions-Leg force as a conductor". In: *IEEE Transactions on Medical Robotics and Bionics*.

M. Sartori, U. . Yavuz, and D. Farina (2017). "In vivo neuromechanics: Decoding causal motor neuron behavior with resulting musculoskeletal function". In: *Scientific reports* 7.1, p. 13465.

A. Seyfarth, S. Grimmer, et al. (2013). "Biomechanical and neuromechanical concepts for legged locomotion: Computer models and robot validation: Andre Seyfarth, Sten Grimmer, Daniel Häufle, Horst-Moritz Maus, Frank Peuker and Karl-Theodor Kalveram". In: *Routledge Handbook of Motor Control and Motor Learning*. Routledge, pp. 99–119.

M. A. Sharbafi and A. Seyfarth (2017). "How locomotion sub-functions can control walking at different speeds?" In: *Journal of biomechanics* 53, pp. 163–170.

M. A. Sharbafi et al. (2016). "A new biarticular actuator design facilitates control of leg function in Bio-Biped3". In: *Bioinspiration & Biomimetics* 11.4, p. 046003.

M. A. Sharbafi et al. (2017). "Reconstruction of human swing leg motion with passive biarticular muscle models". In: *Human movement science* 52, pp. 96–107.

T. Siebert and C. Rode (2014). "Computational modeling of muscle biomechanics". In: *Computational Modelling of Biomechanics and Biotribology in the Musculoskeletal System*. Elsevier, pp. 173–204.

L. H. Ting et al. (2015). "Neuromechanical principles underlying movement modularity and their implications for rehabilitation". In: *Neuron* 86.1, pp. 38–54.

M. C. Tresch and A. Jarc (2009). "The case for and against muscle synergies". In: *Current opinion in neurobiology* 19.6, pp. 601–607.

D. A. Winter (2009). *Biomechanics and motor control of human movement*. John Wiley & Sons.

D. M. Wolpert, Z. Ghahramani, and M. I. Jordan (1995). "An internal model for sensorimotor integration". In: *Science* 269.5232, pp. 1880–1882.

2 Article I: Biarticular muscles in Light of Template Models, Experiments and Robotics: A review

Christian Schumacher, Maziar Sharbafi, André Seyfarth and Christian Rode

Abstract

Leg morphology is an important outcome of evolution. A remarkable morphological leg feature is the existence of biarticular muscles that span adjacent joints. Diverse studies from different fields of research suggest a less coherent understanding of the muscles' functionality in cyclic, sagittal plane locomotion.

We structured this review of biarticular muscle function by reflecting biomechanical template models, human experiments and robotic system designs. Within these approaches, we surveyed the contribution of biarticular muscles to the locomotor subfunctions (*stance*, *balance*, and *swing*).

While mono- and biarticular muscles do not show physiological differences, the reviewed studies provide evidence for complementary and locomotor subfunction-specific contributions of mono- and biarticular muscles. In *stance*, biarticular muscles coordinate joint movements, improve economy (e.g. by transferring energy), and secure the zig-zag-configuration of the leg against joint overextension. These commonly-known functions are extended by an explicit role of biarticular muscles in controlling the angular momentum for *balance* and *swing*.

Human-like leg arrangement and intrinsic (compliant) properties of biarticular structures improve the controllability and energy efficiency of legged robots and assistive devices.

Future interdisciplinary research on biarticular muscles should address their role for sensing and control as well as non-cyclic and/or non-sagittal motions, and non-static moment arms.

Introduction

Animals can easily perform a variety of movements. They coordinate their complex musculoskeletal system in a way that allows a simple description of the movement dynamics with template models (Full and Koditschek, 1999). For example, during running and walking, the dynamics of the human body – with all its segments and muscles – can be described with a leg-spring supporting the body mass (Blickhan, 1989; McMahon and Cheng, 1990; Geyer et al., 2006). These conceptual models suggest that the neural system controls the segmented leg in simplified coordinates like leg length and leg angle rather than individual joint angles (Ivanenko et al., 2007; Bosco and Poppele, 2001; Auyang et al., 2009). The leg architecture and the muscle function could contribute to the simple behaviour of the complex leg. In the human leg, multiple muscles drive a single joint, and single muscles can act on more than one joint. Current biomechanical analyses like inverse dynamics as well as typical robotic designs focus on single joint dynamics (e.g. Winter, 2009). Single-joint analyses neglect inter-joint couplings and their potential in simplifying the realisation of coordinated multi-segment motions (Kuo, 2001).

The specific functions of biarticular muscles (muscles spanning two joints) has spurred the interest of researchers since centuries. Pioneers like DaVinci (1452-1519) exploited the ability of strings spanning multiple joints to transfer energy to move robots. Borelli (1608-1679) linked biarticular muscles to balance (drawing of a standing man with explicit biarticular muscle). The well-known *Lombard's paradox* refers to the ability of a biarticular muscle to extend a joint that it anatomically flexes. The muscle extends the joint through the action of a co-contracted biarticular antagonist (Lombard, 1903; Kuo, 2001). Biarticular muscles are believed to play an important role in efficient (Junius et al., 2017) and robust (Dean and Kuo, 2008) locomotion. However, in spite of the long history of research, the contribution of biarticular muscles for realising locomotion is still not well understood.

The lacking understanding of biarticular muscle functions prevents exploitation of potential benefits of biarticular muscles e.g. in the design of assistive devices. We provide a new functional perspective to the state-of-the-art in biarticular actuation by splitting locomotion into different subfunctions. Based on this scheme, we review relevant conceptual models and existing literature to derive functions of biarticular muscles.

Previously, legged locomotion has been analysed from many perspectives (e.g. external and interal work: Donelan et al. 2002; Saibene and Minetti 2003, potential and kinetic energetics: Cavagna et al. 1976, or by detailed building blocks of neural control: Song and Geyer 2015). Motion related approaches included the decomposition of motion into body posture, leg alignment and energy balance (Raibert, 1986), or into body support and propulsion (Liu et al., 2008; Hamner et al., 2010). Here, we follow the concept of *locomotor subfunctions* comprising *stance*, *balance* and *swing* (Sharbafi et al., 2017a). The main idea of this concept is to consider the main limbs and their functional contribution during locomotion (stance leg, swing leg and trunk) individually. This approach stresses the leg's function-specific kinematics (e.g. distal end of limb) rather than that of the individual joint or muscle, following the idea of simplified leg coordinates (leg length and leg orientation).

We focused on studies that modelled, investigated or replicated fundamental and cyclic tasks of human legged locomotion with a confined range of motion of lower-limb joints. Since the sagittal plane contains the majority of leg muscle action in these tasks, other planes and associated biarticular functions (see e.g. Cleather, 2018) are not considered.

In this review, we first define the framework of the locomotor subfunctions. This perspective is used to examine important conceptual models, followed by experimental studies on biarticular muscle function. Then, we review how hardware designs exploit biarticular structures in legged robots and assistive devices. Finally, we integrate model predictions, human experiments and robotic applications into an overall picture of biarticular muscle function during cyclic locomotion and identify opportunities for future research.

Concepts and models of locomotion

Locomotor subfunctions

Template models (Full and Koditschek, 1999) can help to describe how the dynamics of the movement could be organised. These models have been used to resemble different features of legged locomotion at different levels of the human body (muscles, joints, segments). For instance, the behaviour of the leg during walking or running can be represented by the spring-loaded inverted pendulum, called SLIP model, that is universal for animals with different numbers of legs, humans and a variety of gaits (Blickhan and Full, 1993; Gan et al., 2018a; Gan et al., 2018b). This indicates a global organisation of movement with functional requirements that are independent of the anatomical structure of the body. Agreeing with this, observations of animals and humans showed that individual joints are coordinated together to generate a desired behaviour of the limb or the whole body (Bosco and Poppele, 2001; Auyang et al., 2009; Ivanenko et al., 2007). Legged locomotion can thus be considered as a composition of locomotor subfunctions that resembles the global organisation of the corresponding limb to fulfil the functional requirement of the performed task. Previously, we proposed a set of three locomotor subfunctions, namely *stance*, *balance* and *swing* subfunction (Sharbafi and Seyfarth, 2017a):

- **Stance subfunction.** During ground contact, the stance leg exerts axial leg forces on the ground (at center of pressure, CoP) to counteract gravity and to redirect the movement of the body center of mass (CoM).

- **Balance subfunction.** This subfunction represents a rotational body alignment to keep the upper body aligned vertically with respect to gravity.

- **Swing subfunction.** This subfunction controls the swing leg motion to prepare for the next ground contact. It comprises a rotational leg alignment adjusting the leg angle of attack and an axial leg length change, e.g. for foot clearance during forward swing.

Analysing separated locomotor subfunctions allows for the investigation of each individual subfunction at different levels (Sharbafi et al., 2017a) and their interaction (Sarmadi et al., 2019). These may involve experimental or computational approaches ranging from simplistic mechanical templates to complex neuromechanical models. With this approach, we aim to provide an integrative view on the upper body and limb functions which addresses the motion-dependent requirements of sensing, controlling and actuating all involved joints and corresponding biarticular muscles.

Locomotor subfunctions can be combined to create complex movements. This requires a certain degree of modularity to generate suitable combinations that coexist without disturbing or prohibiting each other. In the current approach, some features of locomotion are simplified. Additional subfunctions could be identified in the future to extend or potentially revise the current composition of three locomotor subfunctions.

Biomechanical template models

In this review, we mainly deal with cyclic motions like walking, running, or hopping. A range of computational template models (Full and Koditschek, 1999) that drastically reduce the complexity of the physical systems have been devised to understand fundamental mechanisms of bipedal locomotion. Most template models of locomotion contain, in a more or less abstract way, a combination of different locomotor subfunctions that in an interplay enable cyclic locomotion. However, a single model often emphasises a specific mechanism or function that particularly influences one or two locomotor subfunctions. According to these priorities, we arranged a number of utilised template models within the spectrum of locomotor subfunctions (Figure 2.1). These template models have been used to analyse a variety of fundamental mechanisms of bipedal locomotion.

To investigate e.g. different gait patterns, gait stability or energy fluctuations, templates realised the specific subfunctions differently. For example, the stance subfunction has been described by rigid massless legs (Figure 2.1A), compliant springs (Figure 2.1B), viscoelastic elements (Figure 2.1D), or time-dependent functions of length and force (Figure 2.1J). The F-SLIP model (Figure 2.1C) included a foot to investigate leg lengthening and the foot rollover.

In templates, the balance subfunction was realised by torques about the hip (Figure 2.1D, F, G, H) or the ankle (Figure 2.1E). Point mass models are reduced to investigating whole-body stability, i.e. CoM dynamics relative to the CoP. The balance subfunction for templates incorporating a trunk segment with finite moment of inertia (Figure 2.1F, G) is more complex, because they simultaneously require upper body stability.

In most templates, the swing phase of the massless leg is reduced to defining an angle of attack (Figure 2.1B). This neglects the leg dynamics. Other models consider motion dynamics (e.g. leg retraction Seyfarth et al., 2003; Andrada et al., 2013, or capture point, Figure 2.1H) to define the leg placement.
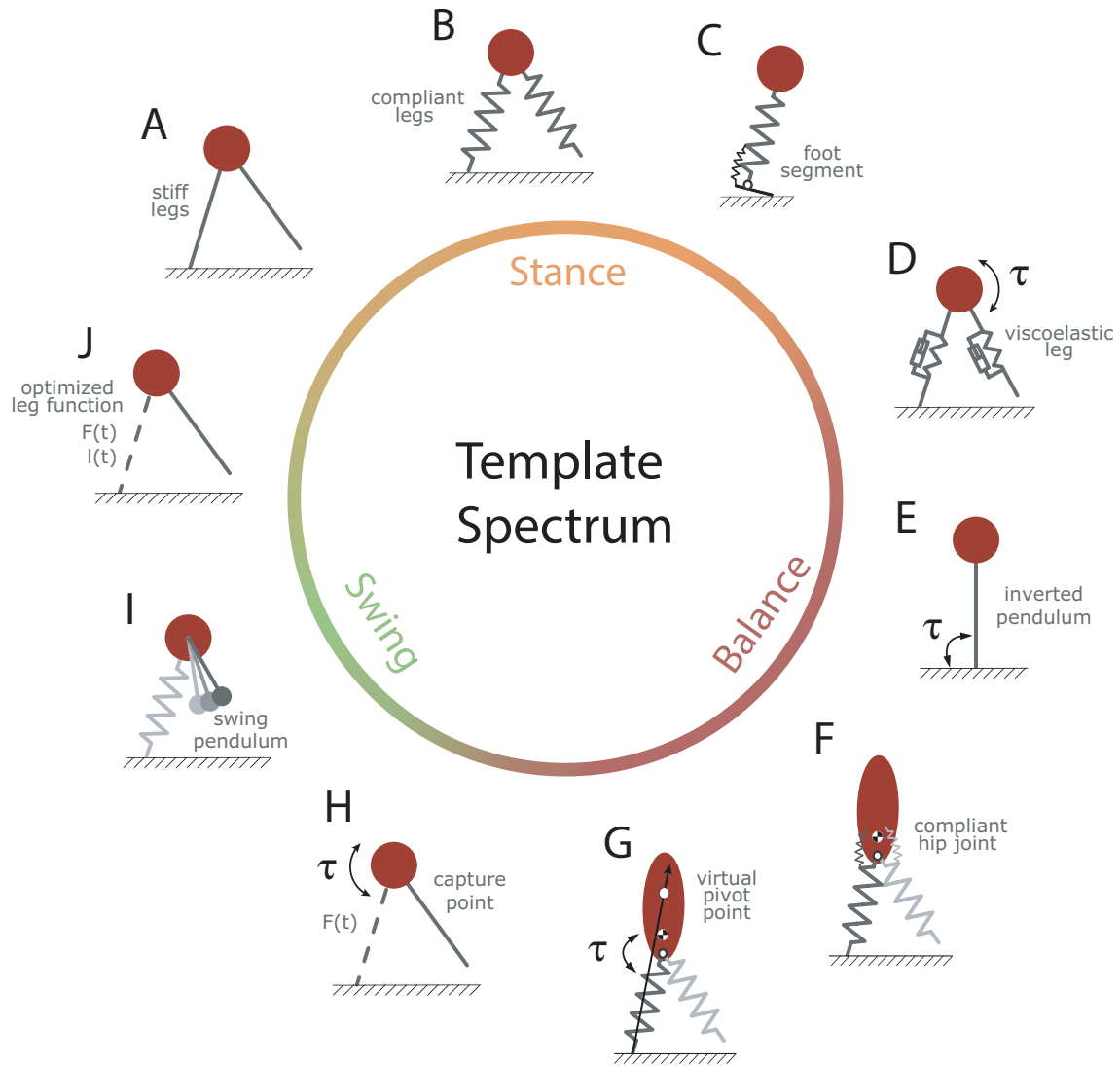
Figure 2.1: Selection of template models in the spectrum of locomotor subfunctions: **A** inverted pendulum (IP) model (Garcia et al., 1998) and linear IP model (Kajita et al., 2001), **B** spring-loaded inverted pendulum (SLIP) model (Blickhan, 1989; McMahon and Cheng, 1990; Geyer et al., 2006; Andrada et al., 2013), **C** SLIP model with foot (F-SLIP) (Maykranz and Seyfarth, 2014), **D** hip-actuated-SLIP (Hip-SLIP) with damped leg (Shen and Seipel, 2012), **E** ankle-actuated-IP model for standing (Winter, 1995), **F** SLIP with compliant hip and trunk (Gomes and Ruina, 2011; Rummel and Seyfarth, 2010), e.g. force-modulated compliant hip (FMCH) model (Sharbafi and Seyfarth, 2015), **G** virtual pivot point (VPP) model (Maus et al., 2010), **H** linearised hip-actuated-IP model with capture point (Pratt et al., 2006), **I** swing pendulum model (Rashty et al., 2014; Knuesel et al., 2005; Lim and Park, 2019) and **J** optimised leg function (Srinivasan and Ruina, 2006). Point masses neglect moment of inertia. Torques τ applied to the hip of a point mass are equivalent to models with upper bodies of infinite moment of inertia. Ellipsoid upper bodies have finite moment of inertia. Note that some references refer to slightly modified or extended versions of the shown models.

Few investigations using templates aimed at analysing the dynamics of the swing leg by representing the swing leg as a simple mechanical pendulum (Figure 2.1I).

Templates are useful to understand locomotion on a global level and this article will show their application in robotic systems (e.g. by virtual model control). However, in nature, legs are segmented and driven by mono- and biarticular muscles. Thus, the muscle's mechanical function is strongly influenced by the leg architecture. This coupling also affects the neural coordination of the muscles. Since the mentioned template models abstracted this level of complexity, they are not suitable to study the neuromechanical realisation of animal or human locomotion. To address questions concerning specific biarticular muscle functions or their neural control, the template models must be extended to segmented legs and (abstracted) muscles while preserving the derived concepts.

Biarticular structures in the segmented leg

This section focuses on the relation between selected template and segmented models with abstracted muscles (Figure 2.2). Compared to template-level analysis, segmented models resemble reality more closely. For example, compared to hip torques in a template model (e.g. Figure 2.1H) which generate ground reaction force (GRF) perpendicular to the leg axis in the sagittal plane (rotary forces), monoarticular hip muscles in a segmented leg generate static forces aligned with the shank segment (Hof, 2001). Thus, the direction of force generation with respect to leg axis depends on knee flexion. Nonetheless, the function of monoarticular hip muscles in the template model can be represented even in a segmented leg structure. This requires biarticular thigh muscles with appropriate muscle moment arms resulting in substantial rotary forces (Hof, 2001). For hip to knee muscle moment arm ratios of 2:1 and equal thigh and shank segment lengths, biarticular muscles generate GRF equal to hip torques in template models (Figure 2.2B, Hosoda et al. 2017). With this leg architecture, the muscle-tendon length is proportional to the angle between the leg and the upper body (Lakatos et al., 2014; Sarmadi et al., 2019).

Similarly, the gastrocnemius (GAS) muscle-tendon length is proportional to the angle between the leg and the ground for ankle-to-knee muscle moment arm ratios of 2:1 (Hof, 2001; Lakatos et al., 2014). For flat foot contacts with the ground, GAS force generation mainly results in a horizontal force on the upper body (Hosoda et al., 2017). This leg architecture was exploited to generate stable running with reduced control effort in a simulation model of a 7-link (trunk, thighs, shanks, feet) robot (Lakatos et al., 2014).

With a similar leg architecture, the segmented model in Figure 2.2C predicted that biarticular muscles can be used to reconstruct the segment motions of the swing leg during human walking (Sharbafi et al., 2017b). Additionally, biarticular springs (with an optimal hip-to-knee moment arm ratio of 3:1) allowed for a greater working range of walking speeds to a comparable subset of monoarticular muscles (Dean and Kuo, 2008). How these theoretical muscle moment arms relate to *in vivo* muscle moment arms will be discussed in the next section.

These concepts suggest a relevant role of biarticular muscles to translate the fundamental mechanisms of legged locomotion – as predicted by the template models – into the segmented and complex leg physiology. By supporting the organism to benefit from these mechanisms (that reflect the underlying structure of locomotion) might be a crucial contribution of biarticular muscles. However, this theory demands further validation because simulation models and hardware demonstrators at this level of complexity are rare.
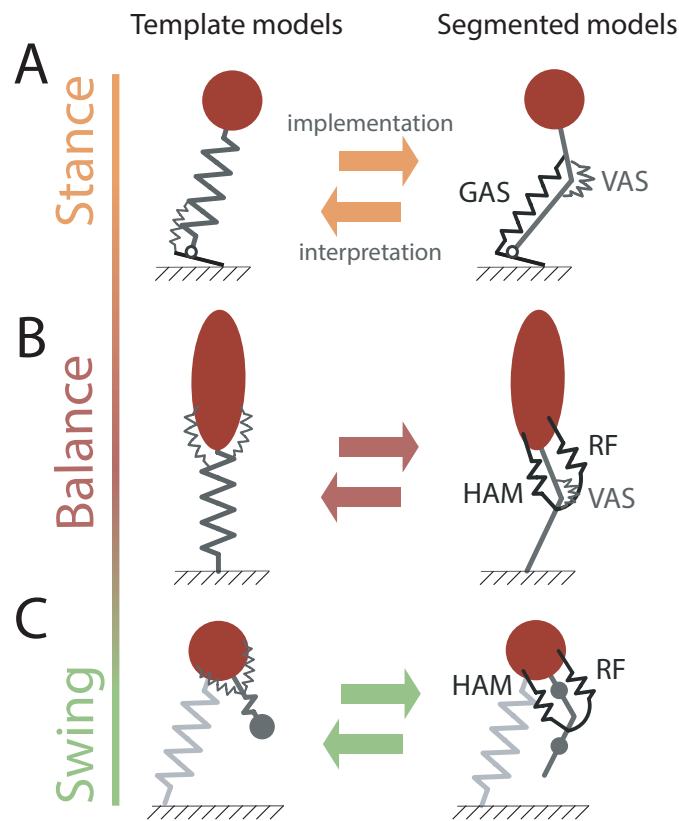
Figure 2.2: Biarticular structures bridge the gap between concepts (templates) and implementations (leg designs). Template models (with a telescopic leg structure) can be approximated with the use of biarticular muscles in the segmented leg (see text). Template models focus on fundamental mechanisms while segmented models can be used to study specific muscle functions. Equivalent template (left side) and segmented models (right side) for stance (**A**), balance (**B**) and swing subfunctions (**C**). Note that, approximations are best for muscle moment arms ratios of 2:1 (hip to knee and ankle to knee) and equal segment lengths (Hosoda et al., 2017).

Evidence of biarticular muscle function in bipedal locomotion

Muscle architecture and muscle properties

This section will discuss functional muscular adaptations like muscle architecture and selected properties. Even molecular muscle mechanics help to simplify control (e.g. Tomalka et al., 2017; Heidlauf et al., 2017; Rode et al., 2009). A more exhaustive discussion of such specific muscle properties can be found in (Hosoda et al., 2017; Siebert and Rode, 2014).

The muscle's architecture and properties determine its ability to generate force and control the fibre length with respect to tendon stretch (Biewener and Roberts, 2000). For example, short pinnate fascicles and long tendons are highly suitable for elastic recoil and economic force generation, while longer contractile fibres with short tendons allow for higher work generation and better controllability of the joint impedance, e.g. when facing perturbations (Biewener and Roberts, 2000; Carroll and Biewener, 2009).

In animals, biarticular muscles were found to cover a wide range of functions. Biarticular muscles damp impact-related oscillations in horse (Wilson et al., 2001), allow for energy transfer in turkey, wallaby and goat distal hindlimbs or generate positive work in dog and goat forelimbs (Biewener, 2016). In contrast to the human leg, where biarticular muscles flex and extend adjacent joints, the biarticular *iliotibialis lateralis pars postacetabularis* in the guinea fowl extends both, hip and knee joints and undergoes a stretch-shortening cycle during stance (Carr et al., 2011a; Carr et al., 2011b). Due to the diverse nature of biarticular muscle function in animal locomotion, we focus our analysis of muscle properties on the human leg.

To check for specialised biarticular muscle designs, we visualised data of human leg muscles (Figure 2.3A) stemming from Rajagopal et al. (2016). Figure 2.3B shows that the muscle-tendon-complex (MTC) of biarticular muscles is generally longer than that of monoarticular muscles. This result is explained by the definition of bi- or multiarticular muscles as they span more than one joint or segment. The additional length of the MTC must thereby stem from longer tendinous structures and/or longer contractile fibres.

The contraction dynamics and function of muscles depends on their fibre-tendon length ratio (Seyfarth et al., 2000; Mörl et al., 2016). Major muscles undergoing stretch-shortening cycles during walking, e.g. during ankle push-off (stance subfunction, e.g. soleus (SOL), vastus (VAS), gastrocnemius (GAS)) or swing leg acceleration (swing subfunction, e.g. rectus femoris (RF), semitendinosus (ST), biceps femoris long head (BFlh)), mainly use longer tendons (Figure 2.3B), supporting principles of energy storage and return to reduce the energy requirement of walking (Simonsen et al., 1985; Roberts, 2002; Ishikawa et al., 2007; Grimmer et al., 2014; Grimmer and Seyfarth, 2014). In addition, due to the serial arrangement of fibres and tendons, these muscles must be able to make use of the tendon's recoil (Biewener and Roberts, 2000). In accordance with this requirement, these muscles show high force capabilities (Figure 2.3C) and highly pennated muscle fibres (Figure 2.3D) generating high output forces to load the relatively long tendons (Figure 2.3E).

Muscles with longer fibres relative to tendon length (Figure 2.3E: sartorius (SAR), gracilis (GRA)) were associated with leg rotation in the transversal plane and thus steering (Cleather, 2018) and might relate to leg joint stability. Their long contractile fibres and short tendons allow a more direct control of the muscular impedance (Biewener and Roberts, 2000). Typically, steering does not involve powerful stretch-shortening cycles of these muscles. This is reflected in their limited output force, as found by a small force-generating capacity (Figure 2.3C) and small pennation angles (Figure 2.3D).

These results show that mono- and biarticular muscles share similar properties (Figure 2.3; Kuo, 2001). The muscle's specific characteristics may be more a result of a continuous adaptation to the organism's lifestyle and its environment (Du Brul, 1962; Lovejoy, 1988).

Moment arms of biarticular muscles are important for understanding their functional contribution to generate torques at the joints they span (Cleather et al., 2015; Sharbafi et al., 2017b; Young et al., 2019). As discussed in the previous section, appropriate biarticular moment arms translated fundamental mechanisms of template models to more elaborate leg designs. To check if these assumptions reflect the human physiology, we visualised data from *in-vivo* and *in-vitro* studies that investigated human muscle moment arms in the sagittal plane. Since muscle moment arms depend on joint angles, results vary due to a wide range of studied joint angles (Figure 2.4). The biarticular GAS moment arm at the ankle was found to be in ranges of 3 cm to 7 cm while its knee arm was in ranges of 1 cm to 4 cm. For biarticular thigh muscles, hip moment arms seem to be greater than knee moment arms (Figure 2.4 and Cleather et al. 2015). The results presented here seem to roughly agree with previously postulated (Winter, 2009) moment arm ratios of GAS (ankle to knee ratio: 2:1), HAM (hip to knee ratio: 2:1) and RF (hip to knee ratio: 4:3).
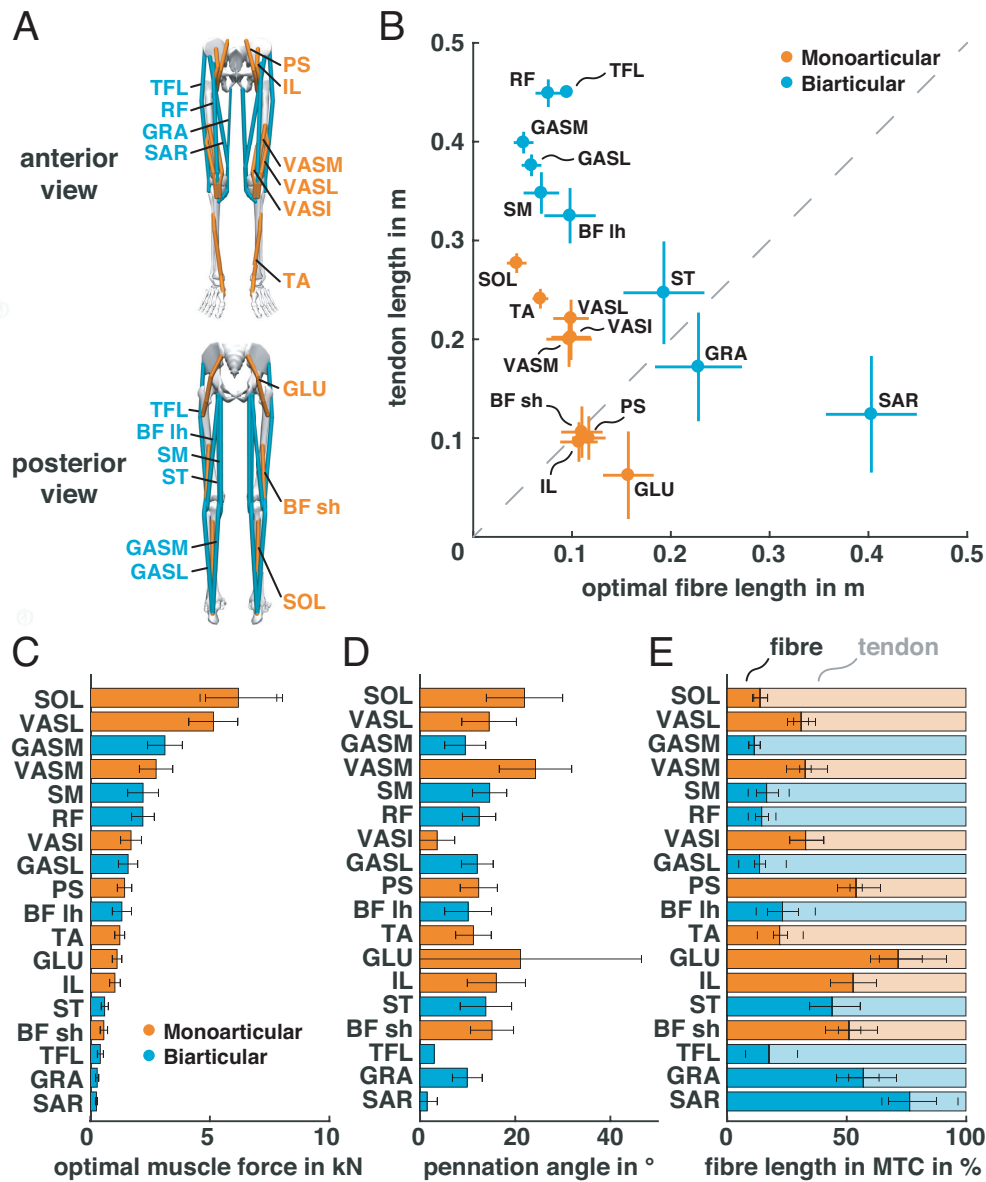
Figure 2.3: Overview of major mono- (orange) and biarticular (cyan) muscle architectures and properties. Figures were generated based on data from Rajagopal et al. (2016). **A** Arrangement of anterior (top panel) and posterior (bottom panel) muscles groups. **B** Mean and standard deviation (SD) of tendon and muscle fibre lengths. **C** Mean and SD force capacity of muscles. **D** Mean and SD pennation angles of muscles fibres. **E** Mean and SD distribution of muscles fibres and tendon lengths in the MTC. Muscle abbreviations: soleus (SOL), vastus lateralis (VASL), gastrocnemius medial head (GASM), vastus medialis (VASM), semimembranosus (SM), rectus femoris (RF), vastus intermedius (VASI), gastrocnemius lateral head (GASL), psoas major (PS), biceps femoris long head (BFlh), tibialis anterior (TA), gluteus maximus (GLU), iliacus (IL), semitendinosus (ST), biceps femoris short head (BFsh), tensor fasciae latae (TFL), gracilis (GRA) and sartorius (SAR). Note that for TFL no variances of optimal fiber length, tendon slack length, and pennation angle were reported in Rajagopal et al. (2016).

Only a limited number of studies quantified the hip moment arms. In addition, moment arms can undergo substantial changes, e.g. during a normal stride, as shown by a hindlimb model of the rat (Young et al., 2019). Even though such changes might be less pronounced for humans – as they use more extended leg configurations during locomotion – the provided overview should only be used as a guideline. In order to draw reliable conclusions further studies are needed.

Biarticular muscles in human locomotion

In this section, we will review evidence from experimental studies that investigated the role of biarticular muscles in human locomotion. We categorise the existing works by locomotor subfunctions and their task- and function-specific context.

Stance

In animals and humans, withstanding or overcoming gravitation is a major requirement for locomotion. During ground contact, leg joints (hip, knee and ankle) are often synchronised such that they undergo a flexion/ extension when the leg is shortened/ extended, respectively (Cleland, 1867; Fenn, 1938; Ivanenko et al., 2007). Due to the zig-zag configuration of the leg, biarticular leg muscles are then simultaneously pulled at one joint and released at the other joint. The length of the biarticular muscle tendon complex has been found to remain almost constant for both extremes of the full leg length range of motion (Cleland, 1867). Other studies have found that the MTC of the GAS does stretch during the stance phase of walking, but that the stretch appeared in the tendon, allowing the fascicles to operate almost isometrically (Fukunaga et al., 2001; Ishikawa et al., 2005; Lichtwark et al., 2007; Farris and Sawicki, 2012). This held even over a range of ground inclines or speeds, when higher work generation is required (Lichtwark and Wilson, 2006). Such isometric contraction of the biarticular fascicles is beneficial for multiple reasons. An isometric contraction delivers a higher force compared to a shortening contraction due to the force-velocity relationship of muscle force production (Hill, 1938). Moreover, the tensed biarticular MTC is able to transmit forces to neighbouring joints, while generating almost no mechanical work (product of force and contraction velocity). This is advantageous because such a close to isometric contraction (almost zero velocity) requires less metabolic cost compared to quicker contractions (Minetti and Alexander, 1997). Two monoarticular muscles substituting the biarticular muscle would have to undergo shortening/ lengthening contractions, respectively, to achieve a similar mechanical outcome at a higher cost (Elftman, 1939; Elftman, 1940; Wells, 1988).

If a biarticular muscle is co-contracted with an adjacent monoarticular muscle, the monoarticular muscle can act on a joint that it does not span. For example, a hip extension (e.g. by gluteus maximus (GLU)) can be transferred via a ligamentous action (Cleland, 1867) of the RF to a knee extension. By such coupling more powerful muscle groups (with greater muscle volume) can contribute to the net torque of an adjacent joint (Morrison, 1970; Gregoire et al., 1984; Prilutsky and Zatsiorsky, 1994). Researchers concluded that such joint coupling is an effective strategy to reduce distal mass of the legs and minimise the mechanical delay of the system in response to neural commands (Elftman, 1939; Morrison, 1970; Gregoire et al., 1984; Schenau, 1989; Prilutsky and Zatsiorsky, 1994).

During push-off in jumping, the major leg joints extend in a temporal sequence from the hip to the ankle enabling an energy flow from proximal to distal joints (Gregoire et al., 1984; Schenau, 1989). It was found that the biarticular joint coupling enabled a more efficient execution of the push-off (Schenau,
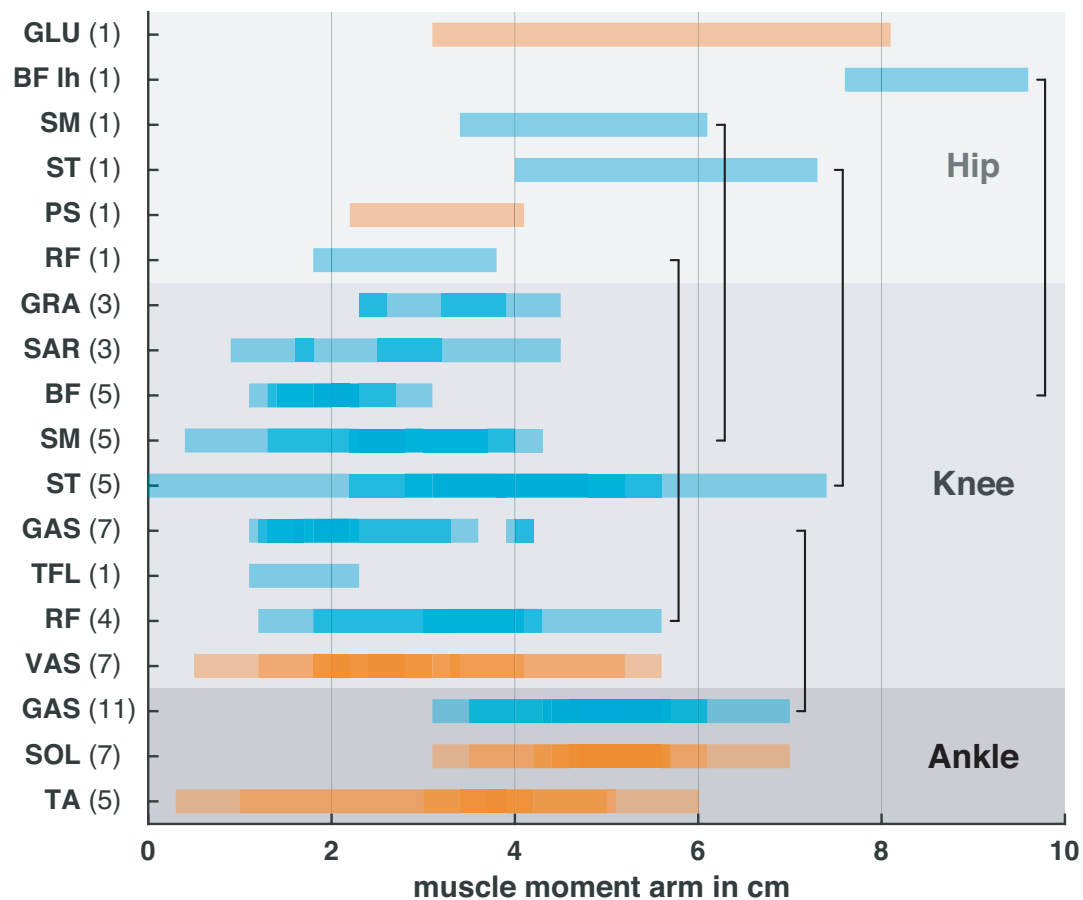
Figure 2.4: Range of sagittal muscle moment arms for human mono- (orange) and biarticular (cyan) leg muscles. Darker colour bars shows overlaying results from multiple studies. Note that working ranges and methods of assessment vary between studies. Numbers in parentheses denote the number of studies that are shown for that muscle. Black lines connect both joint moment arms of the same biarticular muscle. Data for visualisation stems from: Németh and Ohlsén (1985), Visser et al. (1990), and Arnold et al. (2000) (hip), Wretenberg et al. (1996), Buford et al. (1997), Spoor and Van Leeuwen (1992), Maganaris et al. (2006), Herzog and Read (1993), Visser et al. (1990), and Arnold et al. (2000) (knee) and Maganaris et al. (1998), Maganaris et al. (2000), Maganaris (2004a), Maganaris (2004b), Maganaris (2003), Fath et al. (2010), Karamanidis et al. (2011), Hashizume et al. (2012), Rugg et al. (1990), Klein et al. (1996), and Sheehan (2012) (ankle). Used muscle abbrevations are gluteus maximus (GLU), biceps femoris long head (BFlh), semimembranosus (SM), semitendinosus (ST), psoas major (PS), rectus femoris (RF), gracilis (GRA), sartorius (SAR), biceps femoris long head (BFlh), gastrocnemius (GAS), tensor fasciae latae (TFL), vastus (VAS), soleus (SOL) and tibialis anterior (TA). BF denotes knee moment arms of biceps femoris long head (BFlh) and biceps femoris short head (BFsh). For HAM muscle group and GAS, also see Cleather et al. (2015).

1989). Prilutsky and Zatsiorsky (1994) also showed that such energy flow can be effective *vice-versa* (from distal to proximal joints) to dissipate energy in the powerful proximal muscles, e.g. during landing or load response.

During quick knee extensions at the end of stance in hopping, the biarticular GAS transformed rotational kinetic energy of thigh and shank to a translational push-off motion (Ingen Schenau et al., 1987; Schenau, 1989). This not only improved the legs push-off performance but also prevented knee overextension (Ingen Schenau et al., 1987; Schenau, 1989). During hopping, such energy transfer (from knee to ankle) could contribute up to 25 percent to the peak power output at the ankle (Bobbert et al., 1986a; Bobbert et al., 1986b).

Balance

While the term balance usually refers to the task of maintaining stability of the whole body, here, we consider the postural control of the upper body to focus on the involvement of biarticular thigh muscles for generating stabilising hip torques (Horak and Nashner, 1986; Winter, 1995).

The ability of biarticular muscles to mainly contribute to rotary leg forces (Hof, 2001) can be especially useful for controlling angular momentum and thus postural balance. In this context, a study investigated the reaction of subjects who stood on one leg to maintain their posture while being exerted to external (anterior and posterior) forces on the unloaded leg (Hosoda et al., 2017). In response to the introduced joint torques, subjects dominantly (and consistently) recruited biarticular thigh muscles in both legs, while activity of electromyographic data (EMG) in monoarticular muscles changed inconsistently (Hosoda et al., 2017).

Further experiments studied the relation of biarticular muscle function and appropriate combinations of hip and knee joint torques (and associated GRF adaptations). Doorenbosch and Ingen Schenau (1995) reported high correlations (0.935 ± 0.027 SD) between the isometric muscular activity of RF and HAM muscles and the net joint torque of hip and knee. For a desired combination of hip flexion and knee extension torque, increasing RF and decreasing HAM activation was observed. Both antagonistic biarticular thigh muscles were recruited in a reciprocal way, depending on the torque requirements of the tasks (Fujiwara and Basmajian, 1975; Wells and Evans, 1987; Ingen Schenau et al., 1992; Doorenbosch and Ingen Schenau, 1995). Similar patterns for GRF manipulations were also observed in cycling (Gregor et al., 1991) or load lifting tasks (Toussaint et al., 1992; Prilutsky et al., 1998).

To also shed more light on reactive control strategies to unexpected and immediate perturbations, we recently applied impulse-like pitch perturbations to the upper-body during standing (Schumacher et al., 2019). In line with the studies above, biarticular thigh muscles had the strongest increase in muscular activity of all measured muscles (monoarticular hip muscles showed only moderate to no reactions). These results provide further evidence that RF and HAM actively control the required net hip to knee torques coordinating the posture of the upper body (Schumacher et al., 2019).

Swing

In bipedal locomotion, the swing leg performs a forward motion while being unloaded. The swing phase requires suitable swing leg length and orientation trajectories to achieve ground clearance (avoiding obstacles) and a proper foot placement for the next stance phase. Since only inertia is to be overcome, required joint torques are rather small compared to the stance subfunction (Piazza and Delp, 1996). However, an important requirement lies in the proper coordination and synchronisation of different joints.

RF and HAM experience stretch-shortening cycles facilitating energy store-and-release mechanisms during walking, running and sprinting (Nilsson et al., 1985; Simonsen et al., 1985). In late stance, RF length increased (also loading the tendon) due to hip extension. Together with a concentric contraction, this energy was released and helped to initialise the forward swing of the leg. For HAM, the stretch-shortening cycle appeared during the forward swing and subsequent retraction of the leg. While the elastic energy storage serves to improve the horizontal propulsion, previously mentioned template models revealed benefits of such leg retraction strategy (here by HAM) on running stability (Seyfarth et al., 2003; Poggensee et al., 2014). Both biarticular thigh muscles exchanged energy between stance and swing phases (Simonsen et al., 1985). However, only data from two subjects was assessed, revealing the demand for further experimental support of these mechanisms.

Prilutsky et al. (1998) investigated the role of biarticular thigh muscles during the swing phase of walking and running at different speeds. Phase-specific contributions of RF and HAM for specific hip and knee torque combinations were found. Similar to balancing the upper body, RF and HAM of the swing leg showed reciprocal EMG patterns in line with the net hip to knee torque requirement. Muscle activation of the RF was significantly higher during the early half of the swing phase, when hip flexion and knee extension torque occur simultaneously, compared to the second half. For HAM, the opposite was reported. These patterns occurred in both walking and running gaits. Authors also found high correlations for the EMG difference of RF and HAM with the net hip to knee torque (between 0.923 and 0.959 for different speeds). However, since only four subjects participated in the study, and a total of only three swing phases each were used for the analysis, more quantitative data should confirm these results.

Biarticular sensors

In addition to generating appropriate joint torques throughout the segmental chain (Prilutsky and Zatsiorsky, 1994; Jacobs and Macpherson, 1996; Prilutsky et al., 1998), biarticular muscles might also play an important role for sensing limb posture in global coordinates, e.g. limb orientation and length (Bosco et al., 1996; Verschueren et al., 1998; Sharbafi et al., 2016; Poppele et al., 2002; Ivanenko et al., 2007). Potential implementations could involve force feedback, e.g. by the respective Golgi tendon organs (Prochazka et al., 1997; Prilutsky et al., 1998) or by cutaneous receptors in the foot sole, sensing the leg force (Duysens et al., 1996; Prilutsky et al., 1998; Sharbafi and Seyfarth, 2015; Sarmadi et al., 2019). In this context, Lacquaniti and Soechting (1986a), Lacquaniti and Soechting (1986b), and Soechting and Lacquaniti (1988) found that, following torque perturbations at the arm, the effective net torque of the elbow and shoulder was a better predictor for the observed muscle responses than single joint angular velocities (and individual stretch reflexes). Similar results were also found in the leg (Fujiwara and Basmajian, 1975; Wells and Evans, 1987; Doorenbosch and Ingen Schenau, 1995). As the length of HAM and RF remains almost constant when the leg length shortens or extends (Cleland, 1867; Fenn, 1938), these muscles predominantly undergo a change in length when e.g. the trunk orientation changes with respect to the leg orientation. Thus, length feedback pathways of biarticular muscles could sense the orientation of the limb axis directly. By this, biarticular muscles provide a simple solution of postural proprioception, complementing vestibular sensation and other sources in postural equilibrium tasks.

The sensing of leg length and orientation (Bosco et al., 1996; Poppele et al., 2002; Ivanenko et al., 2007) by biarticular muscles could simplify control and coordination of joints (Lakatos et al., 2014; Sharbafi et al., 2016; Lakatos et al., 2016). In this context, a parallel and independent control of axial and perpendicular leg forces by mono- and biarticular have been suggested from studying the perturbation response of standing cats (Lacquaniti and Maioli, 1994; Jacobs and Macpherson, 1996). However, more research is

required to identify specific biarticular reflex pathways and the corresponding involvement in generating appropriate movements, also in the context of muscle synergies (Torres-Oviedo and Ting, 2010; Chvatal et al., 2011).

Applications in robotic devices

In this section, we review the application of biarticular elements (e.g. actuators or springs) in the design of legged robotic systems. For this, we will present how compliant biarticular structures were used to improve the controllability of these systems, before we review different hardware designs and control concepts in the light of the locomotor subfunctions.

Control embodiment via compliance and biarticular mechanism

The morphology and biomechanics of humans and animals have great impact on locomotion control (Pfeifer et al., 2007). This was formulated in the *control embodiment*[1] concept, in which the mechanical structure is considered to be an important contributor for generating appropriate movements and solving control challenges (Pfeifer et al., 2007).

In the context of locomotion, robotic systems utilised biarticular structures with compliant properties of muscles or tendons (Endo et al., 2006; Iida et al., 2008; Hosoda et al., 2010; Radkhah et al., 2011; Ogawa et al., 2011; Nakanishi et al., 2013; Lakatos et al., 2016). Such designs are inspired by biological bodies (Ferris et al., 1998; Seyfarth et al., 2006). Both of these qualities, biarticular arrangement and inherent compliant properties, can be considered tools for control embodiment. They can improve the controllability of the robot, enable energy management and improve robustness against the uncertainty of the environment, e.g. changing terrains (Nakata et al., 2012; Liu et al., 2015). Additionally, passive mechanical structures instantaneously interact with the environment and can thus respond to external perturbation without a control delay. Examples of these benefits can be found in bipedal and quadruped robots, where biarticular springs helped to generate stable gaits even when a simple open loop control (without sensory feedback) was used (Iida et al., 2008; Iida et al., 2009; Ogawa et al., 2011; Spröwitz et al., 2013).

As discussed previously, the length of the biarticular spring – given appropriate moment arm ratios – corresponds to rotational changes of the whole leg with respect to the adjacent segment. For instance, the length of a biarticular thigh spring (similar to HAM or RF) can be proportional to the angle between the leg and the upper body (Lakatos et al., 2014; Sarmadi et al., 2019). By this, a biarticular spring could be used to directly react to perturbations on the upper-body posture. Results of Schumacher et al. (2019) support the beneficial contribution of biarticular structures to recover from upper-body perturbations in human-like leg designs. In another example of a simple swing leg model, the (rest) length of biarticular thigh springs was found to linearly correlate with the target swing leg angle (Sharbafi et al., 2017b). However, in all these applications, biarticular moment arm ratios are an important factor determining the functional contribution of the biarticular actuator or spring, as shown in the *CARL* robot (Nejadfard et al., 2018b). Proper design of moment arm ratios and spring properties (e.g. spring stiffness or rest length) can thus be used as design parameters to determine the desired limb behaviour and incorporate a bio-inspired control

---

[1]Instead of *intelligence embodiment*, introduced in Pfeifer and Bongard (2007), we use the term *control embodiment* focusing on locomotion control.

embodiment strategy in robotic systems (Blickhan et al., 2006; Lakatos et al., 2014; Lakatos et al., 2016; Sharbafi et al., 2016; Nejadfard et al., 2018b).

Biarticular structures in legged robots

Several robotic systems investigated the effect of biarticular actuation (Figure 2.5) to counteract gravity (stance subfunction) in dynamic motions by evaluating the motion performance, e.g. the hopping height. In the study of Hosoda et al. (2010), biarticular pneumatic artificial muscle (PAM) were used to transmit joint torques along multiple segments and coordinate multiple joints in vertical jumping. Further, a hopping robot (Babic, 2009; Babic et al., 2009) was used to test the results of a computational study that predicted improvements in hopping performance due to GAS muscle energy transfer from knee to ankle (Bobbert et al., 1986a). The hopping robot confirmed that hopping height increased due to an additional energy-storage and release in the added GAS as well as improved energy transfer from proximal to distal joints. With an appropriate timing and magnitude of GAS actuation, hopping height increased by 18 % (Babic et al., 2009). For *CARL*, energy transfer of biarticular actuators improved the overall jumping efficiency of the robotic leg (Nejadfard et al., 2018a). Similar effects were also reported in the *BioBiped* robot and free falling experiments (Scholz et al., 2012; Sharbafi et al., 2016). In another study, a three segmented mono-pedal hopping robot with a point foot used electromagnetic linear actuators to mimic compliant mono- and biarticular muscles (Nakata et al., 2012). In this system, biarticular thigh muscles tuned the *stiffness ellipse*[2] at the foot during stance and consequently, controlled the motion direction of the robot in the flight phase.

The mechanism of a proximal-to-distal energy transfer with biarticular muscles was further tested in a human-sized robotic leg that used all major monoarticular (except the knee flexor) and biarticular RF and GAS actuators to perform squatting movements (Klein et al., 2008). It was found that, if force generation of GAS precedes SOL contribution, the total ankle power increased, compared to simultaneous force generation.

Biarticular actuation was used to improve the postural balance function in robots, e.g. by PAM in the *Pneumat-BS* (Ogawa et al., 2011) and the *Pneumat-BB* (Narioka et al., 2013) or by serial elastic actuator (SEA) in the *BioBiped* (Sharbafi et al., 2016). In standing and squatting experiments of the *BioBiped3* robot, the cross-talk between axial and perpendicular terms of GRF was reduced when hip-to-knee moment arm ratios approached values of 2:1 (Sharbafi et al., 2016). By this, VAS and biarticular thigh muscles could respectively control GRF magnitude and direction with minimum interference. This agrees well with results from simulations and experiments (see previous sections for details) and further suggests that the two subfunctions of stance and balance could be assigned to different muscle groups.

Inspired by simulation results (Sharbafi et al., 2017b), a simulation model of the *BioBiped* robot used biarticular thigh actuators to generate an appropriate leg swing motion for forward hopping (Sharbafi et al., 2014; Sharbafi et al., 2016). For this, a pre-tension of the elastic element in the SEA (during late stance) resulted in a passive response of the spring realising the leg swing motion (Sharbafi et al., 2016). Further, simulation results of a running robot (Lakatos et al., 2014) and successful implementation of a simple controller exploiting biarticular SEA in a humanoid robot achieving dynamic walking (Lakatos et al., 2016) indicate that for an appropriate design of biarticular actuators, balance and swing subfunctions could be decoupled from the *stance* control.

---

[2]The stiffness matrix is calculated at the end effector of a manipulator. By calculating the eigenvalues and eigenvectors of the stiffness matrix, the stiffness ellipse illustrates the compliance in different directions at the end effector. In biped robots, calculating the stiffness ellipse during stance can determine the movement direction.
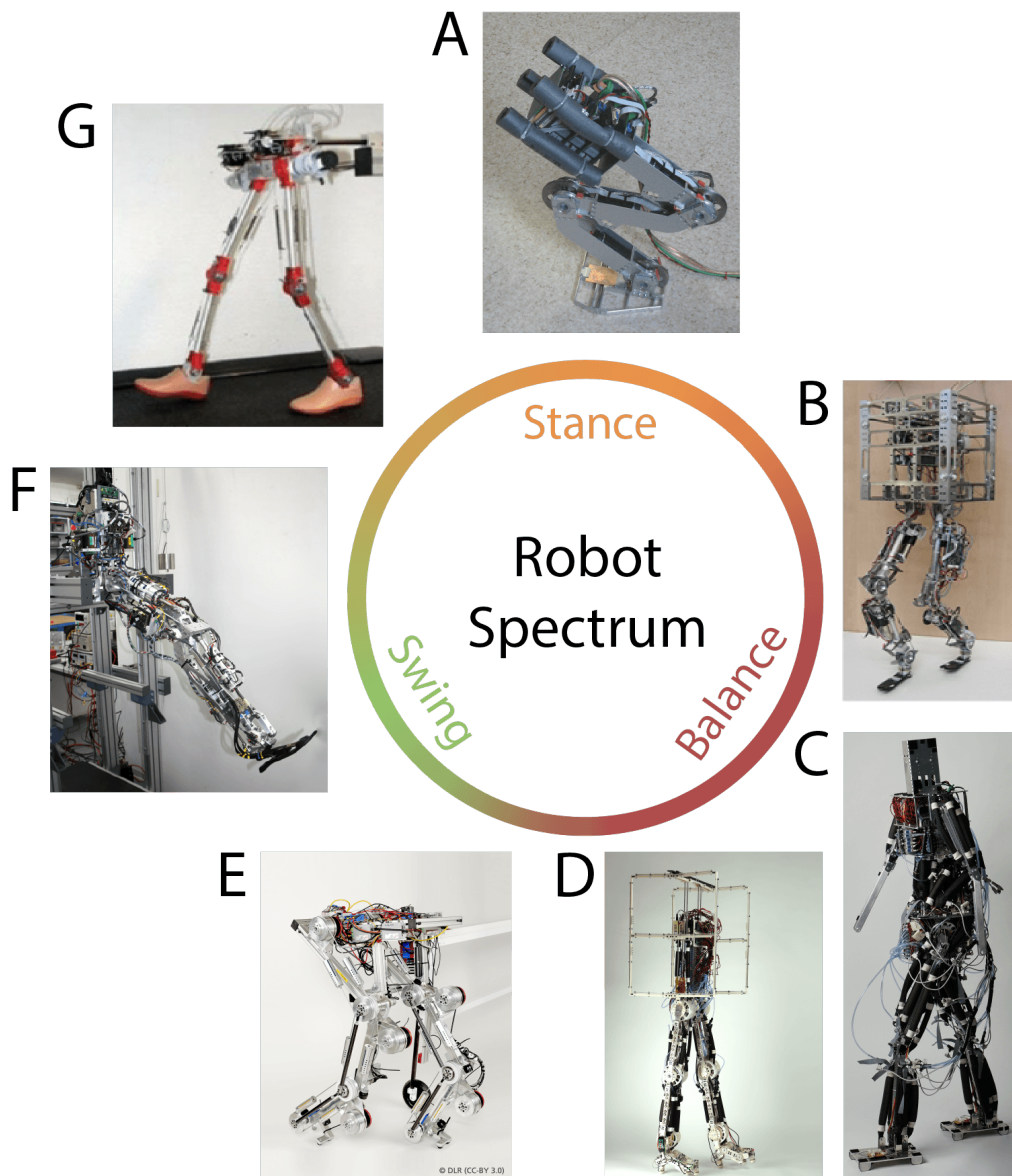
Figure 2.5: Selection of simple and complex legged robots utilising biarticular actuation in the spectrum of locomotor subfunctions. A biarticular legged robot (Babic, 2009; Babic et al., 2009), **B** Bio-Biped (Sharbafi et al., 2016), **C** Pneumat-BS (Ogawa et al., 2011), **D** Pneumat-BB (Narioka et al., 2013), **E** C-Runner humanoid running machine (Loeffl et al., 2016; Lakatos et al., 2016) **F** CARL robot (Schütz et al., 2017) and **G** Jena Walker II (Seyfarth et al., 2009). Note that some of the shown robots also cover multiple subfunctions, but were arranged according to the main functional contribution of biarticular actuation. Photos in the courtesy of: Jan Babic (A), Koh Hosoda (C & D), Patrick Vonwirth (F) as well as under CC BY 3.0 from DLR (E) and Sharbafi et al. 2016 (B & G).

By such muscle-specific task allocation, control approaches could be simplified to setting properties of compliant elements (e.g. spring stiffness or rest length) to a specific value for each gait condition. An

example of this can be found in the *Jena Walker* robot (Iida et al., 2008; Iida et al., 2009). Combining oscillatory feed-forward actuation at the hip for propulsion (push-off and leg swing), a monoarticular spring (like tibialis anterior (TA)) and multiple biarticular springs (similar to RF, HAM and GAS) generated stable walking and running patterns. By this, stance and swing subfunctions were nicely coordinated using passive biarticular springs while the TA spring was mainly used for foot clearance (Iida et al., 2008; Iida et al., 2009). To further coordinate or synchronise different subfunctions, e.g. when facing perturbations, sensory feedback pathways can be used. In that context, leg force feedback could coordinate subfunctions of stance (VAS) and balance (RF and HAM) and improve the robustness against perturbations in simulation (Sarmadi et al., 2019).

Biarticular structures in assistive devices

Recently[3], biarticular structures were used in the design of assistive devices for impaired (Eilenberg, 2017; Eilenberg et al., 2018) and non-impaired people (Quinlivan et al., 2017; Schmidt et al., 2017).

In walking experiments of unilateral amputees, Eilenberg et al. (2018) emulated the healthy human GAS behaviour by combining a powered ankle-foot prosthesis and a robotic knee orthosis. In this study, neuromuscular models of matched non-amputees were used to model the lower limb biarticular muscle. It was hypothesised that by biarticular coupling with an artificial GAS, the active push-off of the prosthesis could be used to reduce the work in the affected-side hip and knee during leg swing initiation. Compared to a monoarticular operation (without knee orthosis contribution), reductions in biological knee flexion moment impulse of the affected-side as well as reduced positive work of the hip during late-stance knee flexion were found. This resulted in decreased metabolic power during walking in some subjects (4 out of 6), although non-significant over all subjects (Eilenberg et al., 2018).

For assisting non-impaired people, the application of biarticular structures in *exosuits* became more popular, due to the soft and flexible design of muscle-like, tension-based actuation principles (Quinlivan et al., 2017; Schmidt et al., 2017). Since actuators can also span multiple joints in these systems, simulation models were used to identify an optimal actuator arrangement in the *exosuit*. Sharbafi et al. (2018) extended the neuromuscular walking model of Geyer and Herr (2010) by a virtual HAM-like actuator with FMCH-based control. While parameters of the original simulation model remained unchanged, simulation results predicted reductions of GLU and HAM muscle activity (due to changed feedback contributions) and 12 % metabolic costs (Sharbafi et al., 2018). In the simulation study of Van den Bogert (2003), *exotendons* – long elastic strings that span different leg joints – were added to an inverse model of walking. By optimising for the most efficient arrangements of *exotendons* in the leg model, it was found that required biological joint torques and powers for generating the same walking patterns can be reduced by up to 71 % and 74 %, respectively. However, in real experiments, when such a passive exoskeleton was applied in conjunction with a human subject, energy expenditure of the subjects increased compared to normal walking without an exoskeleton (Van Dijk et al., 2011).

In Malcolm et al. (2018), a biarticular knee-ankle-foot exoskeleton with a serial arrangement of a PAM and a passive spring reduced the metabolic cost of walking more than a weight-matched monoarticular exoskeleton (to a similar level when not wearing the exoskeleton). Using an exoskeleton, metabolic reductions of up to 23 % compared to walking with the unpowered system were reported in Quinlivan et al. (2017). Here, a multiarticular actuator simultaneously assisted hip flexion and ankle plantarflexion that

---

[3]Here, we mainly consider relevant studies since 2017. Please refer to earlier works in the review of Junius et al. (2017).

reduced the biological ankle and hip torque during push-off (Quinlivan et al., 2017). Next to the direct energy support, it is likely that the multiarticular nature allowed for an advantageous internal energy transfer between joints (Quinlivan et al., 2017). The *Myosuit* aimed at assisting anti-gravitational muscles at the hip and knee by a biarticular arrangement of actuators for sit-to-stand movements (Schmidt et al., 2017). This system supported up to 26 % and 35 % of the biological hip and knee torques, respectively (Schmidt et al., 2017). This shows that biarticular arrangements in an exoskeleton effectively supported propulsion (Quinlivan et al., 2017) as well as gravity compensation (Schmidt et al., 2017). Such biarticular structures might, however, be used in different leg arrangements (e.g. hip flexion and ankle plantarflexion in Quinlivan et al. 2017, hip and knee extension in Schmidt et al. 2017, hip flexion and knee extension in Jin et al. 2016) and different control strategies targeting different mechanisms of assistance (Grimmer et al., 2019a).

In rigid exoskeleton designs, biarticular actuation improved the efficiency of the exoskeleton. In the *WalkON* suit (Choi et al., 2017), the generated end-effector force per motor torque increased in some situations (Choi et al., 2016). In another study, Zhao et al. (2017) demonstrated that support of mono- and biarticular muscles could reduce human metabolic cost (by 10 %). This was achieved by emulating muscle-like actuation at the hip and knee joint (mimicking monoarticular hip and biarticular thigh muscles) using the FMCH control method in the *LOPES II* exoskeleton (Meuleman et al., 2015). However, these results should be used with caution since only two subjects participated in this pilot study (Zhao et al., 2017). Despite these studies, biarticular actuation principles were less common in rigid exoskeleton designs.

Some of the recent developments indicate potential benefits of incorporating biarticular designs in prosthetic and exoskeleton designs. However, for real-world applications and the range of subject populations, technological difficulties remain to be solved, such as human-machine interfaces, durability of hardware designs and flexible control concepts (Grimmer et al., 2019b). Biarticular actuation might be one useful approach to tackle some of these challenges by synchronous joint coordination and improved controllability.

Discussion

In this paper, we integrate model predictions, human experiments and robotic applications into a structured, locomotor subfunction-specific picture of biarticular muscle function. By this, we extend the conventional single joint-focused approach and advocate a generalised and more function-specific multi-joint perspective.

Concepts

The existence of biomechanical template models (Full and Koditschek, 1999) as observed in different animals and during different gaits and speeds (Blickhan and Full, 1993; Gan et al., 2018a; Gan et al., 2018b) indicates a basic structure of locomotion. However, these mechanical concepts need to be reflected in the segmented human leg. Templates work with generalised coordinates (e.g. leg length and orientation) and in a low-dimensional parameter space. These generalised coordinates can be assessed by a sensible arrangement of mono- and biarticlar muscles. This might support the control of the complex human leg (including all its degrees of freedom (DoF) and muscles) in a global, simplified manner (Bosco and Poppele, 2001; Ivanenko et al., 2007; Auyang et al., 2009). While such behaviour might also be generated

by the neural control system in an arbitrary leg architecture, the specific arrangement of biarticular and monoarticular muscles provides a structural solution that can reduce the control effort of the motor control system (Soest and Bobbert, 1993; Pfeifer et al., 2007; Sharbafi et al., 2016) and make leg function more robust (Seyfarth et al., 2001). For a well-designed system, control can be sloppy and allow for a wider range of movements. For example, biarticular springs enlarged the stability region and robustness against spring stiffness adjustments during passive walking as predicted in the model of Dean and Kuo (2008).

Evidence

In the presented studies, biarticular muscles were found to support locomotion by a variety of features, depending on the functional requirements of the specific locomotor subfunctions stance, balance, and swing.

In *stance*, muscular joint-coupling was found to synchronise neighbouring joints and distribute the energy flow along segments that enables efficient (see also review by Junius et al., 2017) and robust movement execution (Seyfarth et al., 2001). Further, almost isometric biarticular muscle operation was found, e.g. during leg extension, which resulted in more efficient torque generation than that of two monoarticular muscles. Additionally, biarticular muscles contribute to fine-tuning and proper coordination of *balance* and *swing*. For instance, multiple studies suggested a net torque based control scheme (net hip minus knee torque, extension torques defined positive) of biarticular thigh muscles (Doorenbosch and Ingen Schenau, 1995; Prilutsky et al., 1998) that allowed for the manipulation of GRF direction and control of angular momentum (Dean and Kuo, 2008; Hosoda et al., 2010; Sharbafi et al., 2017b; Sharbafi and Seyfarth, 2017b).

The multitude of biarticular features points to the idea that mono- and biarticular muscles fulfil different, subfunction-specific tasks. During *stance,* monoarticular muscles mainly power the motion. Simultaneously, by mechanically coupling adjacent joints, biarticular muscles coordinate joint movements, transfer energy, and secure the zig-zag-configuration of the leg against joint overextension. In *balance* and *swing*, the contribution of mono- and biarticular muscles changes. Here, biarticular muscles power dominantly rotational motions and monoarticular muscles fine-tune the required torques since torque generation from biarticular muscles is defined by their moment arms. In some cases, biarticular muscles also synchronise or coordinate individual locomotor subfunctions. For instance, during late stance of human walking, RF and GAS transition between *stance* and *swing* (Nilsson et al., 1985; Simonsen et al., 1985; Ingen Schenau et al., 1987; Schenau, 1989; Prilutsky et al., 1998; Lipfert et al., 2014). Moreover, GAS switches in this contribution from *balance* to *stance* when the heel lifts off the ground. When the whole foot is in contact with the ground, GAS contributes to the *balance* subfunction (by rotary forces, Hof 2001). However, in forefoot stance, GAS supports *stance* because it can only contribute to axial forces.

The specific function of biarticular muscles is strongly coupled to their muscle moment arms (Winter, 2009; Cleather et al., 2015). The overview of relevant sagittal muscle moment arms (Figure 2.4) revealed that GAS follows the suggested moment arm ratio of 2:1 (Winter, 2009). For biarticular thigh muscles, moment arms were greater at the hip than at the knee (Cleather et al., 2015). However, only a small number of studies investigated muscle moment arms at the hip, and study results vary due to different methods and techniques. It is therefore hard to draw clear conclusions; more research is required. For several other properties of human leg muscles, we could not find evidence for physiological differences between mono- and biarticular muscles. Only, the MTC length of biarticular muscles was longer compared to monoarticular muscles. This was expected as biarticular muscles span more than one joint.

Generally, experimental studies supported predictions from conceptual template models. Even though some of these results should be used with caution due to a small number of subjects, reported evidence was very consistent across different study designs (methods) and motions (tasks). While evidence involved unperturbed tasks like standing, walking, running, cycling or load lifting, further research is needed to identify e.g. control strategies of biarticular muscles (predictive and reactive control). Here, studies on non-continuous motion tasks like gait transitions or external perturbations (like in Schumacher et al. 2019) are of particular value.

Applications

Several legged robots utilise biarticular structures to generate performant, robust or efficient motions. The main motivation for this is to outsource the control effort to mechanical components (control embodiment, Pfeifer et al. 2007). This is accomplished by (1) smart morphological leg arrangement and/or by (2) facilitating intrinsic (compliant) properties that allow a certain flexibility in joint behaviour but also inherently react to external perturbations. Depending on the application, passive structures, e.g. springs or dampers, or active elements, e.g. SEA or PAM, realise biarticularity. Often, engineers use the structural compliance or muscle moment arms as design parameters to generate a desired leg behaviour (Blickhan et al., 2006; Lakatos et al., 2014; Lakatos et al., 2016; Sharbafi et al., 2016; Bidgoly et al., 2017; Nejadfard et al., 2018b). In assistive devices, like prostheses or exoskeletons, walking economy of the wearer or efficiency of the device could be improved (Quinlivan et al., 2017; Zhao et al., 2017; Eilenberg et al., 2018; Malcolm et al., 2018).

Currently, most robotic designs including industrial applications utilise a single actuator per DoF, instead of redundant actuation systems, in which e.g. multiple muscle-like actuators can act on a single joint. This prevents most robotic systems to take advantage of the features of biarticular actuation. However, additional actuators might also create further design challenges, like motor redundancy or undesired coupling behaviour due to fixed geometrical constraints. Both of these issues can be resolved by smart design which may be inspired from biology. In this context, abstraction and categorisation as applied in this review may be useful approaches. By this, engineers can learn from template models and animals to improve artificial system designs without suffering from complexity and unwanted coupling. Some of the potentially beneficial concepts of biarticularity to be further exploited in robotic designs, are as follows:

- energy transport within a segment chain,

- improved distribution of leg inertia,

- inter-joint coordination and synchronisation,

- operation of biarticular actuator with reduced power demands,

- resolving kinematic singularities.

Many of these advantages have been introduced several decades ago (Cleland, 1867; Lombard, 1903; Fenn, 1938; Elftman, 1939; Elftman, 1966; Morrison, 1970; Fujiwara and Basmajian, 1975; Gregoire et al., 1984; Wells, 1988). Potential implementations may enable simplified swing leg control for foot placement (as predicted in Sharbafi et al. 2014; Sharbafi et al. 2016) or reactive balance control (Schumacher et al., 2019). Still, some of the features of biarticular actuators are still unexploited in robotics and await their proof-of-concept in hardware systems.

Conclusion

We structured this review of biarticular muscle function in two dimensions: locomotor sub-functions (*stance, balance* and *swing*) and methodological approaches (theoretical concepts, experimental evidence and robotic applications). Templates revealed the general organisation of locomotion in different species. Based on this understanding, we interpreted tangible experimental studies on biarticular muscles. Finally, robotic designs transferred these mechanisms into the physical world and validated these insights and concepts. By this approach, we integrated and combined knowledge from biomechanics, biology and robotics in a unified locomotor sub-function specific perspective. For instance, the global leg function can be described by a simple leg spring (Blickhan, 1989; McMahon and Cheng, 1990). By coordinating individual joints in the leg, biarticular muscles contribute to the generation of such global leg behaviour in human experiments (Gregoire et al., 1984; Schenau, 1989) and robotic systems (Babic et al., 2009; Hosoda et al., 2010). This example shows the benefit of incorporating all three domains of the research trilogy (Kalveram and Seyfarth, 2009): (1) conceptual modelling, (2) human experiments and (3) robotic applications. Combining the expertises of biology, biomechanics and robotics seems promising to generate a deeper understanding of the structures and patterns involved in generating locomotion.

Acknowledgments

Author Contributions

CS, CR and MS reviewed studies. All authors contributed to the conception of this study, drafted and critically revised the manuscript, gave final approval for publication and agree to be held accountable for the work performed therein.

References

E. Andrada, C. Rode, and R. Blickhan (2013). "Grounded running in quails: simulations indicate benefits of observed fixed aperture angle between legs before touch-down". In: *Journal of Theoretical Biology* 335, pp. 97–107.

A. S. Arnold et al. (2000). "Accuracy of muscle moment arms estimated from MRI-based musculoskeletal models of the lower extremity". In: *Computer Aided Surgery* 5.2, pp. 108–119.

A. G. Auyang, J. T. Yen, and Y.-H. Chang (2009). "Neuromechanical stabilization of leg length and orientation through interjoint compensation during human hopping". In: *Experimental brain research* 192.2, pp. 253–264.

J. Babic (2009). "Biarticular legged robot: Design and experiments". In: *2008 IEEE International Conference on Robotics and Biomimetics*. IEEE, pp. 155–159.

J. Babic et al. (2009). "A biarticulated robotic leg for jumping movements: theory and experiments". In: *Journal of mechanisms and robotics* 1.1, p. 011013.

H. J. Bidgoly et al. (2017). "Benefiting From Kinematic Redundancy Alongside Mono-and Biarticular Parallel Compliances for Energy Efficiency in Cyclic Tasks". In: *IEEE Transactions on Robotics* 33.5, pp. 1088–1102.

A. A. Biewener (2016). "Locomotion as an emergent property of muscle contractile dynamics". In: *Journal of Experimental Biology* 219.2, pp. 285–294.

A. A. Biewener and T. J. Roberts (2000). "Muscle and tendon contributions to force, work, and elastic energy savings: a comparative perspective". In: *Exerc Sport Sci Rev* 28.3, pp. 99–107.

R. Blickhan (1989). "The spring-mass model for running and hopping". In: *Journal of Biomechanics* 22, pp. 1217–1227.

R. Blickhan and R. Full (1993). "Similarity in multilegged locomotion: bouncing like a monopode". In: *Journal of Comparative Physiology A* 173.5, pp. 509–517.

R. Blickhan et al. (2006). "Intelligence by mechanics". In: *Philosophical Transactions of the Royal Society A: Mathematical, Physical and Engineering Sciences* 365.1850, pp. 199–220.

M. F. Bobbert, P. A. Huijing, and G. J. van Ingen Schenau (1986a). "A model of the human triceps surae muscle-tendon complex applied to jumping". In: *Journal of biomechanics* 19.11, pp. 887–898.

M. F. Bobbert, P. A. Huijing, and G. J. van Ingen Schenau (1986b). "An estimation of power output and work done by the human triceps surae musle-tendon complex in jumping". In: *Journal of biomechanics* 19.11, pp. 899–906.

G. Bosco and R. Poppele (2001). "Proprioception from a spinocerebellar perspective". In: *Physiological reviews* 81.2, pp. 539–568.

G. Bosco, A. Rankin, and R. Poppele (1996). "Representation of passive hindlimb postures in cat spinocerebellar activity". In: *Journal of Neurophysiology* 76.2, pp. 715–726.

W. L. Buford et al. (1997). "Muscle balance at the knee-moment arms for the normal knee and the ACL-minus knee". In: *IEEE Transactions on Rehabilitation Engineering* 5.4, pp. 367–379.

J. A. Carr, D. J. Ellerby, and R. L. Marsh (2011a). "Function of a large biarticular hip and knee extensor during walking and running in guinea fowl (Numida meleagris)". In: *Journal of Experimental Biology* 214.20, pp. 3405–3413.

J. A. Carr et al. (2011b). "Mechanisms producing coordinated function across the breadth of a large biarticular thigh muscle". In: *Journal of Experimental Biology* 214.20, pp. 3396–3404.

A. M. Carroll and A. A. Biewener (2009). "Mono-versus biarticular muscle function in relation to speed and gait changes: in vivo analysis of the goat triceps brachii". In: *Journal of Experimental Biology* 212.20, pp. 3349–3360.

G. A. Cavagna, H. Thys, and A. Zamboni (1976). "The sources of external work in level walking and running." In: *The Journal of physiology* 262.3, pp. 639–657.

H. Choi, S. Oh, and K. Kong (2016). "Control of a robotic manipulator in the polar coordinate system using a biarticular actuation mechanism". In: *International Journal of Control, Automation and Systems* 14.4, pp. 1095–1105.

J. Choi et al. (2017). "Walkon suit: A medalist in the powered exoskeleton race of cybathlon 2016". In: *IEEE Robotics & Automation Magazine* 24.4, pp. 75–86.

S. A. Chvatal et al. (2011). "Common muscle synergies for control of center of mass and force in non-stepping and stepping postural behaviors". In: *American Journal of Physiology-Heart and Circulatory Physiology*.

D. J. Cleather (2018). "An important role of the biarticular hamstrings is to exert internal/external rotation moments on the tibia during vertical jumping". In: *Journal of theoretical biology* 455, pp. 101–108.

D. J. Cleather, D. F. Southgate, and A. M. Bull (2015). "The role of the biarticular hamstrings and gastrocnemius muscles in closed chain lower limb extension". In: *Journal of theoretical biology* 365, pp. 217–225.

J. Cleland (1867). "On the actions of muscles passing over more than one joint". In: *Journal of anatomy and physiology* 1.1, p. 85.

J. C. Dean and A. D. Kuo (2008). "Elastic coupling of limb joints enables faster bipedal walking". In: *Journal of the Royal Society Interface* 6.35, pp. 561–573.

J. M. Donelan, R. Kram, and A. D. Kuo (2002). "Simultaneous positive and negative external mechanical work in human walking". In: *Journal of biomechanics* 35.1, pp. 117–124.

C. A. Doorenbosch and G. J. van Ingen Schenau (1995). "The role of mono-and bi-articular muscles during contact control leg tasks in man". In: *Human Movement Science* 14.3, pp. 279–300.

E. L. Du Brul (1962). "The general phenomenon of bipedalism". In: *American Zoologist*, pp. 205–208.

J. Duysens et al. (1996). "Backward and forward walking use different patterns of phase-dependent modulation of cutaneous reflexes in humans." In: *Journal of neurophysiology* 76.1, p. 301.

M. F. Eilenberg, J.-Y. Kuan, and H. Herr (2018). "Development and Evaluation of a Powered Artificial Gastrocnemius for Transtibial Amputee Gait". In: *Journal of Robotics* 2018.

M. F. Eilenberg (2017). "Development and evaluation of biarticular transtibial prostheses for level-ground amputee walking". PhD thesis. Massachusetts Institute of Technology.

H. Elftman (1939). "The function of muscles in locomotion". In: *American Journal of Physiology-Legacy Content* 125.2, pp. 357–366.

H. Elftman (1940). "The work done by muscles in running". In: *American Journal of Physiology-Legacy Content* 129.3, pp. 672–684.

H. Elftman (1966). "Biomechanics of muscle: with particular application to studies of gait". In: *JBJS* 48.2, pp. 363–377.

K. Endo, D. Paluska, and H. Herr (2006). "A quasi-passive model of human leg function in level-ground walking". In: *Intelligent Robots and Systems, 2006 IEEE/RSJ International Conference on*. IEEE, pp. 4935–4939.

D. J. Farris and G. S. Sawicki (2012). "Human medial gastrocnemius force–velocity behavior shifts with locomotion speed and gait". In: *Proceedings of the National Academy of Sciences* 109.3, pp. 977–982.

F. Fath et al. (2010). "Direct comparison of in vivo Achilles tendon moment arms obtained from ultrasound and MR scans". In: *Journal of Applied Physiology* 109.6, pp. 1644–1652.

W. Fenn (1938). "The mechanics of muscular contraction in man". In: *Journal of Applied Physics* 9.3, pp. 165–177.

D. P. Ferris, M. Louie, and C. T. Farley (1998). "Running in the real world: adjusting leg stiffness for different surfaces". In: *Proceedings of the Royal Society of London. Series B: Biological Sciences* 265.1400, pp. 989–994.

M. Fujiwara and J. V. Basmajian (1975). "Electromyographic study of two-joint muscles." In: *American journal of physical medicine* 54.5, pp. 234–242.

T. Fukunaga et al. (2001). "In vivo behaviour of human muscle tendon during walking". In: *Proceedings of the Royal Society of London. Series B: Biological Sciences* 268.1464, pp. 229–233.

R. J. Full and D. E. Koditschek (1999). "Templates and anchors: neuromechanical hypotheses of legged locomotion on land". In: *Journal of Experimental Biology* 202.23, pp. 3325–3332.

Z. Gan, Z. Jiao, and C. D. Remy (2018a). "On the dynamic similarity between bipeds and quadrupeds: a case study on bounding". In: *IEEE Robotics and Automation Letters* 3.4, pp. 3614–3621.

Z. Gan et al. (2018b). "All common bipedal gaits emerge from a single passive model". In: *Journal of The Royal Society Interface* 15.146, p. 20180455.

M. Garcia et al. (1998). "The simplest walking model: stability, complexity, and scaling". In: *Journal of biomechanical engineering* 120.2, pp. 281–288.

H. Geyer, A. Seyfarth, and R. Blickhan (2006). "Compliant leg behaviour explains basic dynamics of walking and running". In: *Proceedings of the Royal Society of London B: Biological Sciences* 273, pp. 2861–2867.

H. Geyer and H. Herr (2010). "A muscle-reflex model that encodes principles of legged mechanics produces human walking dynamics and muscle activities". In: *IEEE Transactions on neural systems and rehabilitation engineering* 18.3, pp. 263–273.

M. Gomes and A. Ruina (2011). "Walking model with no energy cost". In: *Physical Review E* 83.3, p. 032901.

L. Gregoire et al. (1984). "Role of mono-and biarticular muscles in explosive movements". In: *International journal of sports medicine* 5.06, pp. 301–305.

R. J. Gregor, J. P. Broker, and M. M. Ryan (1991). "The Biomechanics of Cycling". In: *Exercise and sport sciences reviews* 19.1, pp. 127–170.

M. Grimmer, M. Eslamy, and A. Seyfarth (2014). "Energetic and peak power advantages of series elastic actuators in an actuated prosthetic leg for walking and running". In: *Actuators*. Vol. 3. Multidisciplinary Digital Publishing Institute, pp. 1–19.

M. Grimmer and A. Seyfarth (2014). "Mimicking human-like leg function in prosthetic limbs". In: *Neuro-Robotics*. Springer, pp. 105–155.

M. Grimmer et al. (2019a). "Comparison of the human-exosuit interaction using ankle moment and ankle positive power inspired walking assistance". In: *Journal of biomechanics* 83, pp. 76–84.

M. Grimmer et al. (2019b). "Mobility related physical and functional losses due to aging and disease-a motivation for lower limb exoskeletons". In: *Journal of neuroengineering and rehabilitation* 16.1, p. 2.

S. R. Hamner, A. Seth, and S. L. Delp (2010). "Muscle contributions to propulsion and support during running". In: *Journal of biomechanics* 43.14, pp. 2709–2716.

S. Hashizume et al. (2012). "In vivo determination of the Achilles tendon moment arm in three-dimensions". In: *Journal of biomechanics* 45.2, pp. 409–413.

T. Heidlauf et al. (2017). "A continuum-mechanical skeletal muscle model including actin-titin interaction predicts stable contractions on the descending limb of the force-length relation". In: *PLoS computational biology* 13.10, e1005773.

W. Herzog and L. Read (1993). "Lines of action and moment arms of the major force-carrying structures crossing the human knee joint." In: *Journal of anatomy* 182.Pt 2, p. 213.

A. V. Hill (1938). "The heat of shortening and the dynamic constants of muscle". In: *Proc. R. Soc. Lond. B* 126.843, pp. 136–195.

A. Hof (2001). "The force resulting from the action of mono-and biarticular muscles in a limb". In: *Journal of biomechanics* 34.8, pp. 1085–1089.

F. B. Horak and L. M. Nashner (1986). "Central programming of postural movements: adaptation to altered support-surface configurations". In: *Journal of neurophysiology* 55.6, pp. 1369–1381.

K. Hosoda et al. (2010). "Pneumatic-driven jumping robot with anthropomorphic muscular skeleton structure". In: *Autonomous Robots* 28.3, pp. 307–316.

K. Hosoda et al. (2017). "Actuation in Legged Locomotion". In: *Bioinspired Legged Locomotion*. Elsevier, pp. 563–622.

F. Iida, J. Rummel, and A. Seyfarth (2008). "Bipedal walking and running with spring-like biarticular muscles". In: *Journal of biomechanics* 41.3, pp. 656–667.

F. Iida et al. (2009). "Toward a human-like biped robot with compliant legs". In: *Robotics and Autonomous Systems* 57.2, pp. 139–144.

G. v. van Ingen Schenau, M. Bobbert, and R. Rozendal (1987). "The unique action of bi-articular muscles in complex movements." In: *Journal of anatomy* 155, p. 1.

G. van Ingen Schenau et al. (1992). "The constrained control of force and position in multi-joint movements". In: *Neuroscience* 46.1, pp. 197–207.

M. Ishikawa, J. Pakaslahti, and P. Komi (2007). "Medial gastrocnemius muscle behavior during human running and walking". In: *Gait & posture* 25.3, pp. 380–384.

M. Ishikawa et al. (2005). "Muscle-tendon interaction and elastic energy usage in human walking". In: *Journal of applied physiology*.

Y. P. Ivanenko et al. (2007). "Modular control of limb movements during human locomotion". In: *Journal of Neuroscience* 27.41, pp. 11149–11161.

R. Jacobs and J. M. Macpherson (1996). "Two functional muscle groupings during postural equilibrium tasks in standing cats". In: *Journal of Neurophysiology* 76.4, pp. 2402–2411.

S. Jin et al. (2016). "Experimental evaluation of energy efficiency for a soft wearable robotic suit". In: *IEEE Transactions on Neural Systems and Rehabilitation Engineering* 25.8, pp. 1192–1201.

K. Junius et al. (2017). "Biarticular elements as a contributor to energy efficiency: biomechanical review and application in bio-inspired robotics". In: *Bioinspiration & biomimetics* 12.6, p. 061001.

S. Kajita et al. (2001). "The 3D Linear Inverted Pendulum Mode: A simple modeling for a biped walking pattern generation". In: *Intelligent Robots and Systems, 2001. Proceedings. 2001 IEEE/RSJ International Conference on*. Vol. 1. IEEE, pp. 239–246.

K. T. Kalveram and A. Seyfarth (2009). "Inverse biomimetics: How robots can help to verify concepts concerning sensorimotor control of human arm and leg movements". In: *Journal of Physiology-Paris* 103.3-5, pp. 232–243.

K. Karamanidis et al. (2011). "Lower leg musculoskeletal geometry and sprint performance". In: *Gait & posture* 34.1, pp. 138–141.

P. Klein, S. Mattys, and M. Rooze (1996). "Moment arm length variations of selected muscles acting on talocrural and subtalar joints during movement: an in vitro study". In: *Journal of biomechanics* 29.1, pp. 21–30.

T. J. Klein, T. M. Pham, and M. A. Lewis (2008). "On the design of walking machines using biarticulate actuators". In: *Advances in Mobile Robotics*. World Scientific, pp. 229–237.

H. Knuesel, H. Geyer, and A. Seyfarth (2005). "Influence of swing leg movement on running stability". In: *Human movement science* 24.4, pp. 532–543.

A. D. Kuo (2001). "The action of two-joint muscles: the legacy of WP Lombard". In: *Classics in movement science*, pp. 289–316.

F. Lacquaniti and C. Maioli (1994). "Independent control of limb position and contact forces in cat posture". In: *Journal of Neurophysiology* 72.4, pp. 1476–1495.

F. Lacquaniti and J. Soechting (1986a). "EMG responses to load perturbations of the upper limb: Effect of dynamic coupling between shoulder and elbow motion". In: *Experimental Brain Research* 61.3, pp. 482–496.

F. Lacquaniti and J. Soechting (1986b). "Responses of mono-and bi-articular muscles to load perturbations of the human arm". In: *Experimental Brain Research* 65.1, pp. 135–144.

D. Lakatos et al. (2014). "Design and control of compliantly actuated bipedal running robots: Concepts to exploit natural system dynamics". In: *Humanoid Robots (Humanoids), 2014 14th IEEE-RAS International Conference on*. IEEE, pp. 930–937.

D. Lakatos et al. (2016). "Dynamic bipedal walking by controlling only the equilibrium of intrinsic elasticities". In: *Humanoid Robots (Humanoids), 2016 IEEE-RAS 16th International Conference on*. IEEE, pp. 1282–1289.

G. Lichtwark, K. Bougoulias, and A. Wilson (2007). "Muscle fascicle and series elastic element length changes along the length of the human gastrocnemius during walking and running". In: *Journal of biomechanics* 40.1, pp. 157–164.

G. Lichtwark and A. Wilson (2006). "Interactions between the human gastrocnemius muscle and the Achilles tendon during incline, level and decline locomotion". In: *Journal of Experimental Biology* 209.21, pp. 4379–4388.

H. Lim and S. Park (2019). "A bipedal compliant walking model generates periodic gait cycles with realistic swing dynamics". In: *Journal of biomechanics* 91, pp. 79–84.

S. W. Lipfert et al. (2014). "Impulsive ankle push-off powers leg swing in human walking". In: *Journal of experimental biology* 217.8, pp. 1218–1228.

M. Q. Liu et al. (2008). "Muscle contributions to support and progression over a range of walking speeds". In: *Journal of biomechanics* 41.15, pp. 3243–3252.

Y. Liu et al. (2015). "Trajectory generation for dynamic walking in a humanoid over uneven terrain using a 3d-actuated dual-slip model". In: *Intelligent Robots and Systems (IROS), 2015 IEEE/RSJ International Conference on*. IEEE, pp. 374–380.

F. Loeffl et al. (2016). "The dlr c-runner: Concept, design and experiments". In: *2016 IEEE-RAS 16th International Conference on Humanoid Robots (Humanoids)*. IEEE, pp. 758–765.

W. P. Lombard (1903). "The action of two-joint muscles". In: *American Physical Education Review* 8.3, pp. 141–145.

C. O. Lovejoy (1988). "Evolution of human walking". In: *Scientific American* 259.5, pp. 118–125.

C. N. Maganaris (2003). "Force-length characteristics of the in vivo human gastrocnemius muscle". In: *Clinical Anatomy: The Official Journal of the American Association of Clinical Anatomists and the British Association of Clinical Anatomists* 16.3, pp. 215–223.

C. N. Maganaris (2004a). "A predictive model of moment–angle characteristics in human skeletal muscle: Application and validation in muscles across the ankle joint". In: *Journal of theoretical biology* 230.1, pp. 89–98.

C. N. Maganaris (2004b). "Imaging-based estimates of moment arm length in intact human muscle-tendons". In: *European journal of applied physiology* 91.2-3, pp. 130–139.

C. N. Maganaris, V. Baltzopoulos, and A. J. Sargeant (1998). "Changes in Achilles tendon moment arm from rest to maximum isometric plantarflexion: in vivo observations in man". In: *The Journal of Physiology* 510.3, pp. 977–985.

C. N. Maganaris, V. Baltzopoulos, and A. J. Sargeant (2000). "In vivo measurement-based estimations of the human Achilles tendon moment arm". In: *European journal of applied physiology* 83.4-5, pp. 363–369.

C. N. Maganaris, V. Baltzopoulos, and D. Tsaopoulos (2006). "Muscle fibre length-to-moment arm ratios in the human lower limb determined in vivo". In: *Journal of biomechanics* 39.9, pp. 1663–1668.

P. Malcolm et al. (2018). "Bi-articular knee-ankle-foot exoskeleton produces higher metabolic cost reduction than weight-matched mono-articular exoskeleton". In: *Frontiers in neuroscience* 12, p. 69.

H.-M. Maus et al. (2010). "Upright human gait did not provide a major mechanical challenge for our ancestors". In: *Nature communications* 1, p. 70.

D. Maykranz and A. Seyfarth (2014). "Compliant ankle function results in landing-take off asymmetry in legged locomotion". In: *Journal of theoretical biology* 349, pp. 44–49.

T. McMahon and G. Cheng (1990). "The mechanism of running: how does stiffness couple with speed?" In: *Journal of Biomechanics* 23, pp. 65–78.

J. Meuleman et al. (2015). "LOPES II—design and evaluation of an admittance controlled gait training robot with shadow-leg approach". In: *IEEE transactions on neural systems and rehabilitation engineering* 24.3, pp. 352–363.

A. Minetti and R. M. Alexander (1997). "A theory of metabolic costs for bipedal gaits". In: *Journal of Theoretical Biology* 186.4, pp. 467–476.

F. Mörl, T. Siebert, and D. Häufle (2016). "Contraction dynamics and function of the muscle-tendon complex depend on the muscle fibre-tendon length ratio: a simulation study". In: *Biomechanics and modeling in mechanobiology* 15.1, pp. 245–258.

J. Morrison (1970). "The mechanics of muscle function in locomotion". In: *Journal of Biomechanics* 3.4, pp. 431–451.

Y. Nakanishi et al. (2013). "Design approach of biologically-inspired musculoskeletal humanoids". In: *International Journal of Advanced Robotic Systems* 10.4, p. 216.

Y. Nakata et al. (2012). "Hopping of a monopedal robot with a biarticular muscle driven by electromagnetic linear actuators". In: *Robotics and Automation (ICRA), 2012 IEEE International Conference on*. IEEE, pp. 3153–3160.

K. Narioka, T. Homma, and K. Hosoda (2013). "Roll-over shapes of musculoskeletal biped walker". In: *at-Automatisierungstechnik Methoden und Anwendungen der Steuerungs-, Regelungs-und Informationstechnik* 61.1, pp. 4–14.

A. Nejadfard et al. (2018a). "Coordination of the Biarticular Actuators Based on Mechanical Output Power in an Explosive Jump Experiment". In: *2018 IEEE/ASME International Conference on Advanced Intelligent Mechatronics (AIM)*. IEEE, pp. 220–225.

A. Nejadfard et al. (2018b). "Moment Arm Analysis of the Biarticular Actuators in Compliant Robotic Leg C arl". In: *Conference on Biomimetic and Biohybrid Systems*. Springer, pp. 348–360.

G. Németh and H. Ohlsén (1985). "In vivo moment arm lengths for hip extensor muscles at different angles of hip flexion". In: *Journal of biomechanics* 18.2, pp. 129–140.

J. Nilsson, A. Thorstensson, and J. HALBERTSMA (1985). "Changes in leg movements and muscle activity with speed of locomotion and mode of progression in humans". In: *Acta Physiologica Scandinavica* 123.4, pp. 457–475.

K. Ogawa, K. Narioka, and K. Hosoda (2011). "Development of whole-body humanoid "Pneumat-BS" with pneumatic musculoskeletal system". In: *Intelligent Robots and Systems (IROS), 2011 IEEE/RSJ International Conference on*. IEEE, pp. 4838–4843.

R. Pfeifer and J. Bongard (2007). *How the body shapes the way we think: a new view of intelligence*. MIT press.

R. Pfeifer, M. Lungarella, and F. Iida (2007). "Self-organization, embodiment, and biologically inspired robotics". In: *science* 318.5853, pp. 1088–1093.

S. J. Piazza and S. L. Delp (1996). "The influence of muscles on knee flexion during the swing phase of gait". In: *Journal of biomechanics* 29.6, pp. 723–733.

K. Poggensee, M. Sharbafi, and A. Seyfarth (2014). "Characterizing swing-leg retraction in human locomotion". In: *Mobile Service Robotics*. World Scientific, pp. 377–384.

R. Poppele, G. Bosco, and A. Rankin (2002). "Independent representations of limb axis length and orientation in spinocerebellar response components". In: *Journal of neurophysiology* 87.1, pp. 409–422.

J. Pratt et al. (2006). "Capture point: A step toward humanoid push recovery". In: *2006 6th IEEE-RAS international conference on humanoid robots*. IEEE, pp. 200–207.

B. I. Prilutsky and V. M. Zatsiorsky (1994). "Tendon action of two-joint muscles: transfer of mechanical energy between joints during jumping, landing, and running". In: *Journal of biomechanics* 27.1, pp. 25–34.

B. I. Prilutsky et al. (1998). "Is coordination of two-joint leg muscles during load lifting consistent with the strategy of minimum fatigue?" In: *Journal of Biomechanics* 31.11, pp. 1025–1034.

A. Prochazka, D. Gillard, and D. J. Bennett (1997). "Positive force feedback control of muscles". In: *Journal of neurophysiology* 77.6, pp. 3226–3236.

B. Quinlivan et al. (2017). "Assistance magnitude versus metabolic cost reductions for a tethered multiarticular soft exosuit". In: *Sci Robot* 2.2, p. 4416.

K. Radkhah et al. (2011). "Concept and design of the biobiped1 robot for human-like walking and running". In: *International Journal of Humanoid Robotics* 8.03, pp. 439–458.

M. H. Raibert (1986). *Legged robots that balance*. MIT press.

A. Rajagopal et al. (2016). "Full-Body Musculoskeletal Model for Muscle-Driven Simulation of Human Gait." In: *IEEE Trans. Biomed. Engineering* 63.10, pp. 2068–2079.

A. M. N. Rashty, M. A. Sharbafi, and A. Seyfarth (2014). "Slip with swing leg augmentation as a model for running". In: *2014 IEEE/RSJ International Conference on Intelligent Robots and Systems*. IEEE, pp. 2543–2549.

T. J. Roberts (2002). "The integrated function of muscles and tendons during locomotion". In: *Comparative Biochemistry and Physiology Part A: Molecular & Integrative Physiology* 133.4, pp. 1087–1099.

C. Rode, T. Siebert, and R. Blickhan (2009). "Titin-induced force enhancement and force depression: A 'sticky-spring' mechanism in muscle contractions?" In: *Journal of Theoretical Biology* 259.2, pp. 350–360.

S. Rugg et al. (1990). "In vivo moment arm calculations at the ankle using magnetic resonance imaging (MRI)". In: *Journal of biomechanics* 23.5, pp. 495–501.

J. Rummel and A. Seyfarth (2010). "Passive stabilization of the trunk in walking". In: *Proceedings of SIMPAR 2010 Workshops – International Conference on Simulation, Modeling and Programming for Autonomous Robots*, pp. 127–136.

F. Saibene and A. E. Minetti (2003). "Biomechanical and physiological aspects of legged locomotion in humans". In: *European journal of applied physiology* 88.4-5, pp. 297–316.

A. Sarmadi et al. (2019). "Concerted control of stance and balance locomotor subfunctions-Leg force as a conductor". In: *IEEE Transactions on Medical Robotics and Bionics*.

G. J. V. I. Schenau (1989). "From rotation to translation: Constraints on multi-joint movements and the unique action of bi-articular muscles". In: *Human Movement Science* 8.4, pp. 301–337.

K. Schmidt et al. (2017). "The myosuit: Bi-articular anti-gravity exosuit that reduces hip extensor activity in sitting transfers". In: *Frontiers in neurorobotics* 11, p. 57.

D. Scholz et al. (2012). "Simulation and experimental evaluation of the contribution of biarticular gastrocnemius structure to joint synchronization in human-inspired three-segmented elastic legs". In: *International Conference on Simulation, Modeling, and Programming for Autonomous Robots*. Springer, pp. 251–260.

C. Schumacher et al. (2019). "Biarticular muscles are most responsive to upper-body pitch perturbations in human standing". In: *Scientific reports* 9.1, pp. 1–14.

S. Schütz et al. (2017). "Carl—A compliant robotic leg featuring mono-and biarticular actuation". In: *2017 IEEE-RAS 17th International Conference on Humanoid Robotics (Humanoids)*. IEEE, pp. 289–296.

A. Seyfarth, R. Blickhan, and J. Van Leeuwen (2000). "Optimum take-off techniques and muscle design for long jump". In: *Journal of Experimental Biology* 203.4, pp. 741–750.

A. Seyfarth, H. Geyer, and H. Herr (2003). "Swing-leg retraction: a simple control model for stable running". In: *Journal of Experimental Biology* 206.15, pp. 2547–2555.

A. Seyfarth, M. GuÈnther, and R. Blickhan (2001). "Stable operation of an elastic three-segment leg". In: *Biological cybernetics* 84.5, pp. 365–382.

A. Seyfarth et al. (2006). "Running and walking with compliant legs". In: *Fast motions in biomechanics and robotics*. Springer, pp. 383–401.

A. Seyfarth et al. (2009). "Towards bipedal jogging as a natural result of optimizing walking speed for passively compliant three-segmented legs". In: *The International Journal of Robotics Research* 28.2, pp. 257–265.

M. A. Sharbafi et al. (2017a). "Fundamental Subfunctions of Locomotion". In: *Bioinspired Legged Locomotion: Models, Concepts, Control and Applications*. Ed. by M. A. Sharbafi and A. Seyfarth. Elsevier. Chap. 2, pp. 11–52.

M. A. Sharbafi and A. Seyfarth (2015). "FMCH: a new model for human-like postural control in walking". In: *2015 IEEE/RSJ International Conference on Intelligent Robots and Systems (IROS)*. IEEE, pp. 5742–5747.

M. A. Sharbafi and A. Seyfarth (2017a). "How locomotion sub-functions can control walking at different speeds?" In: *Journal of biomechanics* 53, pp. 163–170.

M. A. Sharbafi and A. Seyfarth (2017b). *Bioinspired Legged Locomotion: Models, Concepts, Control and Applications*. Butterworth-Heinemann.

M. A. Sharbafi et al. (2016). "A new biarticular actuator design facilitates control of leg function in BioBiped3". In: *Bioinspiration & biomimetics* 11.4, p. 046003.

M. A. Sharbafi et al. (2017b). "Reconstruction of human swing leg motion with passive biarticular muscle models". In: *Human movement science* 52, pp. 96–107.

M. A. Sharbafi et al. (2014). "Hopping control for the musculoskeletal bipedal robot: BioBiped". In: *2014 IEEE/RSJ International conference on Intelligent Robots and Systems*. IEEE, pp. 4868–4875.

M. A. Sharbafi et al. (2018). "Leg force control through biarticular muscles for human walking assistance". In: *Frontiers in neurorobotics* 12, p. 39.

F. T. Sheehan (2012). "The 3D in vivo Achilles' tendon moment arm, quantified during active muscle control and compared across sexes". In: *Journal of biomechanics* 45.2, pp. 225–230.

Z. Shen and J. Seipel (2012). "A fundamental mechanism of legged locomotion with hip torque and leg damping". In: *Bioinspiration & Biomimetics* 7.4, p. 046010.

T. Siebert and C. Rode (2014). "Computational modeling of muscle biomechanics". In: *Computational Modelling of Biomechanics and Biotribology in the Musculoskeletal System*. Elsevier, pp. 173–204.

E. B. Simonsen, L. Thomsen, and K. Klausen (1985). "Activity of mono-and biarticular leg muscles during sprint running". In: *European Journal of Applied Physiology and Occupational Physiology* 54.5, pp. 524–532.

J. Soechting and F. Lacquaniti (1988). "Quantitative evaluation of the electromyographic responses to multidirectional load perturbations of the human arm". In: *Journal of Neurophysiology* 59.4, pp. 1296–1313.

A. J. van Soest and M. F. Bobbert (1993). "The contribution of muscle properties in the control of explosive movements". In: *Biological cybernetics* 69.3, pp. 195–204.

S. Song and H. Geyer (2015). "A neural circuitry that emphasizes spinal feedback generates diverse behaviours of human locomotion". In: *The Journal of physiology* 593.16, pp. 3493–3511.

C. Spoor and J. Van Leeuwen (1992). "Knee muscle moment arms from MRI and from tendon travel". In: *Journal of biomechanics* 25.2, pp. 201–206.

A. Spröwitz et al. (2013). "Towards dynamic trot gait locomotion: Design, control, and experiments with Cheetah-cub, a compliant quadruped robot". In: *The International Journal of Robotics Research* 32.8, pp. 932–950.

M. Srinivasan and A. Ruina (2006). "Computer optimization of a minimal biped model discovers walking and running". In: *Nature* 439.7072, p. 72.

A. Tomalka et al. (2017). "The active force–length relationship is invisible during extensive eccentric contractions in skinned skeletal muscle fibres". In: *Proceedings of the Royal Society of London B: Biological Sciences* 284.1854.

G. Torres-Oviedo and L. H. Ting (2010). "Subject-specific muscle synergies in human balance control are consistent across different biomechanical contexts". In: *American Journal of Physiology-Heart and Circulatory Physiology*.

H. Toussaint et al. (1992). "Coordination of the leg muscles in backlift and leglift." In: *Journal of biomechanics* 25.11, p. 1279.

A. J. Van den Bogert (2003). "Exotendons for assistance of human locomotion". In: *Biomedical engineering online* 2.1, p. 17.

W. Van Dijk, H. Van der Kooij, and E. Hekman (2011). "A passive exoskeleton with artificial tendons: Design and experimental evaluation". In: *2011 IEEE International Conference on Rehabilitation Robotics*. IEEE, pp. 1–6.

S. M. Verschueren, P. J. Cordo, and S. P. Swinnen (1998). "Representation of wrist joint kinematics by the ensemble of muscle spindles from synergistic muscles". In: *Journal of neurophysiology* 79.5, pp. 2265–2276.

J. Visser et al. (1990). "Length and moment arm of human leg muscles as a function of knee and hip-joint angles". In: *European journal of applied physiology and occupational physiology* 61.5-6, pp. 453–460.

R. Wells and N. Evans (1987). "Functions and recruitment patterns of one-and two-joint muscles under isometric and walking conditions". In: *Human movement science* 6.4, pp. 349–372.

R. Wells (1988). "Mechanical energy costs of human movement: an approach to evaluating the transfer possibilities of two-joint muscles". In: *Journal of biomechanics* 21.11, pp. 955–964.

A. M. Wilson et al. (2001). "Horses damp the spring in their step". In: *Nature* 414.6866, p. 895.

D. A. Winter (1995). "Human balance and posture control during standing and walking". In: *Gait & posture* 3.4, pp. 193–214.

D. A. Winter (2009). *Biomechanics and motor control of human movement*. John Wiley & Sons.

P. Wretenberg et al. (1996). "Passive knee muscle moment arms measured in vivo with MRI". In: *Clinical Biomechanics* 11.8, pp. 439–446.

F. Young et al. (2019). "Analyzing moment arm profiles in a full-muscle rat hindlimb model". In: *Biomimetics* 4.1, p. 10.

G. Zhao et al. (2017). "Template model inspired leg force feedback based control can assist human walking". In: *2017 International Conference on Rehabilitation Robotics (ICORR)*. IEEE, pp. 473–478.

3 Article II: Biarticular muscles are Most Responsive to Upper-body Pitch Perturbations in Human Standing

Christian Schumacher, Andrew Berry, Daniel Lemus, Christian Rode, André Seyfarth and Heike Vallery

Abstract

Balancing the upper body is pivotal for upright and efficient gait. While models have identified potentially useful characteristics of biarticular thigh muscles for postural control of the upper body, experimental evidence for their specific role is lacking. Based on theoretical findings, we hypothesised that biarticular muscle activity would increase strongly in response to upper-body perturbations. To test this hypothesis, we used a novel Angular Momentum Perturbator (AMP) that, in contrast to existing methods, perturbs the upper-body posture with only minimal effect on center of mass (CoM) excursions. The impulse-like AMP torques applied to the trunk of subjects resulted in upper-body pitch deflections of up to 17° with only small CoM excursions below 2 cm. Biarticular thigh muscles (biceps femoris long head and rectus femoris) showed the strongest increase in muscular activity (mid- and long-latency reflexes, starting 100 ms after perturbation onset) of all eight measured leg muscles which highlights the importance of biarticular muscles for restoring upper-body balance. These insights could be used for improving technological aids like rehabilitation or assistive devices, and the effectiveness of physical training for fall prevention e.g. for elderly people.

Introduction

Dealing with typical perturbations (e.g. pushing, stumbling or walking on uneven ground) comprises coordinating multiple joints (Engelhart et al., 2015). For this, biarticular muscles (that span two joints) might play a key role. In contrast to monoarticular muscles (spanning one joint), biarticular muscles contribute strongly to the leg force that acts perpendicular to the leg axis (Hof, 2001). This seems to make biarticular muscles especially suitable for postural control because the perpendicular component of leg force regulates the angular momentum.

In accordance with this, in static experiments humans mainly used biarticular thigh muscles to control the direction of the ground reaction force (GRF) (Ingen Schenau et al., 1995; Doorenbosch and Ingen Schenau, 1995; Fujiwara and Basmajian, 1975; Wells and Evans, 1987). This ability might also be exploited to achieve stable walking by directing the GRF towards a point above the center of mass (CoM) (Maus et al., 2010; Maus et al., 2008; Gruben and Boehm, 2012; Müller et al., 2017). Further, humans responded quickly with hamstring activity to a perturbation of angular momentum in a stumbling experiment (Pijnappels et al., 2005). Simulations and robotic demonstrators revealed the potential of biarticular structures (e.g. springs or muscles) to stabilise the trunk during walking and generate appropriate leg swing motions (Lakatos et al., 2014; Lakatos et al., 2016; Sharbafi et al., 2017; Dean and Kuo, 2008). However, experimental evidence for the actual use of biarticular muscles for upper-body balance in humans is still missing. Based on their ability to generate appropriate combinations of required hip and knee torques (Doorenbosch and Ingen Schenau, 1995; Fujiwara and Basmajian, 1975; Wells and Evans, 1987; Prilutsky et al., 1998a), we hypothesised that biarticular thigh muscles would react strongly to a perturbation of upper body angular momentum during quiet standing.

Perturbing a system and investigating its response is a standard method to analyse the system's dynamics (Mergner, 2010). To study human balance strategies, unexpected and specific mechanical perturbations such as surface translations (Figure 3.1a) have frequently been used to study the human balance response to slipping (Nashner, 1977; Horak and Nashner, 1986; Mergner, 2010; Welch and Ting, 2009). Recently, research groups have also applied pulls and pushes at the hip or at the shoulder (Rietdyk et al., 1999; Misiaszek et al., 2000; Vashista et al., 2014; Fujimoto et al., 2015; Vlutters et al., 2016; Olenšek et al., 2016;

Wu et al., 2017) to resemble other common perturbation scenarios (Figure 3.1b). By generating a horizontal force, these systems perturb balance of the body as a whole (Tang et al., 1998). Pushes/ pulls and surface movement perturbations require corrections of angular momentum, i.e. keeping the CoM within the base of support and restoring the upright upper-body orientation. Thus, such perturbations necessitate a complex response of the neuro-musculoskeletal system, which might involve multiple response mechanisms. This might complicate or hamper the interpretation of the role of biarticular muscles for upper-body balance.

For the first time, we propose to exert a pure torque, or force couple, on the upper body. Applying a pure torque without a translational (horizontal force) component entails that the whole-body CoM position is only minimally influenced and reduces artefacts of cross-talk between different balance strategies. For this purpose, we use an Angular Momentum Perturbator (AMP) (Lemus et al., 2017). This system opens a new category in the framework of Shirota et al. (2017) and enables a specifically targeted perturbation (Figure 3.1c), making it a suitable tool to study upper-body balance response strategies while maintaining a natural leg axis alignment. The system is portable – the subject can move freely without being bound to a treadmill or a frame construction – and is capable of generating powerful torque bursts.

In this study, we contribute to the ongoing research of human motor control during non-stepping balance recovery by examining the muscular response of major leg muscles for two major perturbation directions: (1) positive torque perturbations resulting in a forward upper-body pitch and (2) negative torque perturbations resulting in a backward pitch. Compared to other commonly used perturbation types, the AMP produced perturbations with a distinct upper-body pitch and only a small shift in CoM position, allowing us to assess the contribution of different leg muscles (using electromyographic data (EMG)) for restoring the upper-body balance in near-absence of whole-body balance corrections.

Methods

Angular Momentum Perturbator (AMP)

The AMP is worn like a backpack and contains a *control moment gyroscope*, an actuator that exerts torques by manipulating the angular momentum of an internal flywheel. This flywheel is mounted to a motorised gimbal frame (Figure 3.1d), which enables the flywheel to be reoriented with respect to the wearer.

For the present study, we modified the AMP prototype described previously (Lemus et al., 2017) to reduce its mass. After replacing the gimbal motor and transmission, the system weighed 16 kg and was capable of exerting a maximum torque of 53 N m.

The AMP exerts torques on the wearer ($\boldsymbol{\tau}_{\mathrm{AMP}}$) by changing the direction or magnitude of the angular momentum of the flywheel (H), described in detail by e.g. Schaub et al. (1998). Changing the direction by rotating the gimbal or rotating the trunk produces *gyroscopic* torques proportional to the angular velocities of the gimbal ($\dot{\boldsymbol{\gamma}}$) and trunk of the wearer ($\boldsymbol{\omega} = [\omega_x, \omega_y, \omega_z]$, using the frame definitions of Figure 3.1d). When exploiting this gyroscopic effect, the gimbal motor applies a torque ($\boldsymbol{\tau}_g$) in the gimbal axis to modulate $\dot{\boldsymbol{\gamma}}$; however, in doing so, this changes the magnitude of H and is experienced by the wearer as an opposite reaction torque in the same axis. The total torque is thus the sum of these components:

$$\boldsymbol{\tau}_{\mathrm{AMP}}(t) = -\dot{H}(t) = -\underbrace{(\dot{\boldsymbol{\gamma}}(t) + \boldsymbol{\omega}(t)) \times H(t)}_{\text{gyroscopic effect}} - \underbrace{\boldsymbol{\tau}_g(t)}_{\text{gimbal motor}} \ . \tag{3.1}$$
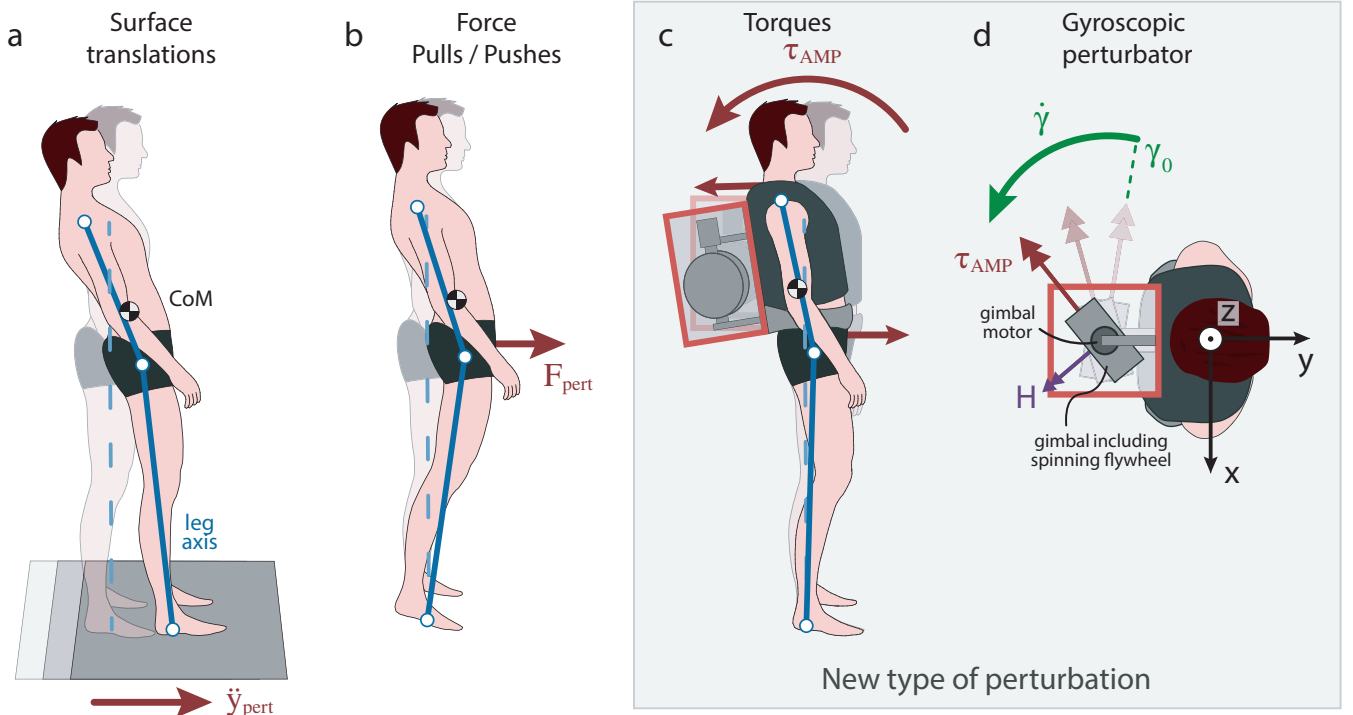
Figure 3.1: Exemplary perturbation types: Schematic visualisation of center of mass (CoM), leg, and upper-body kinematics (transparent: before perturbation, solid: after perturbation). **(a)** Back and forth surface translations result in a whole-body balance perturbation by producing first an acceleration followed by a deceleration. **(b)** Force pushes or pulls can result in irregular body postures with small upper body perturbations. **(c)** Torque perturbation: the generated torque on the upper body (curved red arrow) is equivalent to a force pair (straight red arrows) with zero net horizontal force. This type of perturbation results mainly in rotational acceleration of the upper body. Minimal CoM excursions occur due to the muscular coupling of the upper body to the leg. **(d)** The Angular Momentum Perturbator (AMP) creates external torques by rotating a spinning flywheel (angular momentum H, purple arrow) around a perpendicular gimbal axis (here: longitudinal, angular velocity $\dot{\gamma}$, green arrow, initial gimbal position γ_0). The created torque τ_{AMP} is exerted in the direction perpendicular to both, the rotation of the spinning flywheel and the gimbal axis, and rotates together with the gimbal (red arrow).

By design, the gyroscopic torque is generally much larger than the gimbal torques ($\boldsymbol{\tau}_g$) to allow the use of a relatively small gimbal motor and reduce power requirements. Since this gyroscopic torque depends not only on the controlled gimbal velocity ($\dot{\boldsymbol{\gamma}}$), but also on the angular velocity of the wearer $\boldsymbol{\omega}$, it is in general only partially controllable. However, in the present study, since $\boldsymbol{\omega}$ is relatively small (especially during quiet standing), the uncontrolled gyroscopic torques were typically at least one order of magnitude smaller than those due to $\dot{\boldsymbol{\gamma}}$ and were mostly considered negligible.

When generating controlled gyroscopic torques by rotating the gimbal, the direction of $\boldsymbol{\tau}_{\text{AMP}}$ simultaneously changes with the gimbal angle ($\boldsymbol{\gamma}$). In a human-fixed frame (unit vectors $(\hat{e}_x, \hat{e}_y, \hat{e}_z)$ attached to frame

(x,y,z), Figure 3.1d), the total perturbation torque $\boldsymbol{\tau}_{\text{AMP}}$ consists of components in all three directions:

$$\boldsymbol{\tau}_{\text{AMP}}(t) = \underbrace{-\tau_t(t)\cos(\gamma(t))\hat{e}_x}_{\text{pitch component}} \underbrace{-\tau_t(t)\sin(\gamma(t))\hat{e}_y}_{\text{roll component}} + \underbrace{(\omega_t(t)H(t) - \tau_g(t))\hat{e}_z}_{\text{yaw component}} \tag{3.2}$$

$$\approx -\dot{\gamma}(t)H\cos(\gamma(t))\hat{e}_x - \dot{\gamma}(t)H\sin(\gamma(t))\hat{e}_y + (\omega_x(t)H\cos(\gamma(t)) - \tau_g(t))\hat{e}_z \,,$$

where $\tau_t(t) = (\dot{\gamma}(t) + \omega_z(t))H(t) \approx \dot{\gamma}(t)H(t)$ and $\omega_t(t) = \omega_x(t)\cos(\gamma(t)) + \omega_y(t)\sin(\gamma(t)) \approx \omega_x(t)\cos(\gamma(t))$. All non-bold variables indicate the signed scalar magnitudes of the vector quantities defined previously, and the magnitude of the flywheel angular momentum was approximately constant throughout all experiments ($H(t) \approx H$).

To generate a torque of a specific magnitude and direction requires inversion of Equation 3.2 to produce a reference gimbal motion, described in general by Berry et al. (2016). For discrete open-loop perturbations, this inversion is simplified, and, for a given initial gimbal angle (γ_0) and desired torque profile, the final angle (γ_f) can be computed in advance. To produce a torque primarily in the sagittal plane (around the x-axis) and limit the component in the frontal plane (around the y-axis), the range of gimbal rotation was constrained and γ_0 was chosen such that $\gamma \approx 0$ when the magnitude of $\boldsymbol{\tau}_{\text{AMP}}$ was maximal (Figure 3.1d).

The perturbation torque $\boldsymbol{\tau}_{\text{AMP}}$ was selected to be a symmetric trapezoidal profile (Figure 3.2 inset), consisting of a peak torque of 60 N m with a rise time, hold time, and fall time each of 100 ms. This shape reflects the finite ability of the gimbal motor to accelerate or decelerate rotation of the gimbal structure to produce the gyroscopic effect. A gimbal motor torque (τ_g) of approximately 12 N m was necessary to generate the desired perturbations. Because the roll (frontal) torque components alternated sign throughout the perturbation, all perturbations were repeated with the gimbal inverted (rotated by 180°) to also generate the opposite pattern (of roll torque component) with similar pitch torque component for comparison.

Experimental Protocol

The experimental protocol consisted of three successive sets of measurements involving different settings. In the first setting, the subjects were asked to stand still for 60 s with arms crossed over the chest and without wearing the perturbator ('Unloaded Standing'). In the second setting, they repeated the same task but wore a safety harness and the AMP with spinning flywheel, but no active torque perturbations ('Loaded Standing'). In the final setting of standing, a series of 48 trials were executed involving 40 trials of active torque perturbation of the AMP ('Perturbation Trials') and 8 trials which lacked a perturbation ('Control Trials'). The 40 Perturbation Trials consisted of 4 conditions with 10 repetitions each: positive and negative torque directions with both original ($\gamma_0 = 0°$) and inverted ($\gamma_0 = 180°$) initial gimbal orientations. Conditions of positive and negative torque direction (inducing forward and backward upper-body pitch, respectively) were chosen to investigate a potential direction dependency. Since the AMP generates a complex perturbation that acts in multiple planes (mainly sagittal but also in the frontal plane), the initial gimbal position was altered to investigate potential side effects of the roll torque component. Due to relatively long gimbal re-positioning times before every trial (to reach the initial gimbal position), a blocked protocol was preferred over a fully randomised protocol ('Block 1' with original and 'Block 2' with inverted gimbal position). This was done to reduce the measurement time and subject fatigue. Within the two blocks, both the direction and timing of the active perturbations were randomised. Subject were given time to rest in between measurements. For referencing, subjects conducted ten additional walking trials (distance approx. 7 m) at preferred walking speeds (1.20 ± 0.14 m/s, Mean $\pm$ SD) without any additional loads.

To prevent fall-related injury during the perturbations, a safety harness was used at all times when the AMP was worn. The harness was attached to the Rysen body weight support system (Motekforce Link, Amsterdam, The Netherlands), which is capable of actively detecting and arresting falling motions of the subject (Plooij et al., 2018). To avoid vertical unloading forces during the measurements, the Rysen system was lowered and locked in a position where the harness straps were slack during both quiet and perturbed standing, but could still prevent falls if balance could not be successfully recovered.

Data collection and processing

Subjects

Seventeen healthy adult subjects (two female) participated in the study. All subjects volunteered to participate in the study in summer 2018 and gave written informed consent in advance of the experiment. The experimental protocol was approved by and performed in accordance with the relevant guidelines and regulations of the Human Research Ethics Committee of the Delft University of Technology (Project ID: 350). Before the experiment, all participants gave their consent and filled in the revised Waterloo Footedness Questionnaire (Elias et al., 1998), which was used to assess limb dominance regarding stabilisation tasks.

We collected EMG, kinetic, and kinematic data of the subject. All measurement devices including the data logging of the AMP were synchronised by a manual trigger signal. Before processing the data, one female subject was excluded from the data analysis due to repetitive stepping responses during the experiments. A further five (male) subjects were excluded due to missing EMG data or missing marker data that impeded a calculation of the CoM. Only the data of the remaining eleven subjects (one female), of age 34 ± 14 years (Mean $\pm$ SD), weight 74.8 ± 12.5 kg, and height 1.81 ± 0.08 m, were considered for further analysis.

Measured data

Sixteen surface EMG electrodes (Trigno, Delsys Inc., Natick, USA) were used to record at 2000 Hz the electrical activity of relevant leg muscles. The set of electrodes were placed on the following muscles of each leg: tibialis anterior (TA), soleus (SOL), gastrocnemius (GAS), vastus lateralis (VL), rectus femoris (RF), hamstrings (HAM), tensor fasciae latae (TFL) and gluteus maximus (GLU) (see Appendix Figure A.1). To ensure a good electrical connectivity, the skin was prepared following the SENIAM recommendations (Hermens et al., 1999). After attachment, electrode locations were checked for voluntary muscle signals and low noise values. The raw EMG was band-pass-filtered with cut-off frequencies of 20 Hz (high-pass) and 450 Hz (low-pass), further rectified and low-pass filtered at 50 Hz. For each muscle and subject, the filtered EMG signals were normalised by the mean filtered background activity recorded during unloaded level walking (WEMG), and expressed as a percentage of WEMG (see Appendix Table A.3).

Individual GRF of both legs were measured at a frequency of 1000 Hz (3$^{\text{rd}}$-order analogue Butterworth low-pass filter with 500 Hz cut-off frequency) using two force plates (9260AA3, Kistler Holding AG, Winterthur, Switzerland), each for a single leg. These were combined to compute the whole-body center of pressure (CoP).

An inertial measurement unit (IMU) (MPU-9250, InvenSense, San Jose, USA) within the AMP and a motion capture system (Qualisys, Gothenburg, Sweden) were used to collect kinematic data (200 Hz) of the subject and the AMP. Nineteen reflective markers were placed at relevant body locations (see Appendix

Figure A.1): the tragion (TRA), 7th cervial vertebrae (C7), acromion (ACR), greater trochanter (GTR), lateral femoral condyle (LFC), fibulare (FIB), lateral melleoius (LM), calcaneus (CAL), 1st metatarsal head (MT1), and 5th metatarsal head (MT5). The CoM of the AMP was estimated by suspending the AMP from a single attachment point, and measuring the point of intersection of the vertical axis as the attachment point was changed. Four addition markers were placed on the rigid and static frame of the AMP such that their mean position resembled the CoM of the AMP. All kinematic data was upsampled to 1000 Hz by linear interpolation and filtered using a zero-lag 4th-order low-pass filter with a cut-off frequency of 6 Hz.

Computing Outcome measures

Since the unintended roll torque components created only slight opposing asymmetric behaviours with similar magnitude in both conditions of initial gimbal positions ('Block 1' vs. 'Block 2', see Appendix Figures A.9 to A.14), both sets were merged for comprehensibility reasons. Outcome measures, such as mean and SD of kinematic and kinetic data, were calculated from both blocks together.

Mean muscle stimulation of 'Unloaded Standing' and 'Loaded Standing' was calculated for a 20 s period of quiet standing. The mean signal of the preceding 500 ms prior to perturbation onset (quiet standing) was used as 'Pre-Perturbation' activation. From this signal, the mean of each muscle and subject of the last 10 trials per block ('Block 1' and 'Block 2') was compared against the condition of 'Loaded Standing' to evaluate muscle activity changes due to anticipation.

In order to account for temporal variability of the muscular activity for all 'Perturbation Trials', three time intervals were chosen to evaluate the appearance of medium-latency response (RI1: from 100 ms to 150 ms) and long-latency responses (RI2: from 170 ms to 250 ms, RI3: from 270 ms to 350 ms) that involve contributions from supra-spinal centres or poly-synaptic reflex responses (Horak and Macpherson, 1996; Hof and Duysens, 2018; Torres-Oviedo and Ting, 2007). The relative reflex response of each muscle was defined as the difference between the mean EMG in the response intervals and corresponding mean EMG in the 'Pre-Perturbation' interval of the same trial, each expressed as a percentage of WEMG. As adaptation processes of EMG responses have been found to settle after about 5 trials (Keshner et al., 1987), we considered only the last 5 of the 10 trials per condition, in order to reduce the effects of adaptation processes. We used the Grubbs' test (with a significance level of $\alpha = 0.05$) to identify and remove unphysiological EMG values (outliers), stemming from e.g. physical collisions of the hip belt and hip muscle electrodes. To evaluate the muscular reflexes, we first computed the mean relative reflex response of all analysed trials per subjects (last 5 of the 10 trials per condition, combining 'Block 1' and 'Block 2') before performing the statistical analysis. Outcome measures of pooled data are reported by grand means and SD of the averaged subject data. Data analysis was done using Matlab 2016b (The MathWorks Inc., Natick, USA).

Statistical analysis

We compared different joint angles and activity levels between 'Unloaded Standing' and 'Loaded Standing' as well as 'Loaded Standing' and 'Pre-Perturbation' conditions. First we evaluated the normality of the residuals by the Shapiro–Wilk test. If they were normally distributed we applied a paired two-sided t-test. In other cases we tested for differences with the non-parametric two-sided Wilcoxon signed-rank test. All comparisons were performed using a 5 % significance level.

For comparisons of the relative reflex response, a repeated measures analysis of variance (rmANOVA) with between ('Direction', 'Side' and 'Muscles') and within subject factors ('Response Intervals') was performed. Shapiro–Wilk tests confirmed normality of the data. If Mauchly's test for sphericity revealed that homogeneity of the data was not given, the Greenhouse-Geisser correction was used. Comparisons were performed using a 5 % significance level. If the rmANOVA showed significant interaction effects, post-hoc tests were computed with the Tukey's Honest Significant Difference procedure to adjust for multiple comparisons.

Results

We perturbed upper-body posture during quiet standing by applying external torques – instead of forces – created by a new type of perturbation device, the AMP. This was done to specifically investigate the role of biarticular leg muscles used to control upper-body balance.

The outcome measures of both conditions of initial gimbal positions ('Block 1' and 'Block 2') were merged before computing statistics. The results will thus be presented for both main perturbation directions: positive torque perturbation ($\tau_{AMP} > 0$) with forward upper-body pitch and negative torque perturbation ($\tau_{AMP} < 0$) with backward upper-body pitch. In the following, we will focus on the results of the left leg (the dominant leg for stabilisation of all subjects) as leg behaviour (see Appendix Figures A.12 to A.14 and Table A.2) and response characteristics ('Side' main effect of rmANOVA: $F(1,314) = 0.18, p = 0.676$) were similar for both sides.

AMP produced dynamic and reproducible torque perturbations

To verify that the AMP generated appropriate perturbation profiles, the calculated gyroscopic torque (based on measured gimbal angular velocity $\dot{\gamma}$) was compared to the desired profile (Figure 3.2 insets). For both perturbation directions, the AMP was able to generate repeatable perturbations that closely resembled the shape of the desired profile. The rise and fall dynamics were tracked accurately, but the realised peak torque (53 N m) fell lower than the target of 60 N m. For both perturbation directions, the small standard deviation (SD) of the measured profile confirms a consistent perturbation generation over multiple trials (Figure 3.2 insets).

Torque perturbations resulted in specific upper-body pitch perturbations

In order to study the resulting posture of the subjects, we evaluated upper-body pitch (sagittal-plane rotation), whole-body CoM and CoP (top panels in Figure 3.2a). Following the positive torque perturbation, the upper-body segment pitched forward with a peak rotation of 15° to 17° with respect to the initial posture before perturbation onset. The peak pitch was reached after 300 ms to 400 ms after perturbation onset, and about 1000 ms to 1500 ms were needed to recover the initial posture. This response was accompanied by a backwards movement of the hip joint (see Appendix Figure A.4). In contrast to the substantial upper-body rotation, the CoM moved forward by only about 1 cm to 2 cm. The CoM progression started after 400 ms. The mean CoP moved anterior by 4 cm to reach its peak after 500 ms. The subjects' mechanical response within the first 1000 ms consisted of a distinct early upper-body pitch, mainly due to hip flexion within first 500 ms (see Appendix Figure A.2), followed by a delayed, but subtle CoM forward sway.
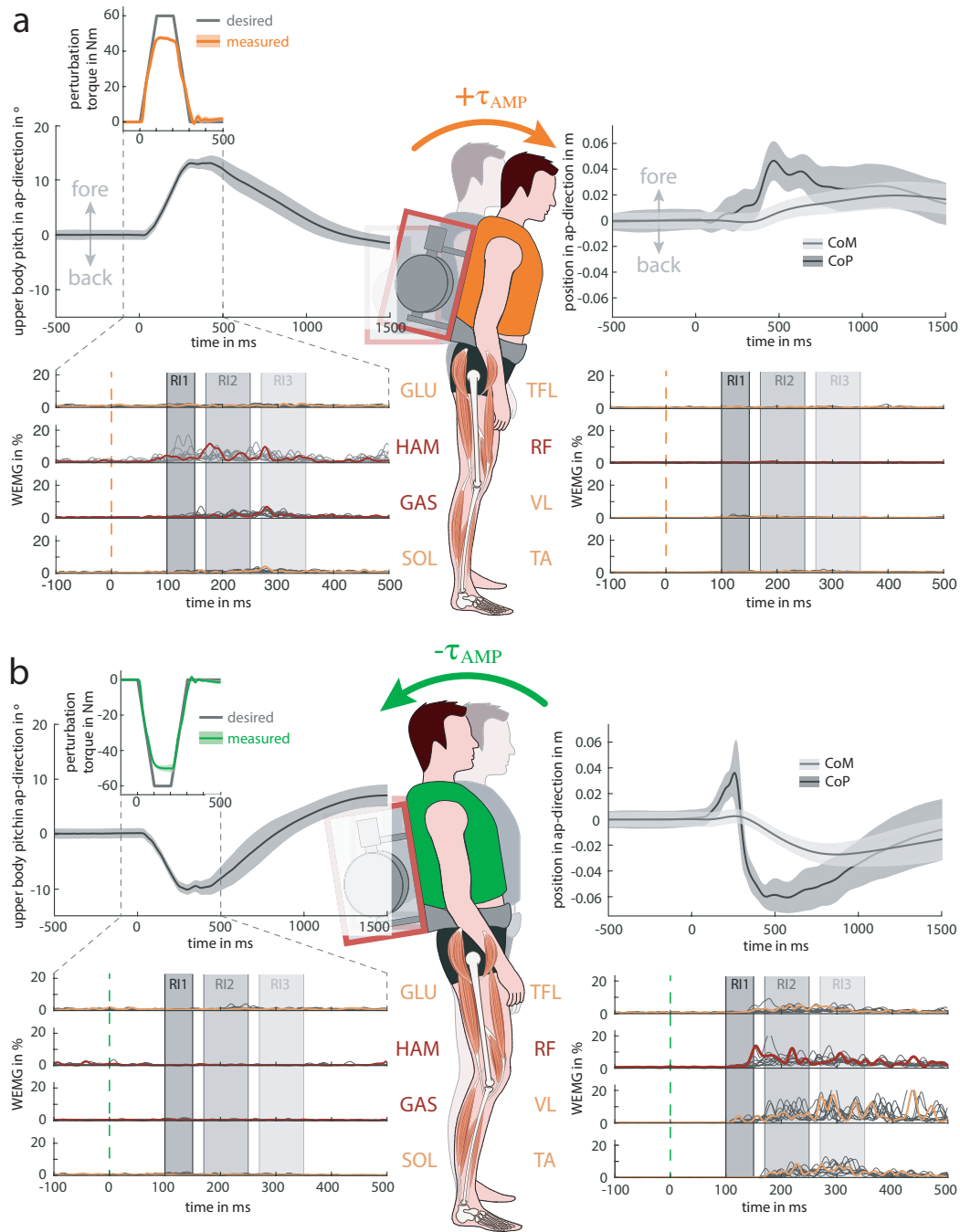
Figure 3.2: AMP generated (a) positive and (b) negative torque perturbations resulting in forward and backward pitch of the upper body, respectively. Change in upper-body pitch angle of one subject (mean and standard deviation from the last 5 trials × 2 gimbal configurations) with respect to the initial upper-body posture (top left). The inset shows the desired (grey, $100\,\mathrm{ms}$ rise, hold and fall time) and actual pitch perturbation torque profile (orange/green: mean and SD). Change in sagittal CoM (grey: mean and SD) and CoP position (black: mean and SD) of the same subject with respect to the initial positions (top right). Exemplary EMG of the same subject (bottom panel): filtered and normalised signals of all trials (grey) and one individual response of mono- (yellow) and biarticular muscles (red).

For negative torque perturbations, the resultant backwards pitch of the upper body (top panels in Figure 3.2b) was smaller (approx. $-12°$) compared to the forward perturbations and appeared at similar timing (300 ms to 400 ms after perturbation onset). During upper-body pitch, the hip joint moved forward (see Appendix Figure A.4). Again delayed, the CoM moved posterior to a peak of about -2 cm from the initial position. A distinct CoP pattern was measured: for the time of backward acceleration of the upper body, the CoP moved forward before quickly moving backwards to around -5 cm. In the backwards condition, the upper-body rotation was not achieved through hip extension (remained in initial posture), but by knee bending such that upper body and thigh segments pivoted together around the knee joint (see Appendix Figure A.2).

Influence of AMP weight, noise, and vibrations

Next, we tested the extent to which the weight, noise, and vibrations of the AMP influenced the initial posture and the EMG. Wearing the AMP led to a more bent hip ($-6.2°$, $t(10) = -5.528$, $p < 0.001$) and more extended knee ($2.1°$, $t(10) = 3.652$, $p = 0.002$) while no difference was found for the ankle joint (see Appendix Table A.1). By comparing EMG data of the two conditions of quiet standing 'Unloaded Standing' and 'Loaded Standing' changes of muscle stimulation were identified (Figure 3.3). The additional weight, noise, and vibration of the rotating flywheel of the AMP resulted in significant reductions of muscular activity in GLU (unloaded: 78 ± 28 %WEMG, loaded: 57 ± 24 %WEMG, $Z = -2.934$, $p = 0.003$) and HAM (unloaded: 108 ± 75 %WEMG, loaded: 62 ± 34 %WEMG, $Z = -2.490$, $p = 0.013$) of the left leg – reflecting the reduced demand of muscle generated hip extension torque to maintain similar upper-body postures – as well as VL of the right leg (see Appendix Table A.2). No other significant differences were found.

Prestimulation of monoarticular hip muscles to prepare for perturbations

We compared the muscular activity in the 'Loaded Standing' and the 'Pre-Perturbation' activation to assess if subjects increased muscular activity in anticipation of perturbation, despite the random timing and direction (Figure 3.3). Significant changes of the monoarticular hip muscles GLU of the left leg (increased by: 8 ± 13 %WEMG, $Z = 2.134$, $p = 0.033$). From all other muscles, only TFL in the right leg showed a significant reduction (see Appendix Table A.2).

Biarticular thigh muscles were major contributors to recover upper-body balance

We next tested which muscles showed the highest response activity to identify the most reactive muscles. For both perturbations, early EMG responses within the first 100 ms after the perturbation were not found. In the analysed response intervals, both perturbation directions evoked different muscular responses ('Direction' main effect: $F(1, 314) = 173.8, p < 0.001$).

For positive torque perturbation with forward upper-body pitch, we found the highest muscle activity levels for the biarticular thigh muscle HAM, the biarticular ankle muscle GAS and the monoarticular ankle muscle SOL. HAM response activity started already in the mid-latency response window (RI1) and lasted until RI3 with up to 366 ± 271 %WEMG. GAS (up to 128 ± 61 %WEMG) and SOL (up to 101 ± 35 %WEMG) responded later in RI2 or RI3. By this, HAM was found to increase its activity (in RI1 and RI2) by more than double of its mean activity during walking (Figure 3.4a) which was significantly higher than in all other muscles (see Appendix Table A.4).
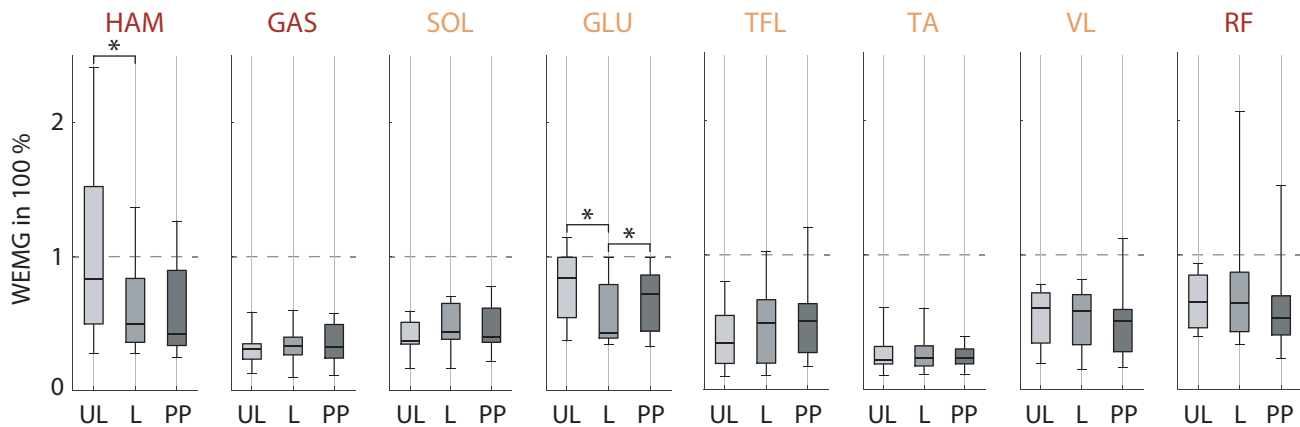
Figure 3.3: Influence of AMP artefacts and prestimulation activity. Boxplots of muscular activity of the left leg in 'Unloaded Standing' (UL), 'Loaded Standing' (L) and the mean 'Pre-Perturbation' activation of the last 10 trials per block ('Block 1' and 'Block 2') for all 11 subjects. Reported EMGs (WEMG) are the mean intervals of the filtered EMG signals normalised by the muscle's mean activity during walking (see Methods). Results are presented with significant ($^*p < 0.05$) comparisons of the paired t-test or two-sided Wilcoxon signed-rank test.

In negative perturbations, the biarticular thigh muscle RF, the monoarticular ankle flexor TA and the monoarticular knee extensor VL were found to have the highest EMG amplitude with respect to their mean activity during normal walking. RF activity was high in all response intervals (up to $866 \pm 341\,\%$WEMG). RF, TA (up to $706 \pm 435\,\%$WEMG) and VL (up to $582 \pm 178\,\%$WEMG) reached the highest response in RI2. TFL activity with a maximum of $428 \pm 257\,\%$WEMG in RI2 increased by half of the RF increase. Since 'Pre-Perturbation' activity was similar for TFL, RF and VL, RF was also the muscle with the strongest and earliest increase in activity (Figure 3.4b). Compared to all other muscles, RF reflex activity was significantly stronger than in all other muscles (see Appendix Table A.4). From a lower activity ($24 \pm 9\,\%$WEMG) before the perturbation onset, TA increased by $678 \pm 433\,\%$WEMG in RI2, but only showed low increase in RI1.

Summarising these results, biarticular thigh muscles (HAM and RF) were found to have the highest activity in the earliest response interval (RI1), the highest overall amplitude with respect to their mean activity during walking and the highest increase compared to unperturbed standing (significantly higher than all other measured muscles). Ankle joint muscles like GAS, SOL or TA contributed moderately with delayed increase, mainly in RI2 and RI3. In contrast to biarticular thigh muscles, monoarticular hip muscles GLU and TFL increased only slightly or moderately in response to the evoked upper-body pitch deflection.

Discussion

Previous research identified beneficial features of biarticular muscles that could potentially contribute to recover balance after postural perturbations (Junius et al., 2017; Sharbafi et al., 2016; Doorenbosch and Ingen Schenau, 1995; Wells and Evans, 1987). Experimental evidence that highlights the specific contribution of biarticular muscles to upper-body balance is however missing. To fill this gap of knowledge, this study examined the muscular response of major leg muscles for recovering from artificial torque perturbations to the upper body. For the first time, an Angular Momentum Perturbator (AMP) was used to
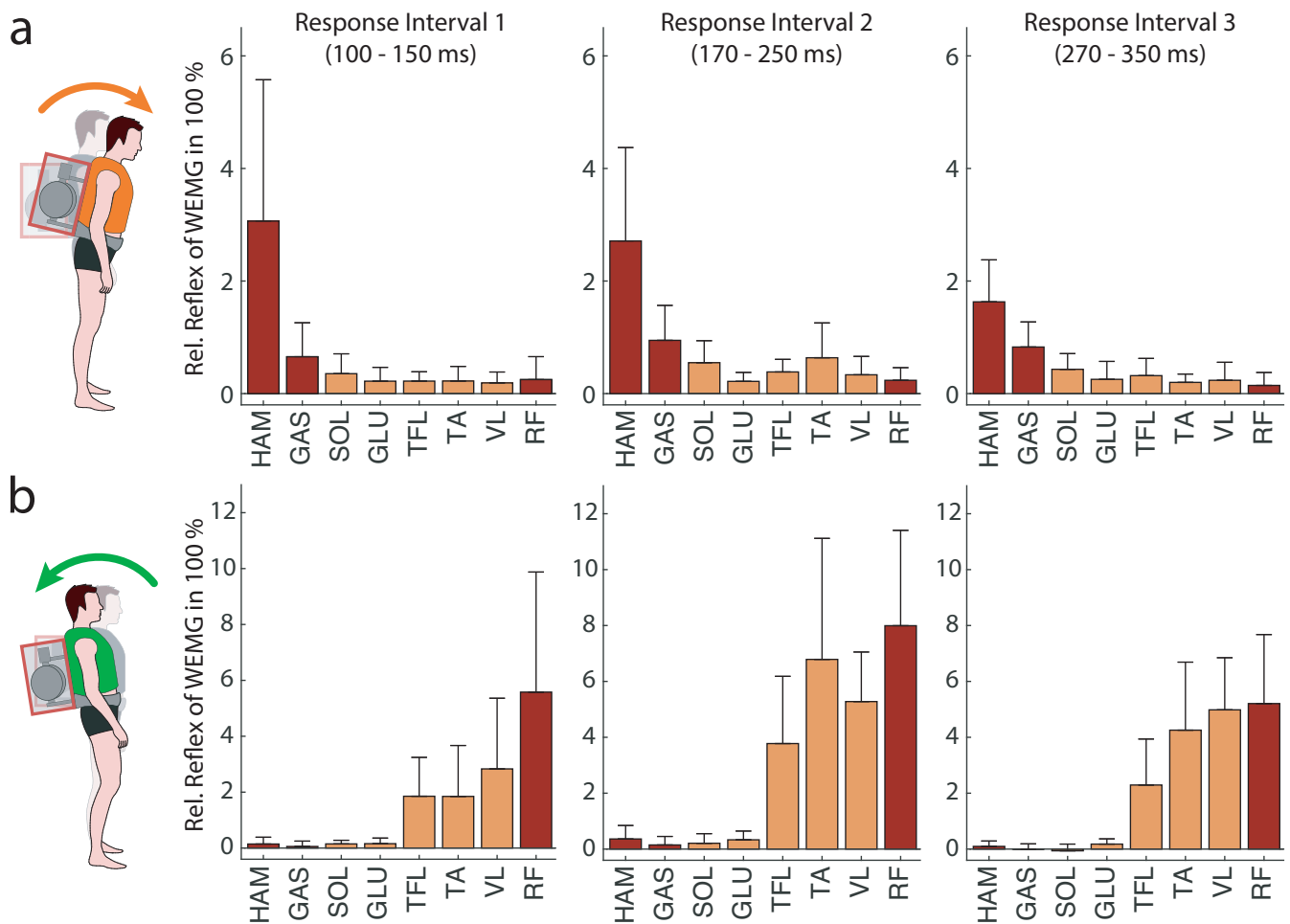
Figure 3.4: Reflex activity of mono- (yellow) and biarticular muscles (red) for (a) positive and (b) negative torque perturbations in different response intervals. Grand mean and SD of averaged relative reflex responses of the left leg (last 5 trials per condition × 2 gimbal configurations) for all 11 subjects. Relative reflex activity in each response interval is computed with respect to 'Pre-Perturbation' and normalised by the muscle's mean activity during walking (see Methods).

directly apply reproducible torques to the upper body during quiet standing without a translational (e.g. horizontal foreward/ backward force) component of other typical perturbations like pushes or pulls. By analysing the mechanical response of the subjects and EMG of major leg muscles, we found that

1. Biarticular thigh muscles HAM and RF showed the strongest increase in activity in response to upper-body balance perturbations of all measured leg muscles;

2. AMP torques resulted in nearly isolated upper-body postural alignment perturbations.

Biarticular muscles and upper-body balance

In our study, biarticular thigh muscles showed the strongest reflex responses. Perturbing the upper-body challenged the motor control system to re-erect the upper-body. The positive perturbation created forward

upper-body pitch (about 17°). Restoring the original body posture requires hip extension torques. These would cause knee overextension which must be counteracted by knee flexion torques. The biarticular HAM muscle group delivers simultaneous hip extension and knee flexion torques. This might explain our finding that the HAM showed the strongest EMG increase of all measured muscles. The negative perturbation led to backwards upper-body pitch (about $-12°$). Conversely, to re-erect the upper-body, hip flexion and knee extension torques are required. The biarticular RF muscle group delivers simultaneous hip flexion and knee extension torques. Correspondingly, the strongest EMG response was found for the biarticular RF.

Our results confirmed our hypothesis of a strong involvement of biarticular thigh muscles for restoring upper-body balance. This result agrees well with the previously suggested torque-based (net hip minus knee torque; extension torques are positive) control scheme of biarticular muscles for joint coordination in tasks involving opposing changes in hip and knee torques. For example, high HAM and RF activity was found during GRF direction manipulations in isometric and isokinetic conditions (Wells and Evans, 1987; Doorenbosch and Ingen Schenau, 1995), load-lifting (Toussaint et al., 1992; Prilutsky et al., 1998b), cycling (Ingen Schenau et al., 1992) as well as in the swing leg during walking and running (Prilutsky et al., 1998a). In contrast to these studies involving planned movements, our experiment targeted perturbation recovery. Studies in this area involving surface translations and force pushes/ pulls (Nashner, 1977; Horak and Nashner, 1986; Mergner, 2010; Welch and Ting, 2009; Rietdyk et al., 1999; Misiaszek et al., 2000; Vashista et al., 2014; Fujimoto et al., 2015; Vlutters et al., 2016; Olenšek et al., 2016; Wu et al., 2017) show that, among other muscles, biarticular muscles react to compensate for these perturbations. Our experiments refined these findings by providing evidence for a strong reactive involvement of biarticular thigh muscles to compensate torque perturbations applied at the upper body. This can most clearly be observed for the positive torque perturbation.

The positive and the negative perturbation generated different responses that might be related to joint range-of-motion constraints. While the positive perturbation lead to strong hip flexion (about 16°) and only small knee extension (about 2°, see Appendix Figure A.2), the negative perturbation generated moderate hip extension (about 6°) and strong knee flexion (about 14°, see Appendix Figure A.2). From a straight configuration as reference, the range of motion of the hip is approximately 120° flexion and only 10° hip extension (Roach and Miles, 1991). The knee constraint is even more strict with approximately 140° flexion and 2° extension (Roach and Miles, 1991). While our positive perturbation induced mainly upper body forward pitch, the negative perturbation resulted in a backwards pitch of the upper body and the thigh segments together. Thus, the asymmetric perturbation responses reflect the joint range-of-motion constraints.

The observed asymmetric perturbation responses induced different torque requirements. In the case of the positive perturbation, biarticular HAM activity seems to be sufficient to re-erect the upper body. For negative perturbations, in addition to pronounced RF activity we observed increases in activity of monoarticular knee extensors (VL) and to a lesser extent of the functionally monoarticular hip flexor muscles (TFL). It seems that despite its ability to provide for simultaneous knee extension and hip flexion torques, RF may not be able to meet the torque requirement at these joints. RF has approximately half of the physiological cross-sectional area and thus half the force capacity of HAM (Rajagopal et al., 2016). In addition, it has a lower lever arm at the hip than HAM (Visser et al., 1990; Cleather et al., 2015), which may explain the increase in activity of the functionally monoarticular hip flexor TFL. The different capacity of the biarticular HAM and RF muscles to generate joint torques may stem from an adaptation towards their daily use, reflecting a dominating use of HAM in walking and running due to a forward lean of the upper body (Grimmer and Seyfarth, 2014). For less intense negative torque perturbations, we expect to see disproportionally less pronounced knee flexion (reducing the kinematic difference between positive

and negative perturbations) and reduced activity of monoarticular muscles. RF torques might then be sufficient to re-erect the upper body.

During perturbations in both directions, different mechanisms led to opposing CoM and CoP patterns. In positive perturbations, the upper body pitched forward about the hip. During this early response, extension hip torques were generated by increased HAM activity. The hip coupling to the leg (and subsequently to the ground) resulted in a delayed acceleration of the CoM in anterior direction (after 400 ms). The CoP travel is due to ankle extension torques provided by the SOL to counteract the forward movement of the CoM. During the backward perturbation, the upper body rotated backwards by extensive bending at the knee joint. This induced a pronounced eccentric stretch of the pre-activated SOL resulting in an instantaneous increase in muscle force (Loeb et al., 1999). This explains the initial anterior CoP travel (within the first 300 ms to 400 ms). This, however, is a critical condition for balance, because both the required hip flexion (to realign the upper body) and the ankle extension accelerate the CoM backwards (Winter, 1995). To counter this, immediate deactivation of the SOL and activation of the TA would be required which we also observed in the EMG responses (RI3 in Figure 3.4b). Further proof of these interpretations requires modelling and simulation of the neuro-muscle-skeletal system.

Reported EMG signals might contain cross-talk from other muscle groups. For example, the RF might have been contaminated by activity from the vastus intermedius (Nene et al., 1999). Using needle electrodes might be a more reliable alternative. However, due to their invasive nature, the intramuscular electrodes require technical expertise, usually more time for preparing the subject and can create discomfort (Meadows, 1970; Strommen and Daube, 2001), which in turn might influence the behaviour of the subject. By following the SENIAM recommendations (Hermens et al., 1999) for skin preparation and electrode placement, and by utilising appropriate surface electrodes (Farina et al., 2002; De Luca et al., 2012), we aimed at reducing the influence of cross-talk to a minimum.

Our experiments show that the biarticular thigh muscles strongly relate to postural upper-body control in standing. We speculate that these muscles could also play a key role for upper-body balance in walking. During walking, GRFs intersect in a point above the CoM which helps to stabilise the angular momentum of the whole body similar to a physical pendulum (Maus et al., 2010; Gruben and Boehm, 2012). However, upper body stability is not achieved in this way, because the resulting forces acting on the upper body intersect below the CoM of the upper body (Müller et al., 2017). Here, biarticular muscles can help to regulate the angular momentum of the upper body by applying torques via the stance leg (Hof, 2001; Gregor et al., 1991; Toussaint et al., 1992; Sarmadi et al., 2019; Lakatos et al., 2014; Jacobs and Macpherson, 1996; Lacquaniti and Maioli, 1994) or the swing leg (Prilutsky et al., 1998a; Sharbafi et al., 2017; Dean and Kuo, 2008). The stabilising function of biarticular structures for the upper body during walking was demonstrated in a dynamically walking robot (Lakatos et al., 2016). Further perturbation experiments will target the role of biarticular muscles for upper-body balance in walking.

Anticipatory and reactive control strategies

When mechanical perturbations are applied, humans use different strategies to prepare or counteract the effect of the perturbation (MacKinnon and Winter, 1993; Mergner, 2010; Ritzmann et al., 2018). For instance, when a perturbation is expected or predicted, activity of antagonistic muscles can be increased simultaneously (co-contraction) in order to build up joint impedance before the perturbation onset (Ruit et al., 2018). This zero-delay mechanism is governed by feed-forward commands of supra-spinal centres and usually called 'prestimulation' (Loeb et al., 1999; Jacobs et al., 2008). Especially when knowledge

about the perturbation (e.g. intensity, timing or direction) is rare, joint impedance can help to preserve the body posture (Mugge et al., 2010).

In our experiment, an anticipatory co-contraction was not found. Only the monoarticular hip extensor GLU of the left leg showed an increased activity level in anticipation of the perturbation. In the right leg, the hip flexor TFL reduced its prestimulation. Explanations of this could be the influence of feed-forward commands (Loeb et al., 1999), e.g. limb dominance, or an unbalanced loading of both legs caused by the natural (lateral) sway (Winter, 1995) that was also present in our study (see Appendix Figure A.7). It is also likely that subjects adapted their prestimulation throughout the progress of the experiment. However, the results of Welch and Ting (2014), which found only modest changes of prestimulation in response to surface translations and only one to two trials with converging behaviour towards a preferred prestimulation activity, suggest that the influence of training-induced adaptation or habituation on prestimulation activity should be small.

Reactive responses ('reflexes') can (with a certain delay) respond to the perturbation by processing sensory feedback with only minimal or no prior knowledge (Mergner, 2010; Horak, 2006; Johansson and Magnusson, 1991). We found that the temporal organisation of observed muscular responses remained (with only some exceptions) similar throughout the three response intervals. However, muscular responses were only found after a delay of 100 ms after the perturbation onset. Similar delays were found for surface translations (Horak and Nashner, 1986; Welch and Ting, 2009), while other (more sudden) upper-body perturbations resulted in shorter delays of e.g. 30 ms to 80 ms (Cresswell et al., 1994; Carlson et al., 1981). Since we measured an initial change of upper-body pitch 50 ms after onset, RI1 responses can be considered medium-latency while RI2 and RI3 denote long-latency responses (Hof and Duysens, 2018). Previous studies (Safavynia and Ting, 2013; Soechting and Lacquaniti, 1988) suggest that short-latency responses (not observed in our experiment) are induced by joint errors (e.g. stretch reflexes) and long-latency responses are the result of a task-level feedback. While these long-latency responses have been found to undergo modulations of task- and context-specific constraints (Horak and Macpherson, 1996; Kurtzer et al., 2008; Shemmell et al., 2010; Martelli et al., 2013; Peterka, 2002; Horak, 2006; Nashner et al., 1982; Fitzpatrick et al., 1994), they also reflect the inter-segmental coupling of joints (Gielen et al., 1988; Lacquaniti and Soechting, 1986b; Lacquaniti and Soechting, 1986a; Koshland et al., 1991). For instance, perturbations to one joint can evoke responses in muscles that only act on unperturbed joints (Nashner, 1977; Koshland et al., 1991). Such patterns were associated with pre-defined coordination patterns (e.g. muscle synergies) that are triggered by a certain stimulus and generate purposeful responses in the context of spartio-temporal or task-specific constraints (Safavynia and Ting, 2013; Kurtzer et al., 2008; Ting, 2007) also reflecting the requirements of everyday activities, such as controlling inertial effects of e.g. accelerated, neighbouring segments (Gielen et al., 1988; Koshland et al., 1991). While reactive and anticipatory control strategies are usually combined (Horak and Nashner, 1986; Park et al., 2004; Allum et al., 1998; Forssberg and Hirschfeld, 1994; Welch and Ting, 2014), our results show that biarticular muscles mainly follow a reactive control strategy.

Such long-latency responses can also undergo adaptation processes (Safavynia and Ting, 2013). While the additional loading (the weight of the AMP) resembled a task that all subjects faced previously (e.g. when wearing a heavy backpack), pure torque perturbations are rare during activities of daily living. It is thus unlikely that subjects were familiar with the type of perturbation, resulting in adaptation or habituation effects from updating an internal model of the AMP and the applied torques. Prior information about the perturbation, learning, or training has been found to guide the selection of long-latency responses towards a strategy that also reduces muscular activity (Horak and Nashner, 1986; Welch and Ting, 2014; Horak, 1996; Keshner et al., 1987). Also, previous studies found a wide variety of adaptation processes, ranging from approximately 5 trials (Keshner et al., 1987) to more than 50 trials (Horak, 1996), so it is difficult

to conclude that adaptation had ceased during the 10 trials per condition in our experiment. However, to reduce influences of learning on the reflex responses (Welch and Ting, 2014), we considered only the last 5 of the 10 trials per condition. Still, we cannot exclude further training or learning of subjects. Nevertheless, given also other factors, such as an accelerated rate of fatigue during load carriage, the number of discarded trials must be kept small for practicality.

Gyroscopic perturbation generation

The AMP is an example of 'reactionless actuation', in which torques are exerted by exchanging angular momentum with the actuator itself, rather than by exerting forces against the ground or an inertially-fixed object (e.g. an immobile robot transmitting forces via linkages or cables). This principle has both theoretical and practical benefits for perturbation experiments.

Specificity of a perturbation is difficult to achieve. Force-controlled systems are generally preferred over position-controlled systems due to their absence of kinematic constraints and more natural responses (Vlugt et al., 2003; Maaswinkel et al., 2016). While it is, in principle, possible to generate a pure torque with a pair of opposing forces, it is, in practice, difficult to synchronise these forces and track the location of the CoM in real-time. Reactionless actuation is attractive because both synchronisation and alignment of the equivalent force couple happens inherently.

A practical benefit of reactionless actuation is that, since there is no necessity to exert forces against an inertially-fixed environment, the actuator can be entirely self-contained and even take the form of a wearable backpack, as in the AMP. This enables the AMP to be portable and suitable for overground experiments, and to be combined with other systems (e.g. treadmills, other perturbators) and measurement apparatus (e.g. motion capture, force plates) with minimal interference. To study other balance mechanisms in the future, wearable reactionless actuators might be placed on other parts of the body to perturb specific limbs. For various other (assistive) applications, such actuators have already been described for placement on the arms (Jarc et al., 2006; Muller and Popovic, 2018), legs (Odajima, 2009; Jabeen et al., 2019), and distributed across the body (Duda et al., 2015).

The gyroscopic torque vector rotates along with the gimbal creating – together with the desired pitch perturbation – roll torque components in the frontal plane (Equation 3.2). While the gimbal initial angle and total rotation were chosen to reduce the magnitude of this roll component, it was nevertheless present. In additional conditions in which the gimbal was rotated by 180°, the same pitch perturbations were produced but with the opposite roll components. From this, it was established that a lateral trunk lean did occur (up to 8°, see Appendix Figure A.9), and that the load shifted from one leg to the other, but that this did not appear with asymmetric magnitudes or dependent of the side of dominance (see Appendix Figures A.10 and A.11).

The frontal balancing of the upper body is mainly achieved by an (un-)loading mechanism of hip abductors (MacKinnon and Winter, 1993; Winter et al., 1996) in which the torque generated by gravity is compensated by hip abductor activity to regulate angular momentum and ensure frontal upper-body balance (Jansen et al., 2014; John et al., 2012; Neptune and McGowan, 2016). Since the AMP also generated roll torque components, it is likely that also frontal balance control strategies were used. This would probably result in altered hip muscle activities (depending on the corresponding perturbation torque) as found by previous multidirectional perturbation studies when applying surface transitions (Moore et al., 1988; Henry et al., 1998; Torres-Oviedo and Ting, 2010; Gruneberg et al., 2005; Torres-Oviedo and Ting, 2007) and rotations (Gruneberg et al., 2005; Carpenter et al., 1999). Given that each leg individually controls the

CoP (MacKinnon and Winter, 1993), cross-talk from the contralateral leg to ipsilateral ankle joint muscles should be small. For the hip, however, neuronal coupling of both legs – next to their mechanical interaction – e.g. by interneurons is very likely. Still, muscular responses did not appear to differ (see Appendix Figures A.12 to A.14) allowing us to merge both conditions of inverted roll but similar pitch perturbations.

To generate a rotation of the gimbal wrt. to the body frame of the subjects, a peak gimbal torque of $12\,\mathrm{Nm}$ was necessary. This torque created an angular acceleration (Equation 3.2) that resulted in upper-body yaw rotations of 3° to 5° (see Appendix Figure A.8). This could especially influence GLU and TFL activity, as both muscles also function to generate a leg rotation in the transversal plane (wrt. to the pelvis). However, since the observed upper-body yaw was small compared to our main perturbation direction, such influence is expected to be small. A future version of the AMP may use instead two or more smaller actuators to allow both the magnitude and direction of the torque vector to be controlled simultaneously, thereby eliminating torques in unintended directions (Brown and Peck, 2008) and allowing multi-directional perturbation studies (Ting, 2007; Torres-Oviedo and Ting, 2007).

A drawback of the selected actuation principle is that the mass of the actuator is borne by the test subject and cannot be placed externally. The prototype AMP in this study weighed $16\,\mathrm{kg}$, or $15\,\%$ to $29\,\%$ of the participant's body weight. Other studies of standing with similar backpack load showed tendencies of increasing activity for anterior and reductions for posterior muscles groups. In particular, non-significant increases of VL, RF and reduced HAM activity as well as increased CoP sway were found (Al-Khabbaz et al., 2008; Schiffman et al., 2006). In our study, significant reductions in muscle activity were only seen in GLU, HAM of the left leg and VL of the right leg. Still, we cannot exclude other influences of e.g. modulation of muscular stiffness or related effects on balance. Also, an increased hip flexion (by 6.2°), more extended knee (by 2.1°) and increased CoP sway were found (see Appendix Table A.1 and Figure A.7). The additional weight makes the balance control more challenging (Schiffman et al., 2006). When being perturbed, it is likely that the added moment of inertia of the AMP helped subjects to maintain the initial upper-body posture. The influence of muscle fatigue should be small, since subjects had sufficient time to rest. Additionally, also the generated vibrations or the noise could result in changed muscle activity, e.g. by stimulating muscle-spindle proprioception (Roden-Reynolds et al., 2015; Kavounoudias et al., 1999) or psychological factors like attention or anxiety (Lacour et al., 2008; Woollacott and Shumway-Cook, 2002; Adkin et al., 2000; Adkin et al., 2002).

In future generations of the AMP it will be possible to reduce the mass substantially by (i) using lightweight components, (ii) scaling down the maximum possible perturbation magnitude, (iii) increasing the diameter of the flywheel, or (iv) rotating the flywheel faster. Lightweight reactionless actuators that are wearable (Jarc et al., 2006; Duda et al., 2015; Muller and Popovic, 2018; De Panisse et al., 2018) or handheld (Yano et al., 2003; Gagne et al., 2012) have been recently developed, and the technology has even been demonstrated on the sub-gram scale (Chang et al., 2010). However, for the same perturbation magnitude, we estimate that it is currently feasible to construct a AMP weighing approximately half the one used in this study.

Conclusion

This study investigated the specific role of biarticular muscles in dealing with upper-body pitch perturbations in human standing. Our main finding was that biarticular thigh muscles (hamstring and rectus femoris) showed the strongest response of all measured major leg muscles. Our results indicate a reactive control for biarticular thigh muscles in line with a previously suggested torque control strategy considering the difference between hip and knee torques. To the knowledge of the authors, this was the first study

on human subjects providing experimental evidence that biarticular muscles play a key role in reactive upper-body balance control.

In order to focus on upper-body balance while reducing method-dependent artefacts (arising e.g. from inter-segmental couplings or global perturbations), a new type of perturbation was applied by the Angular Momentum Perturbator (AMP). Complementing existing perturbation devices, the generated torque perturbation at the trunk provides a new methodology for studying human response strategies.

Future research will involve applying mechanical and neuromechanical models (Winter, 1995; Barin, 1989; Welch and Ting, 2009; Rajagopal et al., 2016; Afschrift et al., 2018) and/or data-driven approaches (Xue et al., 2016) to increase our understanding of underlying control mechanisms as well as classification of user intention, e.g. for controlling wearable robotic devices like the AMP.

A deeper understanding of postural balance control of the upper body and involved muscle responses will facilitate the design of robotic systems for assistance or rehabilitation and improve the effectiveness of physical training for fall prevention e.g. for elderly people.

Data availability

Processed datasets of the AMP, kinematic, kinetic, electromyographic and anthropometric data that were used in this study are available in the 4TU.ResearchData repository (Schumacher et al., 2019).

Acknowledgements

Author Contributions

C.S., A.B., D.L., A.S. and H.V. contributed conception and design of the study; C.S. organised the database; C.S. and C.R. performed the statistical analysis; C.S. wrote the first draft of the manuscript; C.S., A.B., C.R. wrote sections of the manuscript. All authors contributed to revision of the manuscript, and read and approved the submitted version.

Competing interests

The authors declare no competing interests.

References

A. L. Adkin et al. (2000). "Postural control is scaled to level of postural threat". In: *Gait & posture* 12.2, pp. 87–93.

A. L. Adkin et al. (2002). "Fear of falling modifies anticipatory postural control". In: *Experimental brain research* 143.2, pp. 160–170.

M. Afschrift et al. (2018). "Modulation of gluteus medius activity reflects the potential of the muscle to meet the mechanical demands during perturbed walking". In: *Scientific reports* 8.1, p. 11675.

J. Allum et al. (1998). "Proprioceptive control of posture: a review of new concepts". In: *Gait & posture* 8.3, pp. 214–242.

K. Barin (1989). "Evaluation of a generalized model of human postural dynamics and control in the sagittal plane". In: *Biological cybernetics* 61.1, pp. 37–50.

A. Berry et al. (2016). "Directional singularity-robust torque control for gyroscopic actuators". In: *IEEE/ASME Transactions on Mechatronics* 21.6, pp. 2755–2763.

D. Brown and M. A. Peck (2008). "Scissored-pair control-moment gyros: a mechanical constraint saves power". In: *Journal of guidance, control, and dynamics* 31.6, pp. 1823–1826.

H. Carlson et al. (1981). "Motor responses in the human trunk due to load perturbations". In: *Acta Physiologica Scandinavica* 111.2, pp. 221–223.

M. G. Carpenter, J. H. Allum, and F. Honegger (1999). "Directional sensitivity of stretch reflexes and balance corrections for normal subjects in the roll and pitch planes". In: *Experimental brain research* 129.1, pp. 93–113.

H. Chang et al. (2010). "Design and simulation of a MEMS control moment gyroscope for the sub-kilogram spacecraft". In: *Sensors* 10.4, pp. 4130–4144.

D. J. Cleather, D. F. Southgate, and A. M. Bull (2015). "The role of the biarticular hamstrings and gastrocnemius muscles in closed chain lower limb extension". In: *Journal of theoretical biology* 365, pp. 217–225.

A. Cresswell, L. Oddsson, and A. Thorstensson (1994). "The influence of sudden perturbations on trunk muscle activity and intra-abdominal pressure while standing". In: *Experimental brain research* 98.2, pp. 336–341.

C. J. De Luca et al. (2012). "Inter-electrode spacing of surface EMG sensors: reduction of crosstalk contamination during voluntary contractions". In: *Journal of biomechanics* 45.3, pp. 555–561.

P. De Panisse et al. (2018). *Tremor stabilisation apparatus and methods*. US Patent App. 15/539,089.

J. C. Dean and A. D. Kuo (2008). "Elastic coupling of limb joints enables faster bipedal walking". In: *Journal of the Royal Society Interface* 6.35, pp. 561–573.

C. A. Doorenbosch and G. J. van Ingen Schenau (1995). "The role of mono-and bi-articular muscles during contact control leg tasks in man". In: *Human Movement Science* 14.3, pp. 279–300.

K. R. Duda et al. (2015). "The variable vector countermeasure suit (V2Suit) for space habitation and exploration". In: *Frontiers in systems neuroscience* 9, p. 55.

L. J. Elias, M. P. Bryden, and M. B. Bulman-Fleming (1998). "Footedness is a better predictor than is handedness of emotional lateralization". In: *Neuropsychologia* 36.1, pp. 37–43.

D. Engelhart et al. (2015). "Adaptation of multijoint coordination during standing balance in healthy young and healthy old individuals". In: *Journal of neurophysiology* 115.3, pp. 1422–1435.

D. Farina et al. (2002). "Surface EMG crosstalk between knee extensor muscles: experimental and model results". In: *Muscle & Nerve: Official Journal of the American Association of Electrodiagnostic Medicine* 26.5, pp. 681–695.

R. Fitzpatrick, D. K. Rogers, and D. McCloskey (1994). "Stable human standing with lower-limb muscle afferents providing the only sensory input." In: *The Journal of physiology* 480.2, pp. 395–403.

H. Forssberg and H. Hirschfeld (1994). "Postural adjustments in sitting humans following external perturbations: muscle activity and kinematics". In: *Experimental Brain Research* 97.3, pp. 515–527.

M. Fujimoto, W.-N. Bair, and M. W. Rogers (2015). "Center of pressure control for balance maintenance during lateral waist-pull perturbations in older adults". In: *Journal of biomechanics* 48.6, pp. 963–968.

M. Fujiwara and J. V. Basmajian (1975). "Electromyographic study of two-joint muscles." In: *American journal of physical medicine* 54.5, pp. 234–242.

J. Gagne et al. (2012). "Gyrolock: stabilizing the heart with control moment gyroscope (CMG)—from concept to first in vivo assessments". In: *IEEE Transactions on robotics* 28.4, pp. 942–954.

C. Gielen, L. Ramaekers, and E. Van Zuylen (1988). "Long-latency stretch reflexes as co-ordinated functional responses in man." In: *The Journal of physiology* 407.1, pp. 275–292.

R. J. Gregor, J. P. Broker, and M. M. Ryan (1991). "The Biomechanics of Cycling". In: *Exercise and sport sciences reviews* 19.1, pp. 127–170.

M. Grimmer and A. Seyfarth (2014). "Mimicking human-like leg function in prosthetic limbs". In: *Neuro-Robotics*. Springer, pp. 105–155.

K. G. Gruben and W. L. Boehm (2012). "Force direction pattern stabilizes sagittal plane mechanics of human walking". In: *Human movement science* 31.3, pp. 649–659.

C. Gruneberg et al. (2005). "Spatio-temporal separation of roll and pitch balance-correcting commands in humans". In: *Journal of neurophysiology* 94.5, pp. 3143–3158.

S. M. Henry, J. Fung, and F. B. Horak (1998). "EMG responses to maintain stance during multidirectional surface translations". In: *Journal of Neurophysiology* 80.4, pp. 1939–1950.

H. J. Hermens et al. (1999). "European recommendations for surface electromyography". In: *Roessingh research and development* 8.2, pp. 13–54.

A. Hof (2001). "The force resulting from the action of mono-and biarticular muscles in a limb". In: *Journal of biomechanics* 34.8, pp. 1085–1089.

A. Hof and J. Duysens (2018). "Responses of human ankle muscles to mediolateral balance perturbations during walking". In: *Human movement science* 57, pp. 69–82.

F. B. Horak (1996). "Adaptation of automatic postural responses". In: *The acquisition of motor behavior in vertebrates*. The MIT Press, Cambridge, MA, pp. 57–85.

F. B. Horak (2006). "Postural orientation and equilibrium: what do we need to know about neural control of balance to prevent falls?" In: *Age and ageing* 35.suppl_2, pp. ii7–ii11.

F. B. Horak and J. M. Macpherson (1996). "Postural orientation and equilibrium". In: *Handbook of physiology* 1, pp. 255–292.

F. B. Horak and L. M. Nashner (1986). "Central programming of postural movements: adaptation to altered support-surface configurations". In: *Journal of neurophysiology* 55.6, pp. 1369–1381.

G. van Ingen Schenau et al. (1992). "The constrained control of force and position in multi-joint movements". In: *Neuroscience* 46.1, pp. 197–207.

G. van Ingen Schenau et al. (1995). "The control of mono-articular muscles in multijoint leg extensions in man." In: *The Journal of physiology* 484.1, pp. 247–254.

S. Jabeen et al. (2019). "Assisting gait with free moments or joint moments on the swing leg". In: *2019 IEEE 16th International Conference on Rehabilitation Robotics (ICORR)*. IEEE, pp. 1079–1084.

J. V. Jacobs et al. (2008). "Changes in the activity of the cerebral cortex relate to postural response modification when warned of a perturbation". In: *Clinical Neurophysiology* 119.6, pp. 1431–1442.

R. Jacobs and J. M. Macpherson (1996). "Two functional muscle groupings during postural equilibrium tasks in standing cats". In: *Journal of Neurophysiology* 76.4, pp. 2402–2411.

K. Jansen et al. (2014). "How gravity and muscle action control mediolateral center of mass excursion during slow walking: a simulation study". In: *Gait & posture* 39.1, pp. 91–97.

A. Jarc et al. (2006). "The Design and Control of a Low-Power, Upper-Limb Prosthesis". In: *Proceedings of the IEEE 32nd Annual Northeast Bioengineering Conference*. IEEE, pp. 165–166.

R. Johansson and M. Magnusson (1991). "Human postural dynamics." In: *Critical reviews in biomedical engineering* 18.6, pp. 413–437.

C. T. John et al. (2012). "Contributions of muscles to mediolateral ground reaction force over a range of walking speeds". In: *Journal of biomechanics* 45.14, pp. 2438–2443.

K. Junius et al. (2017). "Biarticular elements as a contributor to energy efficiency: biomechanical review and application in bio-inspired robotics". In: *Bioinspiration & biomimetics* 12.6, p. 061001.

A. Kavounoudias et al. (1999). "From balance regulation to body orientation: two goals for muscle proprioceptive information processing?" In: *Experimental Brain Research* 124.1, pp. 80–88.

E. Keshner, J. Allum, and C. Pfaltz (1987). "Postural coactivation and adaptation in the sway stabilizing responses of normals and patients with bilateral vestibular deficit". In: *Experimental Brain Research* 69.1, pp. 77–92.

Y. S. Al-Khabbaz, T. Shimada, and M. Hasegawa (2008). "The effect of backpack heaviness on trunk-lower extremity muscle activities and trunk posture". In: *Gait & posture* 28.2, pp. 297–302.

G. Koshland, Z. Hasan, and L. Gerilovsky (1991). "Activity of wrist muscles elicited during imposed or voluntary movements about the elbow joint". In: *Journal of motor behavior* 23.2, pp. 91–100.

I. L. Kurtzer, J. A. Pruszynski, and S. H. Scott (2008). "Long-latency reflexes of the human arm reflect an internal model of limb dynamics". In: *Current Biology* 18.6, pp. 449–453.

M. Lacour, L. Bernard-Demanze, and M. Dumitrescu (2008). "Posture control, aging, and attention resources: models and posture-analysis methods". In: *Neurophysiologie Clinique/Clinical Neurophysiology* 38.6, pp. 411–421.

F. Lacquaniti and C. Maioli (1994). "Independent control of limb position and contact forces in cat posture". In: *Journal of Neurophysiology* 72.4, pp. 1476–1495.

F. Lacquaniti and J. Soechting (1986a). "EMG responses to load perturbations of the upper limb: Effect of dynamic coupling between shoulder and elbow motion". In: *Experimental Brain Research* 61.3, pp. 482–496.

F. Lacquaniti and J. Soechting (1986b). "Responses of mono-and bi-articular muscles to load perturbations of the human arm". In: *Experimental Brain Research* 65.1, pp. 135–144.

D. Lakatos et al. (2014). "Design and control of compliantly actuated bipedal running robots: Concepts to exploit natural system dynamics". In: *Humanoid Robots (Humanoids), 2014 14th IEEE-RAS International Conference on*. IEEE, pp. 930–937.

D. Lakatos et al. (2016). "Dynamic bipedal walking by controlling only the equilibrium of intrinsic elasticities". In: *Humanoid Robots (Humanoids), 2016 IEEE-RAS 16th International Conference on*. IEEE, pp. 1282–1289.

D. Lemus, J. van Frankenhuyzen, and H. Vallery (2017). "Design and Evaluation of a Balance Assistance Control Moment Gyroscope". In: *Journal of Mechanisms and Robotics* 9.5, p. 051007.

G. E. Loeb, I. E. Brown, and E. J. Cheng (1999). "A hierarchical foundation for models of sensorimotor control". In: *Experimental brain research* 126.1, pp. 1–18.

E. Maaswinkel et al. (2016). "Methods for assessment of trunk stabilization, a systematic review". In: *Journal of Electromyography and Kinesiology* 26, pp. 18–35.

C. D. MacKinnon and D. A. Winter (1993). "Control of whole body balance in the frontal plane during human walking". In: *Journal of biomechanics* 26.6, pp. 633–644.

D. Martelli et al. (2013). "Angular momentum during unexpected multidirectional perturbations delivered while walking". In: *IEEE Transactions on Biomedical Engineering* 60.7, pp. 1785–1795.

H.-M. Maus, J. Rummel, and A. Seyfarth (2008). "Stable upright walking and running using a simple pendulum based control scheme". In: *Advances in Mobile Robotics*. World Scientific, pp. 623–629.

H.-M. Maus et al. (2010). "Upright human gait did not provide a major mechanical challenge for our ancestors". In: *Nature communications* 1, p. 70.

J. Meadows (1970). "Observations on muscle pain in man, with particular reference to pain during needle electromyography". In: *Journal of Neurology, Neurosurgery & Psychiatry* 33.4, pp. 519–523.

T. Mergner (2010). "A neurological view on reactive human stance control". In: *Annual Reviews in Control* 34.2, pp. 177–198.

J. E. Misiaszek et al. (2000). "Early corrective reactions of the leg to perturbations at the torso during walking in humans". In: *Experimental brain research* 131.4, pp. 511–523.

S. Moore et al. (1988). "Human automatic postural responses: responses to horizontal perturbations of stance in multiple directions". In: *Experimental brain research* 73.3, pp. 648–658.

W. Mugge et al. (2010). "A rigorous model of reflex function indicates that position and force feedback are flexibly tuned to position and force tasks". In: *Experimental brain research* 200.3-4, pp. 325–340.

M. K. Muller and M. B. Popovic (2018). *Gyroscopically controlled balance prosthetic*. US Patent App. 15/948,270.

R. Müller et al. (2017). "Force direction patterns promote whole body stability even in hip-flexed walking, but not upper body stability in human upright walking". In: *Proceedings of the Royal Society A: Mathematical, Physical and Engineering Sciences* 473.2207, p. 20170404.

L. M. Nashner, F. O. Black, and C. Wall (1982). "Adaptation to altered support and visual conditions during stance: patients with vestibular deficits". In: *Journal of Neuroscience* 2.5, pp. 536–544.

L. M. Nashner (1977). "Fixed patterns of rapid postural responses among leg muscles during stance". In: *Experimental Brain Research* 30.1, pp. 13–24.

A. Nene, R. Mayagoitia, and P. Veltink (1999). "Assessment of rectus femoris function during initial swing phase". In: *Gait & posture* 9.1, pp. 1–9.

R. R. Neptune and C. P. McGowan (2016). "Muscle contributions to frontal plane angular momentum during walking". In: *Journal of biomechanics* 49.13, pp. 2975–2981.

T. Odajima (2009). *Assist Device and Its Controlling Method*. JP2009254741A.

A. Olenšek, M. Zadravec, and Z. Matja i (2016). "A novel robot for imposing perturbations during overground walking: mechanism, control and normative stepping responses". In: *Journal of neuroengineering and rehabilitation* 13.1, p. 55.

S. Park, F. B. Horak, and A. D. Kuo (2004). "Postural feedback responses scale with biomechanical constraints in human standing". In: *Experimental brain research* 154.4, pp. 417–427.

R. Peterka (2002). "Sensorimotor integration in human postural control". In: *Journal of neurophysiology* 88.3, pp. 1097–1118.

M. Pijnappels, M. F. Bobbert, and J. H. van Dieën (2005). "How early reactions in the support limb contribute to balance recovery after tripping". In: *Journal of Biomechanics* 38.3, pp. 627–634.

M. Plooij et al. (2018). "Design of RYSEN: An Intrinsically Safe and Low-Power Three-Dimensional Overground Body Weight Support". In: *IEEE Robotics and Automation Letters* 3.3, pp. 2253–2260.

B. I. Prilutsky et al. (1998a). "Is coordination of two-joint leg muscles during load lifting consistent with the strategy of minimum fatigue?" In: *Journal of Biomechanics* 31.11, pp. 1025–1034.

B. I. Prilutsky et al. (1998b). "Is coordination of two-joint leg muscles during load lifting consistent with the strategy of minimum fatigue?" In: *Journal of Biomechanics* 31.11, pp. 1025–1034.

A. Rajagopal et al. (2016). "Full-Body Musculoskeletal Model for Muscle-Driven Simulation of Human Gait." In: *IEEE Trans. Biomed. Engineering* 63.10, pp. 2068–2079.

S. Rietdyk et al. (1999). "Balance recovery from medio-lateral perturbations of the upper body during standing". In: *Journal of biomechanics* 32.11, pp. 1149–1158.

R. Ritzmann et al. (2018). "Stimulus prediction and postural reaction: Phase-specific modulation of soleus H-reflexes is related to changes in joint kinematics and segmental strategy in perturbed upright stance". In: *Frontiers in integrative neuroscience* 12, p. 62.

K. E. Roach and T. P. Miles (1991). "Normal hip and knee active range of motion: the relationship to age". In: *Physical therapy* 71.9, pp. 656–665.

D. C. Roden-Reynolds et al. (2015). "Hip proprioceptive feedback influences the control of mediolateral stability during human walking". In: *Journal of neurophysiology* 114.4, pp. 2220–2229.

M. van de Ruit et al. (2018). "Revealing Time-Varying Joint Impedance With Kernel-Based Regression and Nonparametric Decomposition". In: *IEEE Transactions on Control Systems Technology*.

S. A. Safavynia and L. H. Ting (2013). "Long-latency muscle activity reflects continuous, delayed sensorimotor feedback of task-level and not joint-level error". In: *Journal of neurophysiology* 110.6, pp. 1278–1290.

A. Sarmadi et al. (2019). "Concerted control of stance and balance locomotor subfunctions-Leg force as a conductor". In: *IEEE Transactions on Medical Robotics and Bionics*.

H. Schaub, S. R. Vadali, J. L. Junkins, et al. (1998). "Feedback control law for variable speed control moment gyros". In: *Journal of the Astronautical Sciences* 46.3, pp. 307–328.

J. M. Schiffman et al. (2006). "Effects of carried weight on random motion and traditional measures of postural sway". In: *Applied Ergonomics* 37.5, pp. 607–614.

C. Schumacher et al. (2019). *Supplementary data on the research of Gyroscopic upper-body balance perturbations*. en. *4TU.Centre for Research Data*, https://data.4tu.nl/repository/uuid:dcabb475-6d78-4730-afe0-04c6b9d5ea83.

M. A. Sharbafi et al. (2016). "A new biarticular actuator design facilitates control of leg function in BioBiped3". In: *Bioinspiration & biomimetics* 11.4, p. 046003.

M. A. Sharbafi et al. (2017). "Reconstruction of human swing leg motion with passive biarticular muscle models". In: *Human movement science* 52, pp. 96–107.

J. Shemmell, M. A. Krutky, and E. J. Perreault (2010). "Stretch sensitive reflexes as an adaptive mechanism for maintaining limb stability". In: *Clinical Neurophysiology* 121.10, pp. 1680–1689.

C. Shirota et al. (2017). "Robot-supported assessment of balance in standing and walking". In: *Journal of neuroengineering and rehabilitation* 14.1, p. 80.

J. Soechting and F. Lacquaniti (1988). "Quantitative evaluation of the electromyographic responses to multidirectional load perturbations of the human arm". In: *Journal of Neurophysiology* 59.4, pp. 1296–1313.

J. A. Strommen and J. R. Daube (2001). "Determinants of pain in needle electromyography". In: *Clinical neurophysiology* 112.8, pp. 1414–1418.

P.-F. Tang, M. H. Woollacott, and R. K. Chong (1998). "Control of reactive balance adjustments in perturbed human walking: roles of proximal and distal postural muscle activity". In: *Experimental brain research* 119.2, pp. 141–152.

L. H. Ting (2007). "Dimensional reduction in sensorimotor systems: a framework for understanding muscle coordination of posture". In: *Progress in brain research* 165, pp. 299–321.

G. Torres-Oviedo and L. H. Ting (2007). "Muscle synergies characterizing human postural responses". In: *Journal of neurophysiology* 98.4, pp. 2144–2156.

G. Torres-Oviedo and L. H. Ting (2010). "Subject-specific muscle synergies in human balance control are consistent across different biomechanical contexts". In: *American Journal of Physiology-Heart and Circulatory Physiology*.

H. Toussaint et al. (1992). "Coordination of the leg muscles in backlift and leglift." In: *Journal of biomechanics* 25.11, p. 1279.

V. Vashista, X. Jin, and S. K. Agrawal (2014). "Active tethered pelvic assist device (a-tpad) to study force adaptation in human walking". In: *Robotics and Automation (ICRA), 2014 IEEE International Conference on*. IEEE, pp. 718–723.

J. Visser et al. (1990). "Length and moment arm of human leg muscles as a function of knee and hip-joint angles". In: *European journal of applied physiology and occupational physiology* 61.5-6, pp. 453–460.

E. de Vlugt et al. (2003). "A force-controlled planar haptic device for movement control analysis of the human arm". In: *Journal of neuroscience methods* 129.2, pp. 151–168.

M. Vlutters, E. H. Van Asseldonk, and H. Van der Kooij (2016). "Center of mass velocity-based predictions in balance recovery following pelvis perturbations during human walking". In: *Journal of experimental biology* 219.10, pp. 1514–1523.

T. D. Welch and L. H. Ting (2009). "A feedback model explains the differential scaling of human postural responses to perturbation acceleration and velocity". In: *Journal of Neurophysiology* 101.6, pp. 3294–3309.

T. D. Welch and L. H. Ting (2014). "Mechanisms of motor adaptation in reactive balance control". In: *PLoS One* 9.5, e96440.

R. Wells and N. Evans (1987). "Functions and recruitment patterns of one-and two-joint muscles under isometric and walking conditions". In: *Human movement science* 6.4, pp. 349–372.

D. A. Winter (1995). "Human balance and posture control during standing and walking". In: *Gait & posture* 3.4, pp. 193–214.

D. A. Winter et al. (1996). "Unified theory regarding A/P and M/L balance in quiet stance". In: *Journal of neurophysiology* 75.6, pp. 2334–2343.

M. Woollacott and A. Shumway-Cook (2002). "Attention and the control of posture and gait: a review of an emerging area of research". In: *Gait & posture* 16.1, pp. 1–14.

M. Wu, G. Brown, K. E. Gordon, et al. (2017). "Control of locomotor stability in stabilizing and destabilizing environments". In: *Gait & posture* 55, pp. 191–198.

Y. Xue, S. Rodriguez, and P. Bogdan (2016). "A spatio-temporal fractal model for a CPS approach to brain-machine-body interfaces". In: *2016 Design, Automation & Test in Europe Conference & Exhibition (DATE)*. IEEE, pp. 642–647.

H. Yano, M. Yoshie, and H. Iwata (2003). "Development of a non-grounded haptic interface using the gyro effect". In: *11th Symposium on Haptic Interfaces for Virtual Environment and Teleoperator Systems, 2003. HAPTICS 2003. Proceedings.* IEEE, pp. 32–39.

4 Article III: Sensor-motor Maps for Describing Linear Reflex Composition in Hopping

Christian Schumacher and André Seyfarth

Abstract

In human and animal motor control several sensory organs contribute to a network of sensory pathways modulating the motion depending on the task and the phase of execution to generate daily motor tasks such as locomotion. To better understand the individual *and* joint contribution of reflex pathways in locomotor tasks, we developed a neuromuscular model that describes hopping movements. In this model, we consider the influence of proprioceptive length (LFB), velocity (VFB) and force feedback (FFB) pathways of a leg extensor muscle on hopping stability, performance and efficiency (metabolic effort). Therefore, we explore the space describing the blending of the monosynaptic reflex pathway gains. We call this reflex parameter space a *sensor-motor map*. The sensor-motor maps are used to visualize the functional contribution of sensory pathways in multisensory integration. We further evaluate the robustness of these sensor-motor maps to changes in tendon elasticity, body mass, segment length and ground compliance.

The model predicted that different reflex pathway compositions selectively optimize specific hopping characteristics (e.g. performance and efficiency). Both FFB and LFB were pathways that enable hopping. FFB resulted in the largest hopping heights, LFB enhanced hopping efficiency and VFB had the ability to disable hopping. For the tested case, the topology of the sensor-motor maps as well as the location of functionally optimal compositions were invariant to changes in system designs (tendon elasticity, body mass, segment length) or environmental parameters (ground compliance).

Our results indicate that different feedback pathway compositions may serve different functional roles. The topology of the sensor-motor map was predicted to be robust against changes in the mechanical system design indicating that the reflex system can use different morphological designs, which does not apply for most robotic systems (for which the control often follows a specific design). Consequently, variations in body mechanics are permitted with consistent compositions of sensory feedback pathways. Given the variability in human body morphology, such variations are highly relevant for human motor control.

Introduction

The redundancy of the musculoskeletal and neural systems poses a major challenge in human locomotion research. For instance, the motor control system may utilize different strategies for performing specific motions with redundancy in the body's physiology (e.g. many involved muscles), kinematics (e.g. redundant motion trajectories) (Bernstein, 1967), and neuromuscular control (e.g. recruitment of motor units) (Henneman et al., 1965) including neural networks in the spinal cord that contribute substantially to controlling rhythmic and repetitive motions. To date, it is unknown how the neuromuscular system explores and exploits the redundancy and how the different levels are organized and interconnected to achieve functionally relevant activation patterns (Donelan and Pearson, 2004a). Proprioceptive feedback and central pattern generator (CPG) presumably generate appropriate motor control commands depending on the tasks and the phase of the motion (Dietz, 1992; Taube et al., 2012).

Similarly, computational approaches aiming at mimicking human activation patterns and motion trajectories must address the 'redundancy problem' in motor control. Most commonly, these approaches reduce the degrees of freedom by specific neuromuscular structures or hierarchies (e.g. specific combinations of CPG, sensory pathways etc.) that follow certain control policies or rules. For instance, Song and Geyer (2015) used multiple 'spinal modules' (decentralized feedback control) coordinated by a supra-spinal layer to predict several gaits and generate robust behavior even after perturbations (Song and Geyer, 2017). Other

studies used combinations of CPG and proprioceptive feedback (modifying the central patterns) to generate appropriate activation patterns (Taga, 1998; Ogihara and Yamazaki, 2001; Hase et al., 2003; Paul et al., 2005). Moreover, muscle synergies (groups of synchronized co-contracting muscles during a motion) are used to reduce the dimensionality and thus the redundancy of the neuromuscular system (D'Avella et al., 2003; Bizzi et al., 2008). For instance, Ting et al. (2012) used a neuronal network for generating a muscle synergy driven balancing task based on center of mass (CoM) kinematics.

In contrast to previous studies with a detailed representation of the neural networks (including their hierarchies), this study focused on integrating multiple sensory pathways at the elementary sensor-motor-level (Loeb, 1995) to determine how individual reflex pathways of muscle force (FFB), fiber length (LFB) and velocity (VFB) can support – in isolation *and* in combination – the repulsive leg function (Sharbafi and Seyfarth, 2017) during the stance phase of hopping (Haeufle et al., 2012). By blending individual sensory pathways, we investigated the capacity of the neuromuscular feedback system to generate goal-directed motions. We visualized and evaluated the space in which the monosynaptic reflex system can operate to generate functional motions (for generating stable, performant or efficient hopping). We call these reflex parameter spaces sensor-motor maps and suggest that studying their topology can be used to explore the redundancy of multisensory integration. This approach differs from previous approaches because the general concept of such sensor-motor maps only relies on a few primitive assumptions on the neuromuscular structure. The topologies of these sensor-motor maps reflect the task-specific contributions of the sensory pathways that are moderated by the mechanical interaction of the locomotor system with the environment. Our overall goal was to identify enabling and disabling pathways for individual locomotor functions. We expected that several different pathways may generate stable hopping, but that pathway-specific features determine hopping performance and efficiency.

To show the general validity of our approach we varied parameters of the environment (ground compliance) and the body morphology: compliance (tendon elasticity), geometry (segment lengths) and inertia (body mass). Furthermore, we explored the sensitivity of the model to variations of feedback and model parameters.

Material & Methods

To focus on the integration of different sensory pathways, we considered a highly simplified muscle-driven model allowing the evaluation of motion execution with respect to stability, performance and efficiency. Therefore, we used the hopping model by Geyer et al. (2003) with idealized sensory receptors and motorneurons capturing the basic neural control principles with the least possible system complexity (Full and Koditschek, 1999; Brown and Loeb, 2000; Pearson et al., 2006). We chose the signals of three muscle receptors (muscle force of Golgi tendon organs, fibre length and fibre velocity of muscle spindles) to focus on local proprioceptive circuits.

Mechanical hopping model

The model of Geyer et al. (2003) consists of a point mass m (center of mass, CoM) and two massless segments (length l_S) representing the thigh and shank (Figure 4.1). The leg length during flight (l_f) is held constant until the vertical CoM height equals the flight leg length (touch-down). During stance, a muscle-tendon-complex (MTC) modelling the knee extensors counteracts the gravitational force (gravitational constant g). The MTC consists of a contractile element (CE) and a serial elastic element (SE) (Equations 4.1

and 4.2). Take-off occurs when the leg force vanishes or when the vertical displacement of the point mass exceeds the flight leg length.
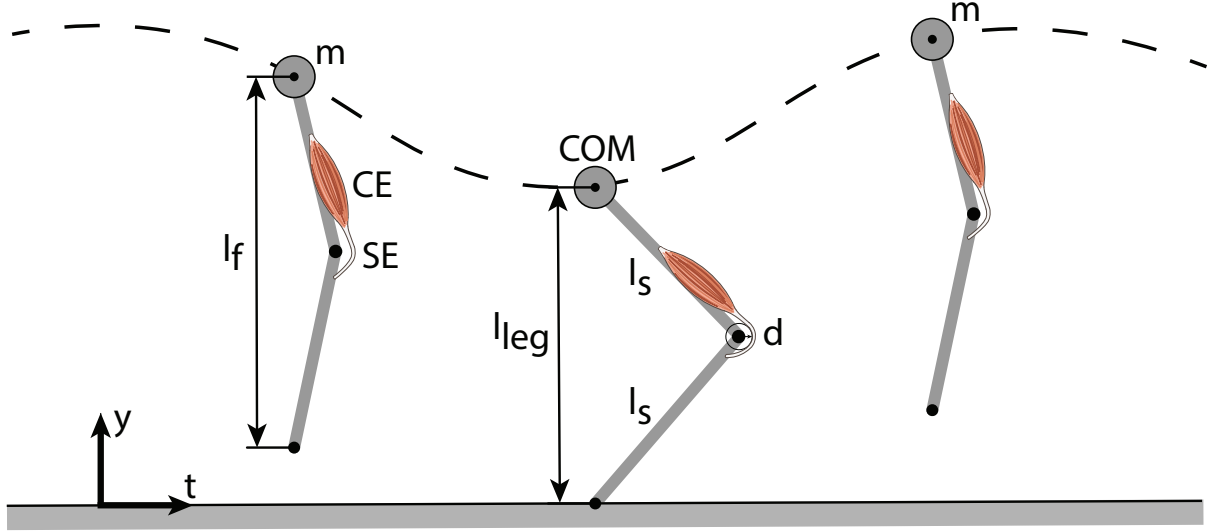
Figure 4.1: Vertical hopping model (Geyer et al., 2003) comprising a point mass (m), two massless leg segments and a leg extensor muscle-tendon-complex (MTC), consisting of a contractile element (CE) and a serial elastic element (SE). During flight phase, the leg flight length (l_f) stays constant. In stance, the MTC generates a pulling force that acts on the lever arm (d) which creates an extension torque. Figure inspired by Geyer et al. (2003).

$$l_{\mathrm{MTC}} = l_{\mathrm{CE}} + l_{\mathrm{SE}} \tag{4.1}$$

$$F_{\mathrm{MTC}} = F_{\mathrm{CE}} = F_{\mathrm{SE}} \tag{4.2}$$

The length of the MTC is defined by a reference length ($l_{\mathrm{MTC,ref}}$), a corresponding reference knee angle (φ_{ref}) and the knee lever arm (d): $l_{\mathrm{MTC}} = l_{\mathrm{MTC,ref}} - d * (\varphi - \varphi_{\mathrm{ref}})$. The force of the CE is calculated as $F_{\mathrm{CE}} = F_{\mathrm{max}} * f_1 * f_v * ACT$ using the maximum isometric force (F_{max}), force-length-relationship (f_1), force-velocity-relationship (f_v) and activation state of the contractile element (ACT, Equation 4.11). The force-length-relationship and force-velocity-relationship are implemented by non-linear approximations (Geyer et al., 2003):

$$f_1(l_{\mathrm{CE}}) = exp\left(c \left| \frac{l_{\mathrm{CE}} - l_{\mathrm{opt}}}{l_{\mathrm{opt}} \, w} \right|^3 \right) \tag{4.3}$$

$$f_v(v_{\mathrm{CE}}) = \begin{cases} N + (N-1) \, \frac{v_{\mathrm{max}} - v_{\mathrm{CE}}}{7.56 K v_{\mathrm{CE}} - v_{\mathrm{max}}} & v_{\mathrm{CE}} \geq 0 \\ \frac{v_{\mathrm{max}} - v_{\mathrm{CE}}}{v_{\mathrm{max}} + K v_{\mathrm{CE}}} & v_{\mathrm{CE}} < 0 \end{cases} \tag{4.4}$$

These equations use a width (w) and a curvature constant (c) of the force-length-curve as well as optimum length of the CE (l_{opt}), eccentric force enhancement (N), maximum shortening velocity (v_{max}) and a second curvature constant (K). The force-length-relationship values can range from 0 to 1. The force-velocity-relationship values can range from 0 to 1 for concentric contractions and from 1 to 1.5 for eccentric

contractions (because of the eccentric force enhancement N). To define the serial elastic element in the MTC a progressive force-length dependency (Equation 4.5) was used (van Ingen Schenau, 1984). Therefore, the reference strain (ε_{ref}) determines the relation of the force acting on the serial element and its corresponding stretch in relation to its rest length (l_{rest}) (Equation 4.6).

$$f_{SE}(\varepsilon) = \begin{cases} (\varepsilon/\varepsilon_{ref})^2 & \varepsilon > 0 \\ 0 & \varepsilon \leq 0 \end{cases} \tag{4.5}$$

$$\varepsilon = \left(\frac{l_{SE}}{l_{rest}}\right) - 1 \tag{4.6}$$

Extension of the neuromuscular model

To consider fused feedback pathways, we extended the neuromuscular feedback model by a linear combination of muscle force (FFB), fibre length (LFB) and fibre velocity feedback (VFB) pathways (Figure 4.2). All three afferent pathway signals are multiplied by a blending factor λ_i weighting the individual pathways resulting in the summation signal $S(t)$ (Equation 4.7) where G_i, F_{max}, L_{off} and V_{off} denote the individual gains, maximum isometric force and offsets of length and velocity pathways, respectively. By restricting the sum of all blending factors (Equation 4.8), one weight can always be calculated from the other two (Seyfarth et al., 2001).
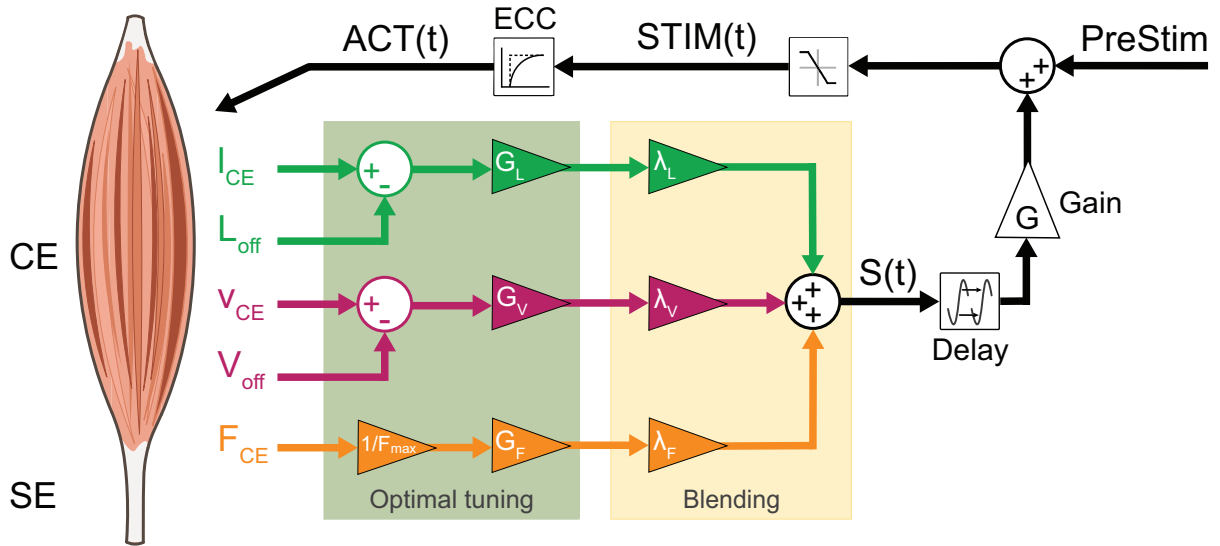
Figure 4.2: Neuromuscular reflex model which fuses Ia afferent signals (l_{CE}, v_{CE} and offsets L_{off}, V_{off}) and normalized Ib afferent (F_{CE}) pathways: All three sensory signals are gained (G_L, G_V, $G_F \geq 0$) and weighted (λ_i). The resulting summation signal $S(t)$ is then delayed (Δ_S) and gained ($G \geq 0$). This signal is then added to a constant pre-stimulation value to mimic a positive excitatoric postsynaptic potential at the α-motoneuron. The stimulation signal $STIM(t)$ is confined to values between 0 and 1 and delayed by the excitation-contraction-coupling (ECC) resulting in the activation signal $ACT(t)$ of the CE.

$$S(t) = \lambda_F * G_F * F_{CE}/F_{max}$$
$$+\lambda_L * G_L * (l_{CE} - L_{off}) \qquad (4.7)$$
$$+\lambda_V * G_V * (v_{CE} - V_{off})$$

$$\lambda_F + \lambda_L + \lambda_V = 1, \quad 0 \leq \lambda_{F, L, V} \leq 1 \qquad (4.8)$$

This normalizes the blending of individual contributions and reduces the dimensionality by projection onto a two-dimensional space (of independent blending factors). Triangles visualize all possible (projected) feedback compositions (Figure 4.3). The corners of the triangle represent the isolated individual feedback pathways (purely FFB, LFB or VFB). Every point within the triangle represents a blending of the individual feedback pathways and refers to two-dimensional Cartesian coordinates (space V, x and y between 0 and 1). The projection to the blending factors (space W) is described by: $f : V \rightarrow W$ (Equation 4.9). Hence, the larger the distance of a point to a corner (e.g. VFB) the smaller is the contribution of that specific feedback pathway in the blended signal $S(t)$. Individual feedback pathways in isolation (corners) are parameterized by optimization.

$$f = \begin{cases} x \rightarrow \lambda_L & 0 \leq x \leq 1 \\ y \rightarrow \lambda_F & 0 \leq y \leq 1 \end{cases} \qquad (4.9)$$

After blending, the proprioceptive signal ($S(t)$) is delayed by Δ_S, gained by G and added to the stimulation bias (*PreStim*) (Equation 4.10). Then, this signal is confined to values between 0 and 1 and input into the excitation-contraction-coupling (ECC) (Equation 4.11) described by a first-order differential equation resulting in the activation signal *ACT(t)* (Geyer et al., 2003; Haeufle et al., 2012).

$$STIM(t) = \begin{cases} PreStim & t < \Delta_S \\ PreStim + G * S(t - \Delta_S) & t \geq \Delta_S \end{cases} \qquad (4.10)$$

$$\tau \frac{\mathrm{d}ACT(t)}{\mathrm{d}t} = STIM(t) - ACT(t) \qquad (4.11)$$

Model parameter and optimization

Model parameters
Parameters of the mechanical model (Table 4.1) were taken from Geyer et al. (2003). The initial position of the point mass was set to 1.05 m and its initial velocity to 0 m/s.

Optimization of feedback parameters
To identify feedback parameters of the extended neuromuscular model (optimal tuning part in Figure 4.2), a pattern search optimization algorithm was used (Torczon, 1997). The pattern search algorithm was implemented to search for parameters sets that result in stable hopping patterns (more than $n = 50$ steps, first criterion). As second optimization criterion, the maximum height of the body mass $h_{max} = y_{max,apex}$ for steady-state hopping ($n = 49$ step) was chosen. Simulations were checked for steady-state motion. Optimizations of all individual feedback pathways (in isolation) were done for 'stiff tendon' and 'rigid
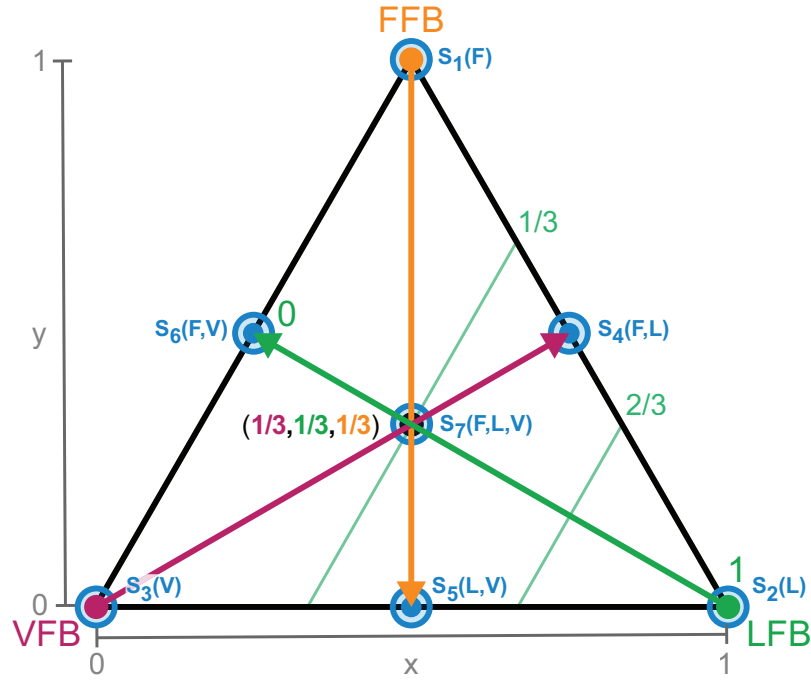
Figure 4.3: Schematic explanation of sensory pathway blending through parameter reduction (Equation 4.8). Corners of the triangle represent a full contribution of one single feedback (e.g. 0 % VFB, 0 % FFB, 100 % LFB). Every point within the triangle (coordinates x and y) represents a unique combination of the three feedback pathways. Arrows (thick) and contour lines (thin) explain the blending of feedback pathways. The larger the distance of a point to a corner (e.g. LFB) the smaller the contribution of that feedback pathway in the blended signal. Exemplary, the middle point describes an equal composition of all feedback pathways ($1/3$ VFB, $1/3$ FFB, $1/3$ LFB). Optimal tuning of the individual feedback pathways is done by optimization for full contribution of only one sensory reflex (corners). These optimal reflex pathways are used for all compositions. The blue circles (S_1(FFB) to S_7(FFB, LFB, VFB)) denote the specific compositions of feedback pathways used for the sensitivity analysis.

ground' and repeated five times each with random starting points to avoid finding local maxima. The limits of parameter values were $0.1 \leq G_F \leq 3$ (FFB), $0.1 \leq G_L \leq 200$ and $0 \leq L_{off} \leq 3$ (LFB) as well as $0.1 \leq G_V \leq 3$ and $-1 \leq V_{off} \leq 0$ (VFB) aligned to results from Geyer et al. (2003). The best performing solution was used for further simulation and analysis.

Simulation and optimization environment

Simulations and optimizations were implemented in *Matlab Simulink* (release 2016b, Mathworks, Natick, Massachusetts, USA). For the simulations, the variable-step solver 'ode45' with relative and absolute tolerances of 10^{-8} was used. Optimization was done using the 'Global Optimization Toolbox' (Version 3.4.1).

Tendon elasticity changes

To change the SE elasticity, three configurations for the reference strain were used: (1) 'stiff tendon' ($\varepsilon_{stiff} = 0.01$), (2) 'moderate tendon' ($\varepsilon_{moderate} = 0.03$), and (3) 'compliant tendon' ($\varepsilon_{compliant} = 0.05$). For equal forces, smaller reference strain values indicated less associated stretch and thus a stiffer length-force dependency of the SE. These SE elasticity levels are in a range used by other simulation studies (Pandy

Table 4.1: Parameters of the hopping model taken from Geyer et al. (2003).

parameter	value	unit
body mass m	80	kg
gravitational constant g	9.81	m/s^2
initial body mass height y_0	1.05	m
flight leg length l_f	0.99	m
segment length l_S	0.5	m
knee lever arm d	0.04	m
MTC reference length $l_{MTC,ref}$	0.5	m
reference knee angle φ_{ref}	110	°
maximum isometric force F_{max}	22 000	m
optimum length of CE l_{opt}	0.1	m
curvature constant of f_l c	0.05	
width w	0.4	
maximum shortening velocity v_{max}	-12	m/s
eccentric force enhancement N	1.5	
curvature constant of f_v K	5	
SE rest length $l_{SE,rest}$	0.4	m
'stiff' reference strain of SE ε_{stiff}	0.01	
'moderate' reference strain of SE $\varepsilon_{moderate}$	0.03	
'compliant' reference strain of SE $\varepsilon_{compliant}$	0.05	
'heavy' body mass m_{heavy}	96	kg
'moderate' body mass $m_{moderate}$	80	kg
'light' body mass m_{light}	64	kg
'long' segment length $l_{S,long}$	0.6	m
'moderate' segment length $l_{S,moderate}$	0.5	m
'short' segment length $l_{S,short}$	0.4	m
'stiff' ground stiffness k_{stiff}	9999	kN/m
'moderate' ground stiffness $k_{moderate}$	500	kN/m
'compliant' ground stiffness $k_{compliant}$	100	kN/m
excitation-contraction time constant τ	0.01	s
feedback signal time delay Δ_S	0.015	s

et al., 1990; Bobbert, 2001; Nagano et al., 2004).

Body mass changes

The body mass of the model (m) was varied to 80 % and 120 % of the original body mass (80 kg): (1) 'light mass' ($m_{light} = 64$ kg), (2) 'moderate mass' ($m_{moderate} = 80$ kg), and (3) 'heavy mass' ($m_{heavy} = 96$ kg).

Segment length changes

The leg geometry was altered by changing the length of both segments (l_S) to 80 % and 120 % of the original segment length (0.5 m): (1) 'short segments' ($l_{S,short} = 0.4$ m), (2) 'moderate segments' ($l_{S,moderate} = 0.5$ m), and (3) 'long segments' ($l_{S,long} = 0.6$ m). To keep the take-off conditions and energy level of the system consistent for all segment length configurations, the initial body mass height ($y_0 = 2 * l_S + 0.05$ m) and the flight leg length ($l_f = 2 * l_S - 0.01$ m) were adjusted accordingly.

Ground compliance changes

To modulate the vertical ground stiffness, the model was slightly adapted. During stance, a linear spring constant (k_{ground}) and the leg force or vertical ground reaction force (F_{leg}) define the foot position (y_{FP}):

$$y_{FP}(F_{leg}) = \begin{cases} y_{CoM} - l_f & \text{during flight} \\ -\frac{F_{leg}}{k_{ground}} & \text{during stance} \end{cases} \tag{4.12}$$

The foot position during stance can only reach values ≤ 0 because the take-off condition is met for vanishing leg force ($F_{leg} < 0$). To change the ground compliance, three configurations for the spring constant were chosen: (1) 'compliant ground' ($k_{compliant} = 100\,kN/m$), (2) 'moderate ground' ($k_{moderate} = 500\,kN/m$), and (3) 'stiff ground' ($k_{stiff} = 9999\,kN/m$). These ground stiffness values are in a range used by other computational or experimental studies (Farley et al. 1998: $20\,kN/m$ to $35.000\,kN/m$, Moritz and Farley 2004: $27\,kN/m$ to $411\,kN/m$, Krogt et al. 2009: $75\,kN/m$ to $3.100\,kN/m$).

Sensitivity analysis

To evaluate the performance of the model for different parameter settings, we analyzed its parametric sensitivity. We randomly altered feedback parameters (G_F, G_L, L_{off}, G_V, V_{off}, $PreStim$, Δ_S) as well as model parameters (ε_{ref}, l_S, m). Physiological parameters were normally distributed (l_S: $\mu = 0.5\,m, \sigma^2 = 0.02\,m$; m: $\mu = 80\,kg, \sigma^2 = 5\,kg$) whereas other parameters were uniformly distributed ($1 \leq G_F \leq 5$; $100 \leq G_L \leq 160$; $0.06m \leq L_{off} \leq 0.1m$; $1 \leq G_V \leq 5$; $-1m/s \leq V_{off} \leq 0m/s$; $0.01 \leq PreStim \leq 0.2$; $0.01s \leq \Delta_S \leq 0.05s$; $0.01 \leq \varepsilon_{ref} \leq 0.05$). For the sensitivity analysis, the ground stiffness remained unchanged (no compliance). Because parametric influences differ depending on the feedback blending, we considered seven reflex pathway compositions for our sensitivity analysis. Figure 4.3 shows the location of these seven compositions (S_1(FFB) to S_7(FFB, LFB, VFB)). For each composition, $n = 1000$ simulations with randomized parameters were performed. Maximum hopping height (Δh_{max}) and hopping efficiency (η) were calculated as performance measures. The sensitivity of these variables was further tested with *SPSS 24.0* (IBM Corporation, Armonk, New York, USA). Spearman's rho correlation coefficients (r) with significance values (two-sided test) and standardized regression coefficients (β) were calculated for simulations that resulted in stable hopping. Correlations were considered to be moderate for $0.5 \leq r < 0.7$ ($-0.5 \geq r > -0.7$) or high for $r \geq 0.7$ ($r \leq -0.7$) if p-values were significant ($p < 0.01$).

Performance metrics

Depending on the force generated during stance, the predicted motion will result in continuous and stable hopping or in a bound motion (leg remains in contact to the ground) where the model lands but does not lift off. In case of hopping, the blending compositions were evaluated by calculating the following metrics.

Stability criterion

To determine if the extended neuromuscular reflex model will result in stable hopping or bound motion, we examined the number of steps to fall, and simulations resulting in at least 50 steps were considered stable.

Hopping metrics

The following criteria were used to evaluate the performance of the hopping model with respect to energetics and motion dynamics for the last step ($n = 49$) of the simulation. Simulations were checked for steady-state motion.

1. The model generates a motion performance or a mechanical output during hopping defined as the steady-state vertical hopping height of the body mass ($\Delta h_{\mathrm{max}} = y_{\mathrm{apex}} - l_{\mathrm{f}}$) at the instance of apex ($v_{\mathrm{y,apex}} = 0$). During flight, the system energy is equivalent to the potential energy at the apex: $E_{\mathrm{system}} = mgh_{\mathrm{max}}$.

2. To describe the hopping motion we calculated the hopping frequency (f_{hop}) and the effective stiffness of the leg $k_{\mathrm{leg}} = F_{\mathrm{leg,max}}/\Delta l_{\mathrm{leg,max}}$.

3. Because the tendon and muscle share the same force (Equation 4.2), knowledge about the relative work generation (and length deflection) of the CE and the MTC is of interest. Hence, we calculated the maximum amount of work generated by the CE ($W_{\mathrm{CE,max}}$) relative to its equivalent of the whole MTC ($W_{\mathrm{MTC,max}}$) that was then simplified to the ratio of the maximum deflection of both elements with respect to the elements' rest lengths:

$$\alpha = \frac{W_{\mathrm{CE,max}}}{W_{\mathrm{MTC,max}}} = \frac{F_{\mathrm{MTC,max}} * \Delta l_{\mathrm{CE,max}}}{F_{\mathrm{MTC,max}} * \Delta l_{\mathrm{MTC,max}}} = \frac{\Delta l_{\mathrm{CE,max}}}{\Delta l_{\mathrm{MTC,max}}} \tag{4.13}$$

This factor describes the maximum amount of work produced in the muscular element relative to the overall maximum contribution of the MTC.

4. To evaluate the metabolic effort of the CE, we used the velocity-dependent metabolic cost model by Minetti and Alexander (1997) and Robertson and Sawicki (2014) favoring eccentric contractions with reduced metabolic effort (Equation 4.15). This is scaled by the activation signal during ground contact ($ACT(t)$), maximum isometric Force (F_{max}) and maximum shortening velocity (v_{max}) to calculate the metabolic rate ($M_{\mathrm{eff}}(t)$) (Krishnaswamy et al., 2011; Robertson and Sawicki, 2014):

$$M_{\mathrm{eff}}(t) = \Phi(v_{\mathrm{CE}}) * ACT(t) * \mid F_{\mathrm{max}} * v_{\mathrm{max}} \mid \tag{4.14}$$

$$\Phi(v_{\mathrm{CE}}) = \begin{cases} 0.23 - 0.16 * e^{\left(-8 * \frac{v_{\mathrm{CE}}}{v_{\mathrm{max}}}\right)} & v_{\mathrm{CE}} \geq 0 \\ 0.01 + 0.11 * \frac{v_{\mathrm{CE}}}{v_{\mathrm{max}}} + 0.06 * e^{\left(-23 * \frac{v_{\mathrm{CE}}}{v_{\mathrm{max}}}\right)} & v_{\mathrm{CE}} < 0 \end{cases} \tag{4.15}$$

We derived the averaged metabolic effort ($\overline{M}_{\mathrm{eff}}$) per hopping cycle by an integration of the metabolic rate ($M_{\mathrm{eff}}(t)$) during ground contact and a normalisation with the body mass (m) and the contact time (T_{contact}) (Robertson and Sawicki, 2014):

$$\overline{M}_{\mathrm{eff}} = \int_{0}^{T_{\mathrm{contact}}} M_{\mathrm{eff}}(t) \, dt / (m * T_{\mathrm{contact}}) \tag{4.16}$$

5. Hopping efficiency was quantified as the ratio of hopping height (Δh_{max}) (output) to averaged metabolic effort of the CE (input): $\eta = \frac{\Delta h_{\mathrm{max}}}{\overline{M}_{\mathrm{eff}}}$.

Results

Individual hopping patterns

The optimization of the individual feedback pathways (with $\varepsilon_{stiff} = 0.01$) resulted in neuromuscular model parameters that produced a maximum hopping height for stable hopping patterns (Table 4.2). For these feedback parameters, FFB was the best performing optimization with a hopping height of 0.126 m. The maximum hopping height of LFB was 0.063 m. VFB did not produce a high performance with a maximum hopping height of 0.002 m just above the flight leg length. The predicted leg forces and activation signals are shown in Figure 4.4. The activation profile and subsequently the leg force profiles of FFB showed an increasing amplification. Compared to leg forces of FFB, LFB produced higher peak leg forces but shorter contact times. The rise of the LFB activation signal was delayed to the instance of touch-down by about 50 ms. Here, the length offset L_{off} suppressed the early activation signal (also reported by Geyer et al. 2003). VFB produced half the leg force and half the contact time compared to FFB and LFB reflected in the small hopping height (0.002 m). While FFB and LFB showed delayed increase in the leg force (more than 50 ms after touch-down), the VFB caused an almost instantaneous response in the activation signal resulting in high (eccentric) force generation and thus high energy losses during leg compression. The CE remained less stretched and started to shorten before reaching optimal fibre length ($f_l < 0.2$) limiting positive (concentric) muscle work during leg extension.

Table 4.2: Optimization results of individual feedback parameters: for $y_0 = 1.05\,m$, $G = 1$, $PreStim = 0.01$, $\varepsilon_{stiff} = 0.01$ and rigid ground.

parameter	Force feedback (FFB)	Length feedback (LFB)	Velocity feedback (VFB)
individual gain	$G_F = 2.6$	$G_L = 130$	$G_V = 2.9$
individual offset	-	$L_{off} = 0.08$	$V_{off} = -0.6$
maximum hopping height Δh_{max}	0.126 m	0.063 m	0.002 m

Sensor-motor maps

The following section describes the results of the blended feedback pathways and the sensor-motor maps for different motion characteristics (e.g. hopping stability, performance and efficiency).

Hopping stability
The blended feedback pathways produced both stable and unstable motions (Figure 4.5A). Motions of stable hopping (more than 50 hops) were found for compositions of FFB and LFB with small proportions of VFB. Here, a balanced composition of FFB and LFB resulted in greater stability (with respect to higher VFB proportion) compared to predominant FFB. A thin envelope of transitions (between 1 and 49 steps) was observed representing a distinct margin of stable and unstable areas.

Hopping performance
The performance map (Figure 4.5B) shows the maximum hopping height (Δh_{max}) for all feedback compositions of steady-state motions where only stable predictions were considered. The contours show greater
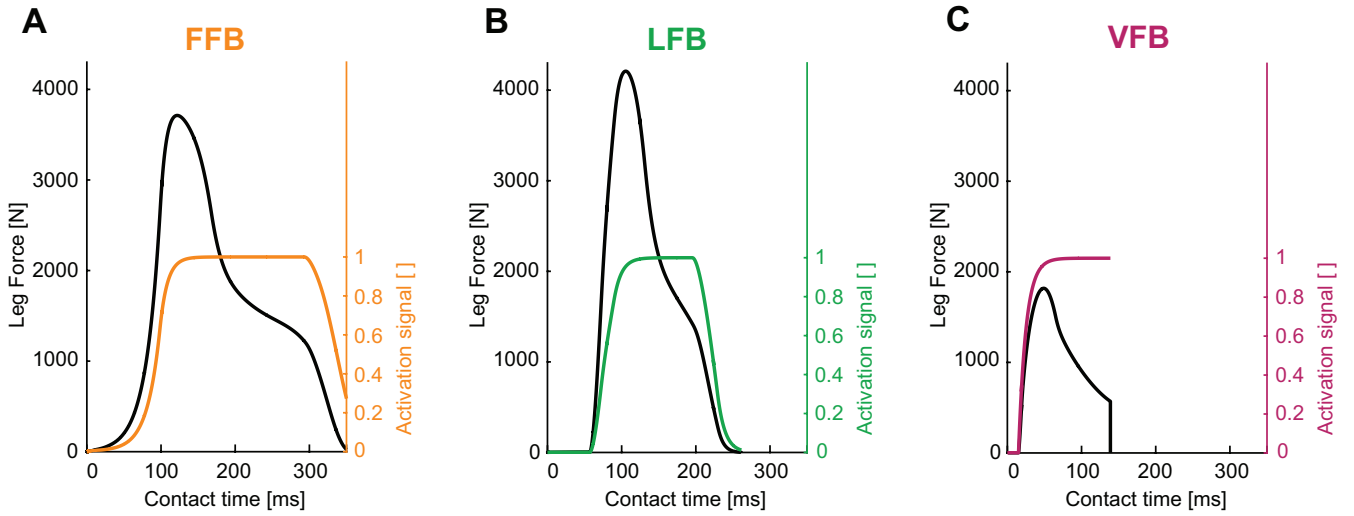
Figure 4.4: Leg forces and activation signals during one stance phase for optimized feedback parameters of individual pathways ($y_0 = 1.05\,m$, $G = 1$, $PreStim = 0.01$, $\varepsilon_{\text{stiff}} = 0.01$, rigid ground): **(A)** force feedback ($G_{\text{F}} = 2.6$), **(B)** length feedback ($G_{\text{L}} = 130$, $L_{\text{off}} = 0.08$) and **(C)** velocity feedback ($G_{\text{V}} = 2.9$, $V_{\text{off}} = -0.6$). Maximum hopping heights are $\Delta h_{\text{max}} = 0.126\,m$ (FFB), $\Delta h_{\text{max}} = 0.063\,m$ (LFB) and $\Delta h_{\text{max}} = 0.002\,m$ (VFB).

hopping heights for smaller proportions of VFB. In areas close to unstable solutions, the maximum hopping height (maximum vertical displacement of CoM) was just above the leg length leading to smooth transitions from unstable (no hopping) to slight hopping patterns. Thus, the energy level of the system (E_{system}) gradually increased when VFB was reduced. Compared to LFB, high proportions of FFB performed better, and higher hopping heights occurred closer to pure FFB. A composition of FFB and LFB (but not VFB) produced maximum performance (see red point in Figure 4.5B). Although compared to individual contributions (e.g. pure FFB or LFB) hopping performance was amplified by blending multiple sensory pathways, the pathway-specific feature enabling motion performance (Geyer et al., 2003) was found for dominant FFB.

Hopping efficiency

To identify feedback compositions resulting in hopping patterns that required less metabolic resources than others, the energetic relation of output and input: $\eta = \frac{\Delta h_{\text{max}}}{\bar{M}_{\text{eff}}}$ was used. In the topology of the efficiency map (Figure 4.5C), efficient motions were predicted in areas with dominant LFB and only small proportions of VFB (below 0.2), and a small band of efficient hopping patterns evolved. The spectrum of this band ranged from small proportions of FFB to pure LFB and gradually spread towards pure LFB. The most efficient feedback blending was found for a combination of small FFB, dominant LFB and no proportion of VFB (see maximum). Because VFB resulted in lower hopping heights (Figure 4.5B), VFB also reduced the hopping efficiency (η). Moreover, only moderate hopping heights led to most efficient hopping (Figure 4.5C). For the used metabolic model, hopping efficiency increased if the amount of positive work used for propulsion (and consequently hopping height) was reduced. Higher proportions of LFB led to lower force (and also work) production during late stance caused by a reduced activation signal in late stance due to the length offset (Figure 4.4B). In areas of higher hopping heights (dominant FFB and minor VFB), the metabolic model predicted a high metabolic effort leading to low efficiency values. As observed for hopping performance, the most efficient hopping pattern was found for a fusion of sensory pathways.
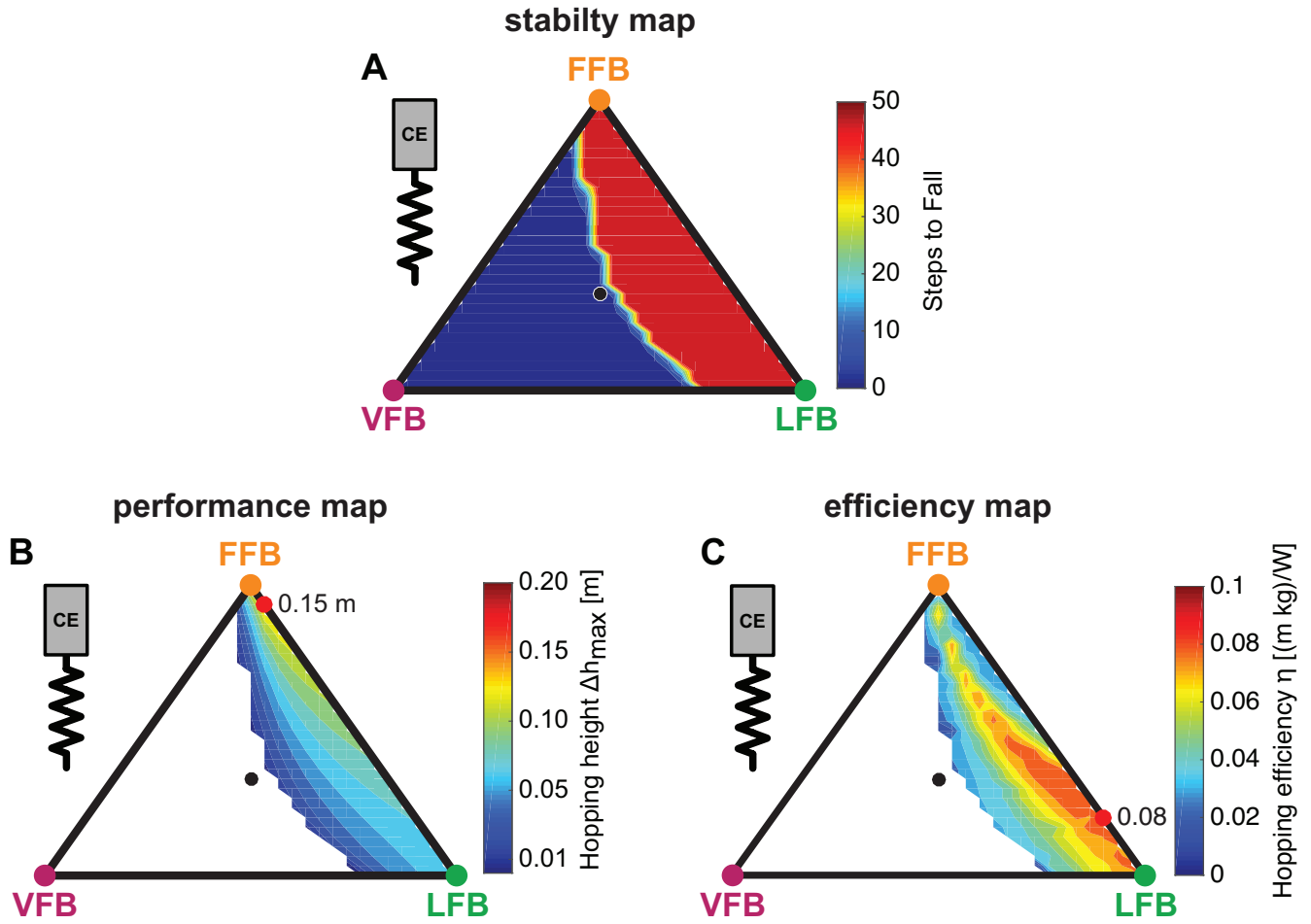
Figure 4.5: Sensor-motor maps: Influence of blended feedback pathways on hopping stability, performance and efficiency ($y_0 = 1.05\,m$, $G = 1$, *PreStim* $= 0.01$, $\varepsilon_{\text{moderate}} = 0.03$, rigid ground). Global maxima are visualized by red points. Every point within the triangle represents a unique combination of the three feedback pathways. The larger the distance of a point to a corner (e.g. LFB) the smaller the contribution of that feedback pathway in the blended signal (see Figure 4.3 for explanation of triangles). **(A)** stability map: steps to fall (max = 50), **(B)** performance map: maximum hopping height (Δh_{max}) and **(C)** efficiency map: hopping efficiency (η).

Hopping motion

To evaluate and compare the predicted hopping motions with human hopping data (where possible), we calculated biomechanical parameters of the motions. Hopping frequencies ranged from $1.5\,\text{Hz}$ to $3.0\,\text{Hz}$ (Figure 4.6A). Higher frequencies were found for higher VFB and hence in areas of smaller hopping heights (Figure 4.5B). The effective leg stiffness of our hopping model ranged from $15\,\text{kN/m}$ to $30\,\text{kN/m}$ (Figure 4.6B). This parameter depended mostly on the relation of VFB and LFB but was slightly influenced by increases in FFB (see vertical contour lines). Thus, the model produced motions of the best performing and most efficient compositions at small hopping frequencies (around $1.5\,\text{Hz}$) and low leg stiffness (around $15\,\text{kN/m}$).

hopping frequency

A

leg stiffness

B
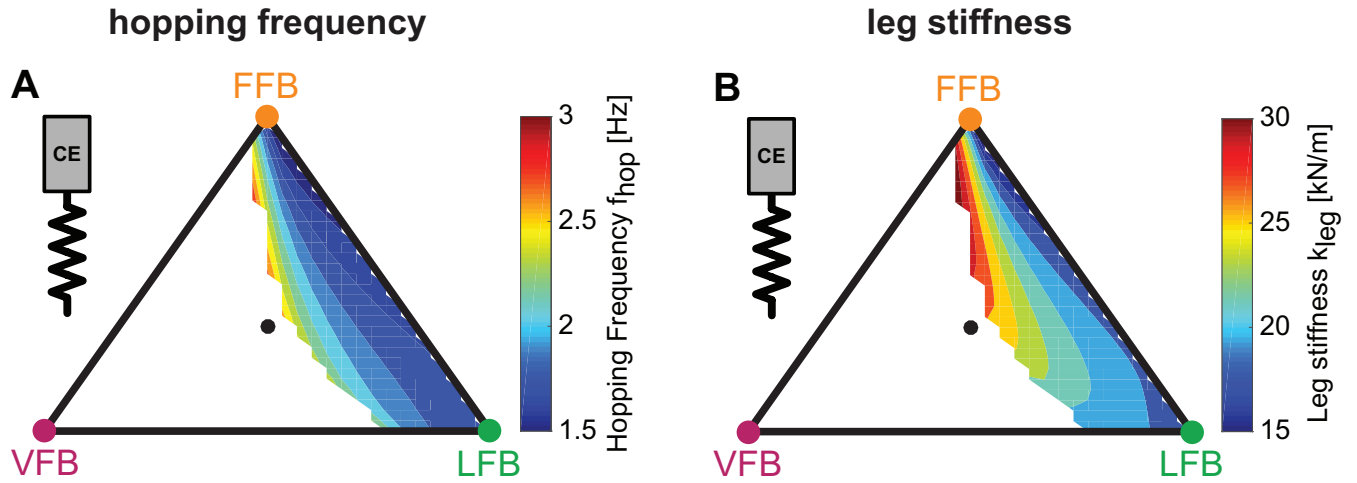
Figure 4.6: Predicted hopping motions: Influence of blended feedback pathways on hopping frequency and leg stiffness ($y_0 = 1.05\,m$, $G = 1$, $PreStim = 0.01$, $\varepsilon_{moderate} = 0.03$, rigid ground). Every point within the triangle represents a unique combination of the three feedback pathways. The larger the distance of a point to a corner (e.g. LFB) the smaller the contribution of that feedback pathway in the blended signal (see Figure 4.3 for explanation of triangles). **(A)** hopping frequency (f_{hop}) and **(B)** leg stiffness (k_{leg}).

Robustness of sensor-motor maps

To explore the robustness of the sensor-motor maps, the effects of parameter variations of the model configuration (tendon elasticity ε_{ref}, body mass m, segment lengths l_S) and the environment (ground compliance k_{ground}) were analyzed. Moreover, we investigated the parametric sensitivity of the model to variations of feedback and model parameters.

Tendon elasticity changes
The three performance maps of altered elasticity of the serial elastic element showed only slight differences (Figure 4.7A). For all three tendon elasticity configurations, the size and location of stable hopping patterns were consistent, and smooth transitions from unstable to stable hopping patterns (with only small hopping heights) were predicted. While the topology of the performance maps remained similar (compared to the 'moderate tendon'), the level of the predicted hopping height changed. The greatest hopping heights were found for a more compliant tendon and gradually decreased for stiffer configurations. Maximum hopping heights for each configuration ranged from 0.18 m ('compliant tendon') to 0.15 m ('moderate tendon') to 0.13 m ('stiff tendon') and were found for consistent feedback compositions. For the stiffest elasticity ($\varepsilon_{stiff} = 0.01$), a second margin of stable solutions for high proportions of the VFB evolved. However, these feedback compositions resulted in hopping patterns just above the leg length (see also Figure 4.4C).

Body mass changes
For all body mass configurations, performance map regions of stable hopping emerging for FFB and LFB remained similar (Figure 4.7B). A reduction of the body mass was predicted to result in higher maximum hopping height while the blending location of the most performant hopping patterns did not change. For the light mass, stable hopping patterns were found for dominant VFB.

Segment length changes
The sensor-motor map topology remained similar for changes in the leg geometry (Figure 4.7C). Only for
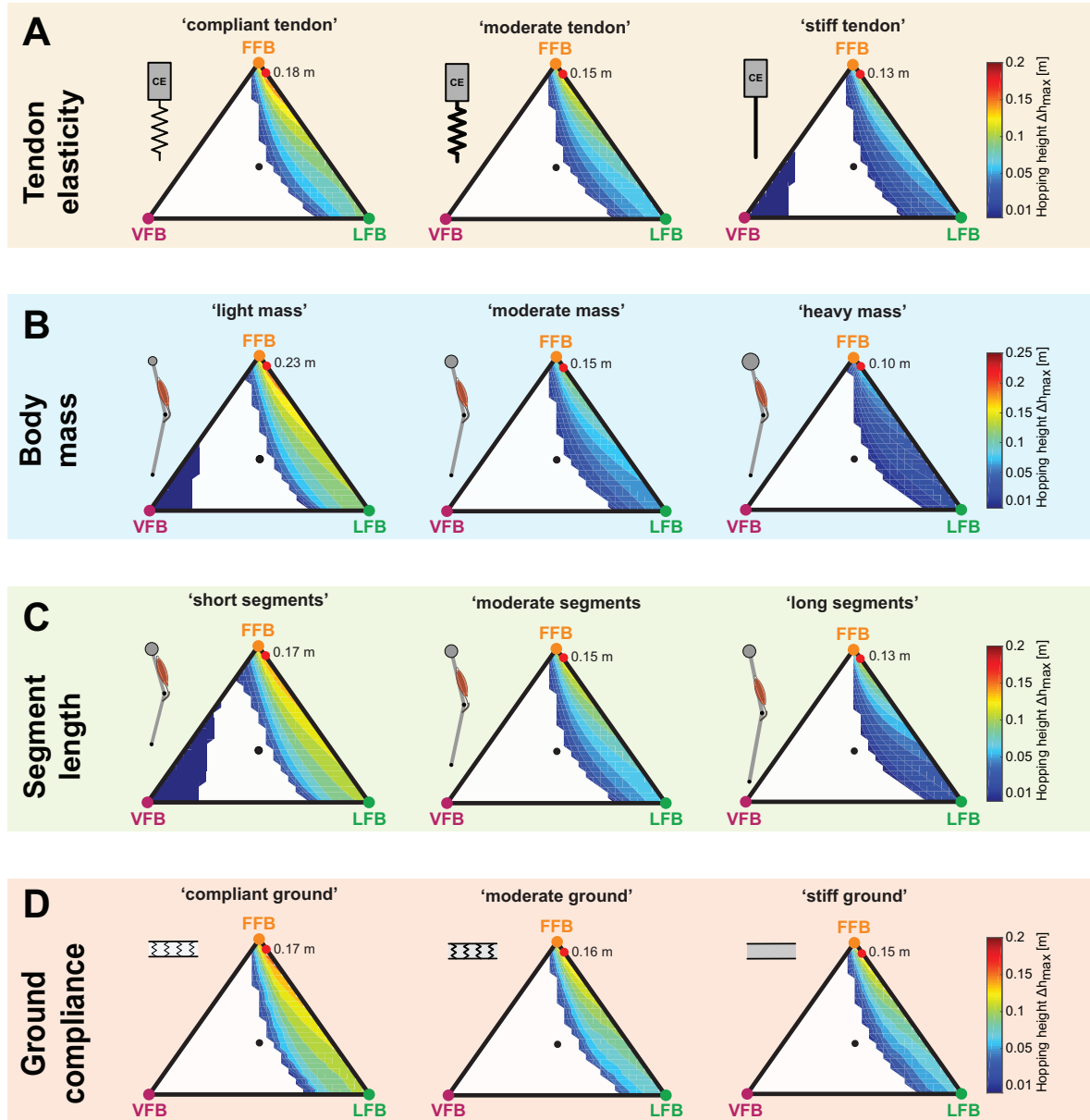
Figure 4.7: Influence of parameter variations on performance maps: Maximum hopping height (Δh_{max}) for blended feedback signals ($y_0 = 1.05\,m$, $G = 1$, $PreStim = 0.01$). Global maxima are visualized by red points. Every point within the triangle represents a unique combination of the three feedback pathways. The larger the distance of a point to a corner (e.g. LFB) the smaller the contribution of that feedback pathway in the blended signal (see Figure 4.3 for explanation of triangles). **(A)** tendon elasticity changes: 'compliant tendon' ($\varepsilon_{compliant} = 0.05$), 'moderate tendon' ($\varepsilon_{moderate} = 0.03$), 'stiff tendon' ($\varepsilon_{stiff} = 0.01$); **(B)** body mass changes: 'light mass' ($m_{light} = 64\,kg$), 'moderate mass' ($m_{moderate} = 80\,kg$), 'heavy mass' ($m_{heavy} = 96\,kg$); **(C)** segment length changes: 'short segments' ($l_{S,short} = 0.4\,m$), 'moderate segments' ($l_{S,moderate} = 0.5\,m$), 'long segments' ($l_{S,long} = 0.6\,m$); and **(D)** ground compliance changes: 'compliant ground' ($k_{compliant} = 100\,kN/m$), 'moderate ground' ($k_{moderate} = 500\,kN/m$), 'stiff ground' ($k_{stiff} = 9999\,kN/m$).

short segment lengths, VFB resulted in stable hopping patterns (with small hopping heights). Motions with the highest performance were found for a consistent sensory pathway blending, and the performance level increased with decreasing segment lengths.

Ground compliance changes

Similar to the other parameter variations, changes in ground stiffness only minimally influenced regions of stable solutions (Figure 4.7D). Steady-state hopping heights decreased with increasing proportions of VFB (for all three ground configurations). Thus, maximum hopping heights were found for no proportions of VFB and dominant FFB, and decreased with decreasing ground compliance. The location of the maxima was consistent for different ground compliance and changes in the other parameter variations. The topology of the performance maps remained similar.

Sensitivity of the model

We evaluated the sensitivity of specific model and feedback parameters to predicted hopping performance ($\Delta h_{\max}$) and hopping efficiency (η) for seven feedback compositions (S_1(FFB) to S_7(FFB, LFB, VFB), Figure 4.3). Correlation coefficients (r), p-values and the standardized regression coefficients (β) are shown in Table 4.3. While pure VFB (S_3) did not generate any stable hopping pattern, for FFB (S_1) and LFB (S_2) 958 out of 1000 simulations resulted in stable hopping. For both individual feedback pathways, hopping height was moderately influenced by the feedback signal time delay (Δ_S): $\beta = 0.637$ ($r = 0.585$, $p < 0.01$, FFB) and $\beta = 0.531$ ($r = 0.521$, $p < 0.01$, LFB). Also, moderate correlations between hopping efficiency and reference strain ($\varepsilon_{\mathrm{ref}}$) were found for FFB ($\beta = 0.628$, $r = 0.643$, $p < 0.01$) and LFB ($\beta = 0.431$, $r = 0.494$, $p < 0.01$). For all feedback compositions, the model was most sensitive to the feedback signal time delay and the reference strain of the serial elastic element. Other feedback parameters such as gains (G_i), offsets (L_{off}, V_{off}), the pre-stimulation bias (*PreStim*) or the model parameters segment length (l_S) and the body mass (m) did not result in moderate or high correlations.

Muscle-tendon interaction

To further explore the robustness of the sensor-motor maps we investigated the muscle-tendon interaction because the elasticity of the SE also influenced the interplay of the CE and the SE. The muscle interaction maps in Figure 4.8 show the calculated index α for each tendon configuration describing the relation of maximum work generated by the CE to the whole MTC. While values of α were mostly determined by the relation of VFB and LFB (see vertical contours), the map topologies were only slightly influenced by changes in serial elasticity. α values decreased with increasing tendon compliance, and α values at the location of maximum hopping heights ranged from 0.9 ('stiff tendon') to 0.75 ('moderate tendon') to 0.57 ('compliant tendon'). The related work loops show the detailed interplay of CE and SE for simulations that predicted the highest hopping heights (red points). At touch-down, the MTC was stretched by a low force. The MTC generated forces (feedback response) while being stretched (eccentric contraction) which led to negative work loops. During leg extension, the MTC shortened during force generation (concentric contraction) and produced a positive work loop. More compliant tendon resulted in slightly higher MTC deflections and less lengthening of the CE. Because maximum MTC forces did not change with different elasticity, a stiffer configuration caused less deflection and reduced the energy recoil. The energy stored in the SE decreased from 728 J ('compliant tendon') to 437 J ('moderate tendon'). For a maximal hopping height of 0.13 m, the 'stiff tendon' stored the least amount of energy with 142 J.

Table 4.3: Results of the sensitivity analysis. For each specific composition, n depicts the number of stable simulations ($\max(n) = 1000$). Correlations r (Spearman-Rho) and standardized regression coefficients β (in parentheses) of predictors on the maximum hopping height (Δh_{max}) and the hopping efficiency (η). Composition S_3 (pure VFB) did not result in any stable hopping simulations ($n = 0$). High ($r \geq 0.7$ or $r \leq -0.7$) and very significant ($p < 0.01$) correlations are highlighted. ($y_0 = 1.05\,m$, $G = 1$, $PreStim = 0.01$, $\varepsilon_{stiff} = 0.03$, rigid ground).

	S_1(FFB) ($n=958$)		S_2(LFB) ($n=958$)		S_4(FFB, LFB) ($n=808$)		S_5(LFB, VFB) ($n=733$)		S_6(FFB,VFB) ($n=959$)		S_7(FFB, LFB, VFB) ($n=950$)	
	Δh_{max}	η	Δh_{max}	η	Δh_{max}	η	Δh_{max}	η	Δh_{max}	η	Δh_{max}	η
G_F	-0.083** (-0.111)	-0.442** (-0.450)	– –	– –	0.115** (0.127)	0.43 (0.066)	– –	– –	0.037 (0.120)	-0.084** (0.005)	0.100** (0.154)	-0.045 (0.020)
G_L	– –	– –	0.016 (0.004)	-0.031 (-0.052)	-0.022 (-0.021)	-0.011 (-0.008)	0.040 (0.016)	0.110** (0.052)	– –	– –	0.010 (0.007)	0.068* (0.057)
L_{off}	– –	– –	0.198** (0.216)	0.428** (0.396)	0.350** (0.538)	0.309** (0.447)	0.097** (-0.157)	0.224** (0.104)	– –	– –	0.138** (0.116)	0.146** (0.117)
G_V	– –	– –	– –	– –	– –	– –	0.038 (0.083)	-0.304** (-0.314)	-0.079* (-0.078)	-0.246** (-0.234)	-0.060 (-0.086)	-0.384** (-0.414)
V_{off}	– –	– –	– –	– –	– –	– –	0.021 (-0.088)	0.224** (-0.014)	0.007 (0.008)	-0.004 (0.009)	0.096** (0.048)	0.050 (0.002)
$PreStim$	-0.483** (-0.530)	-0.190** (-0.231)	0.198** (-0.028)	-0.014 (-0.039)	-0.046 (-0.049)	-0.009 (-0.019)	-0.028 (0.0001)	-0.051 (-0.005)	-0.036 (-0.007)	-0.040 (-0.030)	-0.006 (-0.020)	-0.003 (-0.023)
Δ_S	0.585** (0.637)	0.442** (0.500)	0.521** (0.531)	0.325** (0.304)	0.426** (0.624)	0.233** (0.414)	0.677** (0.740)	0.569** (0.463)	**0.837** (0.843)**	**0.707** (0.709)**	**0.737** (0.731)**	0.523** (0.510)
ε_{ref}	0.287** (0.338)	0.643** (0.628)	0.119** (0.084)	0.494** (0.431)	0.379** (0.429)	0.670** (0.701)	0.268** (0.238)	0.528** (0.492)	0.287** (0.306)	0.504** (0.480)	0.246** (0.264)	0.510** (0.492)
l_S	0.240 (0.029)	-0.010 (-0.024)	0.023 (0.026)	-0.028 (-0.005)	-0.22 (-0.008)	-0.012 (-0.008)	0.017 (0.018)	0.031 (0.004)	0.007 (-0.018)	0.032 (-0.006)	0.008 (0.001)	-0.003 (0.025)
m	-0.304** (-0.411)	-0.014 (-0.107)	-0.246** (-0.263)	-0.123** (-0.112)	-0.313** (-0.360)	-0.196** (-0.231)	-0.225** (-0.298)	-0.092* (-0.077)	-0.233** (-0.272)	-0.140** (-0.151)	-0.303** (-0.313)	-0.105** (-0.112)

*$p < 0.05$; **$p < 0.01$

Discussion

This simulation study investigated the composition of afferent feedback pathways for generating a repulsive leg response in hopping. Therefore, a neuromuscular reflex model (Geyer et al., 2003) was extended by blending length (LFB), force (FFB) and velocity feedback pathways (VFB) of one anti-gravitational leg extensor muscle. *Sensor-motor maps* were derived to evaluate the predicted motion with respect to stability, performance and efficiency. The topology of the sensor-motor maps was further evaluated for different tendon elasticity, body mass, segment lengths and ground compliances. Below, we first highlight the key insights gained by our hopping model, which will then be discussed in more detail.

1. Different feedback pathways had specific functional contributions: Both FFB and LFB pathways enabled hopping. FFB resulted in largest hopping heights, LFB enhanced hopping efficiency (ratio of hopping height to metabolic effort), and VFB had the ability to disable hopping (also in combination with FFB and LFB). These pathway-specific responses established sensor-motor maps with function-selecting and -tuning pathways in hopping (Figure 4.5).
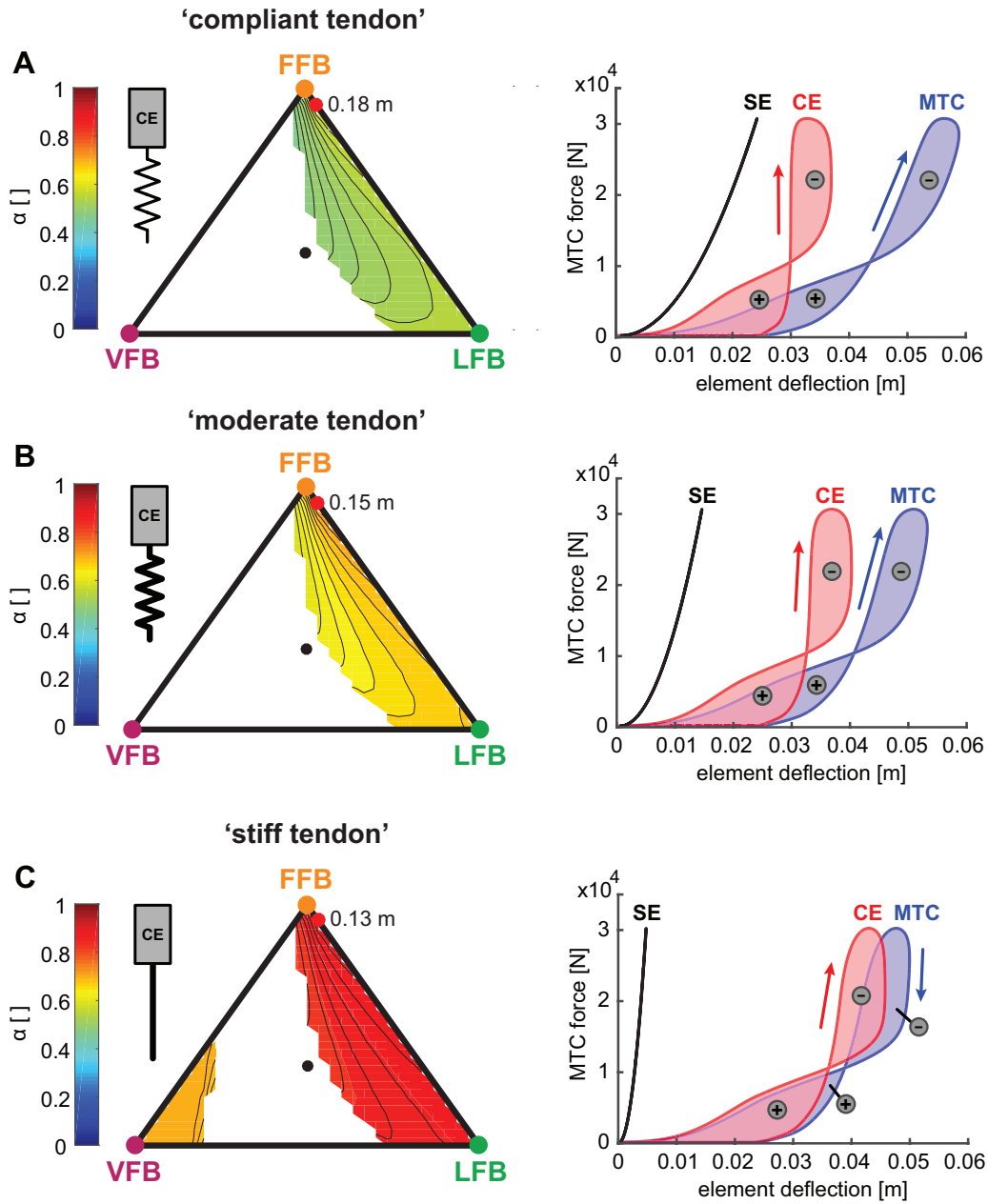
Figure 4.8: Influence of serial elasticity on muscle interaction maps (left side): Maximum work ratio of CE to whole MTC (α) for blended feedback pathways ($y_0 = 1.05\,m$, $G = 1$, $PreStim = 0.01$, rigid ground). Global maxima of hopping heights are visualized by red points. Every point within the triangle represents a unique combination of the three feedback pathways. The larger the distance of a point to a corner (e.g. LFB) the smaller the contribution of that feedback pathway in the blended signal (see Figure 4.3 for explanation of triangles). **(A)** 'compliant tendon' ($\varepsilon_{compliant} = 0.05$), **(B)** 'moderate tendon' ($\varepsilon_{moderate} = 0.03$) and **(C)** 'stiff tendon' ($\varepsilon_{stiff} = 0.01$). **Influence of serial elasticity on individual work loops (right side):** CE (red), SE (black) and MTC (blue) for maximum hopping heights. Positive (energy generation) and negative (energy dissipation) work loops are indicated by positive and negative signs.

2. For the tested case, the topology of these sensor-motor maps as well as the location of functionally optimal compositions was invariant to altered system designs (tendon elasticity, body mass, segment lengths, Figure 4.7A-C) or environmental changes (ground compliance, Figure 4.7D). Thus, in our model the neuromuscular feedback system relied on a consistent topology of feedback compositions.

The modelling framework presented here can be used to establish relations to biomechanical (loco-)motion concepts (e.g. preflex Loeb 1995; Brown and Loeb 2000) and template models (Full and Koditschek, 1999) and to explore the capacity and physiological limitations of the biological neuromuscular system (Pearson et al., 2006), e.g. due to signal delays or muscle dynamics. Moreover, neuromuscular simulation models can be validated, improved and used for different applications, for instance to derive model-based experimental designs for investigating human or animal motor control. The results of our study should be confirmed by experimental studies in biological systems.

Different feedback pathways have different functional contributions

We found pathway-specific features that resulted in different characteristics of the hopping motion. Firstly, FFB was the dominant feedback pathway to produce high hopping heights and thus high hopping performance. Previous studies reported that the combination of the muscle force-velocity-relationship and positive force feedback (FFB) produced stable and high-performing motions (Prochazka et al., 1997a; Prochazka et al., 1997b; Geyer et al., 2003; Haeufle et al., 2012). In contrast to a combination of the force-length-relationship (f_l) and negative LFB (which would result in similar behavior compared to FFB (Prochazka and Yakovenko, 2001)), negative LFB did not provide self-stabilizing behavior (Haeufle et al., 2010). An elastic structure or the f_l helps to achieve energy efficient and spring-like behavior, but does not generate energetically stable hopping on its own (Haeufle et al., 2010). However, experimental evidence for functional force feedback of ankle extensor activity to generate a repulsive leg function has been found for walking cats (Donelan and Pearson, 2004b; Donelan and Pearson, 2004a) and humans (Grey et al., 2007; Klint et al., 2010), but may be different for hopping motions.

Secondly, efficient hopping was found for areas of moderate hopping height in which LFB is dominant. This occurred because the feedback suppression of the length offset (e.g. through fusimotor drive) reduced the positive work production of the CE in late stance phase also reported by Geyer et al. (2003) resulting in high metabolic effort. In our simulations, this suppression could be used to fine-tune the hopping efficiency by determining the length-dependent activation of the CE during stretch-shortening cycle (SSC) (Gollhofer, 2003). This influenced the force-lengthening characteristic of the MTC and thus the energy recoil of the serial elastic element (with the used tendon elasticity). Raburn et al. (2011) suggested that proprioceptive information is used to adjust a periodic bouncing motion pattern to achieve energetically optimal patterns. If afferent pathways of muscle spindles are blocked by an ischemia blockage, the patterns are less adapted (Raburn et al., 2011). It was argued, that the observed effect was most likely caused by an update of the internal model for planning the motion. Nonetheless, implications of direct activation pattern changes as considered in our model could not be ruled out (Dean, 2012). It seems reasonable that reflex contribution directly influences the SSC (e.g. through generating 'muscular stiffness' (Nichols and Houk, 1976; Gollhofer, 2003)) and thus the hopping efficiency (Komi, 2003).

Surprisingly, blending dominant VFB and other feedback pathways did not result in a higher performance, but lead to substantial losses in hopping height resulting from an early rise of the activation signal. Next to this extensive force generation (during leg compression) the CE remained less stretched during stance (force-length-relationship below 0.2) leading to lower push-off forces and hopping performance. This

shift of the CE operation point was also found in the simulation study by Robertson and Sawicki (2014) where higher muscle stimulation frequencies (earlier stimulation onset) and magnitudes resulted in less CE lengthening. In our model, this effect was stronger than the resultant performance increase associated with an increased proportion of FFB. Thus, we found a function disabling behavior for compositions with dominant VFB and small feedback signal time delays. These results indicate that VFB might function as the primary regulator of the system energy in hopping complementing the previous suggestion that FFB might be used to control the energy state of the system (Geyer et al., 2003). McDonagh and Duncan (2002) provided evidence for the contribution of velocity-sensitive afferent signals in their experimental study of landing motions. Increased electromyographic data (EMG) amplitudes of gastrocnemius and rectus femoris muscles were found for increased ankle and knee joint velocities at touchdown (due to different landing heights) during false floor landings compared to expected grounds (McDonagh and Duncan, 2002). For hopping, it might be necessary to delay or inhibit the VFB for example by presynaptic inhibition to functionally enable FFB or LFB pathways. Such inhibition of VFB in hopping were indicated by results by Voigt et al. (1998) who reported a negative correlation between peak stretch velocity and EMG amplitude of the soleus muscle. However, the disabling function of the VFB may not be transferable to other motion tasks such as walking. Because such feedback mechanisms are strongly task and phase dependent the contribution of a feedback pathway may have opposite effects for different motion tasks, e.g. in walking and standing (Pearson et al., 1993; Donelan and Pearson, 2004a). In a biological system this mechanism might be superimposed or modulated by fusimotor action (Prochazka and Ellaway, 2012) or descending signals. Thus, further research is warranted to identify the task-specific role of VFB in generating appropriate leg extensor muscle activation in humans and animals.

Robustness of sensor-motor maps

Regions of stable and unstable hopping motions were only minimally influenced by the changes in tendon stiffness, body mass, segment lengths and ground compliance. Stable solutions for pure VFB were found for 'light mass', 'short segments' or 'stiff tendon' and resulted in very low hopping performance. This result is in agreement with previous studies where VFB produced stable hopping only in the absence of serial compliance (Haeufle et al., 2012; Geyer et al., 2003). More compliance resulted – as expected – in greater hopping heights and more efficient hopping patterns. Similar results were found in experimental and computational studies (Anderson and Pandy, 1993; Kubo et al., 1999; Bobbert, 2001; Nagano et al., 2004). While the level of hopping height was influenced by all altered configurations, the topology of these maps was not affected. Interestingly, we found that for all parameter variations a consistent pathway composition resulted in the maximum hopping performance suggesting a unified sensor-motor map topology with consistent optimal solutions. Apart from this isolated observation, the (multidimensional) sensitivity analysis also revealed only small to moderate dependencies of the predicted hopping height and hopping efficiency for changes in tendon elasticity, body mass or segment lengths.

Our results indicate that sensor-motor maps are robust against these morphological changes. Previous studies showed that the elastic leg function is highly determined by the interplay of the compliant tendomuscular system and the neuronal control system (Nichols and Houk, 1976; Lin and Crago, 2002; Gollhofer, 2003; Taube et al., 2012; Robertson and Sawicki, 2014). In our simulations, a more compliant tendon was able to store and release more energy during hopping agreeing with other studies (Anderson and Pandy, 1993; Bobbert, 2001). Moreover, the model predicted decreasing α values with increasing tendon compliance (increased tendon lengthening) revealing a compensatory behavior of the CE by stiffening (producing equal forces with less deflection). Such behavior was observed by experimental studies, where changes in ground stiffness lead to adaptations of the leg stiffness, such that the total stiffness, consisting

of leg and ground, remains similar (Ferris and Farley, 1997; Moritz and Farley, 2004; Krogt et al., 2009). A similar stiffness adaptation was found for hopping with a passive ankle joint orthesis acting in parallel to the ankle (Ferris et al., 2006). For our model, this effect may be accomplished by the stabilizing function of the non-linear muscle properties (Soest and Bobbert, 1993; Moritz and Farley, 2004; Krogt et al., 2009; Haeufle et al., 2010) as the feedback pathway composition remained the same for all three conditions. These 'exploit mechanics' or 'preflex' function (Loeb et al., 1999) may serve as a selector (functional filter) to offer favorable solutions for the neural motor control system (sensor-motor maps) that allow to learn its simple (Loeb, 1995) and consistent topology.

Integration of spinal reflexes and feed-forward control

Although we did not consider supra-spinal motor commands, we would like to reflect our results on their functional integration with feed-forward commands. Our model suggests that the neuromuscular feedback system alone could generate appropriate adjustments of the muscle activation to permit a fine-tuning of hopping motions. In addition to our results, previous experimental studies revealed the importance of pre-planned feed-forward commands in hopping and drop jumps. Descending commands may contribute during the early contact phase (Zuur et al., 2010) and towards push-off (Taube et al., 2008). Accordingly, the EMG activity of ankle extensor muscles (such as the soleus) was found to be pre-programmed and adjusted dependent on the task (e.g jumping or landing) (Leukel et al., 2008b; Leukel et al., 2012) and with respect to the timing of the touch-down (Santello and McDonagh, 1998; McDonagh and Duncan, 2002). Integrating feed-forward commands would certainly influence the results presented in this study. For example, pre-planned motor commands could compensate the repressive behavior following dominant VFB. Such descending commands could be superposed to our blended feedback signal (as *PreStim* in our model) (Taube et al., 2012) or adapt and suppress the afferent gating (G in our model), for instance by presynaptic inhibition (McDonagh and Duncan, 2002; Leukel et al., 2008b; Leukel et al., 2008a).

The motor control system is likely to rely more on afferent feedback in the case of misplanned motions (if perturbations occur) or if knowledge about the environment is uncertain and planning is difficult (Donelan and Pearson, 2004a). The contribution of afferent feedback pathways may increase under these conditions (McDonagh and Duncan, 2002). A function specific fine-tuning of hopping motions with respect to different movement targets or cost functions (e.g. performance, efficiency), as found for our model, would support the generation of appropriate activation patterns in such conditions. Therefore, supra-spinal centers might plan an appropriate blending of the afferents (setting of λ_i) before touch-down. For example, in our model shifting from targeting hopping performance to hopping efficiency could be moderated by fading from dominant FFB to dominant LFB (see Video in Supplementary Material[1].). By comparing predicted and actual afferents (Wolpert et al., 1995; McDonagh and Duncan, 2002), the overall feedback gain (in our model G) might increase if deviations and errors are detected. If so, the pre-setting of the afferent blending permits a fast and function-oriented contribution (performance, efficiency) of feedback responses. Another advantage would be the reduced control effort due to the low-dimensionality of the blending (setting of λ_i). However, higher centers must be able to learn such feedback blending even in the case of sensorial and mechanical perturbations. Thus, in order to be functionally useful, the solution space of possible feedback compositions (as shown in the sensor-motor maps) must follow a simple and consistent topology (Loeb, 1995). Indeed, we found compact and robust topologies that were invariant to changes of morphological design or environmental parameters with respect to motion stability and optimal compositions. Nonetheless, we can only derive hypotheses about a potential integration of our feedback

[1]The Video can be downloaded from the paper online resource: Link

model and feed-forward commands. The discussion presented here warrants validation and support from experimental studies.

Comparison of the model to human hopping

The neuromechanical hopping model (with a reference strain of $\varepsilon_{moderate} = 0.03$, 'moderate' mass, 'moderate' segment lengths and rigid ground) produced similar hopping motions as those of human hopping. A high effective stiffness of the leg was found for high hopping frequencies. While similar results have been reported in experimental studies (Farley et al., 1999; Riese et al., 2013), other studies reported higher leg stiffness values ranging from 30 kN/m to 55 kN/m (Farley et al., 1991; Kuitunen et al., 2011; Hobara et al., 2011). However, hopping frequency and leg stiffness were in reasonable ranges and changed accordingly (Rapoport, S. et al., 2003). Moreover, our model predicted increasing hopping performance with increasing tendon elasticity agreeing with results of experimental studies (Kubo, 2005; Fukashiro et al., 2006) and other simulation studies (Anderson and Pandy, 1993; Bobbert, 2001; Nagano et al., 2004). Although this study utilises a highly simplified model structure the model predicted the basic dynamics (e.g. hopping frequency and leg stiffness) of human hopping. We thus consider this model a valid simplification for the scope of this study.

Model limitations

We chose a rather simplistic model to integrate multiple sensory pathways at the elementary sensor-motor-level to determine how individual reflex pathways of muscle force (FFB), fiber length (LFB) and velocity (VFB) can support – in isolation *and* in combination – the repulsive leg function during the stance phase of hopping. By blending individual sensory pathways, we investigated the capacity of the neuromuscular feedback system to generate goal-directed motions. These simplifications may have influenced our results.

We selected a bouncing task (one dimensional hopping) as primary locomotor function. The functional contribution of the different feedback pathways predicted for hopping will most likely be different for other motion tasks. The hopping model of Geyer et al. (2003) utilized one anti-gravitational leg extensor muscle representing all involved muscles during the stance phase of hopping. The foot segment and ankle joint were neglected possibly influencing the overall leg stiffness of the model because the ankle joint was found to be the main contributor for leg stiffness modulations at higher hopping frequencies (above 2.2 Hz) (Farley et al., 1998; Farley et al., 1999; Hobara et al., 2011). Nonetheless, the model of Geyer et al. (2003) and our simulations generated biomechanically reasonable results. In addition, we simplified the distributed mass of the human body to a point mass neglecting the effects of wobbling masses and their influence on impact dynamics (Seyfarth et al., 1999; Schmitt and Günther, 2011). This helped to focus on the muscle-tendon interaction and the functional contribution of different feedback pathways. The model of the MTC did not consist of a parallel elastic element that could (additionally to the SE) store and release energy in SSC (Anderson and Pandy, 1993; Lindstedt et al., 2002; Robertson and Sawicki, 2014) when the CE is stretched beyond its optimal length (Soest and Bobbert, 1993). However, in our simulations, the CE did not operate above its optimal length. Hence, we argue that it is tenable to neglect the parallel elastic element in this particular case. In addition, jumping simulation models by Anderson and Pandy (1993) and Seyfarth et al. (2000) showed only insignificant contribution of the parallel elastic elements. Moreover, while in our study damping within the MTC was neglected, a damping element has also been found to be negligible for hopping (Rapoport, S. et al., 2003).

The used neuromuscular feedback model is a highly simplified representation of the complex biological network. Sensory signals were handled as ideal, averaged and analogue physical quantities without frequency modulation and sensory or signal noise. By using simple delays, offsets and gains, we only considered a highly simplified neural processing of the monosynaptic feedback pathways. In particular, no time-variant feedback gains (Pearson, 1995; Pearson et al., 1998) or other sensory signals such as joint position and velocity, mechanoreceptors or cutaneous receptors were considered. Because we found moderate correlations for the feedback time delay, feedback-specific delays (Prochazka et al., 1997a) will certainly influence the performance and efficiency of the model. Possible causes of afferent gain changes as discussed in Sreenivasa et al. (2015) were not investigated here. All these factors were simplified and neglected for the sake of simplicity and comprehensibility (Full and Koditschek, 1999; Brown and Loeb, 2000; Pearson et al., 2006). For this study, it was important to separate and isolate the pathway and task-specific effects in the frame of the mechanical structure and muscle mechanics. Previous studies of similar model complexity (Kuo, 2002; Geyer et al., 2003; Haeufle et al., 2010; Haeufle et al., 2012) not only demonstrated realistic motions but also elucidated the functional roles of the different contributors of feedback, feed-forward or muscle properties.

Outlook and future directions

Based on the results of this study, the robustness of the system against mechanical or sensory perturbations can be investigated. From a control point of view, combinations of multiple sensory pathways or information channels about the system state will result in more robust and more precise estimations of the system state (Donelan and Pearson, 2004a; Green and Angelaki, 2010). Comparing effect sizes resulting from muscle properties (Haeufle et al., 2010), feedback blending and an integration of feed-forward controls (Kuo, 2002; Haeufle et al., 2012) is of high interest. In a next step, we will expand our models to other motions tasks (e.g. running and walking) and underlying locomotor subfunctions (Sharbafi and Seyfarth, 2017) such as swing and balancing (Seyfarth et al., 2012; Sharbafi et al., 2017). For these scenarios, other feedback pathways, e.g. from vestibular organs or as suggested by Song and Geyer (2015), may be used to examine the generalisability of the sensor-motor maps.

Moreover, we would like to explore the use of this type of neuromuscular model as non-invasive distinguishing tool for two purposes: (1) to further explore the mechanisms and interactions of mechanical, neuromuscular and sensory templates and (2) for a model-based design of experimental protocols and settings (e.g. perturbation profiles). While computational modelling approaches help to investigate underlying principles of locomotion, they could potentially help to predict the value and usefulness of experimental settings. Such a model-based identification of experimental settings might improve future experimental designs.

Conclusion

The novel sensor-motor maps provide a tool for analysing human (and animal) motor control strategies and investigating how the biological neural control system recruits function-specific sensor-motor pathways. The maps of muscle force, fibre length and velocity pathways are predicted to be robust with respect to changes in body and environment mechanics (e.g. compliance).

In addition to central (or spinal) pattern generators, muscle-reflex based control circuits are able to generate adjustable cyclic motions by exploiting the musculoskeletal dynamics and gravity. We call these nmPG.

Accordingly, the sensory feedback pathways (e.g. positive force feedback) operate as an antagonist system to the mechanics of the body (muscles, segments) and gravity. The mechanical system is consequently not only the target of (neuronal) control but at the same time an essential part of pattern generating networks.

Acknowledgments

Author Contributions

CS and AS contributed to the design, execution and drafting of this work, and approved the final manuscript. CS implemented the computational model and conducted the simulation studies.

Disclosure/Conflict-of-Interest Statement

The authors declare that the research was conducted in the absence of any commercial or financial relationships that could be construed as a potential conflict of interest.

References

F. C. Anderson and M. G. Pandy (1993). "Storage and utilization of elastic strain energy during jumping". In: *Journal of Biomechanics* 26.12, pp. 1413–1427.

N. A. Bernstein (1967). "The co-ordination and regulation of movements". In:

E. Bizzi et al. (2008). "Combining modules for movement". In: *Brain Research Reviews* 57.1. Networks in Motion, pp. 125–133.

M. F. Bobbert (2001). "Dependence of human squat jump performance on the series elastic compliance of the triceps surae: a simulation study." In: *The Journal of Experimental Biology* 204.3, pp. 533–542.

I. E. Brown and G. E. Loeb (2000). "A Reductionist Approach to Creating and Using Neuromusculoskeletal Models". In: *Biomechanics and Neural Control of Posture and Movement*. Ed. by J. M. Winters and P. E. Crago. New York, NY: Springer New York, pp. 148–163.

A. D'Avella, P. Saltiel, and E. Bizzi (2003). "Combinations of muscle synergies in the construction of a natural motor behavior." In: *Nature neuroscience* 6.3, pp. 300–308.

J. C. Dean (2012). "Proprioceptive Feedback and Preferred Patterns of Human Movement". In: *Exercise and Sport Sciences Reviews* 9, p. 1.

V. Dietz (1992). "Human neuronal control of automatic functional movements: interaction between central programs and afferent input." In: *Physiol Rev* 72.1, pp. 33–69.

J. M. Donelan and K. G. Pearson (2004a). "Contribution of sensory feedback to ongoing ankle extensor activity during the stance phase of walking". In: *Canadian Journal of Physiology and Pharmacology* 82.8-9, pp. 589–598.

J. M. Donelan and K. G. Pearson (2004b). "Contribution of force feedback to ankle extensor activity in decerebrate walking cats." In: *Journal of neurophysiology* 92.4, pp. 2093–104.

C. T. Farley et al. (1998). "Mechanism of leg stiffness adjustment for hopping on surfaces of different stiffnesses." In: *Journal of applied physiology (Bethesda, Md. : 1985)* 85.3, pp. 1044–55.

C. T. Farley et al. (1999). "Leg stiffness primarily depends on ankle stiffness during human hopping". In: *Journal of Experimental Biology* 32.3, pp. 267–273.

C. T. Farley et al. (1991). "Hopping frequency in humans: a test of how springs set stride frequency in bouncing gaits." In: *Journal of applied physiology (Bethesda, Md. : 1985)* 71.6, pp. 2127–2132.

D. P. Ferris and C. T. Farley (1997). "Interaction of leg stiffness and surfaces stiffness during human hopping." In: *Journal of applied physiology (Bethesda, Md. : 1985)* 82.1, pp. 15–22.

D. P. Ferris et al. (2006). "Neuromechanical adaptation to hopping with an elastic ankle-foot orthosis." In: *Journal of Applied Physiology* 100.1, pp. 163–170.

S. Fukashiro, D. C. Hay, and A. Nagano (2006). "Biomechanical Behavior of Muscle-Tendon Complex During Dynamic Human Movements reutilization of elastic energy by the tendinous structures play an important role in enhancing work output and movement efficiency in many sorts of human movements". In: *Journal of Applied Biomechanics* 22, pp. 131–147.

R. Full and D. Koditschek (1999). "Templates and anchors: neuromechanical hypotheses of legged locomotion on land". In: *Journal of Experimental Biology* 202.23, pp. 3325–3332.

H. Geyer, A. Seyfarth, and R. Blickhan (2003). "Positive force feedback in bouncing gaits?" In: *Proceedings of the Royal Society of London. Series B: Biological Sciences* 270.1529, pp. 2173–2183.

A. Gollhofer (2003). "Proprioceptive training: considerations for strength and power production". In: *Strength and power in sport*. Ed. by P. V. Komi. Blackwell Science Ltd, pp. 331–342.

A. M. Green and D. E. Angelaki (2010). "Multisensory integration: Resolving sensory ambiguities to build novel representations". In: *Current Opinion in Neurobiology* 20.3, pp. 353–360.

M. J. Grey et al. (2007). "Positive force feedback in human walking." In: *The Journal of physiology* 581.Pt 1, pp. 99–105.

D. F. B. Haeufle, S. Grimmer, and a. Seyfarth (2010). "The role of intrinsic muscle properties for stable hopping–stability is achieved by the force-velocity relation." In: *Bioinspiration & biomimetics* 5.1, p. 16004.

D. F. B. Haeufle et al. (2012). "Integration of intrinsic muscle properties, feed-forward and feedback signals for generating and stabilizing hopping". In: *Journal of The Royal Society Interface* 9.72, pp. 1458–1469.

K. Hase et al. (2003). "Human gait simulation with a neuromusculoskeletal model and evolutionary computation". In: *Journal of Visualization and Computer Animation* 14.2, pp. 73–92.

E. Henneman, G. Somjen, and D. O. Carpenter (1965). "Functional Significance of Cell Size in Spinal Motoneurons." In: *Journal of neurophysiology* 28.3, pp. 560–580.

H. Hobara et al. (2011). "Determinant of leg stiffness during hopping is frequency-dependent". In: *European Journal of Applied Physiology* 111.9, pp. 2195–2201.

R. af Klint et al. (2010). "Load Rather Than Length Sensitive Feedback Contributes to Soleus Muscle Activity During Human Treadmill Walking". In: *Journal of Neurophysiology* 103.5, pp. 2747–2756.

P. V. Komi (2003). "Stretch-Shortening Cycle". In: *Strength and power in sport*. Ed. by P. V. Komi. Blackwell Science Ltd, pp. 184–202.

P. Krishnaswamy, E. N. Brown, and H. M. Herr (2011). "Human leg model predicts ankle muscle-tendon morphology, state, roles and energetics in walking". In: *PLoS Computational Biology* 7.3. Ed. by K. J. Friston, e1001107.

M. M. van der Krogt et al. (2009). "Robust passive dynamics of the musculoskeletal system compensate for unexpected surface changes during human hopping." In: *Journal of applied physiology (Bethesda, Md. : 1985)* 107.3, pp. 801–808.

K. Kubo (2005). "In Vivo Elastic Properties of Human Tendon Structures in Lower Limb". In: *International Journal of Sport and Health Science* 3.Special_Issue_2, pp. 143–151.

K. Kubo, Y. Kawakami, and T. Fukunaga (1999). "Influence of elastic properties of tendon structures on jump performance in humans." In: *Journal of applied physiology (Bethesda, Md. : 1985)* 87.6, pp. 2090–6.

S. Kuitunen, K. Ogiso, and P. V. Komi (2011). "Leg and joint stiffness in human hopping". In: *Scandinavian Journal of Medicine and Science in Sports* 21.6, e159–e167.

A. D. Kuo (2002). "The relative roles of feedforward and feedback in the control of rhythmic movements." In: *Motor control* 6.2, pp. 129–145.

C. Leukel et al. (2008a). "Influence of falling height on the excitability of the soleus H-reflex during drop-jumps". In: *Acta Physiologica* 192.4, pp. 569–576.

C. Leukel et al. (2008b). "Phase- and task-specific modulation of soleus H-reflexes during drop-jumps and landings". In: *Experimental Brain Research* 190.1, pp. 71–79.

C. Leukel et al. (2012). "Changes in predictive motor control in drop-jumps based on uncertainties in task execution". In: *Human Movement Science* 31.1, pp. 152–160.

C. C. K. Lin and P. E. Crago (2002). "Neural and mechanical contributions to the stretch reflex: A model synthesis". In: *Annals of Biomedical Engineering* 30.1, pp. 54–67.

S. L. Lindstedt et al. (2002). "Do muscles function as adaptable locomotor springs?" In: *The Journal of Experimental Biology* 205.Pt 15, pp. 2211–2216.

G. E. Loeb, I. E. Brown, and E. J. Cheng (1999). "A hierarchical foundation for models of sensorimotor control". In: *Experimental Brain Research* 126.1, pp. 1–18.

G. Loeb (1995). "Control implications of musculoskeletal mechanics". In: *Proceedings of 17th International Conference of the Engineering in Medicine and Biology Society* 2, pp. 1393–1394.

M. J. N. McDonagh and A. Duncan (2002). "Interaction of pre-programmed control and natural stretch reflexes in human landing movements." In: *The Journal of physiology* 544.Pt 3, pp. 985–94.

A. E. Minetti and R. M. Alexander (1997). "A theory of metabolic costs for bipedal gaits." In: *Journal of theoretical biology* 186.4, pp. 467–76.

C. T. Moritz and C. T. Farley (2004). "Passive dynamics change leg mechanics for an unexpected surface during human hopping." In: *Journal of applied physiology (Bethesda, Md. : 1985)* 97.4, pp. 1313–1322.

A. Nagano, T. Komura, and S. Fukashiro (2004). "Effects of Series Elasticity of the Muscle Tendon Complex on an Explosive Activity Performance with a Counter Movement". In: *Journal of Applied Biomechanics* 20.1, pp. 85–94.

T. Nichols and J. Houk (1976). "Improvement in linearity and regulation of stiffness that results from actions of stretch reflex." In: *J Neurophysiol* 39.1, pp. 119–142.

N. Ogihara and N. Yamazaki (2001). "Generation of human bipedal locomotion by a bio-mimetic neuro-musculo-skeletal model." In: *Biological cybernetics* 84.1, pp. 1–11.

M. G. Pandy et al. (1990). "An optimal control model for maximum-height human jumping". In: *Journal of Biomechanics* 23.12, pp. 1185–1198.

C. Paul et al. (2005). "Development of a human neuro-musculo-skeletal model for investigation of spinal cord injury". In: *Biological Cybernetics* 93.3, pp. 153–170.

K. G. Pearson, J. E. Misiaszek, and K. Fouad (1998). "Enhancement and resetting of locomotor activity by muscle afferents". In: *Annals of the New York Academy of Sciences* 860.1 NEURONAL MECH, pp. 203–215.

K. G. Pearson et al. (1993). "Reversal of the influence of group Ib afferents from plantaris on activity in medial gastrocnemius muscle during locomotor activity". In: *Journal of Neurophysiology* 70.3, pp. 1009–1017.

K. G. Pearson (1995). *Proprioceptive regulation of locomotion*.

K. Pearson, Ö. Ekeberg, and A. Büschges (2006). *Assessing sensory function in locomotor systems using neuro-mechanical simulations*.

A. Prochazka, D. Gillard, and D. J. Bennett (1997a). "Positive force feedback control of muscles." In: *Journal of neurophysiology* 77.6, pp. 3226–3236.

A. Prochazka and P. Ellaway (2012). "Sensory systems in the control of movement." In: *Comprehensive Physiology* 2.4, pp. 2615–2627.

A. Prochazka, D. Gillard, and D. J. Bennett (1997b). "Implications of positive feedback in the control of movement". In: *Journal of Neurophysiology* 77.6, pp. 3237–3251.

A. Prochazka and S. Yakovenko (2001). "Locomotor Control: From Spring-like Reactions of Muscles to Neural Prediction". In: *The Somatosensory System: Deciphering the Brain's Own Body Image* November 2016, pp. 141–181.

C. E. Raburn, K. J. Merritt, and J. C. Dean (2011). "Preferred movement patterns during a simple bouncing task". In: *Journal of Experimental Biology* 214.22, pp. 3768–3774.

Rapoport, S. et al. (2003). "Constant and Variable Stiffness and Damping of the Leg Joints in Human Hopping". In: *Journal of Biomechanical Engineering* 125.4, pp. 507–514.

S. Riese, A. Seyfarth, and S. Grimmer (2013). "Linear center-of-mass dynamics emerge from non-linear leg-spring properties in human hopping". In: *Journal of Biomechanics* 46.13, pp. 2207–2212.

B. D. Robertson and G. S. Sawicki (2014). "Exploiting elasticity: Modeling the influence of neural control on mechanics and energetics of ankle muscle-tendons during human hopping". In: *Journal of Theoretical Biology* 353, pp. 121–132.

M. Santello and M. J. McDonagh (1998). "The control of timing and amplitude of EMG activity in landing movements in humans." In: *Experimental Physiology* 83.6, pp. 857–74.

S. Schmitt and M. Günther (2011). "Human leg impact: Energy dissipation of wobbling masses". In: *Archive of Applied Mechanics* 81.7, pp. 887–897.

A. Seyfarth, R. Blickhan, and J. L. Van Leeuwen (2000). "Optimum take-off techniques and muscle design for long jump." In: *Journal of Experimental Biology* 203.Pt 4, pp. 741–50.

A. Seyfarth, M. Günther, and R. Blickhan (2001). "Stable operation of an elastic three-segment leg". In: *Biological Cybernetics* 84.5, pp. 365–382.

A. Seyfarth et al. (2012). "Can robots help to understand human locomotion?" In: *At-Automatisierungstechnik* 60.11, pp. 653–661.

A. Seyfarth et al. (1999). "Dynamics of the long jump". In: *Journal of Biomechanics* 32.12, pp. 1259–1267.

M. A. Sharbafi and A. Seyfarth (2017). "How locomotion sub-functions can control walking at different speeds?" In: *Journal of Biomechanics* 53, pp. 163–170.

M. Sharbafi et al. (2017). "Reconstruction of human swing leg motion with passive biarticular muscle models". In: *Human Movement Science* 52, pp. 96–107.

A. J. van Soest and M. F. Bobbert (1993). "The contribution of muscle properties in the control of explosive movements". In: *Biological Cybernetics* 69.3, pp. 195–204.

S. Song and H. Geyer (2015). "A neural circuitry that emphasizes spinal feedback generates diverse behaviours of human locomotion". In: *The Journal of physiology* 593.16, pp. 3493–3511.

S. Song and H. Geyer (2017). "Evaluation of a Neuromechanical Walking Control Model Using Disturbance Experiments". In: *Frontiers in Computational Neuroscience* 11, p. 15.

M. Sreenivasa, K. Ayusawa, and Y. Nakamura (2015). "Modeling and identification of a realistic spiking neural network and musculoskeletal model of the human arm, and an application to the stretch reflex". In: *IEEE Transactions on Neural Systems and Rehabilitation Engineering* 4320.Section III, pp. 1–1.

G. Taga (1998). "A model of the neuro-musculo-skeletal system for anticipatory adjustment of human locomotion during obstacle avoidance." In: *Biological cybernetics* 78.1, pp. 9–17.

W. Taube, C. Leukel, and A. Gollhofer (2012). "How neurons make us jump: the neural control of stretch-shortening cycle movements." In: *Exercise and sport sciences reviews* 40, pp. 106–15.

W. Taube et al. (2008). "Differential modulation of spinal and corticospinal excitability during drop jumps." In: *Journal of neurophysiology* 99.3, pp. 1243–1252.

L. H. Ting et al. (2012). *Review and perspective: Neuromechanical considerations for predicting muscle activation patterns for movement.*

V. Torczon (1997). "On the convergence of pattern search algorithms". In: *SIAM Journal on optimization* 7.1, pp. 1–25.

G. J. van Ingen Schenau (1984). "An alternative view of the concept of utilisation of elastic energy in human movement". In: *Human Movement Science* 3.4, pp. 301–336.

M. Voigt, P. Dyhre-Poulsen, and E. B. Simonsen (1998). "Modulation of short latency stretch reflexes during human hopping". In: *Acta Physiologica Scandinavica* 163.2, pp. 181–194.

D. M. Wolpert, Z. Ghahramani, and M. I. Jordan (1995). "An internal model for sensorimotor integration." In: *Science (New York, N.Y.)* 269.5232, pp. 1880–2.

A. T. Zuur et al. (2010). "Contribution of afferent feedback and descending drive to human hopping." In: *The Journal of physiology* 588.Pt 5, pp. 799–807.

5 Thesis Conclusions

This chapter will discuss the main insights and implications of the presented articles, and put these into a larger picture. Further, the limitations of this work are discussed and future research directions will be delivered.

General discussion

Early mentions on the origins of locomotion go back to philosophers like Plato (428-348 BC) and Aristotle (384-322 BC). After the recognition of electrical potentials in nerve and muscle by Galvani (1791), scientists like Helmholtz, Pavlov and Sherrington (1906) shaped the early understanding of proprioceptive signals in the generation of movements. Then, Bernstein (1967) was one of the first to formulate the integration of feed forward and feedback signals to control the underdetermined[1] body and generate actions for achieving the desired movement goal. To date, however, it remains open how the neuromuscular system exploits this redundancy and how the different systems in the motor control loop (Figure 1.1) are organised and interconnected to achieve cyclic motion patterns (Donelan et al., 2004).

Thus, this thesis investigated the contribution of motor and sensor networks to translate between the structure of locomotion and the neural control system. In order to test this hypothesis, two examples of cyclic locomotion were investigated using different perspectives and methodological approaches to reflect the specific requirements of these systems.

In Chapter 2, a macro-perspective based on a meta-analysis examined functions of motor networks by integrating research from conceptual models, human experiments and robotic applications. Based on previous research, this chapter worked out beneficial features of biarticular muscles in the leg to simplify multi-joint coordination in the stance leg, swing leg and upper-body balance. Further, Chapter 3 validated one of these results in a human experiment by applying a novel perturbation type to study upper-body balance. Finally, Chapter 4 addressed the composition of the sensor network from a micro-perspective. Here, sensor-motor maps were developed to visualise and evaluate the capacities and limitations of blended feedback pathways for generating a repulsive stance leg function. A neuromechanical template model identified simple relations between sensor network topologies and task-specific motions.

Motor and sensor networks that were investigated in this thesis provided structural solutions to support the neural system. This *control embodiment*[2] was achieved by exploiting the fundamental dynamics of locomotion. Network topologies of muscles and receptors translated the segmented leg structure into the generalised coordinates of the template models (Chapters 2 and 3) and promoted goal-directed movements

---

[1]Due to the redundancy at the anatomical, kinematic (Bernstein, 1967) or neurophysiological level (Henneman et al., 1965), different movements can result in the same movement goal. Therefore, multiple motor solutions to one motor problem exist.

[2]While initially called *intelligent embodiment* (Pfeifer and Bongard, 2007), in this thesis, the term *control embodiment* is used to emphasise the specific contribution to locomotion control.

by elementary compositions of feedback pathways (Chapter 4). By this, these networks bridged the gap between the simple structure of locomotion and the complex physical realisation of the human body.

Motor networks

Biarticular muscles mainly operate in global leg coordinates

The human leg architecture is complex due to its asymmetric and redundant muscle arrangement. However, this does not inevitably require complex neural control strategies. Indeed, Chapter 2 identified how structures in the motor network could help to simplify coordination or control. Conceptual models suggest that biarticular structures in the leg approximate fundamental mechanisms of legged locomotion into the complex leg physiology (Lakatos et al., 2014; Sharbafi et al., 2017; Sarmadi et al., 2019). Given appropriate segment lengths and muscle moment arms, biarticular muscles can sense and act in global leg coordinates (leg orientation and length) instead of local joint coordinates (Chapter 2). These results agree well with other studies, which suggest that the neural system controls the segmented leg in these global coordinates (Bosco and Poppele, 2001; Ivanenko et al., 2007; Auyang et al., 2009). Proprioceptive circuits might facilitate such limb-centred control strategies (Nichols et al., 2016). Biarticular muscles may thus be able to approximate the global leg behaviour as described in biomechanical template models (Chapter 2). This would be highly beneficial for the neural control system, since these template models showed that already simple mechanisms could generate cyclic locomotion or improve the stability region of the motion (Blickhan, 1989; Seyfarth et al., 2002; Seyfarth et al., 2003; Rummel et al., 2008; Maus et al., 2010; Riese and Seyfarth, 2011; Ludwig et al., 2012). These results indicate that the neural control can use simple logics or mechanisms through the translation of biarticular structures in the motor network. However, more research is needed to support this theory (see Limitations & Outlook).

Contributions of biarticular muscles may simplify control strategies

Reviewing evidence from human experiments (in Chapter 2) showed that biarticular muscles coordinate multi-joint movements, secure the zig-zag-configuration of the leg against joint overextension, improve motion economy (e.g. by transferring energy), and contribute to control angular momentum, e.g. during balance or swing leg motions. However, most of these results were based on unperturbed movements. Therefore, Chapter 3 examined muscle contributions to recover from upper-body balance perturbations in standing to investigate also predictive and reactive control strategies. Since previous perturbation types did not allow to study the upper-body posture in isolation, a new device, an Angular Momentum Perturbator (AMP), was used to produce specific upper-body pitch perturbations. Biarticular thigh muscles showed the strongest reflex responses of all tested leg muscles (Chapter 3). This study firstly provided strong evidence that biarticular muscles are preferably used to realign the upper-body, indicating a higher efficacy for controlling angular momentum, compared to monoarticular muscles. In this context, Lacquaniti and Maioli (1994) and Jacobs and Macpherson (1996) suggested independent control strategies of axial and perpendicular leg forces by mono- and biarticular muscles. By this, the motor network of mono- and biarticular muscles would directly embody a structural solution of a simple but functional control strategy.

Sensor networks

Reflex pathways can exploit template-like locomotion

In Chapter 4, simple sensor networks were sufficient to generate appropriate motor commands to perform steady-state hopping in a simulation model. Changed compositions of sensory signals stemming from muscle spindles and Golgi tendon organs resulted in specific characteristics of the predicted hopping pattern.

Both enabling and disabling behaviours were predicted, suggesting that different feedback compositions serve different functional roles: muscle force feedback (FFB) resulted in performant movements, muscle fibre length feedback (LFB) enhanced hopping efficiency and muscle fibre velocity feedback (VFB) disabled hopping (safe landing). These simulation results indicate that already simple logics in the sensor network (weighted summation) can be sufficient to generate task-relevant movements. This example demonstrates that the requirement of bouncing gaits (Blickhan, 1989; Geyer et al., 2006), namely a compliant leg behaviour, can be easily exploited by the neuromuscular system. In order to generate suitable motor commands to drive anti-gravitational muscles, simple reflex signals from force or length feedback can be recruited (Chapter 4). Simple or elementary connections in the neural network (as shown here) would allow improving the efficiency of motor control and facilitate learning. In this context, however, also other sources of activation like feed forward signals, e.g. from supra-spinal centres (Zuur et al., 2010) or central pattern generator (CPG) (Ijspeert, 2008; Kiehn, 2016), can contribute to generating steady-state behaviours reflecting the high level of control redundancy if mechanical, sensor and motor systems are designed appropriately. In the centipede model of Yasui et al. (2019), combinations of feed forward commands, local pattern generators and sensory feedback produced adaptive behaviours like gait changes from walking to swimming and *vice versa*. Their model suggests that sensory feedback is used to coordinate neural oscillators (Yasui et al., 2019). In the future, CPGs could also be integrated and evaluated in the model of Chapter 4 to study the topology of the sensor-motor maps for an interplay of central and peripheral control strategies. Based on results from Haeufle et al. (2012), it is expected that both feedback and feed forward systems complement each other to generate more robust motor commands.

Simple behaviour may also require only simple control strategies

A simple neuromechanical model was used to capture fundamental control principles and the dynamic interplay of the mechanical and neural system with matching complexity levels (Chapter 4). The hypothesis of this approach, namely that mechanics and neural control can be represented by similar and parsimony representations, is based on the existence of simple, biomechanical template models (Full and Koditschek, 1999; Brown and Loeb, 2000; Pearson et al., 2006). This approach assumes that networks of the neural control system match the low-dimensional representation of the motion task, as identified by biomechanical template models (Geyer et al., 2006). Another basis for this hypothesis comes from the long co-evolution of the periphery (motor, sensor and body mechanics) and the nervous system (Chiel and Beer, 1997). Both, the body morphology as well as the nervous system[3] undergo changes within the organism's lifespan and at evolutionary time scales that result in an 'ecological balance' of frequently performed motions (Pfeifer and Iida, 2004). For instance, changes in the vestibular organ from hominid fossils (of early erect-walking hominids) compared to living primates (great apes) suggest changes of the sensory apparatus favouring balancing for bipedal locomotion (Spoor et al., 1994). For fundamental locomotion tasks like walking, running or hopping, these results further indicate that the mechanical and the neural system operate with matching complexity levels to distribute tasks between systems (Chiel and Beer, 1997; Pfeifer and Iida, 2004). However, more research is needed to validate this hypothesis. Recently, the simulation study of Davoodi et al. (2019) demonstrated that simple template-like control mechanisms could effectively be incorporated in more complex neuromuscular control, including adaptive feedback strategies.

Simple sensor-motor connections may facilitate learning

Novel sensor-motor maps helped to predict the solution space and relate blendings of different feedback pathways to the predicted leg behaviour. This approach helped to visualise the contribution of the sensor network concerning its functional outcome to improve the comprehensibility of the complex interplay of sensory integration. It was found that these mappings of the solution space were compact and united

---

[3]Due to learning processes, the nervous system is usually considered to be more plastic than the body morphology.

(without multiple fragments) and showed smooth gradients (Chapter 4). Moreover, the topology of the sensor-motor maps, as well as the location of functionally optimal compositions, were invariant to changes in system designs and environmental parameters. This robustness might be a result of self-stabilising features stemming from (1) the feedback signals directly, (2) the interplay of the compliant tendomuscular system and the neuronal control system (Nichols and Houk, 1976; Lin and Crago, 2002; Robertson and Sawicki, 2014) or (3) the control embodiment of muscle preflexes (Loeb et al., 1999). Previous studies suggest that the preflex function of intrinsic muscle properties (Hill, 1938; Gordon et al., 1966; Rode et al., 2009; Heidlauf et al., 2017; Tomalka et al., 2017) pre-filter suitable solutions for the neural control system and thereby improve the robustness of the system to withstand perturbations (Krogt et al., 2009; Niiyama et al., 2007; Haeufle et al., 2010; Davoodi et al., 2019) and reduce control effort (Yakovenko et al., 2004; Paul, 2006; Haeufle et al., 2014). The observed consistency of the sensor-motor map topologies (Chapter 4) further suggest a simple learning problem (Loeb, 1995). The study of Anand et al. (2019), which used deep reinforcement learning to learn a walking controller in a complex simulation model, found faster and more precise learning when muscle models and associated muscle properties were included instead of simple torque generators. Another study, which used a neural network to learn a control policy of a robotic system, found that muscle properties could reduce the dimensionality of the learning problem (Driess et al., 2018). In future, machine learning approaches should be combined with parsimony neuromechanical models to evaluate to what extent sensor-motor mappings facilitate learning of task-specific behaviours.

Limitations & Outlook

This thesis, however, has its limitations. Therefore, this section will discuss these issues and give suggestions for future research. Please note that the specific shortcomings and limitations of the articles are considered in the individual discussions (in Chapters 2 to 4).

Robotic systems should exploit biarticular structures and validate control embodiment
The previously discussed contribution of biarticular muscles for simplifying the control task by translating between concepts of locomotion and human leg designs (Chapter 2) warrants further validation. Here, robotic systems that incorporate the specific designs of the motor control systems can become testbeds of the mentioned concepts and hypotheses (Brooks, 1991; Kalveram and Seyfarth, 2009; Floreano et al., 2014). Depending on the investigated movement or locomotor subfunction, different technological challenges like actuator transparency, performance, bandwidth, friction or system inertia need to be considered when designing a suitable system. Unfortunately, most of the robotic designs that are currently used in research or industry use single-joint actuation principles that refrain these systems to be used for the validation of biarticular actuator functions. Therefore, only few robotic demonstrators like the *BioBiped* robot (Sharbafi et al., 2016) or the *C Runner* (Lakatos et al., 2014; Lakatos et al., 2016) were used to investigate these hypotheses in control embodiment (see Chapter 2).

Experiments should study muscular contributions in non-continous motions
As identified in Chapter 2, most computational, experimental and robotic studies that address biarticular muscles considered steady-state behaviours, e.g. level ground walking or running with a constant speed. However, in realistic environments, these situations are more an exception than the typical scenario (Dickinson et al., 2000). In real-world scenarios, humans, animals and robotics have to face mechanical or sensory perturbation (Tokur et al., 2020). Moreover, movements are usually not uniform, but instead involve accelerations and transitions of different movements, e.g. changes in direction, speed or motion task. All these factors pose additional challenges to the motor control system. Despite of their frequent

appearance in the activities of daily living, most of these situations are currently underrepresented in state of the art about biarticular actuation (Chapter 2). Therefore, there is a high demand of research that also considers non-continuous motion tasks to better understand the function of motor and sensor networks in the motor control loop (Figure 1.1) and the changing interplay of the involved systems in response to transitions or external perturbations. In this thesis, Chapter 3 provided a first step in this direction by investigating the contribution of reactive and anticipatory control strategies of the motor network. However, this study only looked at non-stepping responses following upper-body balance perturbations. Also, perturbations of other motion tasks as well as movement transitions like sit-to-stand or gait initiation should be considered in the future.

Sensor-motor maps should be applied in robotic and human experiments
Also, the topology of the predicted sensor-motor map, as developed in Chapter 4, remains to be validated by human experiments or robotic demonstrators. Unfortunately, the specific separation of individual pathways is very challenging and requires the application of complex system identification and modelling techniques (Kearney et al., 1997; Kiemel et al., 2006; Mugge et al., 2010). Also, sensory perturbations like ischemic nerve blockade (Raburn et al., 2011) or local anaesthesia can only partially manipulate specific reflex pathways. However, these methods are often not very specific, laborious and inconvenient for the subjects. Subsequently, experimental protocols and measurement techniques need to be developed to isolate individual reflex pathways. In robotic demonstrators, the implementation and evaluation of the reflex control are less complicated. In Zhao et al. (2020), an accurate simulation model of a two-segmented hopping robot with comparable leg design and reflex pathways predicted similar behaviours of the individual reflex pathways as in Chapter 4: positive FFB and LFB resulted in stable motions, while positive VFB led to unstable behaviors[4]. Furthermore, FFB was found to generate the highest hopping performance. These results support simulations in Chapter 4 since the model of (Zhao et al., 2020) also considered realistic joint damping, ground contact model and segment inertia. However, combinations of multiple feedback signals remain to be validated. Potentially, comparison of simulated and demonstrated sensor-motor maps could help to identify shortcomings of the simulation model as well as influences from hardware or real-world conditions like friction and impacts.

Sensor-motor maps should be extended to other locomotor subfunctions
The here-presented neuromechanical template model investigated the *stance subfunction* in the framework of locomotor subfunctions (Seyfarth, Grimmer, et al., 2013; Sharbafi and Seyfarth, 2017). Sensor-motor maps can be extended to a wide spectrum of applications and should be used to study also other types of locomotion and subfunctions (*swing* and *balance*) to investigate specific compositions of sensory pathways in these behaviours. The sensor-motor map concept is open to integrate also other sensory stimuli. For instance, compositions of mechanoreceptors in the hip joint capsule (measuring joint position) and the vestibular organ could be mapped for the regulation of upper-body postures (Horak, 2006; Chiba et al., 2016). Moreover, different subfunctions should be combined to investigate contributions from inter- *and* intra-limb proprioceptive circuits (Nichols et al., 2016) and their robustness against mechanical perturbations (Haeufle et al., 2012). An example of this is found in another study of the thesis author (Sarmadi et al., 2019), where the neuromechanical template model from Chapter 4 is extended by an upper-body that is balanced by two biarticular thigh muscles. By using leg force feedback, both subfunctions *stance* and *balance* could be synchronised to improve the robustness of the model against ground level drops or changes in angular momentum of the upper-body (Sarmadi et al., 2019). This example shows that this approach is well-extendable to other motions or tasks.

---

[4]In line with Haeufle et al. (2010), Zhao et al. (2020) predicted unstable hopping for simplified muscle mechanics.

Integration of cognitive science to investigate more complex behaviour
This thesis addressed the functions of sensor and motor networks to translate between biomechanical template models and neural control. Thereby, in Marr's level of analysis (Marr, 1982), this thesis mainly covered the projection of the algorithmic level into the physical implementation level (Table 5.1). For instance, Chapter 2 discussed the role of biarticular muscles to bridge the gap between biomechanical template models (*algorithmic level*) and the segmented human leg structure (*implementation level*).

Table 5.1: Marr's level of analysis (Marr, 1982) and an example from human locomotion.

Marr's level of analysis	example	description
computational level "what is done?" / "why?"	walk from current position to target position in a certain amount of time and precision and with minimum metabolic effort	motion task or function and its constraints
algorithmic level "how is this done?"	generate spring-like leg function, swing leg motion and upright upper-body	'structure' of locomotion, biomechanical templates
implementation level "how is this realized?"	generate joint torques by controlling muscles, e.g. by reflex, CPG or supra-spinal control	physical representation of the motor control loop

What remains to be the interest of future research is Marr's computational level. How are motions in the redundant system encoded at the computational level? Research produced different models and hypotheses for this problem, like the optimal control hypothesis (Todorov, 2004), muscle synergies (d'Avella et al., 2003; Tresch and Jarc, 2009), the equilibrium point hypothesis (Feldman, 1966), internal models (Francis and Wonham, 1976; Wolpert et al., 1995) or the uncontrolled manifold hypothesis (Scholz and Schöner, 1999).

With respect to the results of this thesis, the higher regulation of cyclic movements could be realised by simple logics or rules, as suggested by control embodiment (Pfeifer and Bongard, 2007) and simple template models. Similar to grammar in languages or algebra in math, these rules may organise the synthesis of motion goals and tasks and translate these into simple sets of appropriate motor commands (as observed e.g. by muscle synergies). In this context, Chapter 4 showed that simple blendings of different sensory pathways could realise different movement characteristics (like performance, efficiency and safety). However, these synthesising rules might be expressed in different modalities than that of conventional movement analysis (e.g. metabolic effort, muscle stimulation, joint impedance or variability). In order to identify suitable task representations, this line of research should be closely coupled to the cognitive sciences and include influences from prior knowledge as well as probabilistic and uncertain processes (e.g. problems of 'probabilistic inference') to mimic realistic scenarios more closely (Dickinson et al., 2000; Ernst and Banks, 2002). Further research is needed to improve our understanding of the mechanisms of motor control such that we can make sense of the tremendous motor control performance seen in e.g. rhythmic gymnastics, darts or long jump.

References

A. S. Anand et al. (2019). "A deep reinforcement learning based approach towards generating human walking behavior with a neuromuscular model". In: *2019 IEEE-RAS 19th International Conference on Humanoid Robots (Humanoids)*, pp. 537–543.

A. G. Auyang, J. T. Yen, and Y.-H. Chang (2009). "Neuromechanical stabilization of leg length and orientation through interjoint compensation during human hopping". In: *Experimental brain research* 192.2, pp. 253–264.

N. A. Bernstein (1967). "The co-ordination and regulation of movements". In:

R. Blickhan (1989). "The spring-mass model for running and hopping". In: *Journal of biomechanics* 22.11-12, pp. 1217–1227.

G. Bosco and R. Poppele (2001). "Proprioception from a spinocerebellar perspective". In: *Physiological reviews* 81.2, pp. 539–568.

R. A. Brooks (1991). "New approaches to robotics". In: *Science* 253.5025, pp. 1227–1232.

I. E. Brown and G. E. Loeb (2000). "A Reductionist Approach to Creating and Using Neuromusculoskeletal Models". In: *Biomechanics and Neural Control of Posture and Movement*. Ed. by J. M. Winters and P. E. Crago. New York, NY: Springer New York, pp. 148–163.

R. Chiba et al. (2016). "Human upright posture control models based on multisensory inputs; in fast and slow dynamics". In: *Neuroscience research* 104, pp. 96–104.

H. J. Chiel and R. D. Beer (1997). "The brain has a body: adaptive behavior emerges from interactions of nervous system, body and environment". In: *Trends in neurosciences* 20.12, pp. 553–557.

A. d'Avella, P. Saltiel, and E. Bizzi (2003). "Combinations of muscle synergies in the construction of a natural motor behavior". In: *Nature neuroscience* 6.3, p. 300.

A. Davoodi et al. (2019). "From template to anchors: transfer of virtual pendulum posture control balance template to adaptive neuromuscular gait model increases walking stability". In: *Royal Society open science* 6.3, p. 181911.

M. H. Dickinson et al. (2000). "How animals move: an integrative view". In: *science* 288.5463, pp. 100–106.

J. M. Donelan et al. (2004). "Mechanical and metabolic requirements for active lateral stabilization in human walking". In: *Journal of biomechanics* 37.6, pp. 827–835.

D. Driess et al. (2018). "Learning to Control Redundant Musculoskeletal Systems with Neural Networks and SQP: Exploiting Muscle Properties". In: *2018 IEEE International Conference on Robotics and Automation (ICRA)*. IEEE, pp. 6461–6468.

M. O. Ernst and M. S. Banks (2002). "Humans integrate visual and haptic information in a statistically optimal fashion". In: *Nature* 415.6870, p. 429.

A. G. Feldman (1966). "Functional tuning of the nervous system with control of movement or maintenance of a steady posture-II. Controllable parameters of the muscle". In: *Biofizika* 11, pp. 565–578.

D. Floreano, A. J. Ijspeert, and S. Schaal (2014). "Robotics and neuroscience". In: *Current Biology* 24.18, R910–R920.

B. A. Francis and W. M. Wonham (1976). "The internal model principle of control theory". In: *Automatica* 12.5, pp. 457–465.

R. J. Full and D. E. Koditschek (1999). "Templates and anchors: neuromechanical hypotheses of legged locomotion on land". In: *Journal of Experimental Biology* 202.23, pp. 3325–3332.

L. Galvani (1791). "D viribus electricitatis in motu musculari: Commentarius". In: *Bologna: Tip. Istituto delle Scienze, 1791; 58 p.: 4 tavv. ft; in 4.; DCC. f. 70*.

H. Geyer, A. Seyfarth, and R. Blickhan (2006). "Compliant leg behaviour explains basic dynamics of walking and running". In: *Proceedings of the Royal Society of London B: Biological Sciences* 273, pp. 2861–2867.

A. Gordon, A. F. Huxley, and F. Julian (1966). "The variation in isometric tension with sarcomere length in vertebrate muscle fibres". In: *The Journal of physiology* 184.1, pp. 170–192.

D. F. B. Haeufle et al. (2012). "Integration of intrinsic muscle properties, feed-forward and feedback signals for generating and stabilizing hopping". In: *Journal of The Royal Society Interface* 9.72, pp. 1458–1469.

D. Haeufle, S. Grimmer, and A. Seyfarth (2010). "The role of intrinsic muscle properties for stable hopping—stability is achieved by the force–velocity relation". In: *Bioinspiration & biomimetics* 5.1, p. 016004.

D. Haeufle et al. (2014). "Quantifying control effort of biological and technical movements: an information-entropy-based approach". In: *Physical Review E* 89.1, p. 012716.

T. Heidlauf et al. (2017). "A continuum-mechanical skeletal muscle model including actin-titin interaction predicts stable contractions on the descending limb of the force-length relation". In: *PLoS computational biology* 13.10, e1005773.

E. Henneman, G. Somjen, and D. O. Carpenter (1965). "Functional significance of cell size in spinal motoneurons". In: *Journal of neurophysiology* 28.3, pp. 560–580.

A. V. Hill (1938). "The heat of shortening and the dynamic constants of muscle". In: *Proc. R. Soc. Lond. B* 126.843, pp. 136–195.

F. B. Horak (2006). "Postural orientation and equilibrium: what do we need to know about neural control of balance to prevent falls?" In: *Age and ageing* 35.suppl_2, pp. ii7–ii11.

A. J. Ijspeert (2008). "Central pattern generators for locomotion control in animals and robots: a review". In: *Neural networks* 21.4, pp. 642–653.

Y. P. Ivanenko et al. (2007). "Modular control of limb movements during human locomotion". In: *Journal of Neuroscience* 27.41, pp. 11149–11161.

R. Jacobs and J. M. Macpherson (1996). "Two functional muscle groupings during postural equilibrium tasks in standing cats". In: *Journal of Neurophysiology* 76.4, pp. 2402–2411.

K. T. Kalveram and A. Seyfarth (2009). "Inverse biomimetics: How robots can help to verify concepts concerning sensorimotor control of human arm and leg movements". In: *Journal of Physiology-Paris* 103.3-5, pp. 232–243.

R. E. Kearney, R. B. Stein, and L. Parameswaran (1997). "Identification of intrinsic and reflex contributions to human ankle stiffness dynamics". In: *IEEE transactions on biomedical engineering* 44.6, pp. 493–504.

O. Kiehn (2016). "Decoding the organization of spinal circuits that control locomotion". In: *Nature Reviews Neuroscience* 17.4, p. 224.

T. Kiemel, K. S. Oie, and J. J. Jeka (2006). "Slow dynamics of postural sway are in the feedback loop". In: *Journal of neurophysiology* 95.3, pp. 1410–1418.

M. M. van der Krogt et al. (2009). "Robust passive dynamics of the musculoskeletal system compensate for unexpected surface changes during human hopping." In: *Journal of applied physiology (Bethesda, Md. : 1985)* 107.3, pp. 801–808.

F. Lacquaniti and C. Maioli (1994). "Independent control of limb position and contact forces in cat posture". In: *Journal of Neuroscience* 72.4, pp. 1476–1495.

D. Lakatos et al. (2014). "Design and control of compliantly actuated bipedal running robots: Concepts to exploit natural system dynamics". In: *Humanoid Robots (Humanoids), 2014 14th IEEE-RAS International Conference on*. IEEE, pp. 930–937.

D. Lakatos et al. (2016). "Dynamic bipedal walking by controlling only the equilibrium of intrinsic elasticities". In: *Humanoid Robots (Humanoids), 2016 IEEE-RAS 16th International Conference on*. IEEE, pp. 1282–1289.

C. C. K. Lin and P. E. Crago (2002). "Neural and mechanical contributions to the stretch reflex: A model synthesis". In: *Annals of Biomedical Engineering* 30.1, pp. 54–67.

G. Loeb (1995). "Control implications of musculoskeletal mechanics". In: *Proceedings of 17th International Conference of the Engineering in Medicine and Biology Society* 2, pp. 1393–1394.

G. E. Loeb, I. E. Brown, and E. J. Cheng (1999). "A hierarchical foundation for models of sensorimotor control". In: *Experimental brain research* 126.1, pp. 1–18.

C. Ludwig et al. (2012). "Multiple-step model-experiment matching allows precise definition of dynamical leg parameters in human running". In: *Journal of biomechanics* 45.14, pp. 2472–2475.

D. Marr (1982). "Vision: A computational investigation into the human representation and processing of visual information". In:

H.-M. Maus et al. (2010). "Upright human gait did not provide a major mechanical challenge for our ancestors". In: *Nature communications* 1, p. 70.

W. Mugge et al. (2010). "A rigorous model of reflex function indicates that position and force feedback are flexibly tuned to position and force tasks". In: *Experimental brain research* 200.3-4, pp. 325–340.

T. R. Nichols, N. E. Bunderson, and M. A. Lyle (2016). "Neural regulation of limb mechanics: insights from the organization of proprioceptive circuits". In: *Neuromechanical modeling of posture and locomotion*. Springer, pp. 69–102.

T. Nichols and J. Houk (1976). "Improvement in linearity and regulation of stiffness that results from actions of stretch reflex." In: *J Neurophysiol* 39.1, pp. 119–142.

R. Niiyama, A. Nagakubo, and Y. Kuniyoshi (2007). "Mowgli: A bipedal jumping and landing robot with an artificial musculoskeletal system". In: *Proceedings 2007 IEEE International Conference on Robotics and Automation*. IEEE, pp. 2546–2551.

C. Paul (2006). "Morphological computation: A basis for the analysis of morphology and control requirements". In: *Robotics and Autonomous Systems* 54.8, pp. 619–630.

K. Pearson, Ö. Ekeberg, and A. Büschges (2006). *Assessing sensory function in locomotor systems using neuro-mechanical simulations*.

R. Pfeifer and J. Bongard (2007). *How the body shapes the way we think: a new view of intelligence*. MIT press.

R. Pfeifer and F. Iida (2004). "Embodied artificial intelligence: Trends and challenges". In: *Embodied artificial intelligence*. Springer, pp. 1–26.

C. E. Raburn, K. J. Merritt, and J. C. Dean (2011). "Preferred movement patterns during a simple bouncing task". In: *Journal of Experimental Biology* 214.22, pp. 3768–3774.

S. Riese and A. Seyfarth (2011). "Stance leg control: variation of leg parameters supports stable hopping". In: *Bioinspiration & biomimetics* 7.1, p. 016006.

B. D. Robertson and G. S. Sawicki (2014). "Exploiting elasticity: Modeling the influence of neural control on mechanics and energetics of ankle muscle-tendons during human hopping". In: *Journal of Theoretical Biology* 353, pp. 121–132.

C. Rode, T. Siebert, and R. Blickhan (2009). "Titin-induced force enhancement and force depression: A 'sticky-spring' mechanism in muscle contractions?" In: *Journal of Theoretical Biology* 259.2, pp. 350–360.

J. Rummel et al. (2008). "Enlarging regions of stable running with segmented legs". In: *2008 IEEE International Conference on Robotics and Automation*. IEEE, pp. 367–372.

A. Sarmadi et al. (2019). "Concerted control of stance and balance locomotor subfunctions-Leg force as a conductor". In: *IEEE Transactions on Medical Robotics and Bionics*.

J. P. Scholz and G. Schöner (1999). "The uncontrolled manifold concept: identifying control variables for a functional task". In: *Experimental brain research* 126.3, pp. 289–306.

A. Seyfarth, H. Geyer, and H. Herr (2003). "Swing-leg retraction: a simple control model for stable running". In: *Journal of Experimental Biology* 206.15, pp. 2547–2555.

A. Seyfarth, S. Grimmer, et al. (2013). "Biomechanical and neuromechanical concepts for legged locomotion: Computer models and robot validation: Andre Seyfarth, Sten Grimmer, Daniel Häufle, Horst-Moritz Maus, Frank Peuker and Karl-Theodor Kalveram". In: *Routledge Handbook of Motor Control and Motor Learning*. Routledge, pp. 99–119.

A. Seyfarth et al. (2002). "A movement criterion for running". In: *Journal of biomechanics* 35.5, pp. 649–655.

M. A. Sharbafi and A. Seyfarth (2017). "How locomotion sub-functions can control walking at different speeds?" In: *Journal of biomechanics* 53, pp. 163–170.

M. A. Sharbafi et al. (2016). "A new biarticular actuator design facilitates control of leg function in BioBiped3". In: *Bioinspiration & biomimetics* 11.4, p. 046003.

M. A. Sharbafi et al. (2017). "Reconstruction of human swing leg motion with passive biarticular muscle models". In: *Human movement science* 52, pp. 96–107.

C. S. Sherrington (1906). "The integrative action of the nervous system." In:

F. Spoor, B. Wood, and F. Zonneveld (1994). "Implications of early hominid labyrinthine morphology for evolution of human bipedal locomotion". In: *Nature* 369.6482, p. 645.

E. Todorov (2004). "Optimality principles in sensorimotor control". In: *Nature neuroscience* 7.9, p. 907.

D. Tokur, M. Grimmer, and A. Seyfarth (2020). "Review of balance recovery in response to external perturbations during daily activities". In: *Human Movement Science* 69, p. 102546.

A. Tomalka et al. (2017). "The active force–length relationship is invisible during extensive eccentric contractions in skinned skeletal muscle fibres". In: *Proceedings of the Royal Society of London B: Biological Sciences* 284.1854.

M. C. Tresch and A. Jarc (2009). "The case for and against muscle synergies". In: *Current opinion in neurobiology* 19.6, pp. 601–607.

D. M. Wolpert, Z. Ghahramani, and M. I. Jordan (1995). "An internal model for sensorimotor integration". In: *Science* 269.5232, pp. 1880–1882.

S. Yakovenko, V. Gritsenko, and A. Prochazka (2004). "Contribution of stretch reflexes to locomotor control: A modeling study". In: *Biological Cybernetics* 90.2, pp. 146–155.

K. Yasui et al. (2019). "Decoding the essential interplay between central and peripheral control in adaptive locomotion of amphibious centipedes". In: *Scientific Reports* 9.1, p. 18288.

G. Zhao, F. Szymanski, and A. Seyfarth (2020). "Bio-inspired neuromuscular reflex based hopping controller for a segmented robotic leg". In: *Bioinspiration & Biomimetics*.

A. T. Zuur et al. (2010). "Contribution of afferent feedback and descending drive to human hopping." In: *The Journal of physiology* 588.Pt 5, pp. 799–807.

A Appendix

Supplementary Material of

Article II: Biarticular muscles are Most Responsive to Upper-body Pitch Perturbations in Human Standing

Christian Schumacher, Andrew Berry, Daniel Lemus, Christian Rode, André Seyfarth and Heike Vallery
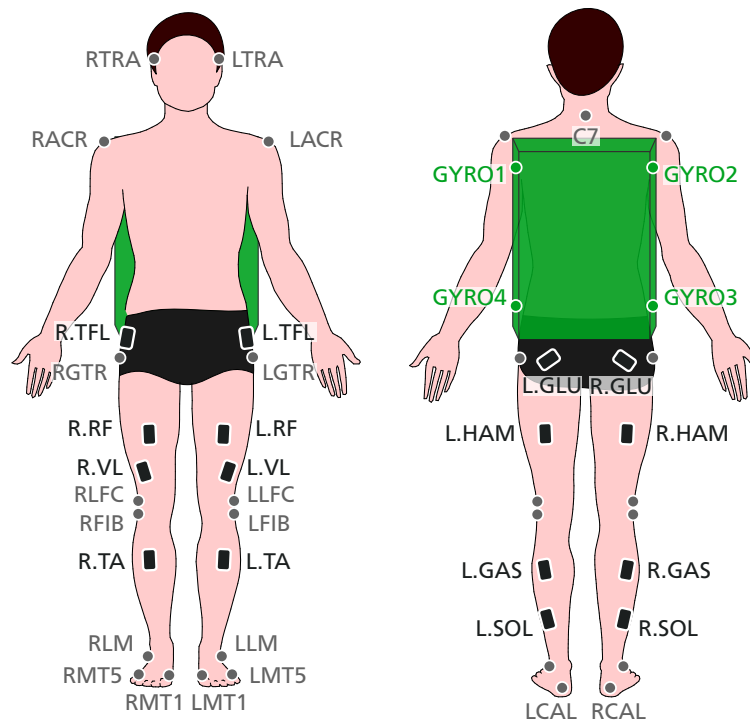
Experimental setup

In August and September 2018, we collected kinematic, kinetic and electromyographic (EMG) data in the Delft Biorobotics Lab. All measurement devices including the data logging of the Angular Momentum Perturbator (AMP) were synchronized by a 5 V trigger signal.

The used marker and EMG electrode locations can be found in Figure A.1.

Figure A.1: Location of EMG sensors and used marker model. EMG electrodes (black) and passive motion capture markers: body markers (grey) and AMP (green).

Mechanical analysis of all subjects

To evaluate the body posture after perturbations were applied, joint angles are shown in Figure A.2. The resultant body postures of positive and negative torque perturbations showed slightly different response behavior. The subjects' mechanical response consisted of a distinct early trunk pitch (hip flexion, within first 500 ms) while other major leg joints, knee and ankle, were only slightly flexed or extended, respectively. In the case of negative perturbations, subjects mainly bend their knees resulting in backwards motion of the trunk and thigh instead of a clearly extended hip (only 5° to 10°).
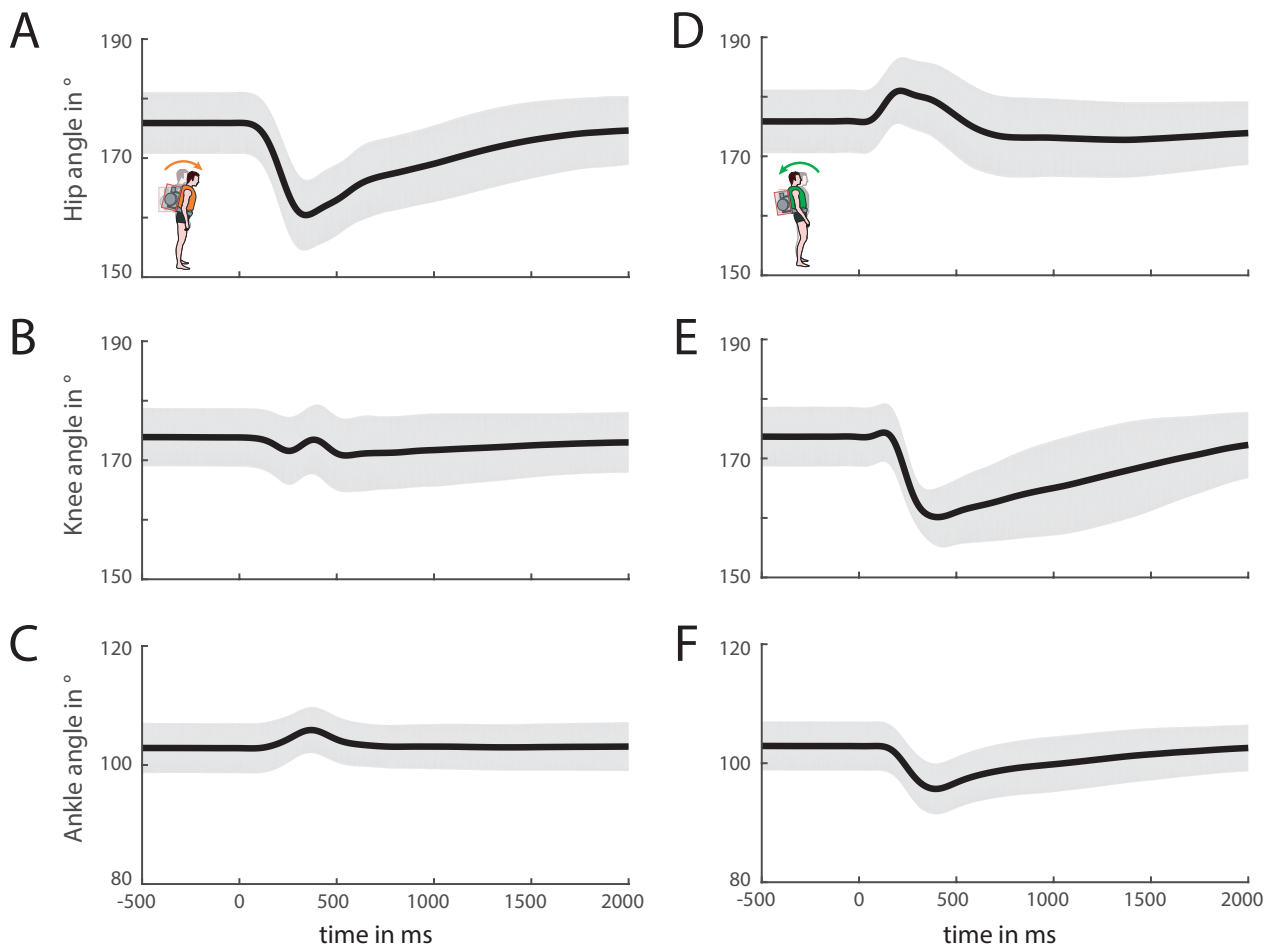
Figure A.2: Grand mean and SD of major sagittal joint angles of all eleven subjects. Hip **(A, D)**, knee **(B, E)** and ankle angles **(D, F)** of positive (left side) and negative torques (right side) are shown. Increasing joint angle changes denote a joint extension.

The following figures show the resultant motion of all subjects. Figures A.3 to A.6 show the mean changes in trunk lean, hip joint position CoM position and CoP position of all subjects in ap-direction, respectively. Observed response patterns were quite similar with some intra-subject variability. The applied torques are equal to a force pair with equal magnitudes and opposing directions. In forward perturbations, the shoulder and hip joints were accelerated forwards and backwards, respectively.
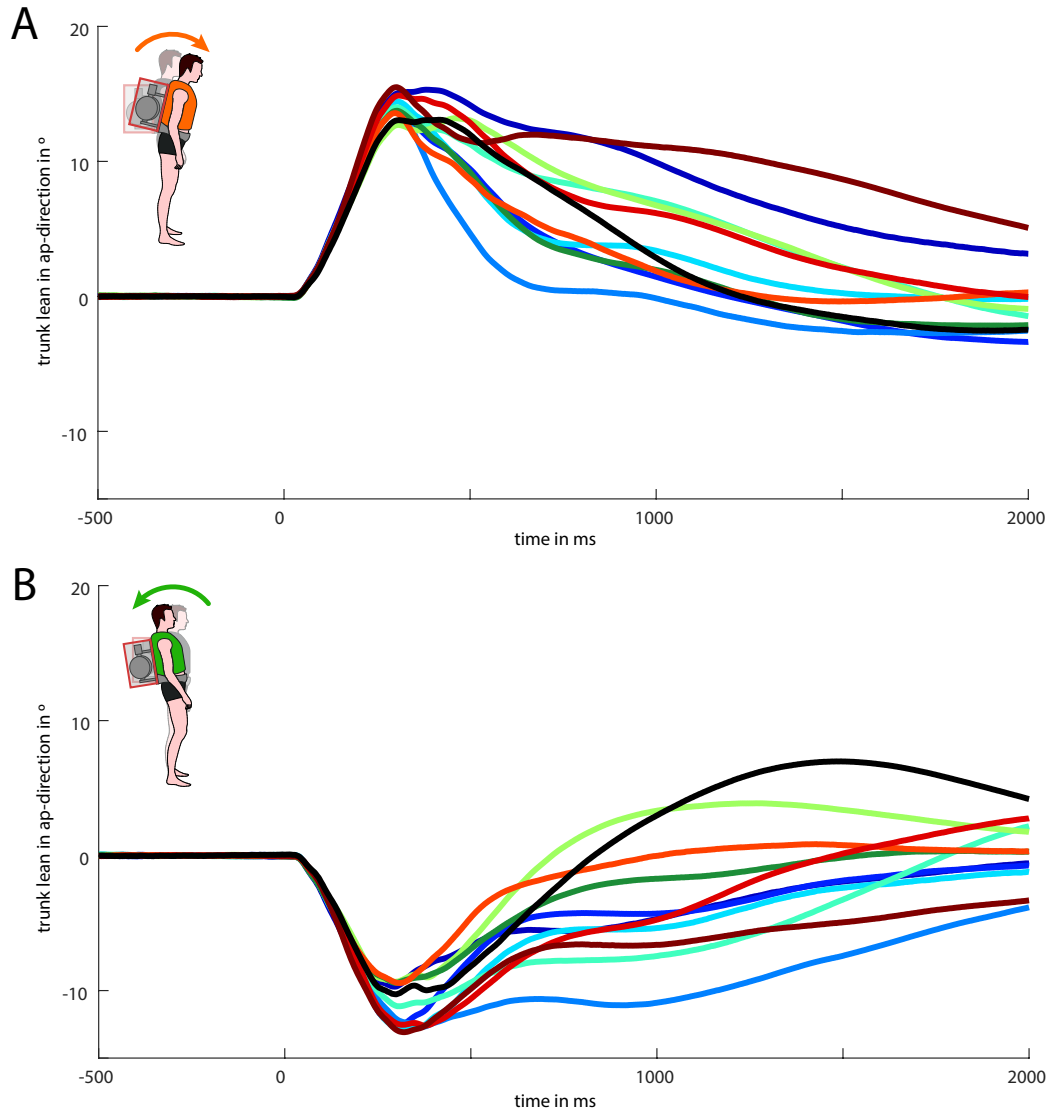
Figure A.3: Change in mean trunk lean in ap-direction of all eleven subjects in positive (A) and negative (B) direction. The single subject shown in the manuscript is colored black here.

Figure A.4 shows the resultant hip joint position of all subjects. In positive perturbations, the hip joint moved posterior by about 5 cm, while, in negative perturbations, slightly less anterior movement was observed.
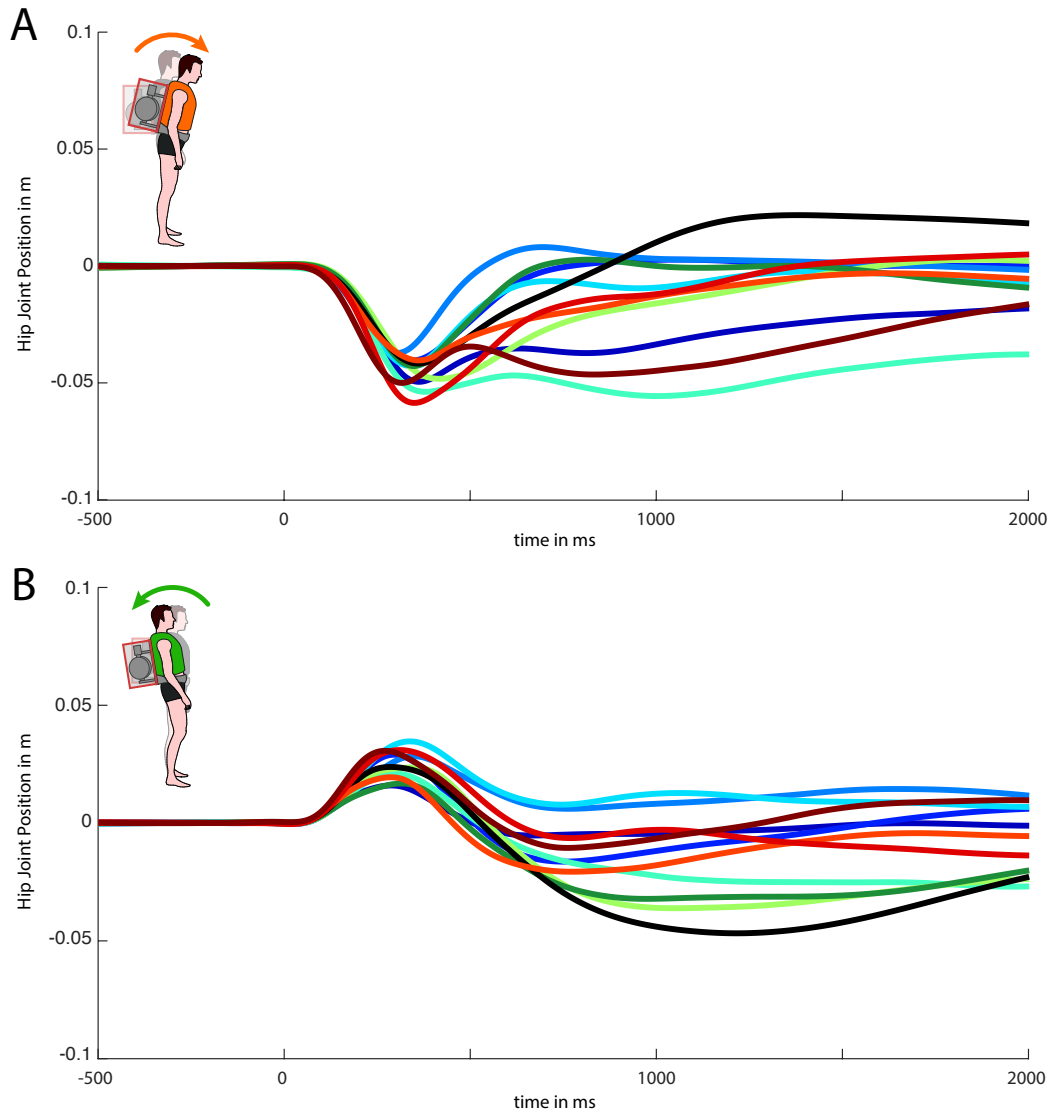
Figure A.4: Change in mean hip joint position in ap-direction of all eleven subjects in positive (A) and negative (B) direction. The single subject shown in the manuscript is colored black here.

The biggest difference was observed for the CoM trajectory in positive perturbations (Figure A.5). Here one subject deviated from all other subjects by moving its CoM in posterior direction. This may have be caused by the posterior position of the CoP (Figure A.6).
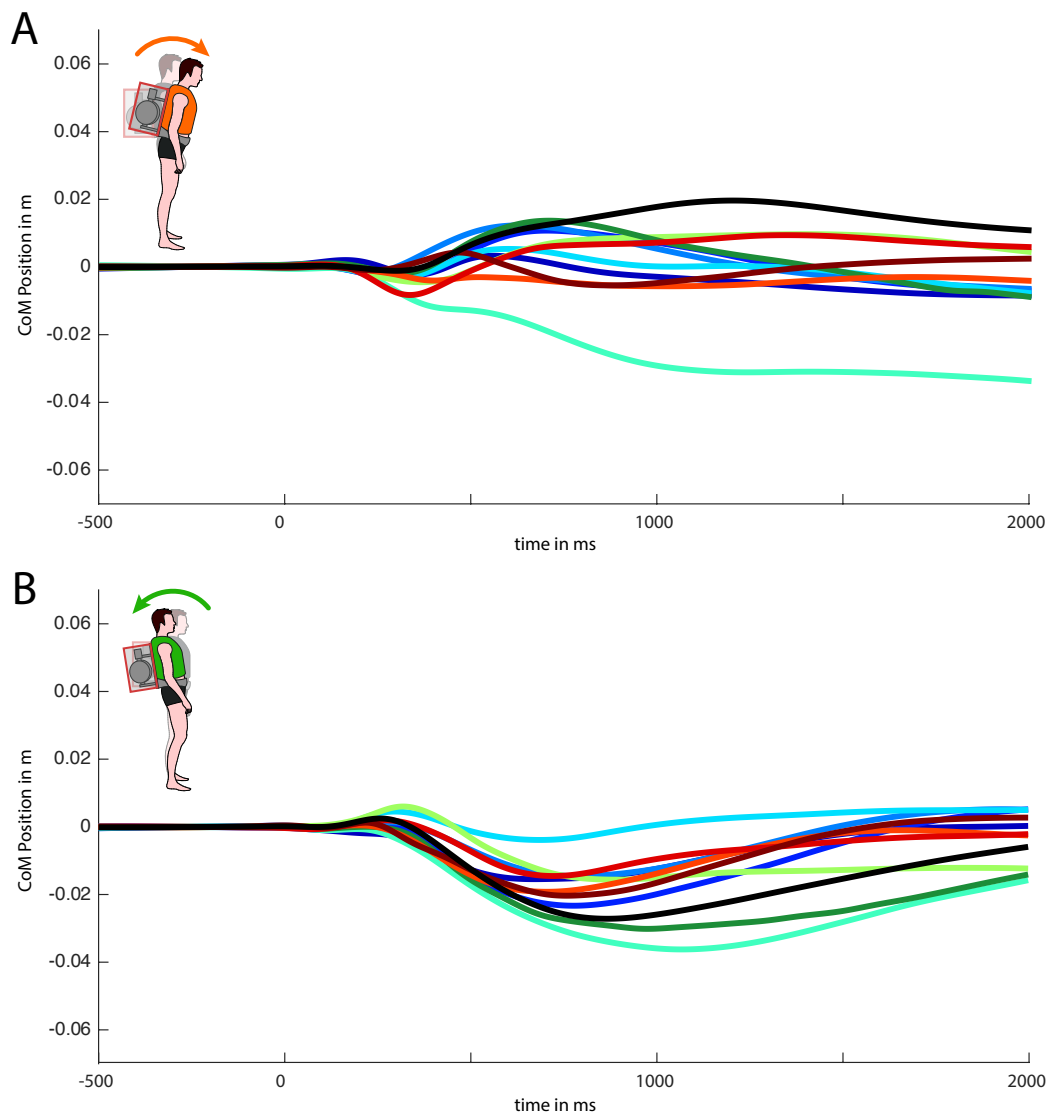

Figure A.5: Change in mean CoM position in ap-direction of all eleven subjects in positive (A) and negative (B) direction. The single subject shown in the manuscript is colored black here.
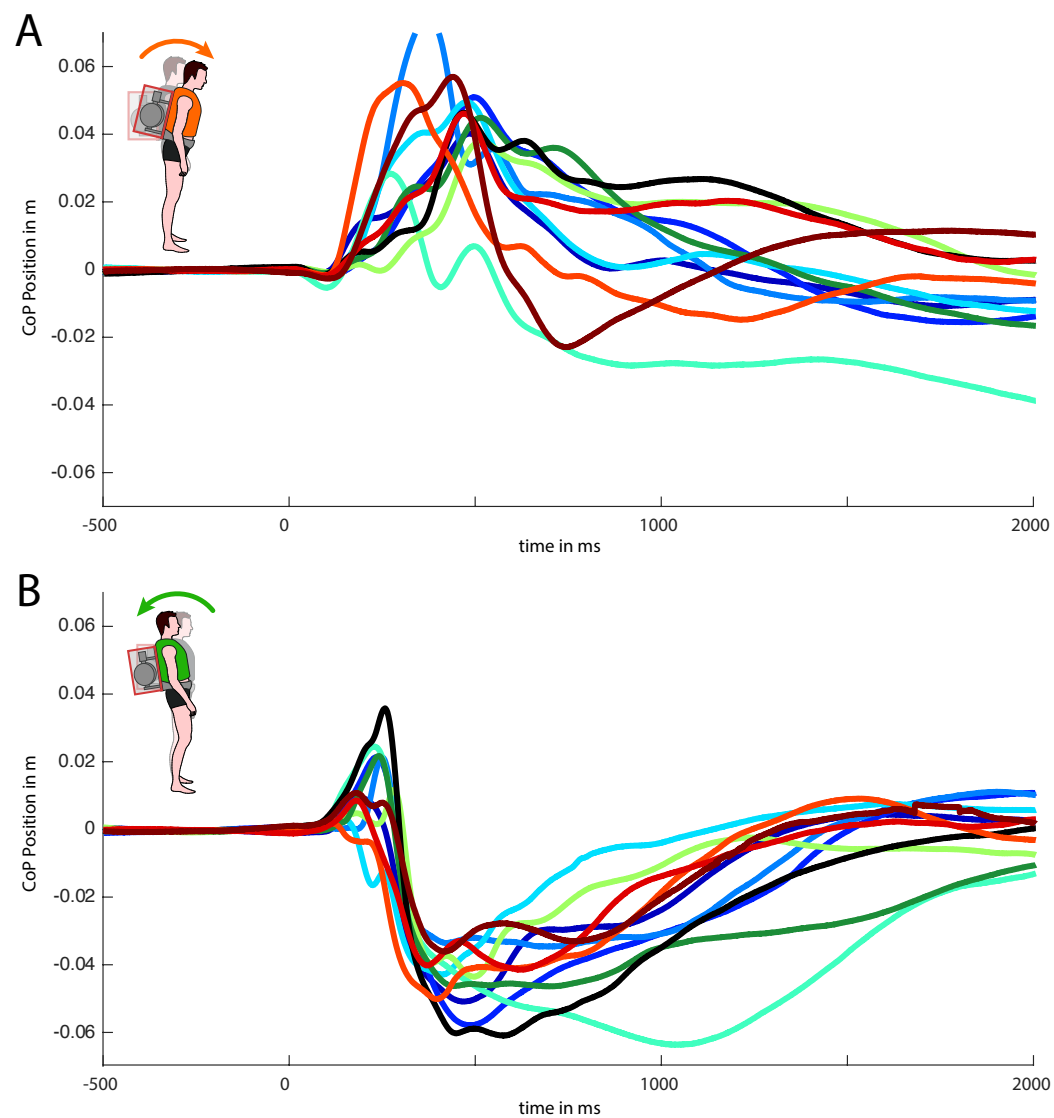
Figure A.6: Change in mean CoP position in ap-direction of all eleven subjects in positive (A) and negative (B) direction. The single subject shown in the manuscript is colored black here.

Influence of AMP weight, vibration and noise

To check to what extent the weight, vibration and noise of the AMP may have influenced the initial posture, mean joint angles in the 'Unloaded Standing' and 'Loaded Standing' conditions of all major joints are shown in Table A.1. Subsequently, wearing the AMP resulted in a slightly more bend hip ($-6.2°$) and more extended knee ($2.1°$).

Table A.1: Comparison of postural changes due to AMP weight, vibration and noise. Mean major joint angles (in °) of all subjects of $20\,\text{s}$ periods of quiet standing in the 'Unloaded Standing' and 'Loaded Standing' conditions. $\Delta\phi$ denotes mean change. For normally distributed comparisons, the paired two-sided t-test was used. In case of non-normal comparisons, the non-parametric two-sided Wilcoxon signed-rank test was used. Significant values ($p < 0.05$) are highlighted by bold text.

joints	'Unloaded Standing'	'Loaded Standing'	$\Delta\phi$	p-value
hip	183.6	177.4	-6.2	**2.52E-04**
knee	172.3	174.4	+2.1	**0.002**
ankle	102.4	102.9	+0.4	0.235

We further compared the CoP trajectory of both conditions of 'Unloaded Standing' and 'Loaded Standing' (Figure A.7). Here, for most subjects a slight increase in CoP sway can be observed, agreeing with results from Al-Khabbaz et al. (2008) and Schiffman et al. (2006).
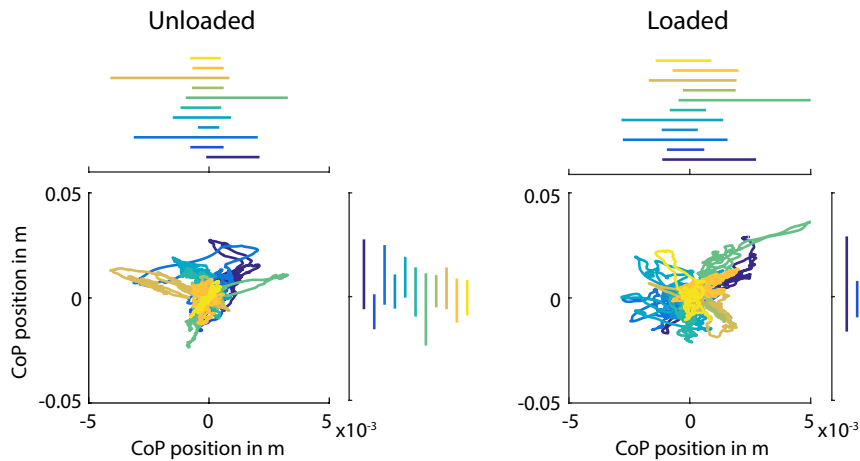
Figure A.7: Change in CoP position of all eleven subjects during $20\,\text{s}$ intervals of 'Unloaded Standing' and 'Loaded Standing' measurements. Bars denote the maximum range of CoP sway. For each subject a different color is used.

Influence of Gimbal torque

To further check the influence of the gimbal torque, the trunk yaw rotation (around the longitudinal axis of the trunk) is shown in Figure A.8. Here, for different conditions of initial gimbal position, the change in trunk yaw resulted in trajectories of opposing direction with a magnitude of 3° to 5°.
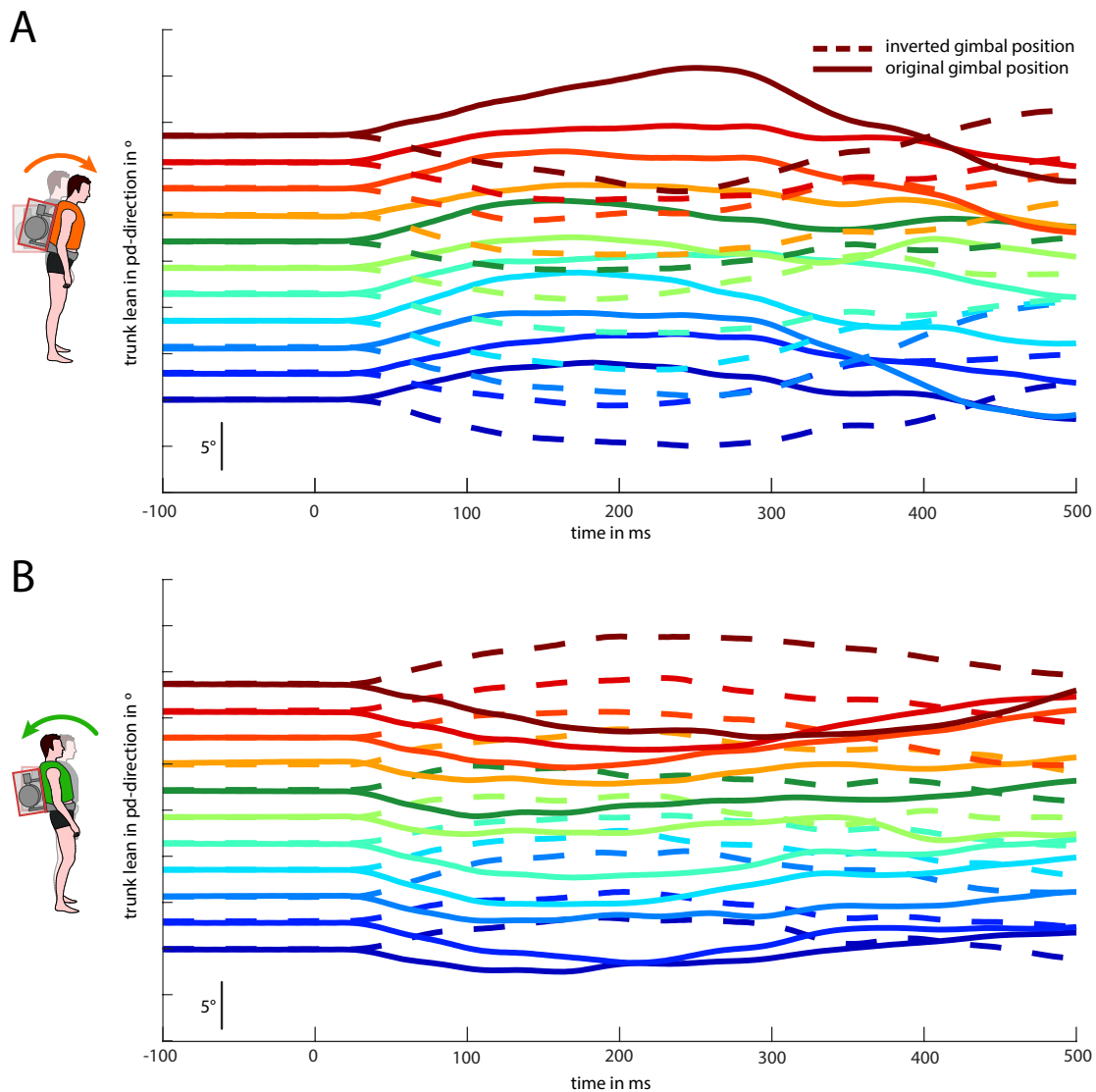
Figure A.8: **Change of mean trunk yaw of all eleven subjects in different conditions of initial gimbal positions:** positive **(A)** and negative perturbation **(B)**. Solid and dashed lines denote the original and inverted gimbal position, respectively.

Influence of roll torque component

In Figure A.9 the resultant trunk roll about the frontal plane for all four conditions is shown (positive and negative torque perturbation, original and inverted gimbal position). For positive perturbation directions, a maximum of 8° of trunk roll was found while most subjects leaned by only 2° to 4°. In negative perturbation, the trunk rolled up to 4°.
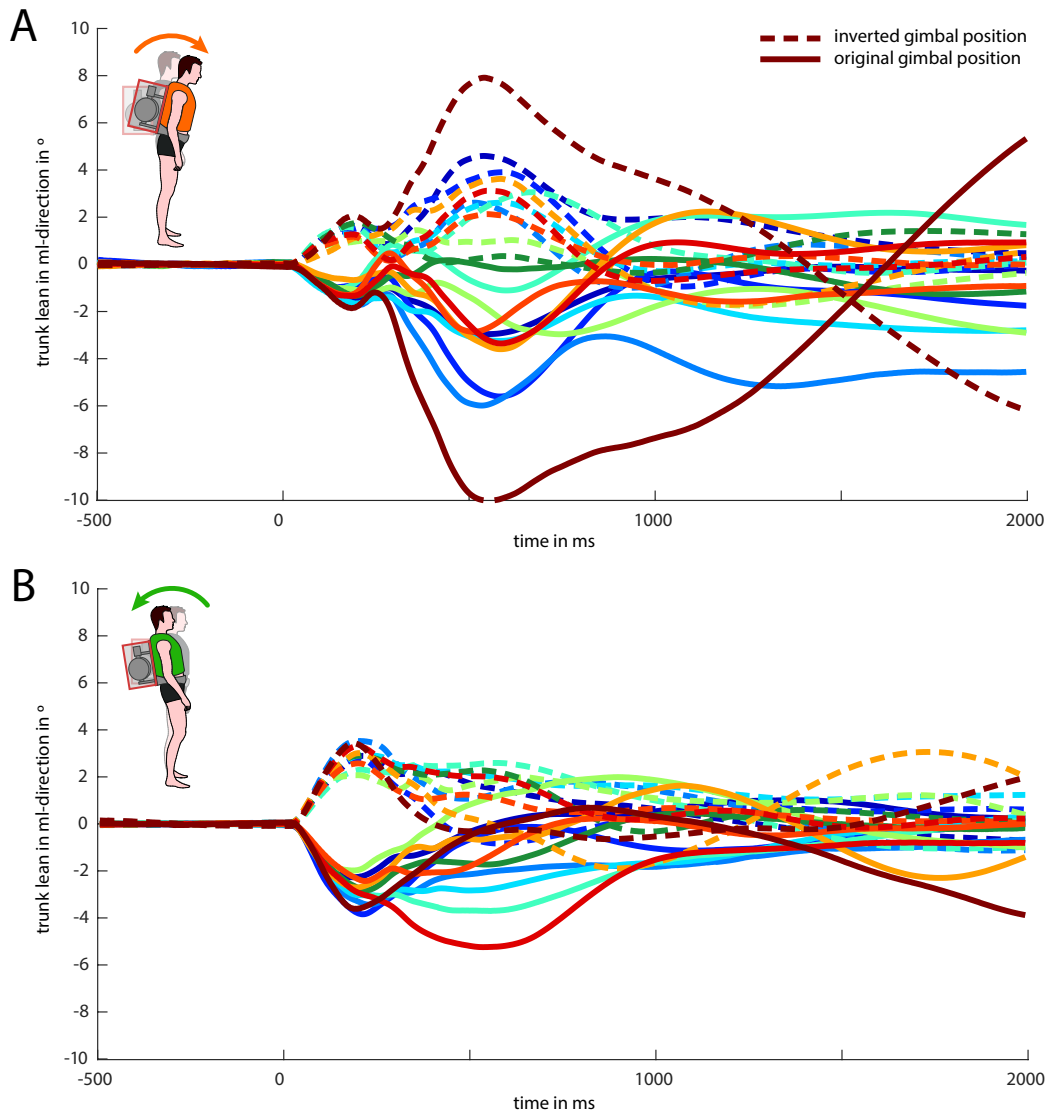
Figure A.9: Change of mean trunk roll of all eleven subjects in different conditions of initial gimbal positions: positive **(A)** and negative perturbation **(B)**. Solid and dashed lines denote the original and inverted gimbal position, respectively.

Both conditions of original and inverted gimbal positions show trunk rolls with similar magnitudes but opposing directions. For positive torques, higher magnitudes and delayed timings of peak deflections occurred compared to negative torque perturbations.

Also the corresponding leg loading as measured by the vertical GRF show changes in opposite directions but with similar magnitudes for both conditions of inverted roll torque components, starting after about 50 ms to 100 ms (Figure A.10).
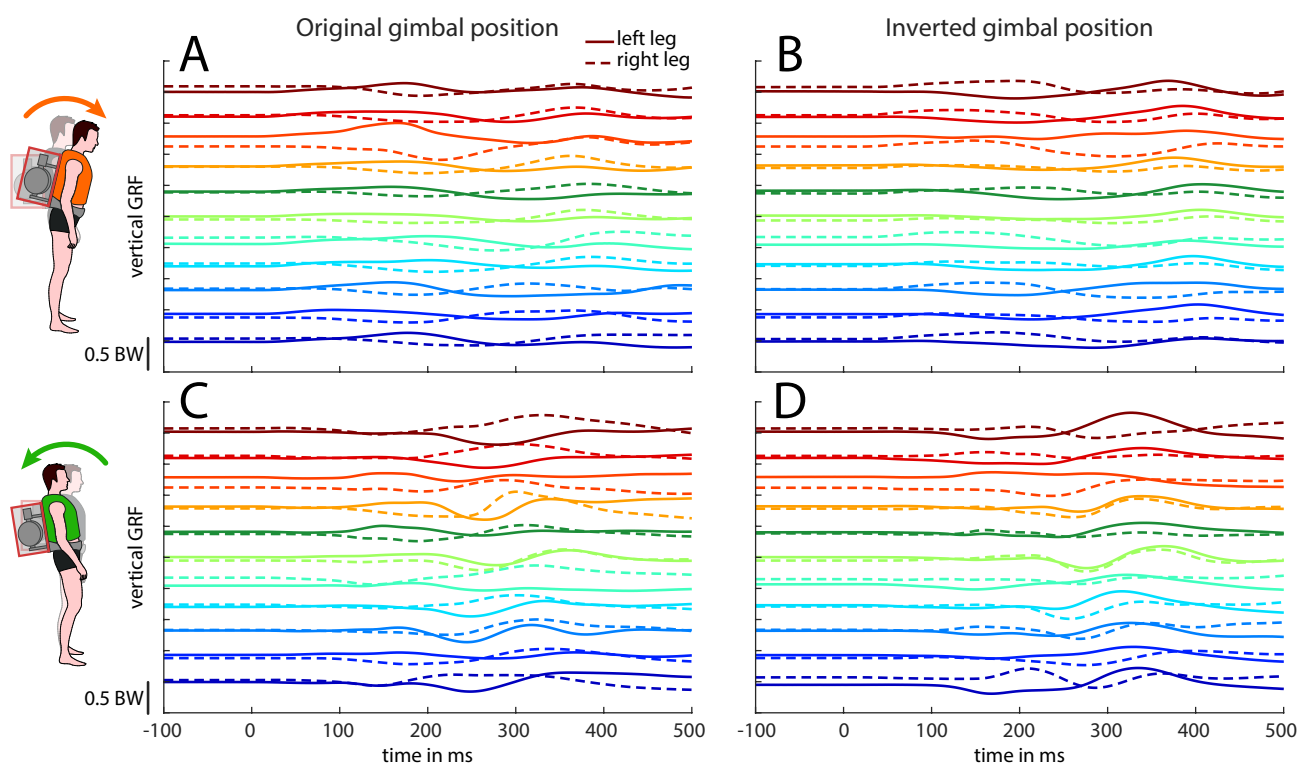
Figure A.10: Change in mean leg loading (vertical GRF) of all eleven subjects in different conditions: positive with original gimbal position **(A)**, positive with inverted gimbal position **(B)**, negative with original gimbal position **(C)**, negative with inverted gimbal position **(D)**. Solid and dashed lines denote the left and right leg, respectively.

In positive perturbation direction, this change in leg loading had only slight impact on the CoP positions (Figure A.11A,B). Both legs still resemble quite similar trajectories. Bigger differences between both legs can be seen in the negative perturbations (Figure A.11C,D).
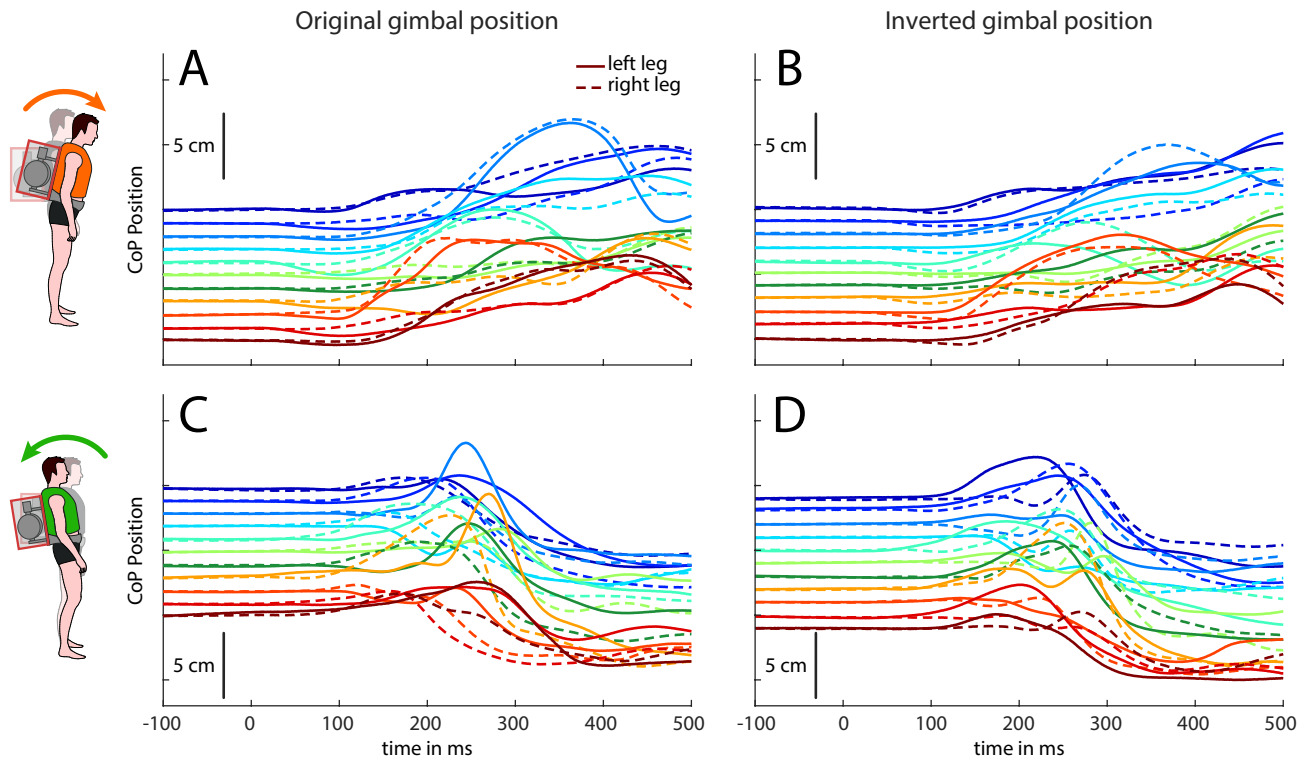
Figure A.11: Change in mean CoP position in ap-direction of all eleven subjects in different conditions: positive with original gimbal position **(A)**, positive with inverted gimbal position **(B)**, negative with original gimbal position **(C)**, negative with inverted gimbal position **(D)**. Solid and dashed lines denote the left and right leg, respectively.

To further check influences of the roll torque component on the muscular response, muscular activity levels of both legs of all conditions are compared. Figure A.12 to Figure A.14 denote the responses in the corresponding response intervals RI1, RI2 and RI3.

Based on these results, only slight differences of muscular response amplitudes were observed for both conditions of initial gimbal position.
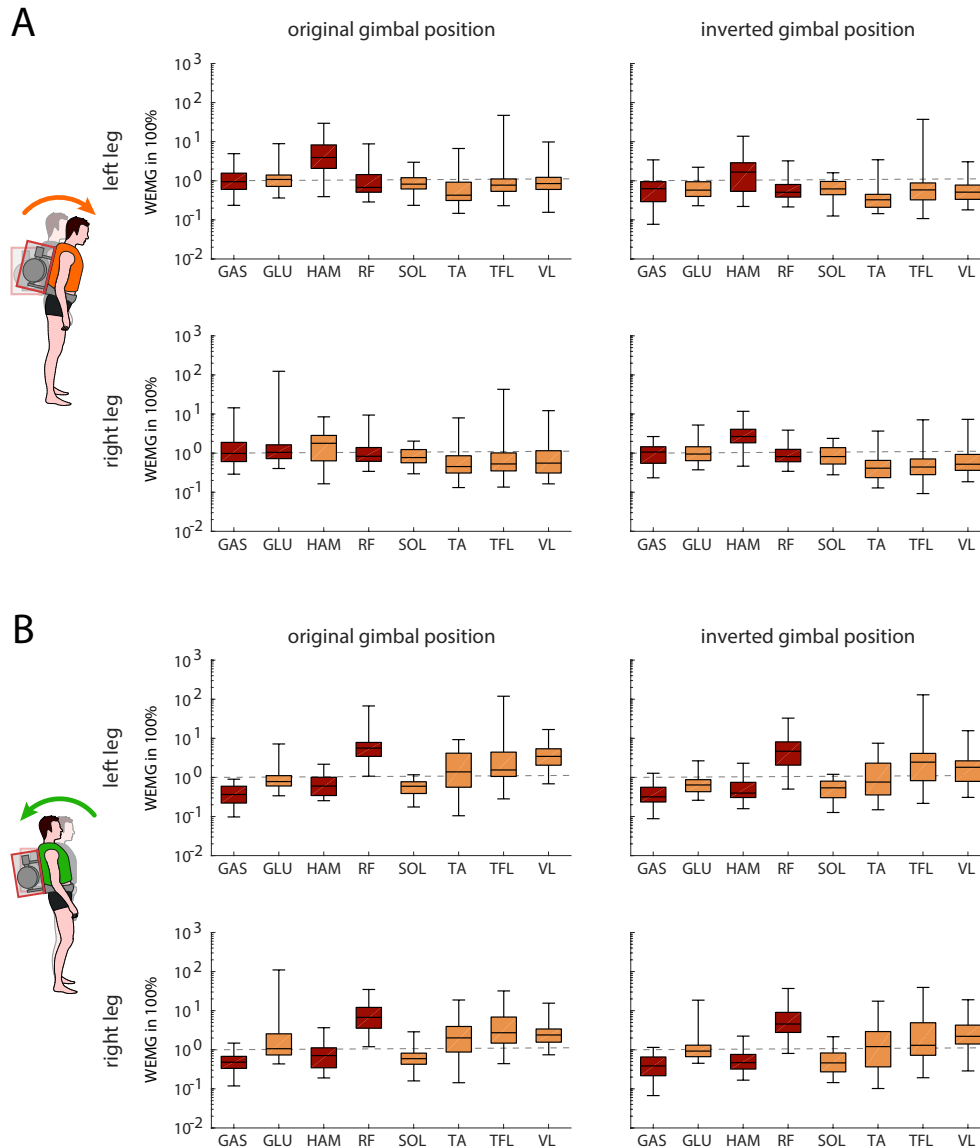
Figure A.12: Comparison of muscular activity levels in response interval RI1 ($100-150\,\text{ms}$**) of all conditions and both legs:** Boxplots (pooled data of all analyzed trials) of the normalized and mean response amplitudes (WEMG) for positive torque perturbations **(A)** and negative torque perturbations **(B)**, left (upper panels) and right leg (bottom panels) and original (left side) and inverted gimbal position (right side). Results of mono- (yellow) and biarticular muscles (red) are presented in a logarithmic scaling. Mean EMGs were normalized by the individuals mean muscle stimulation during walking trials (see Methods).
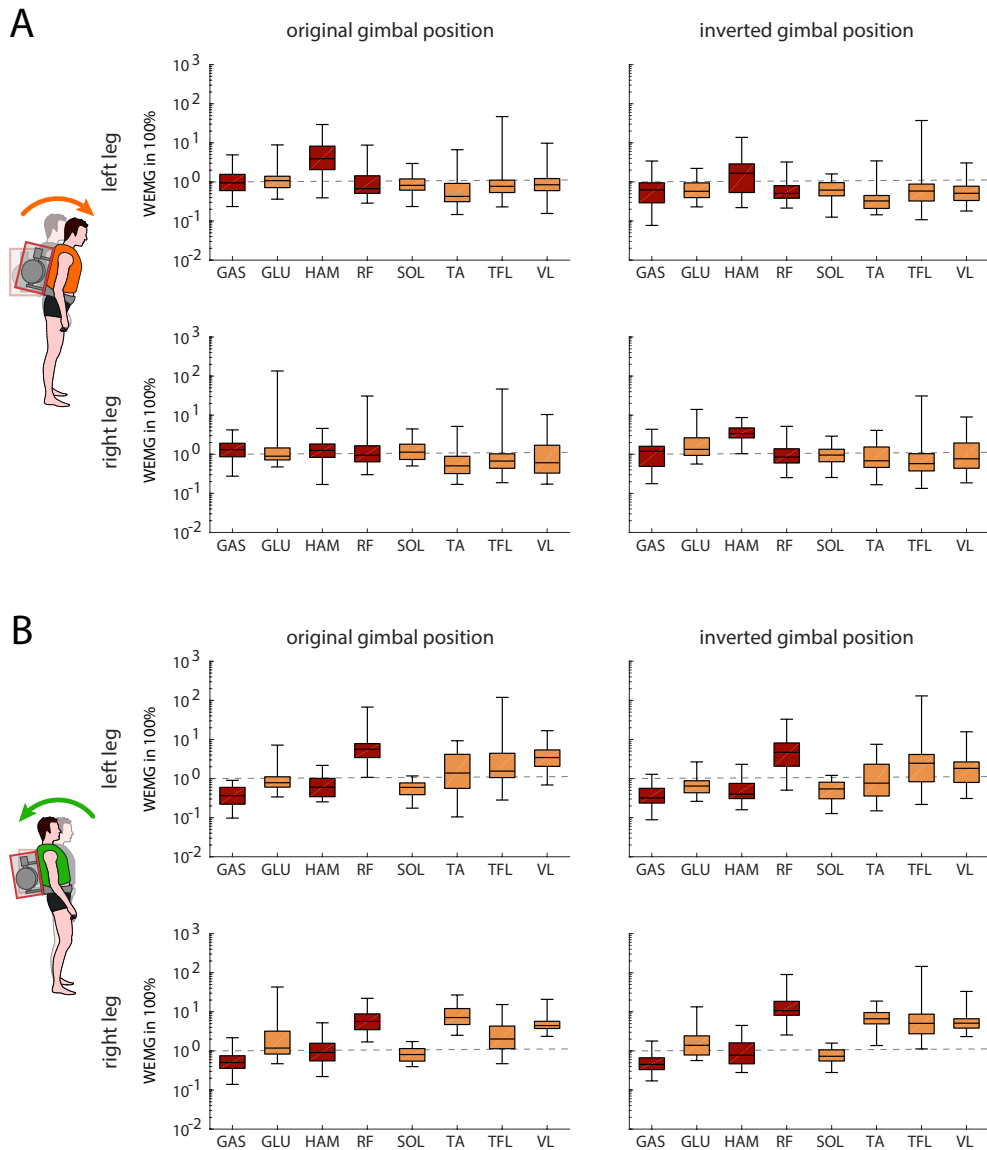
Figure A.13: Comparison of muscular activity levels in response interval RI2 ($170 - 250\,\mathrm{ms}$**) of all conditions and both legs:** Boxplots (pooled data of all analyzed trials) of the normalized and mean response amplitudes (WEMG) for positive torque perturbations **(A)** and negative torque perturbations **(B)**, left (upper panels) and right leg (bottom panels) and original (left side) and inverted gimbal position (right side). Results of mono- (yellow) and biarticular muscles (red) are presented in a logarithmic scaling. Mean EMGs were normalized by the individuals mean muscle stimulation during walking trials (see Methods).
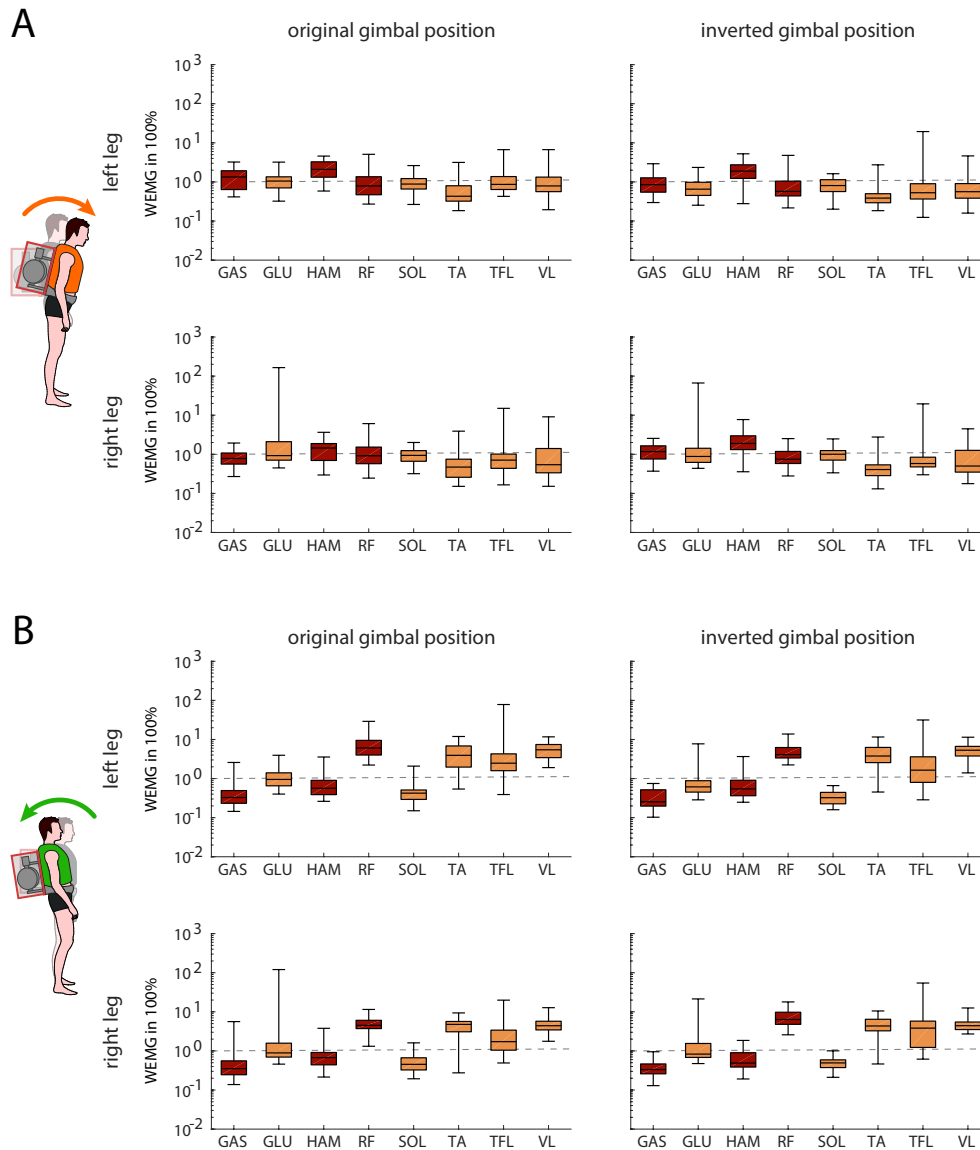
Figure A.14: Comparison of muscular activity levels in response interval RI3 ($270 - 350\,\mathrm{ms}$**) of all conditions and both legs:** Boxplots (pooled data of all analyzed trials) of the normalized and mean response amplitudes (WEMG) for positive torque perturbations **(A)** and negative torque perturbations **(B)**, left (upper panels) and right leg (bottom panels) and original (left side) and inverted gimbal position (right side). Results of mono- (yellow) and biarticular muscles (red) are presented in a logarithmic scaling. Mean EMGs were normalized by the individuals mean muscle stimulation during walking trials (see Methods).

Comparison of muscular prestimulation of left and right leg

Table A.2 shows the calculated changes and significance levels from comparisons of 'loaded Standing' and mean 'Pre-Perturbation' activations of both legs.

Table A.2: Comparison of left and right leg prestimulation. Mean and SD changes (Δ in WEMG) and p-values of normalized and mean response amplitudes for comparisons of 'Unloaded Standing' (UL), 'Loaded Standing' (L) and the mean 'Pre-Perturbation' activation for all 10 trials (averaged over last 5 trials per condition $\times$ 2 gimbal configurations) for all 11 subjects. For comparisons, the paired two-sided t-test (for normal distribution) or the non-parametric two-sided Wilcoxon signed-rank test (if assumption of normality was violated) was used. Significant values ($p < 0.05$) are highlighted by bold text.

side	muscle	'L' vs. 'UL'		'PP' vs. 'L'	
		Δ WEMG	p-values	Δ WEMG	p-values
left	GLU	-20 $\pm$22	**0.003**	+8 $\pm$13	**0.033**
	HAM	-46 $\pm$57	**0.013**	-5 $\pm$14	0.308
	GAS	+2 $\pm$03	0.061	0 $\pm$11	0.213
	SOL	+7 $\pm$12	0.078	-2 $\pm$07	0.345
	TFL	+7 $\pm$12	0.155	+5 $\pm$07	0.065
	RF	+10 $\pm$36	0.790	-9 $\pm$48	0.790
	VL	+1 $\pm$07	0.730	0 $\pm$28	0.213
	TA	0 $\pm$03	0.695	-1 $\pm$08	0.182
right	GLU	-7 $\pm$35	0.051	-20 $\pm$41	0.091
	HAM	-7 $\pm$42	0.091	-5 $\pm$30	0.930
	GAS	+1 $\pm$16	0.862	+1 $\pm$10	0.792
	SOL	+8 $\pm$13	0.058	+2 $\pm$07	0.354
	TFL	+19 $\pm$30	0.061	-15 $\pm$22	**0.048**
	RF	+8 $\pm$31	0.790	-30 $\pm$44	0.051
	VL	-10 $\pm$13	**0.027**	-8 $\pm$14	0.075
	TA	+1 $\pm$03	0.364	-2 $\pm$04	0.098

Peak to mean ratios of background walking activity

Table A.3 provides ratios of the filtered background activity during unloaded level walking to convert the mean background activity (WEMG, this study) to peak background activity (for comparisons with other studies).

Table A.3: EMG Ratio of peak to mean background walking activity of all muscles averaged over 10 trials.

muscle	left side	right side
GLU	6.72	6.65
HAM	7.30	8.04
GAS	5.72	8.87
SOL	4.29	6.90
TFL	5.00	6.37
RF	5.32	5.23
VL	7.85	10.99
TA	7.29	6.14

Comparison of muscular reflex response of positive and negative perturbations

Table A.4 shows the comparisons (mean differences and significance levels) of the reflex responses of all muscles. For positive perturbation, HAM responded with significantly higher activity levels than any other muscle. In negative perturbations, anterior and posterior muscle groups were significantly different. Additionally, RF stimulation was higher than all other muscles.

Table A.4: Comparison of relative reflex responses for positive (upper panel) and negative (lower panel) perturbations. Results from the rmANOVA post-hoc test of the interaction effect 'Muscle' x 'Direction' ($F(7,314) = 65.2, p < 0.001$). Mean differences (upper value, in WEMG) and p-values (lower value) of comparisons between muscles per perturbation direction (over both legs and all response intervals). Comparisons were done for the averaged relative reflex responses of the left leg (last 5 trials per condition $\times$ 2 gimbal configurations) for all 11 subjects. Significant values ($p < 0.05$) are highlighted by bold text.

positive perturbation	HAM	GAS	SOL	GLU	TFL	TA	VL	RF
HAM	-	+117	+156	+190	+177	+184	+166	+193
	-	**< 0.001**	**< 0.001**	**< 0.001**	**< 0.001**	**< 0.001**	**< 0.001**	**< 0.001**
GAS		-	+39	+72	+60	+67	+49	+76
		-	0.942	0.378	0.637	0.483	0.833	0.318
SOL			-	+34	+21	+28	+10	+37
			-	0.974	0.999	0.990	1.000	0.956
GLU				-	−13	−5	−24	+3
				-	0.999	1.000	0.997	1.000
TFL					-	+7	−11	+16
					-	1.000	1.000	0.999
TA						-	−18	+9
						-	0.999	1.000
VL							-	+27
							-	0.993
RF								-
								-

negative perturbation	HAM	GAS	SOL	GLU	TFL	TA	VL	RF
HAM	-							
	-							
GAS	−17	-						
	0.999	-						
SOL	−11	+6	-					
	1.000	1.000	-					
GLU	+1	+18	+12	-				
	1.000	0.999	1.000	-				
TFL	+257	+274	+268	+256	-			
	< 0.001	**< 0.001**	**< 0.001**	**< 0.001**	-			
TA	+325	+342	+337	+324	+69	-		
	< 0.001	**< 0.001**	**< 0.001**	**< 0.001**	0.452	-		
VL	+385	+402	+396	+383	+128	+59	-	
	< 0.001	**< 0.001**	**< 0.001**	**< 0.001**	**0.004**	0.628	-	
RF	+586	+603	+597	+585	+329	+261	+202	-
	< 0.001	**< 0.001**	**< 0.001**	**< 0.001**	**< 0.001**	**< 0.001**	**< 0.001**	-

References

Y. S. Al-Khabbaz, T. Shimada, and M. Hasegawa (2008). "The effect of backpack heaviness on trunk-lower extremity muscle activities and trunk posture". In: *Gait & posture* 28.2, pp. 297–302.

J. M. Schiffman et al. (2006). "Effects of carried weight on random motion and traditional measures of postural sway". In: *Applied Ergonomics* 37.5, pp. 607–614.

Achnowledgements

I am very grateful for the last 5 years that comprise my PhD in the Locomotion Laboratory at Technische Universität Darmstadt and the Delft Biorbotics Lab at the Delft University of Technology. This period of my life taught me to critically reflect information and develop my own standpoint in complex debates. I value this ability higher than the knowledge that I gathered, because – as everything in research – this knowledge might be extended or revised at some point in time. I am very thankful for my mistakes and the feedback that I received from all the great and patient people that helped me to grow professionally and personally.

I want to express my sincere thanks to my advisor Prof. André Seyfarth for his continuous support and guidance. Thank you for the many deep discussions that stimulated my scientific progress and changed my perspective on many – also non-scientific – topics. You are a visionary and broad-thinking person who has a learning-oriented mindset! Thanks for your bright personality and positive charisma. Thank you for giving me the room to fail, learn from my mistakes and develop my character. Your supervision taught me to walk on my own instead of following others; I appreciate the time and dedication you invested into me. Thank you!

Many thanks also belong to Prof. Heike Vallery for her encouraging support and, scientific and personal guidance during my guest stay in Delft. Thank you for your openness to welcome me, your demanding and critical thinking that challenged me and helped me to grow. It was enlightening and inspirational to work with such a bright and innovative mind and learn how you approach academia, science and technology.

I also thank Christian Rode, who I appreciate. I am grateful for your catching enthusiasm for research, broad and reflected thinking, your high-quality standards and your persistence to go the extra mile. I learned a lot form your striving for sound scientific practice.

I want to thank my labmates in Darmstadt for all the fun and stimulating discussions, the lab events and retreats. Thank you, Guoping Zhao, it was a remarkable journey with you! Thank you for all the great memories during our conference visits, countless moments of laughter, tasty chinese dinner and last but not least, great photography. To you, Martin Grimmer, thank you for having a friendly ear, for sharing your experience and constant advice on whatever topics. Thank you Aida, Ryan and Maziar Sharbafi for your company; you are a great family! I appreciate your graciousness and our open and honest discussions about science, culture and politics. From Prof. Karl Kalveram, who sadly passed away recently, I learned how honest curiosity and open-mindedness look like. Thank you for that, Karl! To all students or international interns of the Lab, like Sarah Dorsch, Sebastian Haufe, Rustam Galljamov and many more, thank you for sharing your insights and perspectives. I highly appreciate all these memories – I will keep them in my heart.

To the great people I got to learn in Delft, thank you very much for the support and companionship you gave me. Thank you, Patricia Baines, Saher Jabeen, Ivan Koryakovskiy, Joost van der Weijde, Mukunda Bharatheesha, Carlos Hernándes Corbato and the many more for our coffee breaks and gym sessions. You

are great personalities, and I will always remember the fun lunch discussions, hard-fought football table matches and friday evening events. Special thanks belong to Andrew Berry, who helped me countless times without getting tired to educate me. Thank you for your deep comments & insights and fun conversations. Daniel Lemus, thank you for sharing your vast expertise and your ideological view about science, it left a lasting impression on me.

My "Schafti-Team", Veronika Noll and Kathin Neuheuser, thank you for a great time during the research project and the conference visits. You became friends, and I am very happy that we kept the contact, even after the end of the project!

Thanks to the administrative personnel in the Sports Insitute, Wiebke Sittmann and Brigitte Schult. Thanks to both of you, you are doing a great job every day. Thanks for your open door, friendly chats and your support, e.g. to overcome big bureaucratic hurdles!

I want to acknowledge those who gave me the strength and support to conduct this research, my friends and family. Special thanks to my parents, Cornelia & Joachim Schumacher, and my brother Niklas, who's support always has been unconditional. A lot of what you taught me is incorporated in this thesis!

Finally and most importantly, I like to express my highest appreciation to my wife, Katharina. Thank you for your trust, patience and moral support through this journey. You cheered with me in times of success and encouraged me in hard times. I appreciate the sacrifices you had to make that I could pursue my interests. Our relationship and love always gave me strength and support. Thank you very much!

Christian Schumacher
Darmstadt, November 2019

List of Publications

Journal Papers

- **Schumacher, C.**, Sharbafi, M. A., Seyfarth, A. & Rode, C. (2020, February). Biarticular muscles in light of template models, experiments and robotics: A review. *Journal of the Royal Society Interface*. [Article I of this thesis]

- Verstraten, T., **Schumacher, C.**, Furnémont, R., Seyfarth, A. & Beckerle, P. (2020). Redundancy in Biology and Robotics: Potential of Kinematic Redundancy and its Interplay with Elasticity. *Journal of Bionic Engineering*. (accepted)

- **Schumacher, C.**, Berry, A., Lemus, D., Rode, C., Seyfarth, A., & Vallery, H. (2019, October). Biarticular muscles are most responsive to upper-body pitch perturbations in human standing. *Scientific reports*. [Article II of this thesis]

- Sarmadi, A., **Schumacher, C.**, Seyfarth, A., & Sharbafi, M. A. (2019, January). Concerted Control of Stance and Balance Locomotor Subfunctions—Leg Force as a Conductor. *IEEE Transactions on Medical Robotics and Bionics*.

- Seyfarth, A., & **Schumacher, C.** (2019, January). Teaching locomotion biomechanics-From concepts to applications. *European Journal of Physics*.

- **Schumacher, C.**, & Seyfarth, A. (2017, November). Sensor-motor maps for describing linear reflex composition in hopping. *Frontiers in computational neuroscience*. [Article III of this thesis]

- Noll, V., Eschner, N., **Schumacher, C.**, Beckerle, P., & Rinderknecht, S. (2017, March). A physically-motivated model describing the dynamic interactions between residual limb and socket in lower limb prostheses. *Current Directions in Biomedical Engineering*.

- Noll, V., **Schumacher, C.**, Neuheuser, K., Braun, M., Blab, F., Kleiner, B., ... & Schneider, U. (2016, May). Optimierte Anpassung von Beinprothesenschäften. *Orthopädie-Technik*.

Conference Papers

- Seyfarth, A., Sharbafi, M. A., Zhao, G., & **Schumacher, C.** (2018, October). Modular Composition of Human Gaits Through Locomotor Subfunctions and Sensor-Motor-Maps. In *International Symposium on Wearable Robotics*.

- Seyfarth, A., Zhao, G., & **Schumacher, C.** (2018, October). ANSYMB-Interdisciplinary Teaching for Human-Centered Robotics. In *International Conference on Inclusive Robotics for a better Society*.

- **Schumacher, C.**, Grimmer, M., Scherf, A., Zhao, G., Beckerle, P., & Seyfarth, A. (2018, August). A Movement Manipulator to Introduce Temporary and Local Perturbations in Human Hopping. In *7th IEEE International Conference on Biomedical Robotics and Biomechatronics (Biorob)*.

- Sarmadi, A., Sharbafi, M. A., **Schumacher, C.**, & Seyfarth, A. (2018, August). Force-Feedback Coordinates Stance and Balance Locomotor Subfunctions in Hopping. In *7th IEEE International Conference on Biomedical Robotics and Biomechatronics (Biorob)*.

- Firus, A., Schneider, J., Seyfarth, A., & **Schumacher, C.** (2017, September). Investigation of the human-structure interaction on a full scale experimental footbridge. In *Footbridge 2017*

About the Author

Christian Schumacher

Born on 24 August 1987 in Bonn, Germany

Research Experience

Guest researcher at Delft Biorobotics Lab, TU Delft   **2018 - 2020**

- Research project *'Torque perturbations of the upper-body balance with a control moment gyroscope'* funded by scholarships from the German Academic Exchange Service (DAAD) and the COST Action for Wearable Robotics (CA16116).

Researcher at Lauflabor Locomotion Laboratory, TU Darmstadt   **2014 - 2020**

- Joint research project *'Better balance and reduced risk of falling due to contactless coupling of vibrations'* funded by FiF TU Darmstadt.

- Joint research project *'Optimized Measurement, Adjustment, and Manufacturing of Lower Limb Prosthetic Sockets'* funded by AiF/IGF under grant no. 18873 N/2.

- Joint research project *'Modular Orthopedic Means with Robust EMG and Force Sensing (MorHRoSe)'* funded by the LOEWE framework under grant No. 436/14-26.

- Collaborative research project with adidas AG (Herzogenaurach, Germany), *'System Identification of a Bio-inspired Robotic Leg for Running Gaits'*.

- Collaborative research project with Olympic Training Center (Frankfurt, Germany), *'Model-based Performance Diagnostics for Long Jumping'*.

- Collaborative research project with Össur hf (Reyjkavik, Iceland), *'Experimental Investigation of the Long Jump of a Unilateral Transtibial Amputee'*.

Education

Technische Universität Darmstadt   Darmstadt, Germany
Lauflabor Locomotion Laboratory   **Nov. 2014 - Jun. 2020**
Institute of Sport Science
Centre for Cognitive Science
Department of Human Sciences
Dr. rer. nat. in Biomechanics, summa cum laude (passed with distinction)
Dissertation: 'Motor and Sensor Network Topologies as Translators between Motor Control and
　　　　　Human Locomotion'

Technische Universität Darmstadt   Darmstadt, Germany
Department of Mechanical Engineering   **Nov. 2011 - Oct. 2014**
M.Sc. in Mechanical and Process Engineering
Thesis: 'The Influence of Muscle Properties on Optimizing Leg Design for Long Jump Performance'

Technische Universität Darmstadt   Darmstadt, Germany
Department of Mechanical Engineering   **Oct. 2008 - Oct. 2011**
B.Sc. in Mechanical and Process Engineering
Thesis: 'Investigation of Energy Efficiency Potentials in the Use Phase of Capital Goods'